THE UNIVERSITY
of EDINBURGH

Arctic tundra plant phenology and greenness across space and time

Jakob J Assmann

Thesis submitted for the degree of Doctor of Philosophy
The University of Edinburgh
2018

For my father Winni.

“Die Arbeit läuft nicht davon während du dem Kind den Regenbogen zeigst, aber der Regenbogen wartet nicht.“

Unbekannter Autor

„Work does not run away while you are showing the rainbow to the child, but the rainbow does not wait.”

Unknown Author

Declaration

I declare that this thesis has been composed by myself and that the work has not been submitted for any other degree or professional qualification. I confirm that the work submitted is my own, except where work which has formed part of jointly-authored publications has been included. My contribution and those of the other authors to this work are explicitly detailed below.

Chapter 2

The work in Chapter 2 has been submitted to Global Change Biology as *Snow-melt and temperature – but not sea-ice – explain variation in spring phenology in coastal Arctic tundra* by Jakob J. Assmann, Isla H. Myers-Smith (supervisor), Albert B. Phillimore (supervisor), Anne D. Bjorkman (collaborator), Richard E. Ennos (supervisor), Janet S. Prevéy (collaborator), Greg H.R. Henry (collaborator), Niels M. Schmidt (collaborator), Robert D. Hollister (collaborator). At the time of submission of this thesis, the article had received the assessment of major revisions at the Journal Global Change Biology (decision letter 6th November 2018).

Author Contributions: JJA, IHMS and ABP conceived the study with input from REE. ADB, JSP, GHRH, NMS and RDH contributed data. JJA carried out the analysis and wrote the manuscript with input from all authors.

Chapter 3

The work in Chapter 3 has been accepted by the Journal of Unmanned Vehicle Systems as *Vegetation monitoring using multispectral sensors – best practices and lessons learned from high latitudes* by Jakob J. Assmann, Jeffrey T. Kerby (collaborator), Andrew M. Cunliffe (collaborator) and Isla H. Myers-Smith (supervisor). At the time of submission of this thesis, the article was in press.

Author Contributions: JJA and IHMS conceived the study. JJA performed the analysis and wrote the manuscript with input from all authors.

Chapter 4

The work in Chapter 4 has been prepared for submission as *Drone data reveals fine-scale variation of tundra greenness and phenology that is missed by satellite and in situ monitoring* by Jakob J. Assmann, Isla H. Myers-Smith, Andrew M. Cunliffe and Jeffrey T. Kerby. At the time of submission of this thesis, this article had not yet been submitted to a journal.

Author Contributions: JJA and IHMS conceived the study with input from JTK. JJA carried out the data processing and analysis. AMC lead the field campaign for the drone data collection in 2017. JJA wrote the manuscript with input from all authors.

_____

Jakob J. Assmann

Abstract

The Arctic is warming at twice the rate of the rest of the planet with dramatic consequences for Northern ecosystems. The rapid warming is predicted to cause shifts in plant phenology and increases in tundra vegetation productivity. Changes in phenology and productivity can have knock-on effects on key ecosystem functions. They directly influence plant-herbivore and plant-pollinator interactions creating the potential for mismatches and changes in food web structure, and they alter carbon and nutrient cycling, which in turn influence feedback mechanisms that couple the tundra biome with the global climate system. Improving our understanding of changes in tundra phenology and productivity is therefore critical to projecting not only the future state of Arctic ecosystems, but also the magnitude of potential feedbacks to global climate change. In this thesis, I combine observations from ground-based ecological monitoring, satellites and drones (also known as unmanned aerial vehicles or remotely piloted aircraft systems) to investigate how tundra plant phenology and productivity are changing across space and time, and to test how observational scales influences our ability to detect these changes.

Spring plant phenology is tightly linked to temperatures, and advances in spring phenology are one of the most well documented effects of climate change on global biological systems. With rapid and near-ubiquitous Arctic warming, the absence of consistent trends in tundra spring phenology among sites suggests that additional environmental factors may exert important controls on tundra plant phenology. Indeed, further to temperature, snowmelt and sea-ice have been reported to strongly influence tundra phenology. Yet, the relative influence of these three factors has yet to be evaluated in a single cross-site analysis. In Chapter 2, I tested the importance of local average spring temperatures, local snowmelt and the timing of the drop in regional spring sea-ice extent as controls on variation in spring leaf out and flowering of 14 plant species from long-term records at four coastal sites in Arctic Alaska, Canada and Greenland. I found that spring phenology was best explained by snowmelt and spring temperature. In contrast to previous studies, sea-ice did not predict spring plant phenology at these study sites. This contrasting finding is likely explained by differences in the scale of the sea-ice measures employed. While many previous studies used descriptors of circum-polar sea-ice conditions that serve as

aggregate measures for global weather conditions, I tested for the indirect effects of sea-ice conditions at a regional scale. My findings (re)emphasize the importance of snowmelt timing for tundra spring plant phenology and therefore highlight the localised nature of some of the key drivers of tundra vegetation change.

Discrepancies between conventional scales of observation and underlying ecological processes could limit our ability to explain variation in tundra plant phenology and vegetation productivity. In the remote biome, ground-based monitoring is logistically challenging and restricted to comparably few sites and small plot sizes. Multispectral satellite observations cover the whole biome but are coarse in scale (tens of meters to kilometres) and uncertainties persist in how trends in vegetation indices like the Normalised Differential Vegetation Index (NDVI) relate to *in situ* ecological processes. Recent advances in drone technologies allow for the collection of multispectral fine-grain imagery at landscape level and have the potential to bridge the gap in observational scales. However, collecting high-quality multispectral drone imagery that is comparable across sensors, space and time remains challenging particularly when operating in extreme environments such as the tundra. In Chapter 3 of this thesis, I discuss the key error sources associated with solar angle, weather conditions, geolocation and radiometric calibration and estimate their relative contributions to the uncertainty of landscape level NDVI measurements at Qikiqtaruk in the Yukon Territory of Canada. My findings show that these errors can lead to uncertainties of greater than ± 10% in peak season NDVI, but also demonstrate they can be accounted for by improved flight planning, meta-data collection, ground control point deployment, use of reflectance targets and quality control.

Satellite data suggest that vegetation productivity in the Arctic tundra has been increasing in recent decades: the tundra is greening. However, the observed trends show a lot of variation: although many parts of the tundra are greening, others show reductions in vegetation productivity (sometimes known as browning), and the satellite-based trends do not always match *in situ* records of change. Our ability to explain this variation has been limited by the coarse grain sizes of the satellite observations. In Chapter 4, I combined time-series of multispectral drone and satellite imagery (Sentinel 2 and MODIS) of coastal tundra plots at my focal study site Qikiqtaruk to quantify the correspondence among satellite and drone observations of

vegetation productivity change across spatial scales. My findings show that NDVI estimates of tundra productivity collected with both platform types correspond well at landscape scales (10 m – 100 m) but demonstrate that the majority of spatial variation in NDVI at the study sites occurs at distances below 10 m and is therefore not captured by the latest generation of publicly available satellite products, like those of the Sentinel 2 satellites. I observed strong differences in mean estimates and variation of vegetation productivity between the dominant vegetation types at the field site. When comparing greening observations over two years, I detected differences in the amount of variation amongst years and a within-season decline in variation towards peak growing season for both years. These results suggest that not only the timing, but also the heterogeneity of tundra landscape phenology can vary within and among years, and if lowered by warming could alter trophic interactions between species.

The findings presented in this thesis highlight the importance of the localised processes that influence large-scale patterns and trends in tundra vegetation phenology and productivity. Localised snowmelt timing best explained variation in tundra plant phenology and drone imagery revealed meter-scale heterogeneity in tundra productivity. Research that identifies the most relevant scales at which key biological processes occur is therefore critical to improving our forecasts of ecosystem change in the tundra and resulting feedbacks on the global climate system.

Lay Summary

Human-made climate change is affecting the natural environment around the world, but the impacts are particularly dramatic in the far north of the planet – the Arctic. Over the last fifty years, air temperatures in the Arctic have risen at twice the rate compared to the rest of the globe. The rapid warming is leading to dramatic consequences for the Arctic environment: Sea-ice is declining, glaciers are melting, and previously frozen ground is thawing. However, warming also affects Arctic plants, particularly in the tundra biome north of the latitudinal treeline, where extremely cold temperatures have previously restricted plant growth. The rapid rise in temperature is changing tundra plants. Warmer summers are thought to be increasing plant growth and warmer springs are thought to cause earlier emergence of leaves in the season. Such changes will not only affect the animals that rely on plants for food and shelter, but are also likely to result in feedbacks to the global climate, potentially accelerating or slowing down global warming. My thesis aims to improve our understanding of how the plants and their seasonal timing are changing so that we can better predict future changes in the ecosystems of the tundra and their knock-on effects on the global climate.

Even though satellite observations suggest an earlier onset of spring in the Arctic, ground-based measurements of spring leaf out and flowering do not show consistent changes across the tundra. On the ground, spring is getting earlier at some locations, while no changes - or even delays - are observed elsewhere. The fact that tundra plants are not always greening up earlier is particularly surprising considering both the rapid warming of the tundra and the fact that tundra plants have been shown to change their timing of leaf out and flowering in warmer years at some sites. Other environmental influences must therefore also control the timing of green up and flowering of tundra plants. In addition to temperature, snow-melt and sea-ice conditions have been shown to influence the timing of spring and summer in the tundra. Yet, to date, no study has tested the relative influence of these three environmental factors on the timing of spring in one combined analysis across multiple sites. In Chapter 2, I use ground-based observations of spring leaf-out and flowering from long-term records at four tundra sites located on the coasts of Alaska, Canada and Greenland to test the relative influence of temperature, snowmelt and sea-ice

conditions on the timing of spring. My findings demonstrate that snowmelt and temperature, but not sea-ice conditions, are influencing tundra leaf-out and flowering. This analysis of tundra plants from multiple sites highlights the power of localised environmental influences such as snowmelt as agents of change in the tundra.

Satellite observations suggest that the tundra vegetation is changing. The north of the planet is “greening” and spring green up is happening earlier. Though plant measurements on the ground generally agree with the satellites, the satellite trends themselves are highly varied - some parts of the tundra are getting ‘greener’ while others are getting ‘browner’, their ‘greenness’ is decreasing over time. The large size of the satellite pixels makes it difficult to interpret these changes. Pixel-widths range from tens of meters to 8 km (that’s two times the length of Central Park in Manhattan). Modern drone technology can provide high-resolution aerial imagery (5 cm drone pixel sizes and smaller) that allows us to bridge this gap. However, the drone technology is new and new procedures need to be developed to provide high-quality data for scientific purposes. Particularly in the extreme environments of the Arctic, drone data collection can be challenging. In Chapter 3 of this thesis, I estimate the errors in drone imagery collected in the tundra and provide guidance on how to control for them – for example, by suggesting best practises on how to account for changes in light conditions between drone surveys. In Chapter 4, I then use the newly developed methods to test the agreement between satellite and drone observations of tundra greenness in the Canadian Yukon, and to determine how seasonal changes in tundra landscape greenness vary in the high-resolution drone imagery. I found that even though drone and satellite products agree at the landscape level, a considerable amount of detail in variation is lost when changing resolution from drone to the satellite pixel sizes. Furthermore, I show that tundra landscape greenness varies considerably over short distances and between vegetation types, and that the landscape becomes more uniform in greenness as the growing season progresses. These findings allow us to better our predictions of future changes in the tundra landscape and the impacts thereof on the tundra animals that rely on the variation in plant resources for food, nesting and shelter.

Overall, the research in this thesis demonstrates that we can use high-resolution drone imagery to study fine-scale changes in the tundra, and that satellite and drone observations of tundra greenness agree at the landscape level. Furthermore, it highlights that there is a considerable variation in landscape greenness over short distances and underlines the importance of snowmelt and temperature in determining tundra spring leaf-out and flowering. These findings are important as they allow us to better understand how future seasons and greenness patterns in the tundra landscape will look like, whether these changes will affect the animals that rely on the tundra plants for food, nesting and shelter, and whether there will be any knock-on effects on the global climate.

Acknowledgements

First of all, I would like to say thank you to my supervisors for their continuous encouragement and support. Without you this PhD would not have happened.

Isla, thank you for taking me on board after re-starting my PhD, for introducing me to Canada, the Yukon and the tundra, as well as the many wonderful people that study and live in it. For being so supportive of my research and career development, for putting up with my continentality and German frankness, and of course for making it all possible financially by letting me work on the NERC Shrub Tundra Grant. Your enthusiasm and scientific mind have been an inspiration and I will fondly remember our music jams, at conferences and in the field.

Ally, it has been a great pleasure working with you. Thank you for always being there when I needed advice, for the many stimulating scientific discussion and welcoming me into your lab group. For asking the right questions at the right time, for making me think “phenology”, for continuously reminding me to look after myself and for being a family father and runner. You showed me that it is possible to combine work in academia with the other important parts of life.

Richard, you have been a great support throughout my time at the University of Edinburgh. From my undergrad dissertation to PhD thesis, your advice and mentorship has been an integral part of it all. Thank you for supporting me in all my decisions - even though they were difficult at times, for being an inspirational ecologist and for showing continued interest in my PhD even after your retirement.

Next, I would like to thank the UK Natural Environment Research Council (NERC) for providing funding for the research in this thesis through a NERC E3 Doctoral Training Partnership PhD studentship (NE/L002558/1) and the NERC ShrubTundra standard grant (NE/M016323/1), as well as my examiners Toke Høye and Ed Mitchard for providing valuable feedback on the initial submission of this thesis.

And then of course, there are all the people that helped me along over the last few years and contributed to making this thesis happen. In particular I would like to thank:

Santeri Lehtonen for being a top-notch field assistant, co-pilot and friend. Thanks for putting up with the many long days we had to pull off to make it all happen. Because of you, the two field seasons in the Yukon were an absolute blast. I could have not wished for a better partner to cover my back out on the tundra!

Sandra and Haydn: How do you appropriately thank your PhD sister and brother?
I do not know… But what I know is that has been an incredible joy embarking on the PhD journey with you. I could have not wished for better companions. You are both truly wonderful people.

Jeff Kerby for being an awesome colleague and injecting energy into our drone team. Anne Bjorkman for being a great scientific friend, inspiration and so supportive of my research. Andrew Cunliffe for all the joint drone research projects. Janet Prevéy, Greg Henry, Bob Hollister and Niels Martin Schmidt for allowing me to use their phenological observations and feedback on the manuscript.

Tom Wade and Simon Gibson Poole from the Airborne GeoSciences facility, for giving me my “wings”, their ongoing support and collegiality in all possible drone related endeavours. It has been tremendous fun working without you and thank you for putting many hours into making it all happen. And of course, there are Chris McLellan and Andrew Gray from the NERC FSF who kindly shared their spectroscopy wisdom with me and allowed me to use their lab.

The Team Shrub field-teams for helping with the drone building and data collection. Joe Boyle for being an awesome field support and student on Team Shrub. Andrew Cunliffe, Will Palmer, Gergana Daskalova for collecting the 2017 drone data. Callum Tyler for getting the drones ready for 2016. Mariana who surprised us as a great new addition to Team Shrub during my final year. The Yukon people and the Qikiqtaruk family: The rangers Ed and Sam McLeod, Ricky Joe and Paden Lennie. Cameron “Right-on” Eckert, Megan Grabowski and her parents Toni and Patt for their support and warm welcome to the Yukon. The AWI field crews, particularly, Isabell, Caro, Sam, George and Hugues. The Kluane team for their support. Lance and Sian - I can’t be grateful enough for your generosity. You made us feel welcome in one of the most beautiful places in this world.

My desk neighbour Keiko Nomura, for being a wonderful friend and colleague. For feedback on many of my figures and putting up with the chill-hop quietly trickling out of my headphones. A haiku:

I finished up
My PhD
Puppy plays in leaves

My flatmates and fellow GeoScience PhD students of 1F 11 Melville Terrace for coping with the German cleaning rota, being awesome friends and making our flat such a homely place for the four years of my PhD:.Particularly Robyn Butler, Rachel Kilgallon, Nick Roberts, Rachel Bartlett, Davide Foffa, Alexis Moyer, Johannes Miocic and Lucy Peters. Not to forget Hannah and Darren, Tabi and Anne, Haydn and Nadine as well as Davide and Isla for lending me their spare rooms during the last weeks of my PhD. And my friends in Edinburgh, Jenny Farrar, Tabi Ewing, Archie Crofton and Anja Liski, who have been with me for so many years. And the all PhD students that have come and gone through the Crew Attic PhD office over the years. Anna, Claudia, Andy and Gill have been particular victims of my rants, questions and cheeky distractions. You have all been a wonderful support!

Further thanks need to go to the Gatsby Plant Science Network and the NERC E3 DTP for their great communities and providing with ever so many training opportunities. Particularly, my Gatsby cohort: Alex Blackwell, Emma Lawrence and Jaynee Hardt – I'll miss our regular meetings. Pete Nienow, Simon Mudd, Pat Ferguson and Stephanie Robyn from the E3 for supporting my rollercoaster PhD path both financially and administratively. Emma Cunningham for making sure my PhD ticked all the boxes, you have been a great advisor!

Finally, I would like to thank my parents and family for being there whenever needed, and Nina for taking my mind off work in the final year of my PhD.

Thank you all.

Contents

Declaration i

Abstract iii

Lay Summary vii

Acknowledgements xi

Contents xv

List of Figures xix

List of Tables xxi

Chapter 1 Introduction 1

Environmental and Vegetation Change in the Arctic tundra 4

Aims and structure of this thesis 15

Methods and datasets 17

References 21

Chapter 2 Snow-melt and temperature – but not sea-ice – explain variation in spring phenology in coastal Arctic tundra 33

Abstract 35

Introduction 36

Materials and methods 40

Results 49

Discussion 53

Conclusions 59

Acknowledgements 59

References 61

Chapter 3 Vegetation monitoring using multispectral sensors – best practices and lessons learned from high latitudes 73

Abstract 75

Introduction 76

Technical Background on Multispectral Drone Sensors (Section 1) 78
Data collection and processing – Workflow overview (Section 2) 83
Flight planning and overlap (Section 3) 85
Weather and Sun (Section 4) 88
Geolocation and Ground Control Points (Section 5) 91
Radiometric calibration (Section 6) 94
Estimated combined error 100
Conclusions 102
Acknowledgements 103
References 103
Chapter 4 Drone data reveals fine-scale variation of tundra greenness and phenology that is missed by satellite and *in situ* monitoring 109
Abstract 111
Introduction 112
Methods 116
Results 124
Discussion 132
Conclusions 137
Acknowledgements 138
References 139
Chapter 5 Discussion 151
Localised and regional drivers of tundra phenology 155
Drones can bridge the scale gap between satellite and *in situ* observations 159
Drones reveal fine-scale variation in tundra productivity and phenology 163
Conclusions 165
References 166
Appendix 169

Contents 175

Appendix for Chapter 3 176

Appendix for Chapter 4 188

List of Figures

Chapter 1

Figure 1-1 | Trends in Northern Hemisphere surface temperature, sea-ice extent and vegetation greenness for the high-latitudes and the time-period 1981-2015. 5
Figure 1-2 | Trends in leaf-out and flowering phenology across the tundra biome. ... 9
Figure 1-3 | Observational scales of satellite, manned aircraft, drone and ground-based monitoring (*in situ*) methods employed in tundra ecology. 11
Figure 1-4 | Spectral reflectance curves for vegetation and soil, as well as empirical line relationship between phytomass and GIMMS3g NDVI..... 13
Figure 1-5 | Diagram of the thesis structure. 15
Figure 1-6 | Map of study sites included in this thesis and map of tundra biome. 18
Figure 1-7 | Temperature trends for the study sites. 18

Chapter 2

Figure 2-1 | Map of study sites in the phenology dataset. 41
Figure 2-2 | Spring phenology trends for the species in the phenology dataset. 49
Figure 2-3 | Trends in temperature, snowmelt and sea-ice at the study sites. 51
Figure 2-4 | Scaled effect sizes for the effects of temperature, snowmelt and sea-ice on spring phenology. 53

Chapter 3

Figure 3-1 | Conceptual diagram of the sensing flow for multispectral drone sensors. 80
Figure 3-2 | Multispectral drone data collection workflow overview. 84
Figure 3-3 | Flight patterns that may aid reconstruction. 87
Figure 3-4 | Effect of diurnal solar variation on measured landscape scale mean NDVI. 89
Figure 3-5 | RGB photographs of different cloud and sun angle conditions and their effect on scene illumination. 90
Figure 3-6 | The effect of Ground Control Point (GCP) marker placement effort on geolocation and co-registration accuracy. 92
Figure 3-7 | Chequerboard pattern for GCP design. 94
Figure 3-8 | Radiometric calibration image example. 96

Figure 3-9 | Degradation of reflectance targets. 98
Figure 3-10 | The effect of radiometric calibration on mean NDVI values for three graminoid tundra sites on Qikiqtaruk. 99
Figure 3-11 | Transmissivity of Parrot Sequoia Lens-Protector 100
Figure 3-12 | Effect of Parrot Sequoia Lens-Protector – pixel by pixel differences in NDVI. 100
Figure 3-13 | Key sources of errors in multispectral drone surveys and estimated error values. 101

Chapter 4

Figure 4-1 | Map of the study plots and sites on Qikiqtaruk included in the time-series analysis. 117
Figure 4-2 | Drone and satellite-time-series of tundra greenness on Qikiqtaruk across the growing seasons of 2016 and 2017. And drone-derived mid-season NDVI estimates for the Herschel and Komakuk vegetation types. 126
Figure 4-3 | Spatial variation and pixel-by-pixel differences in drone and sentinel NDVI for the Bowhead Ridge Site (Site 2) on the 17 July 2017. 128
Figure 4-4 | Pixel by pixel correlation between Sentinel 2 L2A pixel values and resampled drone data for 2017. 129
Figure 4-5 | Variograms and model fits of drone derived NDVI for the Herschel and Komakuk vegetation plots at Bowhead Ridge (Site 2). 130
Figure 4-6 | Change in standard deviation of NDVI across the growing season. 131
Figure 4-7 | Influence of grain size on the trends in standard deviation of NDVI across the growing seasons. 132

Chapter 5

Figure 5-1 | Updated flow diagram of the thesis. 155
Figure 5-2 | Conceptual heat-map of the key environmental drivers of tundra plant phenology. 157
Figure 5-3 | Conceptual illustration of the loss of variation in tundra landscape phenology across scales. 165

List of Tables

Chapter 2

Table 2-1 | Species included in the coastal phenology dataset. 42

Chapter 3

Table 3-1 | Band wavelengths of drone and satellite sensors 78
Table 3-2 | Sky-codes for meta-data collection for multispectral drone surveys. 91

Chapter 4

Table 4-1 | Number of drone surveys included in the time-series analysis 121
Table 4-2 | Offset in plot-level July mean NDVI between drone and satellites..... 125

Chapter 1 Introduction

The tundra on Qikiqtaruk Herschel Island, YT, Canada.

Chapter 1 Introduction

The Arctic is undergoing rapid environmental change. Surface temperatures are rising at twice the rate of the global average (IPCC, 2014), precipitation patterns are changing and sea-ice is declining (AMAP, 2017). The rapidly changing environment has considerable consequences for the ecosystems of the North, including those in the Arctic tundra. Phenology (Høye, Post, Meltofte, Schmidt, & Forchhammer, 2007; Zeng, Jia, & Forbes, 2013), plant community composition (Elmendorf et al., 2015; Myers-Smith et al., 2011) and traits (Bjorkman et al., 2018) are changing, and as a result vegetation productivity is thought to be increasing (Guay et al., 2014; Keenan & Riley, 2018; Myneni, Keeling, Tucker, Asrar, & Nemani, 1997). Tundra vegetation change might lead to feedbacks to the global climate system (Chapin et al., 2005; Ernakovich et al., 2014; Loranty & Goetz, 2012; Pearson et al., 2013) and affect ecosystem services with direct consequences for plant-consumer interactions in the tundra (Doiron, Gauthier, & Lévesque, 2015; Gustine et al., 2017; Kerby & Post, 2013b). Improving our understanding of changes in tundra phenology and productivity is therefore critical to projecting the future state of Arctic ecosystems and the magnitude of potential feedbacks to global climate change.

Evidence for tundra vegetation change comes from localised *in situ* observations (Elmendorf et al., 2015; Myers-Smith et al., 2015; Oberbauer et al., 2013) and coarse-scale satellite data (Keenan & Riley, 2018; Myneni et al., 1997; Tucker et al., 2001; Zeng et al., 2013), but a discrepancy in observational-scales between the two has limited our ability to fully identify the key ecological processes and their mechanistic drivers of change (Myers-Smith et al., 2011; Raynolds, Walker, Verbyla, & Munger, 2013; Stow et al., 2004). This thesis combines observations from ground-based ecological monitoring, satellites and drones (also known as unmanned aerial vehicles or remotely piloted aircraft systems) to investigate how plant phenology and productivity are changing across space, time and observational scales in the warming tundra biome. In this chapter, I 1) discuss the relevant background to the research presented in this thesis, 2) identify the knowledge gaps, 3) outline the structure of this thesis and the key research questions addressed, and 4) summarise the key datasets used.

Environmental and Vegetation Change in the Arctic tundra

Arctic Change: Temperature, snow and ice

The environmental change in the Arctic is rapid and influences the vegetation in tundra ecosystems via three main parameters: rising temperatures, changing precipitation / snow patterns and sea-ice decline (AMAP, 2017). The particularly high speed of warming compared to the rest of the globe (Figure 1-1 A) is the result of a complex interaction of feedback mechanisms in the region, which are collectively referred to as “Arctic amplification” (Serreze & Barry, 2011). Temperature directly affects plant metabolic rate and developmental processes and the effects of the rapid warming are particularly forceful in the cold ecosystems of the tundra where plant growth is highly temperature limited (Callaghan et al., 2005). In addition, the increase in temperature affects the permanently frozen soils ubiquitous throughout the biome (Tarnocai et al., 2009), causing thaw and erosion (AMAP, 2017), which in turn release carbon and nutrients from the previously frozen soil (Natali, Schuur, & Rubin, 2012; Schuur et al., 2009), potentially alleviating constraints on plant growth in the nutrient limited biome (Mack, Schuur, Bret-Harte, Shaver, & Chapin Iii, 2004). Declining snow fall and snow cover duration (AMAP, 2017), as well as increased rain on snow events (Bintanja & Andry, 2017) are extending the growing season and increase plant productivity, but also expose the plants to higher risk of frost damage and herbivory, as well as modifying water and nutrient availability (Wipf & Rixen, 2010). The dramatic decline of sea-ice in the Arctic ocean (Figure 1-1 B) has not only considerable effects on the marine (AMAP, 2017) but also the adjacent terrestrial environments, affecting regional temperatures (Macias-Fauria & Post, 2018) and cloud cover in the tundra, which is thought to be increasing, affecting heat and light availability (McGuire, III, Walsh, & Wirth, 2006). Overall, these environmental changes are thought to be the drivers behind two main lines of evidence for vegetation change that have been documented in the Arctic tundra, a satellite observed “greening” and variety of vegetation changes documented by ground-based monitoring and experiments.

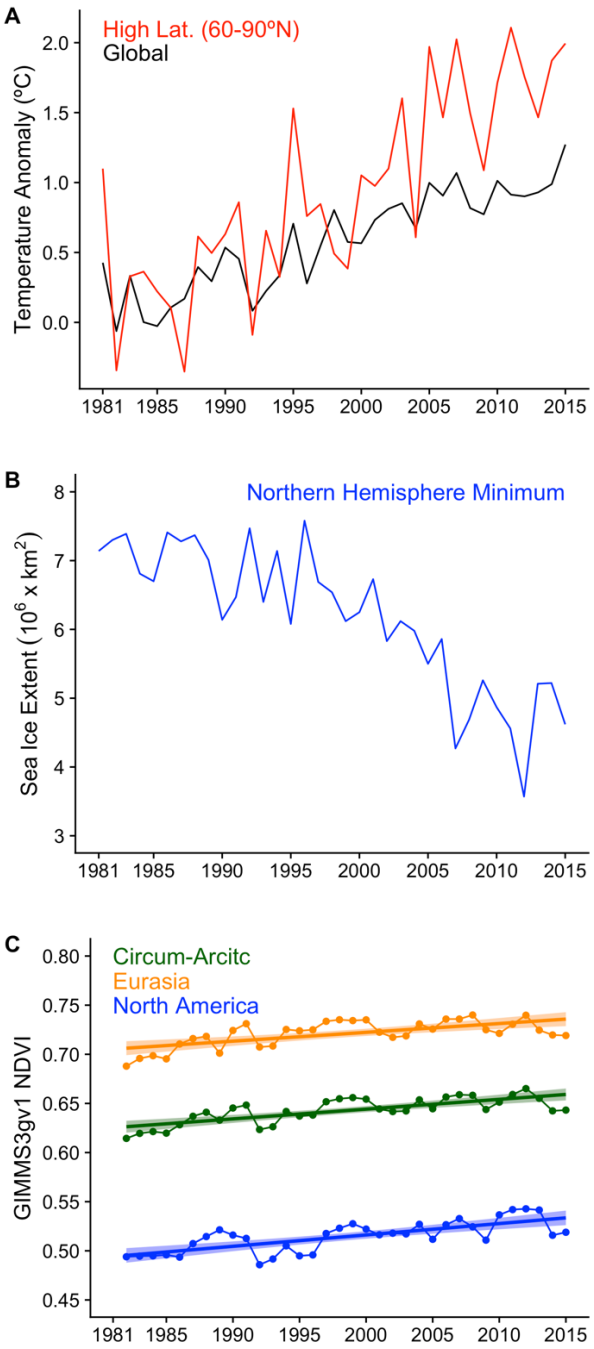

Figure 1-1 | (A) Global and Northern Hemisphere high latitude (60-90°N) temperature anomalies for the years 1981-2015 relative to the 1960-1990 average. Data from the CRUTEMP4 dataset (Jones et al. 2012). (B) Northern Hemisphere minimum sea-ice extent (September mean extent) for the years 1981-2015. Data from the Sea Ice Index Version 3 (Fetterer et al. 2017). (C) Trends in the Normalised Difference Vegetation Index (NDVI) – a proxy for vegetation productivity - of the circumpolar Arctic (green) and two continental Arctic regions derived from the GIMMS3g product based on NOAA AVHRR surface reflectance measurements. Modified from (Myers-Smith et al., 2019).

The Arctic is greening

Satellite observations indicate that vegetation productivity in the high latitudes is increasing, and thus that the north is greening (Figure 1-1 C). These observations (Keenan & Riley, 2018; Myneni et al., 1997; Tucker et al., 2001) primarily include trends in the normalised difference vegetation index (NDV) derived from surface reflectance data (Tucker, 1979). Despite the Arctic wide trends, a lot of heterogeneity in the greening is observed at global (Guay et al., 2014), continental (Ju & Masek, 2016) and regional extents (Lara, Nitze, Grosse, Martin, & McGuire, 2018; Miles & Esau, 2016; Thompson & Koenig, 2018). While some areas are greening, others show no trends or even declines in greenness ("browning") (e.g. Guay et al., 2014; Lara et al., 2018; D. A. Walker et al., 2009). Temperature is thought to be a primary driver of the high latitude greening (Keenan & Riley, 2018; Reichle, Epstein, Bhatt, Raynolds, & Walker, 2018), but linkages to sea-ice conditions (Bhatt et al., 2010; Macias-Fauria, Karlsen, & Forbes, 2017), predominant vegetation types (Loranty et al., 2018), landforms and disturbance events (Lara et al., 2018) have also been reported. Explaining the heterogeneity in the satellite trends and linking it to *in situ* (ground based) observations of tundra vegetation change is one of the key challenges of current ecological research in the tundra biome (Myers-Smith et al., 2011).

The ecology of greening and browning

A diversity of ecological changes is thought to contribute to the mixture of greening and browning trends observed in satellite datasets. Amongst the changes that have been suggested to cause greening are: (1) colonisation of previously non-vegetated surfaces by vegetation (Elmendorf, Henry, Hollister, Björk, Boulanger-Lapointe, et al., 2012), (2) increases in biomass due to changes in community composition - for example through the expansion of shrubs and graminoids (Elmendorf, Henry, Hollister, Björk, Boulanger-Lapointe, et al., 2012), and (3) increases in biomass due to changes in existing vegetation (Hudson & Henry, 2009) – including trait changes such as height, leaf area and phenology (Elmendorf, Henry, Hollister, Björk, Boulanger-Lapointe, et al., 2012, Helman, 2018; Steltzer & Post, 2009). The literature is less clear on whether browning encompasses only long-term trends or whether short-term events are also included (Myers-Smith et al. 2019). However, the following ecological changes have been linked to decreases in satellite perceived greenness of the Arctic: (1) loss of biomass due to extreme climate events including episodes of

severe cold (Bjerke et al., 2014; Bokhorst et al,. 2009; Richardson et al., 2018), (2) disease or herbivore outbreaks (Jepsen et al. 2013; Lund et al., 2017; Post et al., 2008), (3) coastal erosion (Fritz et al., 2017) and degradation of permafrost (Grosse et al., 2016), (4) altered surface water hydrology (Nitze et al., 2017; Smith et al., 2005) and (5) increases in the frequency of fire or individual extreme fire events (Ju & Masek, 2016; Mack et al., 2011; Rocha et al., 2012). The broad variety of these changes underlines the complexity of Arctic vegetation change and re-emphasizes the need for research that identifies which of these changes will be the key processes in determining future Arctic ecosystems.

In situ *observations of tundra vegetation change*

Ground-based evidence of tundra vegetation change and its attribution to the environmental changes has been provided by *in situ* ecological monitoring (Elmendorf, Henry, Hollister, Björk, Boulanger-Lapointe, et al., 2012), experiments (Elmendorf, Henry, Hollister, Björk, Bjorkman, et al., 2012), dendroecology (Myers-Smith et al. 2015) and repeat photography (Tape et al. 2006). Together these sources highlight a complexity of changes, which encompass the following overall trends: 1) changes in plant traits, including phenology (Høye et al., 2007; Kerby & Post, 2013a; Post, Kerby, Pedersen, & Steltzer, 2016; Zeng et al., 2013) and plant height (Bjorkman et al., 2018); 2) climate sensitivity of shrub growth (Myers-Smith et al. 2015); 3) changes in community composition, particularly the expansion of woody shrubs (Myers-Smith et al., 2011; Tape, Strum, & Racine, 2006), declines of mosses, lichens and bare ground cover (Elmendorf, Henry, Hollister, Björk, Boulanger-Lapointe, et al., 2012; M. D. Walker et al., 2006) and a thermophilization of tundra plant communities (Elmendorf et al. 2015); and 4) changes in vegetation abundance and productivity (Elmendorf, Henry, Hollister, Björk, Boulanger-Lapointe, et al., 2012). Collectively, these lines of evidence have enabled the attribution of tundra vegetation change to the observed warming in biome (IPCC 2014).

What drives in situ *observations of tundra vegetation change*

The direct effects of increasing temperatures are likely the principal driver of the tundra vegetation change observed *in situ*, but a considerable amount of heterogeneity in responses among species and sites (Elmendorf, Henry, Hollister, Björk, Bjorkman, et al., 2012) highlights the importance of interactions with other

environmental factors, including (amongst others) soil moisture (Bjorkman et al., 2018; Elmendorf, Henry, Hollister, Björk, Bjorkman, et al., 2012), snow conditions (Wipf & Rixen, 2010; Bjorkman, Elmendorf, Beamish, Vellend, & Henry, 2015; Semenchuk et al., 2016), herbivory (Plante et al., 2014; Ravolainen, Bråthen, Yoccoz, Nguyen, & Ims, 2014; Väisänen et al., 2014), permafrost (Schuur et al., 2009), glacial history as well as macro- and microtopography (Lara et al., 2018; Raynolds et al., 2013). Quantifying the relative influence of the different drivers of vegetation change remains an important knowledge gap in tundra ecology.

No net trend in tundra plant phenology

Advances in phenology is one of the most well documented impacts of global climate change on the Earth's biota (Parmesan & Yohe, 2003; Cleland, Chuine, Menzel, Mooney, & Schwartz, 2007; IPCC, 2014). The direct effects of rising temperatures are generally considered to be the primary driver of phenological change (Menzel et al., 2006; Sparks & Carey, 1995) and the sensitivity of plant phenology to temperature has been demonstrated across the tundra biome (Prevéy et al., 2017). Furthermore, satellite data suggest advances in spring and, to a lesser degree, delays in autumn phenology (Zeng, Jia, & Epstein, 2011; Zeng et al., 2013; Zhao et al., 2015). Yet, *in situ* observations show no globally coherent direction in the trends of tundra spring and summer phenology (Bjorkman et al., 2015; Oberbauer et al., 2013; Post et al., 2016). This is exemplified by the International Tundra Experiment (ITEX) phenology control plot dataset, showing no net change in spring leave out and flowering phenology (Figure 1-2). While disagreement between the satellite and *in situ* trends may be partially explained by high uncertainties in satellite predictions of phenology (Beck et al., 2007; White et al., 2009), the absence of a coherent directional trend in *in situ* tundra phenology despite the rapid warming suggests that multiple environmental factors in addition to temperature may control tundra plant phenology.

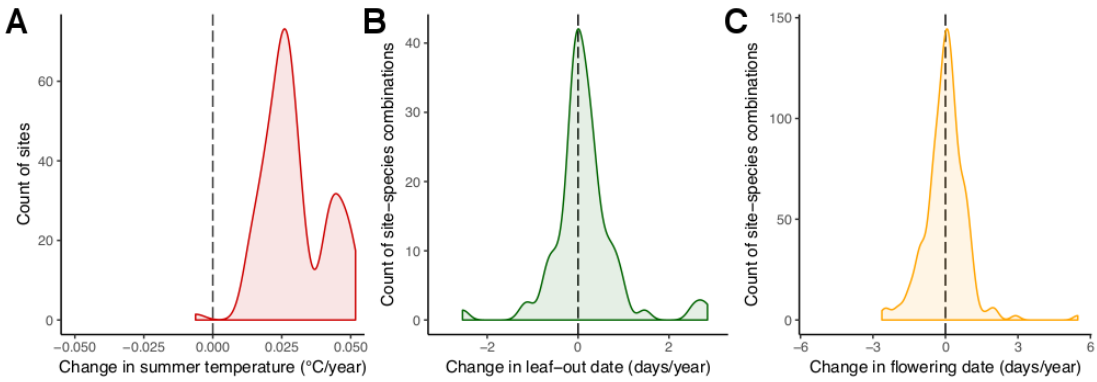

Figure 1-2 | Histograms of change in summer temperature (A), leaf-out date (B) and flowering date (C) from long-term time-series in the International Tundra Experiment's (ITEX) phenology control dataset (Prevéy et al., 2017) including observations from 19 tundra species at 9 sites for leaf-out (A) and 45 species at 18 sites for flowering (B). Reproduced with permission from Bjorkman et al. (in prep).

What environmental factors best explain tundra plant phenology?

Three environmental factors are generally considered as important drivers of tundra phenology and their interactions may be the cause of the observed absence of a directional trend across the biome. These are temperature (Bjorkman et al., 2015; Oberbauer et al., 2013; Panchen & Gorelick, 2017; Wheeler, Høye, Schmidt, Svenning, & Forchhammer, 2015), snowmelt (Bjorkman et al., 2015; Iler, Inouye, Schmidt, & Høye, 2017; Semenchuk et al., 2016) and sea-ice conditions (Kerby & Post, 2013a; Post et al., 2016). Understanding the relative importance of the key drivers of tundra plant phenology is critical for predicting future plant-consumer interactions (Doiron et al., 2015; Gustine et al., 2017; Kerby & Post, 2013b) and growing season length – which itself influences key ecosystem parameters including vegetation productivity (Ernakovich et al., 2014). Yet the relative importance of temperature, snowmelt and sea-ice conditions has not been tested in one comprehensive multi-site and multi-species analysis.

The scale gap – new methods needed!

Our ability to scale up tundra observations of vegetation productivity and phenology has been limited by discrepancies in observational scale. While the grain sizes of satellite datasets with long-term observations are coarse - ranging from 30 meters to 8 kilometres - *in situ* ecological monitoring in the tundra is logistically challenging and has been restricted to focal research sites and small plot sizes (Myers-Smith et al., 2011; Raynolds et al., 2013; Stow et al., 2004). We have therefore only developed a

limited understanding of the hierarchical structure of the ecological processes in the biome (Allen & Starr, 1982). Though great progress has been made in documenting tundra vegetation change, we need to test the correspondence of observations across local, regional and global scales to be able to scale up the complexity of tundra vegetation change and predict its feedbacks (Ernakovich et al. 2014). Only a cross-scale understanding of the changes will allow us to identify the key spatial and temporal scales at which the drivers of tundra vegetation change act and inter-act (Levin, 1992; Marceau, 1999; Turner, O'Neill, Gardner, & Milne, 1989). Recently emerging drone technologies and associated sensors have the potential to provided fine-grain data at landscape extents (Figure 1-3) that can bridge the gap between *in situ* observations and satellite records (Anderson & Gaston, 2013; Klosterman et al., 2018). However, first we need to develop new methods and standardised workflows (sensu Aasen & Bolten, 2018) that allow us to incorporate drone-derived data in to our multi-scale understanding of the tundra biome.

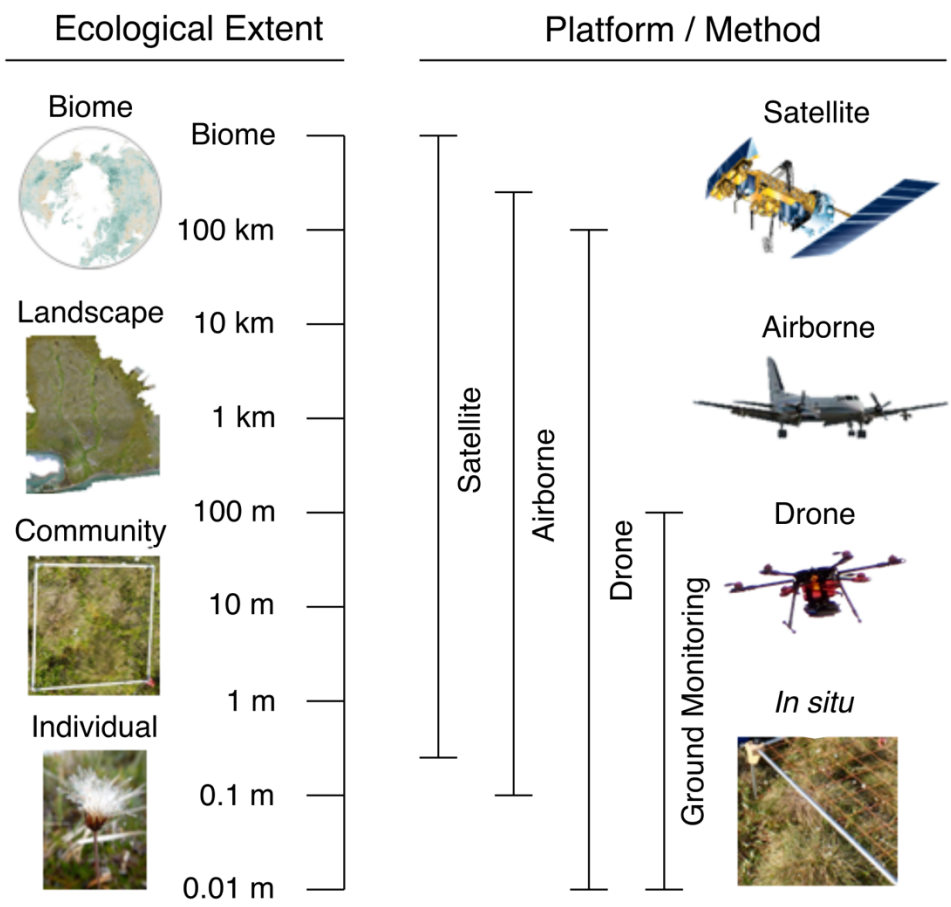

Figure 1-3 | Observational scales of satellite, manned aircraft, drone and ground-based monitoring (*in situ*) methods employed in tundra ecology. Satellites operate on large ecological extents (biome), while ground based monitoring usually only covers small ecological extents (<10 m is common in the Arctic). Even though optical satellite imagery with grain sizes finer than 10 m is available commercially, the costs can be high (Anderson and Gaston, 2013) especially when time-series analyses are conducted. Publicly available satellite imagery provided by national and international agencies such as NASA and the EU is currently limited to grain sizes ranging from tens of meters (Sentinel 2) to kilometres, exceeding the extents of ground-based monitoring. Airborne observations with conventional aircraft and drones have the potential to bridge the spatial gap between the grain sizes of publicly available satellite datasets and ground-based ("*in situ*") observations in the Arctic. However, the deployment of conventional manned aircraft can be logistically challenging and costly (Kampe et al., 2010) particularly at high latitudes where infrastructure is sparse and the weather often extreme. Recently emerging drones technologies on the other hand can be low in cost and allow for data collection at flexible temporal intervals (Anderson and Gaston, 2013). Modified from: (Cunliffe, Assmann, Kerby, & Myers-Smith, 2018)

Uncertainties in explaining satellite greening trends – drones can help

A central problem limiting our ability to understanding the heterogeneity in the greening trends (Guay et al., 2014; Reichle et al., 2018) has been the interpretation of NDVI values. Though generally associated with plant biomass and productivity in tundra ecosystems (Figure 1-4 , Blok et al., 2011; Raynolds, Walker, Epstein, Pinzon, & Tucker, 2012) the coarse grain sizes of the satellite observations likely integrates a variety of ecological processes (D. A. Walker et al., 2009) into the NDVI pixel-values through sub-pixel spectral mixing. Considerable disagreement between the major satellite platforms (Guay et al., 2014) further complicate the interpretation of high latitude greening trends. Differences in grain sizes, as well as spectral band width and position of the multispectral imaging sensors likely cause some of the disagreement in NDVI trends among these satellite products (Teillet, Staenz, & William, 1997; Guay et al., 2014). Differences in grain sizes create discrepancies between satellite products through the complexities in sub-pixel mixing of the spectral properties (Figure 1-4 A) of the diverse surfaces found in Arctic landscapes, including vegetation, soil and snow, as well as the non-linear behaviour of biomass-NDVI relationships (Figure 1-4 B, Huete et al., 2002.; Martínez-Beltrán, Jochum, Calera, & Meliá, 2009). Simple aggregations of finer grain products are therefore not directly comparable to those with larger grain sizes, unless the specific cross-product relationships have been explicitly determined for the landscape types under investigation (Martínez-Beltrán et al., 2009; Guay et al., 2014). Repeated calls for ground and cross-sensor validation of the satellite observations have therefore been made (Fraser, Olthof, Carrière, Deschamps, & Pouliot, 2011; Guay et al., 2014; Ju & Masek, 2016; Myers-Smith et al., 2011; Raynolds et al., 2013). Novel data collection methods such as drone technology can be used to facilitate such validation and test the correspondence among *in situ* monitoring and satellite datasets.

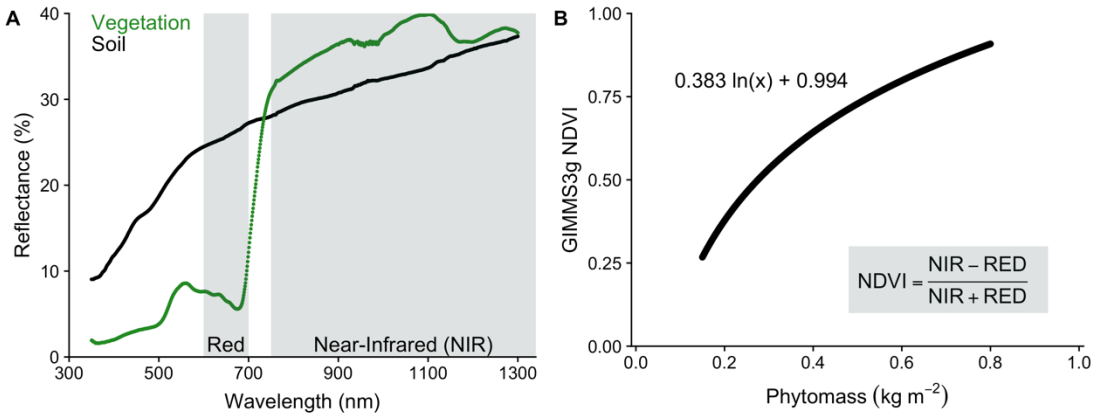

Figure 1-4 | (A) Spectral reflectance curve examples for vegetation and soil in the visible and near-infrared spectrum. Data were obtained with Spectra Vista Corporation (Poughkeepsie, NY, USA) spectroradiometers in Scotland (vegetation) and the USA (soil) and are courtesy of the NERC Field Spectroscopy Facility, Edinburgh, UK. (B) Empirical line relationship between phytomass (kg m^{-2}) and GIMMS3g NDVI for tundra vegetation determined by Raynolds et al. (2012) from above ground biomass samples collected across two latitudinal transects in the European and North American Arctic. The reflectance signature of healthy vegetation, characterised by a low reflectance in the red (absorption by chlorophyll) and high reflectance in the near-infrared (radiation by mesophyll leaf tissues), is utilised when calculating the Normalised Difference Vegetation Index (NDVI) as a proxy for plant biomass (B). Non-vegetated surfaces or unhealthy vegetation do not show this characteristic response (Campbell & Wynne, 2011), see for example the reflectance curve of soil (A). However, empirical biomass-NDVI relationships are subject to errors introduced by a complexity of factors, including atmospheric disturbance (Campbell & Wynne, 2011), and behave non-linearly due to the mathematical nature of the NDVI (B). A variety of alternative vegetation indices have been developed that account for some of these errors by including additional parts of the spectrum and the use different mathematical formulations that produce linear behaviours, but the NDVI is still frequently used due to its legacy (Campbell & Wynne, 2011). In this thesis, I only use the NDVI, as calibration errors restrained the outputs from the drone sensors to the red and near-infrared parts of the spectrum.

Implications of landscape-level phenology for trophic interactions

Spatial and temporal variation in vegetation productivity can allow plant consumers and pollinators to maximise resource availability across the landscape – to “surf” resource waves (Armstrong, Takimoto, Schindler, Hayes, & Kauffman, 2016). Plant-herbivore and -pollinator interactions may be affected through phenological mismatch and fluctuations in plant primary productivity (Berg et al., 2008) altering trophic interactions and food webs. Such mismatches could have both positive as well as negative effects on the vegetation itself. While mismatches in plant-herbivore interactions could lead to a release of grazing pressures (Miller-Rushing, Høye,

Inouye, & Post, 2010), asynchrony between plant and pollinator phenology could have determinantal effects on plant reproduction (Hegland, Nielsen, Lázaro, Bjerknes, & Totland, 2009). Evidence for phenological mismatch in the tundra has been observed for caribou (Kerby & Post, 2013b; Post et al., 2009; but see Gustine et al., 2017) and migratory birds such as snow geese (Doiron et al., 2015). However, few studies have investigated variation in tundra landscape phenology at landscape and regional scales (Kerby, 2015; Thompson & Koenig, 2018). Spatially explicit landscape-level data can be used to test the localised drivers of plant phenology and establishing scaling relationships (Klosterman et al., 2018; Klosterman & Richardson, 2017) and could be used to test the representativeness of *in situ* monitoring plots. As drone technology advances, we will be able to better link resource availability to trophic interactions and quantify mismatches as the tundra continues to warm.

Implications for climate feedbacks

Tundra vegetation change – observed on the ground or from satellites – is linked to the global climate system via positive and negative feedback mechanisms (Chapin et al., 2005; Ernakovich et al., 2014; Loranty & Goetz, 2012; Pearson et al., 2013). For example, increased plant productivity leads to increased carbon uptake in plant biomass (negative feedback), while taller vegetation lowers the surface albedo, leading to more heat to be trapped at the Earth's surface (positive feedback) (Chapin et al., 2005; Pearson et al., 2013; Swann, Fung, Levis, Bonan, & Doney, 2010). Furthermore, slow decomposition rates have turned the tundra into an important carbon reservoir on the global scale (Schuur et al., 2009) with about 50% of the world's soil carbon located in the tundra (Tarnocai et al., 2009), increased plant root activity might prime microbial activity and stimulate the release of carbon from soils and could therefore provide a potentially powerful positive feedback to global climate change (Kuzyakov, 2002; but see Lynch, Machmuller, Cotrufo, Paul, & Wallenstein, 2018). Quantifying tundra vegetation change and identifying its drivers is the first step in predicting the direction and strength of the associated feedback mechanisms and is therefore critical to improving our projections of future impacts on the biome and the Earth's system as a whole.

Aims and structure of this Thesis

Overall, this thesis aims to improve our abilities to observe and understand tundra vegetation change across space and observational scales, with a specific focus on tundra productivity and phenology. In Chapter 2, I use long-term *in situ* records of phenological observations to test which environmental factors best explain variation in spring phenology at four coastal tundra sites across the biome. In Chapter 3 I develop and test a standardised method to collect time-series of fine-grain multispectral drone imagery to study tundra productivity. In Chapter 4, I combine time-series of multispectral drone observations – acquired at my focal research site Qikiqtaruk (YT, Canada) with the methods developed in Chapter 3 - with satellite data to test for cross-platform correspondence of tundra greenness observations and to study fine-scale variation in tundra productivity across space and time (Figure 1-5). The specific research questions addressed in Chapter 2, 3 and 4 are outline below.

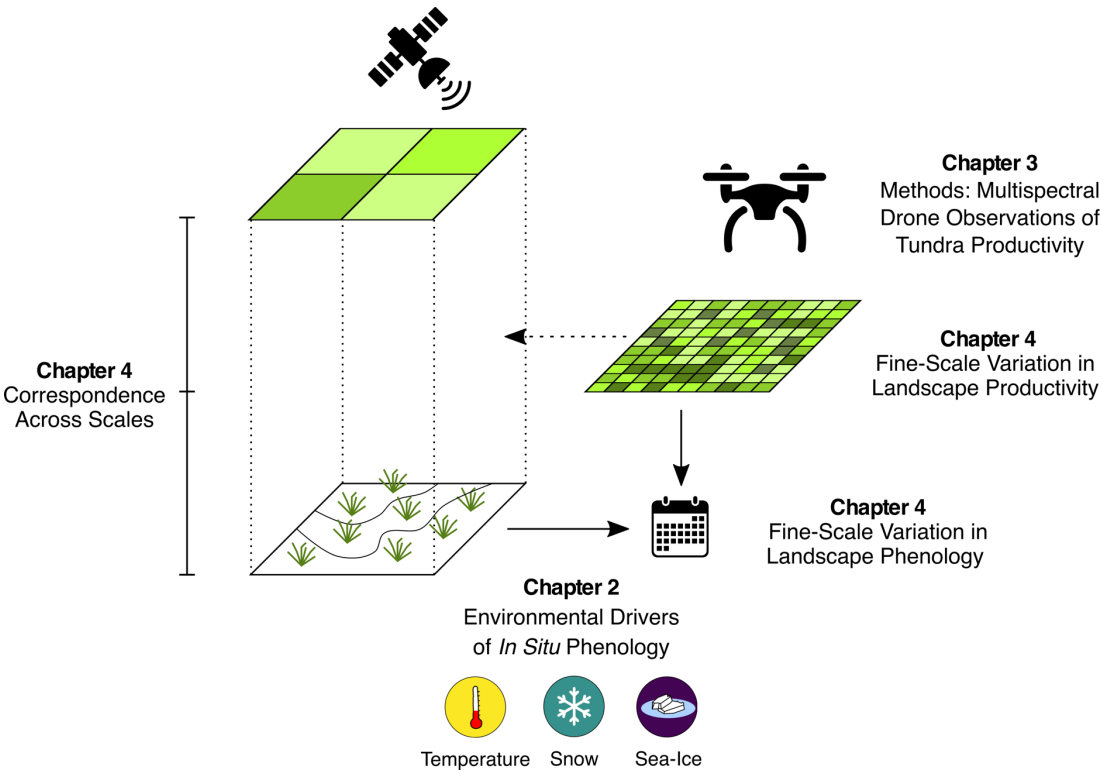

Figure 1-5 I Diagram of the thesis structure and the main research themes addressed in Chapters 2, 3 and 4. Satellite symbol by ProSymbols and drone symbol by Mike Rowe, both reproduced under a creative-commons license from the Noun Project [www.thenounproject.com].

Specific research questions addressed in Chapters 2, 3 and 4:

Chapter 2: Snow-melt and temperature – but not sea-ice – explain variation in spring phenology in coastal Arctic tundra

1) *To what extent do trends in plant spring phenology vary among coastal sites across the tundra biome?*
2) *Which environmental factors control spring flowering and green up at coastal tundra sites?*

Chapter 3: Vegetation monitoring using multispectral sensors – best practises and lessons learned from high latitudes

1) *What are the key error sources contributing to uncertainties in time-series of multispectral drone imagery of tundra vegetation?*
2) *How can these errors be best accounted for?*

Chapter 4: Drone data reveals fine-scale variation of tundra greenness and phenology not captured by satellite and *in situ* monitoring

1) *Do observations of tundra greenness correspond between drones and satellites?*
2) *How is fine-scale variation in tundra landscape greenness distributed across space?*
3) *How does landscape-level variation in tundra landscape greenness change across the growing season?*

Altogether, this PhD thesis therefore contributes to three overarching research themes:

Chapter 2: Which environmental factors best explain tundra vegetation phenology?
Chapter 3: Can novel methods improve our ability to detect and monitor tundra vegetation change across multiple scales?
Chapter 4: How does tundra vegetation productivity and phenology vary across space and time?

By addressing these questions, the research in this thesis furthers our ability to improve predictions of future tundra vegetation change, its implication for plant consumer interactions and feedbacks on global climate change.

Methods and datasets

Study Sites

This thesis contains observations from four study sites distributed across the tundra biome (Figure 1-6): Qikiqtaruk – Herschel Island (YT, Canada), Alexandra Fiord (NU, Canada), Utqiaġvik – formerly Barrow (AK, USA) and Zackenberg (Greenland). The sites cover a wide geographical range and a diversity of tundra types. The vegetation on Qikiqtaruk (138.91 W, 69.57 N) in the mid-Arctic is erect dwarf shrub tundra, while Alexandra Fiord (75.92 W, 78.88 N) on Ellesmere Island has high-Arctic tundra communities on glacio-fluvial sediment composed of mixtures of granitic and carbonate rocks, Utqiaġvik (156.62 W, 71.317 N) consists of wet meadow and heath tundra, and the Zackenberg (20.56 W, 74.47 N) site has high-Arctic tundra on noncarbonated bedrock. While *in situ* observations of phenology from all sites are included in the research of Chapter 2, Qikiqtaruk is the focal study site of Chapter 3 and 4, and is the location where I conducted two field seasons, collecting data that contributed to the analysis of the two chapters. The climate at all four sites has been warming over the last 20 years at different rates (Figure 1-7).

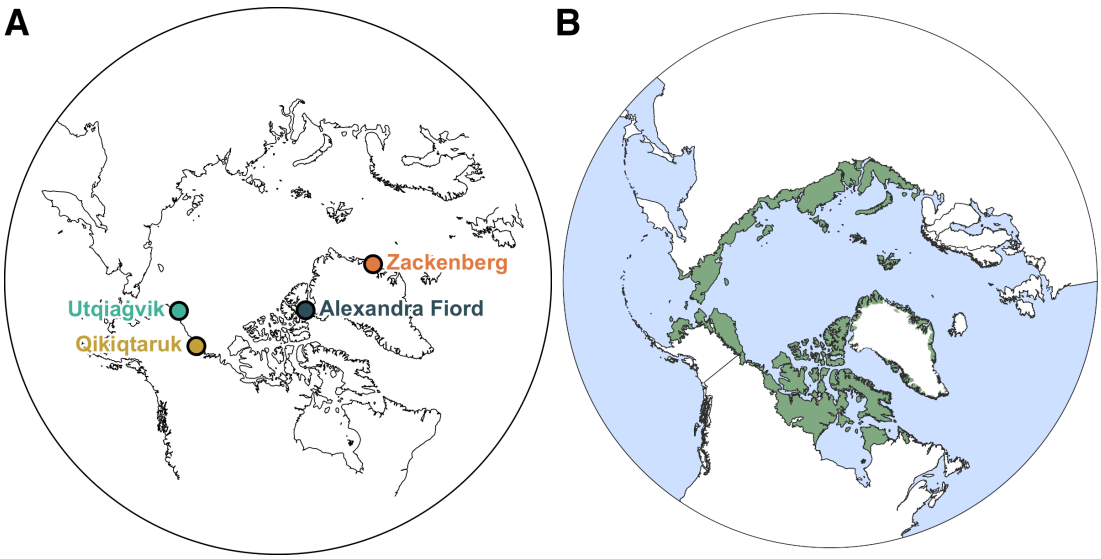

Figure 1-6 | (A) Map of the sites studied in this thesis. Including Qikiqtaruk, YT Canada; Utqiaġvik, AK, USA; Alexandra Fiord, Nunavut, Canada; and Zackenberg in Eastern Greenland. (B) Boundaries of the tundra (green) as defined by the Circumpolar Arctic Vegetation Map (CAVM, 2003).

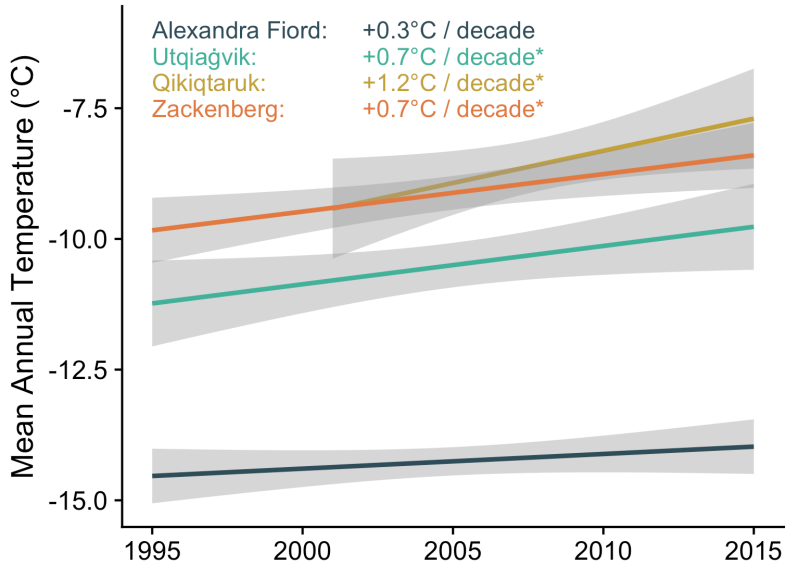

Figure 1-7 | Mean annual temperature trends for the four study sites included in this thesis: Alexandra Fiord on Ellesmere Island, NU, Canada; Utqiaġvik – formerly known as Barrow, AK, USA; Qikqitaruk – Herschel Island, YT, Canada; and Zackenberg, Greenland. Asterisk (*) indicates a statistically significant linear trend.

In situ phenology and snowmelt observations

Phenological observations for the four research sites used in Chapter 2 were obtained as a subset of the most recent version of the International Tundra Experiment (ITEX) (Henry & Molau, 1997; Webber & Walker, 1991) phenology control dataset (Prevéy et al., 2017). Snowmelt observations for the study sites are also included. The subset contained a total of 8469 of observations for 14 species and two phenological events (spring green up and flowering), resulting in a total of 24 time-series of unique site-species-phenological event combinations with an average span of 18 years. Additional data for 2016 was included for the Qikiqtaruk site and plot-level data added for the Zackenberg site. The dataset was originally compiled by Oberbauer et al. (2013) and updated by Prevéy et al. (2017) and is openly available via the Polar Data Catalogue (CCIN reference Number 12722, www.polardata.ca/pdcsearch/PDCSearchDOI.jsp?doi_id=12722).

Weather station temperature data

Temperature data for the analysis of the effect of the environmental predictor on variation in *in situ* phenological observations (Chapter 2), were obtained from publicly available weather station data at the four study sites: Environment Canada - Qikiqtaruk and Alexandra Fiord, NOAA Earth System Research Laboratory - Utqiaġvik, and Greenland Ecological Monitoring (GEM) Programme - Zackenberg. The temperature observations were cleaned and, in the case of Qikiqtaruk and Alexandra Fiord, gap filled as detailed in Chapter 2.

Sea-ice concentrations from passive-microwave satellite data

Passive-microwave satellite observations estimates of Arctic sea-ice concentrations from the US Defence Meteorological Satellite Program (DMSP) and NOAA Nimbus satellites are used to test the effect of sea-ice conditions on tundra spring phenology in Chapter 2. Pre-processed data was obtained from the NOAA/NSIDC Climate Data Record (CDR) version 3 (Meier et al., 2017; Peng, Meier, Scott, & Savoie, 2013).

Multispectral Satellite Observations

Satellite NDVI products for the tests of cross-platform correspondence of satellite and drone observations of tundra vegetation productivity at Qikiqtaruk (Chapter 4) were obtained from the following two publicly available datasets:

MODIS - MOD13Q10 version 6

NDVI values derived from 16-day composites of multispectral reflectance observations by the Moderate Resolution Imaging Spectrometer (MODIS) on the NASA Terra satellite. The data has a ground sampling distance of 250 m and has been highly pre-processed including atmospheric correction, maximum cloud free pixel selection in the 16 day composites and quality estimates (Didan, 2015). Pixel values of the study plots used in Chapter 4 were obtained through the Google Earth Engine (Gorelick et al., 2017).

Sentinel 2 MSI - L2A

Multispectral imagery from the European Union's Multispectral Imager (MSI) on the Sentinel 2 satellites at a 10 m ground sampling resolution. Images were obtained from the Copernicus Open Access Hub (https://scihub.copernicus.eu/) and processed to L2A bottom of the atmosphere reflectance products using Sen2Cor 2.4.0 (Mueller-Wilm, 2017).

Multispectral Drone Imagery

Within-growing season time-series of fine-grain multispectral drone imagery for observations of tundra greenness at Qikiqtaruk (Chapters 3 and 4) were obtained with Parrot Sequoia (Parrot, France - https://www.parrot.com) compact multispectral drone sensors mounted on light-weight multi-copter drones during the growing seasons of 2016 and 2017. In 2016, a Tarot 680 Pro (Tarot, Wenzhou, China - http://tarotrc.com) based hexa-copter was used, while the 2017 surveys were conducted using either a 3DR Iris Pro (3DR Robotics, Berkley, CA, USA - https://3dr.com/) or DJI Phantom 4 Pro (Shenzen, China - https://www.dji.com/) . Data was collected over two field seasons in 2016 and 2017, and post processed using Pix4D Desktop (Pix4D, Lausanne - https://www.pix4d.com/) to obtain surface reflectance maps from which the NDVI values were calculated.

References

Aasen, H., & Bolten, A. (2018). Multi-temporal high-resolution imaging spectroscopy with hyperspectral 2D imagers – From theory to application. *Remote Sensing of Environment*, *205*, 374–389. https://doi.org/10.1016/j.rse.2017.10.043

Allen, T. F. H., & Starr, T. B. (1982). *Hierarchy*. Chicago: Univeristy of Chicago Press.

AMAP. (2017). *Snow, Water, Ice and Permafrost. Summary for Policy-makers.* (p. 20). Oslo, Norway: Arctic Monitoring and Assessment Programme (AMAP). Retrieved from https://www.amap.no/documents/doc/Snow-Water-Ice-and-Permafrost.-Summary-for-Policy-makers/1532

Anderson, K., & Gaston, K. J. (2013). Lightweight unmanned aerial vehicles will revolutionize spatial ecology. *Frontiers in Ecology and the Environment*, *11*(3), 138–146. https://doi.org/10.1890/120150

Armstrong, J. B., Takimoto, G., Schindler, D. E., Hayes, M. M., & Kauffman, M. J. (2016). Resource waves: phenological diversity enhances foraging opportunities for mobile consumers. *Ecology*, *97*(5), 1099–1112. https://doi.org/10.1890/15-0554.1

Beck, P. S. A., Jönsson, P., Høgda, K.-A., Karlsen, S. R., Eklundh, L., & Skidmore, A. K. (2007). A ground-validated NDVI dataset for monitoring vegetation dynamics and mapping phenology in Fennoscandia and the Kola peninsula. *International Journal of Remote Sensing*, *28*(19), 4311–4330. https://doi.org/10.1080/01431160701241936

Berg, T. B., Schmidt, N. M., Høye, T. T., Aastrup, P. J., Hendrichsen, D. K., Forchhammer, M. C., & Klein, D. R. (2008). High-Arctic Plant—Herbivore Interactions under Climate Influence. In *Advances in Ecological Research* (Vol. 40, pp. 275–298). Academic Press. https://doi.org/10.1016/S0065-2504(07)00012-8

Bhatt, U. S., Walker, D. A., Raynolds, M. K., Comiso, J. C., Epstein, H. E., Jia, G., … Webber, P. J. (2010). Circumpolar Arctic Tundra Vegetation Change Is Linked to Sea Ice Decline. *Earth Interactions*, *14*(8), 1–20. https://doi.org/10.1175/2010EI315.1

Bintanja, R., & Andry, O. (2017). Towards a rain-dominated Arctic. *Nature Climate Change*, *7*(4), 263–267. https://doi.org/10.1038/nclimate3240

Bjorkman, A. D., Elmendorf, S. C., Beamish, A. L., Vellend, M., & Henry, G. H. R. (2015). Contrasting effects of warming and increased snowfall on Arctic tundra plant phenology over the past two decades. *Global Change Biology*, *21*, 4651–4661. https://doi.org/10.1111/gcb.13051

Bjerke, J. W., Karlsen, S. R., Høgda, K. A., Malnes, E., Jepsen, J. U,, Lovibond, S., … Tømmervik, H. (2014). Record-Low Primary Productivity and High Plant

Damage in the Nordic Arctic Region in 2012 Caused by Multiple Weather Events and Pest Outbreaks. *Environmental Research Letters, 9*(8): 084006. https://doi.org/10.1088/1748-9326/9/8/084006.

Bjorkman, A. D., Myers-Smith, I. H., Elmendorf, S. C., Normand, S., Rüger, N., Beck, P. S. A., … Weiher, E. (2018). Plant functional trait change across a warming tundra biome. *Nature*, *562*(7725), 57–62. https://doi.org/10.1038/s41586-018-0563-7

Blok, D., Schaepman-Strub, G., Bartholomeus, H., Heijmans, M. M. P. D., Maximov, T. C., & Frank Berendse. (2011). The response of Arctic vegetation to the summer climate: relation between shrub cover, NDVI, surface albedo and temperature. *Environmental Research Letters*, *6*(3), 035502. https://doi.org/10.1088/1748-9326/6/3/035502

Bokhorst, S., Bjerke J. W., Bowles F. W., Melillo J., Callaghan T. V., & Phoenix G. K. (2008). Impacts of Extreme Winter Warming in the Sub-Arctic: Growing Season Responses of Dwarf Shrub Heathland. *Global Change Biology, 14*(11), 2603–12. https://doi.org/10.1111/j.1365-2486.2008.01689.x.

Bokhorst, S. F., Bjerke, J. W., Tømmervik, H., Callaghan, T. V., & Phoenix, G. K. (2009). Winter Warming Events Damage Sub-Arctic Vegetation: Consistent Evidence from an Experimental Manipulation and a Natural Event. *Journal of Ecology 97*(6), 1408–15. https://doi.org/10.1111/j.1365-2745.2009.01554.x.

Callaghan, T. V., Lars Olof Björn, F. Stuart Chapin III, Yuri Chernov, Torben R. Christensen, Brian Huntley, … Gus Shaver. (2005). Chapter 7 - Arctic Tundra and Polar Desert Ecosystems. In *Arctic Climate Impact Assessment* (pp. 243–352). Cambridge: Cambridge University Press.

Campbell, J. B., & Wynne, R. H. Introduction to Remote Sensing, Fifth Edition. New York, USA: Guilford Publications, 2011.

CAVM. (2003). Circumpolar Arctic Vegetation Map. Anchorage, Alaska: U.S. Fish and Wildlife Service.

Chapin, F. S., Sturm, M., Serreze, M. C., McFadden, J. P., Key, J. R., Lloyd, A. H., … Welker, J. M. (2005). Role of Land-Surface Changes in Arctic Summer Warming. *Science*, *310*(5748), 657–660. https://doi.org/10.1126/science.1117368

Cleland, E. E., Chuine, I., Menzel, A., Mooney, H. A., & Schwartz, M. D. (2007). Shifting plant phenology in response to global change. *Trends in Ecology & Evolution*, *22*(7), 357–365. https://doi.org/10.1016/j.tree.2007.04.003

Cunliffe, A. M., Assmann, J. J., Kerby, J. T., & Myers-Smith, I. H. (2018). Drone-based monitoring for studying patterns and processes of tundra vegetation change. *Manuscript in Preparation*.

Didan, K. (2015). MOD13Q1 MODIS/Terra Vegetation Indices 16-Day L3 Global 250m SIN Grid V006. NASA EOSDIS Land Processes DAAC. Retrieved from doi: 10.5067/MODIS/MOD13Q1.006

Doiron, M., Gauthier, G., & Lévesque, E. (2015). Trophic mismatch and its effects on the growth of young in an Arctic herbivore. *Global Change Biology*, *21*(12), 4364–4376. https://doi.org/10.1111/gcb.13057

Elmendorf, S. C., Henry, G. H. R., Hollister, R. D., Björk, R. G., Bjorkman, A. D., Callaghan, T. V., … Wookey, P. A. (2012). Global assessment of experimental climate warming on tundra vegetation: heterogeneity over space and time. *Ecology Letters*, *15*(2), 164–175. https://doi.org/10.1111/j.1461-0248.2011.01716.x

Elmendorf, S. C., Henry, G. H. R., Hollister, R. D., Björk, R. G., Boulanger-Lapointe, N., Cooper, E. J., … Wipf, S. (2012). Plot-scale evidence of tundra vegetation change and links to recent summer warming. *Nature Climate Change*, *2*(6), 453–457. https://doi.org/10.1038/nclimate1465

Elmendorf, S. C., Henry, G. H. R., Hollister, R. D., Fosaa, A. M., Gould, W. A., Hermanutz, L., … Walker, M. (2015). Experiment, monitoring, and gradient methods used to infer climate change effects on plant communities yield consistent patterns. *Proceedings of the National Academy of Sciences*, *112*(2), 448–452. https://doi.org/10.1073/pnas.1410088112

Ernakovich, J. G., Hopping, K. A., Berdanier, A. B., Simpson, R. T., Kachergis, E. J., Steltzer, H., & Wallenstein, M. D. (2014). Predicted responses of arctic and alpine ecosystems to altered seasonality under climate change. *Global Change Biology*, *20*(10), 3256–3269. https://doi.org/10.1111/gcb.12568

Fetterer, F., K. Knowles, W. Meier, M. Savoie, & Windnagel, A. K. (2017). *Sea Ice Index, Version 3*. Monthly Sea Ice Extent. Boulder, Colorado USA. NSIDC: National Snow and Ice Data Center. https://doi.org/10.7265/N5K072F8.

Fritz, M., Vonk, J. E., & Lantuit, H. (2017). Collapsing Arctic coastlines. *Nature Climate Change*, *7*, 6–7. https://doi.org/10.1038/nclimate3188

Fraser, R. H., Olthof, I., Carrière, M., Deschamps, A., & Pouliot, D. (2011). Detecting long-term changes to vegetation in northern Canada using the Landsat satellite image archive. *Environmental Research Letters*, *6*(4), 045502. https://doi.org/10.1088/1748-9326/6/4/045502

Gorelick, N., Hancher, M., Dixon, M., Ilyushchenko, S., Thau, D., & Moore, R. (2017). Google Earth Engine: Planetary-scale geospatial analysis for everyone. *Remote Sensing of Environment*, *202*, 18–27. https://doi.org/10.1016/j.rse.2017.06.031

Grosse, G., Goetz, S., McGuire, A. D., Romanovsky, V. E., & Schuur, E. A. G. (2016). Changing permafrost in a warming world and feedbacks to the Earth system. *Environmental Research Letters*, *11*(4), 040201. https://doi.org/10.1088/1748-9326/11/4/040201

Guay, K. C., Beck, P. S. A., Berner, L. T., Goetz, S. J., Baccini, A., & Buermann, W. (2014). Vegetation productivity patterns at high northern latitudes: a multi-sensor satellite data assessment. *Global Change Biology*, *20*(10), 3147–3158. https://doi.org/10.1111/gcb.12647

Gustine, D., Barboza, P., Adams, L., Griffith, B., Cameron, R., & Whitten, K. (2017). Advancing the match-mismatch framework for large herbivores in the Arctic: Evaluating the evidence for a trophic mismatch in caribou. *PLOS ONE*, *12*(2), e0171807. https://doi.org/10.1371/journal.pone.0171807

Hegland, S. J., Nielsen, A., Lázaro, A., Bjerknes, A.-L., & Totland, Ø. (2009). How does climate warming affect plant-pollinator interactions? *Ecology Letters*, *12*(2), 184–195. https://doi.org/10.1111/j.1461-0248.2008.01269.x

Helman, D. (2018). Land Surface Phenology: What Do We Really "See" from Space?. *Science of The Total Environment*, *618*, 665–73. https://doi.org/10.1016/j.scitotenv.2017.07.237.

Henry, G. H. R., & Molau, U. (1997). Tundra plants and climate change: the International Tundra Experiment (ITEX). *Global Change Biology*, *3*(S1), 1–9. https://doi.org/10.1111/j.1365-2486.1997.gcb132.x

Høye, T. T., Post, E., Meltofte, H., Schmidt, N. M., & Forchhammer, M. C. (2007). Rapid advancement of spring in the High Arctic. *Current Biology*, *17*(12), R449–R451. https://doi.org/10.1016/j.cub.2007.04.047

Hudson, J. M. G., & Henry, G. H. R. (2009). Increased Plant Biomass in a High Arctic Heath Community from 1981 to 2008. *Ecology 90*(10), 2657–63. https://doi.org/10.1890/09-0102.1.

Huete, A., Didan, K., Miura, T., Rodriguez, E. P., Gao, X., & Ferreira, L. G. (2002). Overview of the radiometric and biophysical performance of the MODIS vegetation indices. *Remote Sensing of Environment*, *83*(1), 195–213. https://doi.org/10.1016/S0034-4257(02)00096-2

Iler, A. M., Inouye, D. W., Schmidt, N. M., & Høye, T. T. (2017). Detrending phenological time series improves climate–phenology analyses and reveals evidence of plasticity. *Ecology*, *98*(3), 647–655.

IPCC. (2014). *Climate change 2014: Synthesis Report. Contribution of Working Groups I, II and III to the Fifth Assessment Report of the Intergovernmental Panel on Climate Change*. (R. K. Pachauri & L. Mayer, Eds.). Geneva, Switzerland: IPCC.

Ju, J., & Masek, J. G. (2016). The vegetation greenness trend in Canada and US Alaska from 1984–2012 Landsat data. *Remote Sensing of Environment*, *176*, 1–16. https://doi.org/10.1016/j.rse.2016.01.001

Jepsen, J. U., Biuw, M., Ims, R. A., Kapari, L., Schott, T., Vindstad, O. P. L., & Hagen, S. B. (2013). Ecosystem Impacts of a Range Expanding Forest Defoliator at the Forest-Tundra Ecotone. *Ecosystems*, *16*(4), 561–575. https://doi.org/10.1007/s10021-012-9629-9

Jones, P.D., Lister, D.H., Osborn, T.J., Harpham, C., Salmon, M., & Morice, C.P. (2012) Hemispheric and large-scale land surface air temperature variations: an extensive revision and an update to 2010. *Journal of Geophysical Research,* 117, D05127. http://doi:10.1029/2011JD017139.

Keenan, T. F., & Riley, W. J. (2018). Greening of the land surface in the world's cold regions consistent with recent warming. *Nature Climate Change*, 1. https://doi.org/10.1038/s41558-018-0258-y

Kerby, J. T. (2015). Phenology in a chancing Arctic: Linking trophic interactions across scales. Retrieved from https://etda.libraries.psu.edu/catalog/26992

Kerby, J. T., & Post, E. (2013a). Advancing plant phenology and reduced herbivore production in a terrestrial system associated with sea ice decline. *Nature Communications*, *4*. https://doi.org/10.1038/ncomms3514

Kerby, J. T., & Post, E. (2013b). Capital and income breeding traits differentiate trophic match–mismatch dynamics in large herbivores. *Philosophical Transactions of the Royal Society of London B: Biological Sciences*, *368*(1624), 20120484. https://doi.org/10.1098/rstb.2012.0484

Klosterman, S. T., Melaas, E., Wang, J., Martinez, A., Frederick, S., O'Keefe, J., … Richardson, A. D. (2018). Fine-scale perspectives on landscape phenology from unmanned aerial vehicle (UAV) photography. *Agricultural and Forest Meteorology*, *248*, 397–407. https://doi.org/10.1016/j.agrformet.2017.10.015

Klosterman, S. T., & Richardson, A. D. (2017). Observing Spring and Fall Phenology in a Deciduous Forest with Aerial Drone Imagery. *Sensors*, *17*(12), 2852. https://doi.org/10.3390/s17122852

Kuzyakov, Y. (2002). Review: Factors affecting rhizosphere priming effects. *Journal of Plant Nutrition and Soil Science*, *165*(4), 382–396. https://doi.org/10.1002/1522-2624(200208)165:4<382::AID-JPLN382>3.0.CO;2-#

Lara, M. J., Nitze, I., Grosse, G., Martin, P., & McGuire, A. D. (2018). Reduced arctic tundra productivity linked with landform and climate change interactions. *Scientific Reports*, *8*(1), 2345. https://doi.org/10.1038/s41598-018-20692-8

Levin, S. A. (1992). The Problem of Pattern and Scale in Ecology: The Robert H. MacArthur Award Lecture. *Ecology*, *73*(6), 1943–1967. https://doi.org/10.2307/1941447

Loranty, M. M., Davydov, S., Kropp, H., Alexander, H., Mack, M., Natali, S., … Zimov, N. S. (2018). Vegetation Indices Do Not Capture Forest Cover Variation in Upland Siberian Larch Forests. *Remote Sensing*, *10*(11), 1686. https://doi.org/10.3390/rs10111686

Loranty, M. M., & Goetz, S. J. (2012). Shrub expansion and climate feedbacks in Arctic tundra. *Environmental Research Letters*, *7*(1), 011005. https://doi.org/10.1088/1748-9326/7/1/011005

Lund, M., Raundrup, K., Westergaard-Nielsen, A., López-Blanco, E., Nymand, J., & Aastrup, P. (2017). Larval outbreaks in West Greenland: Instant and subsequent effects on tundra ecosystem productivity and CO2 exchange. *Ambio*, *46*(1), 26–38. https://doi.org/10.1007/s13280-016-0863-9

Lynch, L. M., Machmuller, M. B., Cotrufo, M. F., Paul, E. A., & Wallenstein, M. D. (2018). Tracking the fate of fresh carbon in the Arctic tundra: Will shrub expansion alter responses of soil organic matter to warming? *Soil Biology and Biochemistry*, *120*, 134–144. https://doi.org/10.1016/j.soilbio.2018.02.002

Macias-Fauria, M., Karlsen, S. R., & Forbes, B. C. (2017). Disentangling the coupling between sea ice and tundra productivity in Svalbard. *Scientific Reports*, *7*(1), 8586. https://doi.org/10.1038/s41598-017-06218-8

Macias-Fauria, M., & Post, E. (2018). Effects of sea ice on Arctic biota: an emerging crisis discipline. *Biology Letters*, *14*(3), 20170702. https://doi.org/10.1098/rsbl.2017.0702

Mack, M. C., Schuur, E. A. G., Bret-Harte, M. S., Shaver, G. R., & Chapin Iii, F. S. (2004). Ecosystem carbon storage in arctic tundra reduced by long-term nutrient fertilization. *Nature*, *431*(7007), 440–443. https://doi.org/10.1038/nature02887

Mack, M. C., Bret-Harte, M. S., Hollingsworth, T. N., Jandt, R. R., Schuur, E. A. G., Shaver, G. R., & Verbyla, D. L. (2011). Carbon loss from an unprecedented Arctic tundra wildfire. *Nature*, *475*(7357), 489–492. https://doi.org/10.1038/nature10283

Marceau, D. J. (1999). The Scale Issue in the Social and Natural Sciences. *Canadian Journal of Remote Sensing*, *25*(4), 347–356. https://doi.org/10.1080/07038992.1999.10874734

Martínez-Beltrán, C., Jochum, M. A. O., Calera, A., & Meliá, J. (2009). Multisensor comparison of NDVI for a semi-arid environment in Spain. *International Journal of Remote Sensing*, *30*(5), 1355–1384. https://doi.org/10.1080/01431160802509025

McGuire, A. D., III, F. S. C., Walsh, J. E., & Wirth, C. (2006). Integrated Regional Changes in Arctic Climate Feedbacks: Implications for the Global Climate System. *Annual Review of Environment and Resources*, *31*(1), 61–91. https://doi.org/10.1146/annurev.energy.31.020105.100253

Meier, W. N., Fetterer, F., Savoie, M., Mallory, S., Duerr, R., & Stroeve, J. (2017). *NOAA/NSIDC Climate Data Record of Passive Microwave Sea Ice Concentration, Version 3. NOAA/NSIDC daily sea Ice CDR.* Boulder, Colorado USA: NSIDC: National Snow and Ice Data Center. Retrieved from https://doi.org/10.7265/N59P2ZTG

Menzel, A., Sparks, T. H., Estrella, N., Koch, E., Aasa, A., Ahas, R., … Zust, A. (2006). European phenological response to climate change matches the warming pattern. *Global Change Biology*, *12*(10), 1969–1976. https://doi.org/10.1111/j.1365-2486.2006.01193.x

Miles, V. V., & Esau, I. (2016). Spatial heterogeneity of greening and browning between and within bioclimatic zones in northern West Siberia.

Environmental Research Letters, *11*(11), 115002. https://doi.org/10.1088/1748-9326/11/11/115002

Miller-Rushing, A. J., Høye, T. T., Inouye, D. W., & Post, E. (2010). The effects of phenological mismatches on demography. *Philosophical Transactions of the Royal Society B: Biological Sciences*, *365*(1555), 3177–3186. https://doi.org/10.1098/rstb.2010.0148

Mueller-Wilm, U. (2017, January 7). Sen2Cor Software Release Note: Ref.: S2-PDGS-MPC-L2A-SRN-V2.4.0. Retrieved from http://step.esa.int/thirdparties/sen2cor/2.4.0/Sen2Cor_240_Documenation_PDF/S2-PDGS-MPC-L2A-SRN-V2.4.0.pdf

Myers-Smith, I. H., Elmendorf, S. C., Beck, P. S. A., Wilmking, M., Hallinger, M., Blok, D., … Vellend, M. (2015). Climate sensitivity of shrub growth across the tundra biome. *Nature Climate Change*, *5*(9), 887–891. https://doi.org/10.1038/nclimate2697

Myers-Smith, I. H., Forbes, B. C., Wilmking, M., Hallinger, M., Lantz, T., Blok, D., … Hik, D. S. (2011). Shrub expansion in tundra ecosystems: dynamics, impacts and research priorities. *Environmental Research Letters*, *6*(4), 045509. https://doi.org/10.1088/1748-9326/6/4/045509

Myers-Smith, I. H., Kerby, J. T., Phoenix, G. K., Bjerke, J. W., Epstein, H. E., Assmann, J. J., … Blok, D. (2019). Complexity revealed in the “greening of the Arctic” - satellite-observations and associated vegetation dynamics. *Manuscript in Preparation*.

Myneni, R. B., Keeling, C. D., Tucker, C. J., Asrar, G., & Nemani, R. R. (1997). Increased plant growth in the northern high latitudes from 1981 to 1991. *Nature*, *386*(6626), 698–702. https://doi.org/10.1038/386698a0

Natali, S. M., Schuur, E. A. G., & Rubin, R. L. (2012). Increased plant productivity in Alaskan tundra as a result of experimental warming of soil and permafrost. *Journal of Ecology*, *100*(2), 488–498. https://doi.org/10.1111/j.1365-2745.2011.01925.x

Nitze, I., Grosse, G., Jones, B. M., Arp, C. D., Ulrich, M., Fedorov, A., & Veremeeva, A. (2017). Landsat-Based Trend Analysis of Lake Dynamics across Northern Permafrost Regions. *Remote Sensing*, *9*(7), 640. https://doi.org/10.3390/rs9070640

Oberbauer, S. F., Elmendorf, S. C., Troxler, T. G., Hollister, R. D., Rocha, A. V., Bret-Harte, M. S., … Welker, J. M. (2013). Phenological response of tundra plants to background climate variation tested using the International Tundra Experiment. *Philosophical Transactions of the Royal Society of London B: Biological Sciences*, *368*(1624), 20120481. https://doi.org/10.1098/rstb.2012.0481

Panchen, Z. A., & Gorelick, R. (2017). Prediction of Arctic plant phenological sensitivity to climate change from historical records. *Ecology and Evolution*, *7*(5), 1325–1338. https://doi.org/10.1002/ece3.2702

Parmesan, C., & Yohe, G. (2003). A globally coherent fingerprint of climate change impacts across natural systems. *Nature*, *421*(6918), 37–42. https://doi.org/10.1038/nature01286

Pearson, R. G., Phillips, S. J., Loranty, M. M., Beck, P. S. A., Damoulas, T., Knight, S. J., & Goetz, S. J. (2013). Shifts in Arctic vegetation and associated feedbacks under climate change. *Nature Climate Change*, *3*(7), 673–677. https://doi.org/10.1038/nclimate1858

Peng, G., Meier, W. N., Scott, D. J., & Savoie, M. H. (2013). A long-term and reproducible passive microwave sea ice concentration data record for climate studies and monitoring. *Earth System Science Data*, *5*(2), 311–318. https://doi.org/10.5194/essd-5-311-2013

Plante, S., Champagne, E., Ropars, P., Boudreau, S., Lévesque, E., Tremblay, B., & Tremblay, J.-P. (2014). Shrub cover in northern Nunavik: can herbivores limit shrub expansion? *Polar Biology*, *37*(5), 611–619. https://doi.org/10.1007/s00300-014-1461-6

Post, E., Pedersen, C., Wilmers, C. C., & Forchhammer, M. C. (2008). Warming, plant phenology and the spatial dimension of trophic mismatch for large herbivores. *Proceedings of the Royal Society of London B: Biological Sciences*, *275*(1646), 2005–2013. https://doi.org/10.1098/rspb.2008.0463

Post, E., Forchhammer, M. C., Bret-Harte, M. S., Callaghan, T. V., Christensen, T. R., Elberling, B., … Aastrup, P. (2009). Ecological Dynamics Across the Arctic Associated with Recent Climate Change. *Science*, *325*(5946), 1355–1358. https://doi.org/10.1126/science.1173113

Post, E., Kerby, J. T., Pedersen, C., & Steltzer, H. (2016). Highly individualistic rates of plant phenological advance associated with arctic sea ice dynamics. *Biology Letters*, *12*(12), 20160332. https://doi.org/10.1098/rsbl.2016.0332

Prevéy, J., Vellend, M., Rüger, N., Hollister, R. D., Bjorkman, A. D., Myers-Smith, I. H., … Rixen, C. (2017). Greater temperature sensitivity of plant phenology at colder sites: implications for convergence across northern latitudes. *Global Change Biology*, *23*(7), 2660–2671. https://doi.org/10.1111/gcb.13619

Ravolainen, V. T., Bråthen, K. A., Yoccoz, N. G., Nguyen, J. K., & Ims, R. A. (2014). Complementary impacts of small rodents and semi-domesticated ungulates limit tall shrub expansion in the tundra. *Journal of Applied Ecology*, *51*(1), 234–241. https://doi.org/10.1111/1365-2664.12180

Raynolds, M. K., Walker, D. A., Epstein, H. E., Pinzon, J. E., & Tucker, C. J. (2012). A new estimate of tundra-biome phytomass from trans-Arctic field data and AVHRR NDVI. *Remote Sensing Letters*, *3*(5), 403–411. https://doi.org/10.1080/01431161.2011.609188

Raynolds, M. K., Walker, D. A., Verbyla, D., & Munger, C. A. (2013). Patterns of Change within a Tundra Landscape: 22-year Landsat NDVI Trends in an Area of the Northern Foothills of the Brooks Range, Alaska. *Arctic, Antarctic,*

and Alpine Research, *45*(2), 249–260. https://doi.org/10.1657/1938-4246-45.2.249

Reichle, L. M., Epstein, H. E., Bhatt, U. S., Raynolds, M. K., & Walker, D. A. (2018). Spatial Heterogeneity of the Temporal Dynamics of Arctic Tundra Vegetation. *Geophysical Research Letters*. https://doi.org/10.1029/2018GL078820

Richardson, A. D., Hufkens, K., Milliman, T., Aubrecht, D. M., Chen, M., Gray, J. M., … Frolking, S. (2018). Tracking vegetation phenology across diverse North American biomes using PhenoCam imagery. *Scientific Data*, *5*, 180028. https://doi.org/10.1038/sdata.2018.28

Rocha, A. V., Loranty, M. M., Higuera, P. E., Mack, M. C., Hu, F. S., Jones, B. M., … Shaver, G. R. (2012). The footprint of Alaskan tundra fires during the past half-century: implications for surface properties and radiative forcing. *Environmental Research Letters*, *7*(4), 044039. https://doi.org/10.1088/1748-9326/7/4/044039

Schuur, E. A. G., Vogel, J. G., Crummer, K. G., Lee, H., Sickman, J. O., & Osterkamp, T. E. (2009). The effect of permafrost thaw on old carbon release and net carbon exchange from tundra. *Nature*, *459*(7246), 556–559. https://doi.org/10.1038/nature08031

Semenchuk, P. R., Gillespie, M. A. K., Rumpf, S. B., Baggesen, N., Elberling, B., & Cooper, E. J. (2016). High Arctic plant phenology is determined by snowmelt patterns but duration of phenological periods is fixed: an example of periodicity. *Environmental Research Letters*, *11*(12), 125006. https://doi.org/10.1088/1748-9326/11/12/125006

Serreze, M. C., & Barry, R. G. (2011). Processes and impacts of Arctic amplification: A research synthesis. *Global and Planetary Change*, *77*(1–2), 85–96. https://doi.org/10.1016/j.gloplacha.2011.03.004

Smith, L. C., Sheng, Y., MacDonald, G. M., & Hinzman, L. D. (2005). Disappearing Arctic Lakes. *Science*, *308*(5727), 1429–1429. https://doi.org/10.1126/science.1108142

Sparks, T. H., & Carey, P. D. (1995). The Responses of Species to Climate Over Two Centuries: An Analysis of the Marsham Phenological Record, 1736-1947. *Journal of Ecology*, *83*(2), 321–329. https://doi.org/10.2307/2261570

Steltzer, H. & Post, E. (2009). Seasons and Life Cycles. *Science, 324*(5929), 886–87. https://doi.org/10.1126/science.1171542.

Stow, D. A., Hope, A., McGuire, D., Verbyla, D., Gamon, J., Huemmrich, F., … Myneni, R. (2004). Remote sensing of vegetation and land-cover change in Arctic Tundra Ecosystems. *Remote Sensing of Environment*, *89*(3), 281–308. https://doi.org/10.1016/j.rse.2003.10.018

Swann, A. L., Fung, I. Y., Levis, S., Bonan, G. B., & Doney, S. C. (2010). Changes in Arctic vegetation amplify high-latitude warming through the greenhouse

effect. *Proceedings of the National Academy of Sciences*, *107*(4), 1295–1300. https://doi.org/10.1073/pnas.0913846107

Tape, K. D., Strum, & Racine, C. H. (2006). The evidence for shrub expansion in Northern Alaska and the Pan-Arctic. Glob. Change Biol. 12, 686–702 (2006). *Global Change Biology*, *12*, 686–702.

Tarnocai, C., Canadell, J. G., Schuur, E. a. G., Kuhry, P., Mazhitova, G., & Zimov, S. (2009). Soil organic carbon pools in the northern circumpolar permafrost region. *Global Biogeochemical Cycles*, *23*(2), GB2023. https://doi.org/10.1029/2008GB003327

Teillet, P. M., Staenz, K., & William, D. J. (1997). Effects of spectral, spatial, and radiometric characteristics on remote sensing vegetation indices of forested regions. *Remote Sensing of Environment*, *61*(1), 139–149. https://doi.org/10.1016/S0034-4257(96)00248-9

Thompson, J. A., & Koenig, L. S. (2018). Vegetation phenology in Greenland and links to cryospheric change. *Annals of Glaciology*, 1–10. https://doi.org/10.1017/aog.2018.24

Tucker, C. J. (1979). Red and photographic infrared linear combinations for monitoring vegetation. *Remote Sensing of Environment*, *8*(2), 127–150. https://doi.org/10.1016/0034-4257(79)90013-0

Tucker, C. J., Slayback, D. A., Pinzon, J. E., Los, S. O., Myneni, R. B., & Taylor, M. G. (2001). Higher northern latitude normalized difference vegetation index and growing season trends from 1982 to 1999. *International Journal of Biometeorology*, *45*(4), 184–190. https://doi.org/10.1007/s00484-001-0109-8

Turner, M. G., O'Neill, R. V., Gardner, R. H., & Milne, B. T. (1989). Effects of changing spatial scale on the analysis of landscape pattern. *Landscape Ecology*, *3*(3), 153–162. https://doi.org/10.1007/BF00131534

Väisänen, M., Ylänne, H., Kaarlejärvi, E., Sjögersten, S., Olofsson, J., Crout, N., & Stark, S. (2014). Consequences of warming on tundra carbon balance determined by reindeer grazing history. *Nature Climate Change*, *4*(5), 384–388. https://doi.org/10.1038/nclimate2147

Walker, D. A., Leibman, M. O., Epstein, H. E., Forbes, B. C., Bhatt, U. S., Raynolds, M. K., … Yu, Q. (2009). Spatial and temporal patterns of greenness on the Yamal Peninsula, Russia: interactions of ecological and social factors affecting the Arctic normalized difference vegetation index. *Environmental Research Letters*, *4*(4), 045004. https://doi.org/10.1088/1748-9326/4/4/045004

Walker, M. D., Wahren, C. H., Hollister, R. D., Henry, G. H. R., Ahlquist, L. E., Alatalo, J. M., … Wookey, P. A. (2006). Plant community responses to experimental warming across the tundra biome. *Proceedings of the National Academy of Sciences*, *103*(5), 1342–1346. https://doi.org/10.1073/pnas.0503198103

Webber, P. J., & Walker, M. D. (1991). The International Tundra Experiment (ITEX): resolution. *Arctic Antarctic and Alpine Research*, *23*, 124.

Wheeler, H. C., Høye, T. T., Schmidt, N. M., Svenning, J.-C., & Forchhammer, M. C. (2015). Phenological mismatch with abiotic conditions—implications for flowering in Arctic plants. *Ecology*, *96*(3), 775–787. https://doi.org/10.1890/14-0338.1

White, M. A., De BEURS, K. M., Didan, K., Inouye, D. W., Richardson, A. D., Jensen, O. P., … Lauenroth, W. K. (2009). Intercomparison, interpretation, and assessment of spring phenology in North America estimated from remote sensing for 1982–2006. *Global Change Biology*, *15*(10), 2335–2359. https://doi.org/10.1111/j.1365-2486.2009.01910.x

Wipf, S., & Rixen, C. (2010). A review of snow manipulation experiments in Arctic and alpine tundra ecosystems. *Polar Research*, *29*(1), 95–109. https://doi.org/10.1111/j.1751-8369.2010.00153.x

Zeng, H., Jia, G., & Epstein, H. (2011). Recent changes in phenology over the northern high latitudes detected from multi-satellite data. *Environmental Research Letters*, *6*(4), 045508. https://doi.org/10.1088/1748-9326/6/4/045508

Zeng, H., Jia, G., & Forbes, B. C. (2013). Shifts in Arctic phenology in response to climate and anthropogenic factors as detected from multiple satellite time series. *Environmental Research Letters*, *8*(3), 035036. https://doi.org/10.1088/1748-9326/8/3/035036

Zhao, J., Zhang, H., Zhang, Z., Guo, X., Li, X., & Chen, C. (2015). Spatial and Temporal Changes in Vegetation Phenology at Middle and High Latitudes of the Northern Hemisphere over the Past Three Decades. *Remote Sensing*, *7*(8), 10973–10995. https://doi.org/10.3390/rs70810973

Chapter 2 Snow-melt and temperature – but not sea-ice – explain variation in spring phenology in coastal Arctic tundra

The end of winter on Qikiqtaruk: snow, sea-ice and cold temperatures.

Chapter 2 Snow-melt and temperature – but not sea-ice – explain variation in spring phenology in coastal Arctic tundra

The following chapter has been submitted to Global Change Biology as a primary research article. At the time of submission of this thesis, the article had received the assessment of major revisions (decision letter 6th November 2018).

Authors: Jakob J. Assmann[1*], Isla H. Myers-Smith[1], Albert B. Phillimore[1], Anne D. Bjorkman[2], Richard E. Ennos[1], Janet S. Prevéy[3], Greg H.R. Henry[4], Niels M. Schmidt[5], Robert D. Hollister[6]

Affiliations:
[1] The University of Edinburgh, Edinburgh, Scotland, United Kingdom
[2] Senckenberg Biodiversity and Climate Research Centre, Frankfurt, Germany
[3] Pacific Northwest Research Station, United States Department of Agriculture - Forest Service, Olympia, WA, United States
[4] University of British Columbia, Vancouver, Canada
[5] Arctic Research Centre, Aarhus University, Roskilde, Denmark
[6] Grand Valley State University, Allendale, MI, USA

Author Contributions: JJA, IHMS and ABP conceived the study with input from REE. ADB, JSP, GHRH, NMS and RDH contributed data. JJA carried out the analysis and wrote the manuscript with input from all authors.

Abstract

Changes in phenology are amongst the most well-documented effects of climate change on global biological systems and directly affect ecosystem functions such as net productivity and trophic interactions. The Arctic is undergoing dramatic environmental change with rapidly rising surface temperatures, accelerating sea-ice decline and changing snow regimes, all of which are expected to influence tundra plant phenology. Despite these changes, no globally consistent trends in Arctic spring phenology have been reported. Instead a more complicated picture is emerging: while spring advances are reported for some sites, others show delays or no change, highlighting a substantial amount of unexplained variation amongst the trends. Though temperature, snowmelt and sea-ice have been identified as environmental controls on tundra spring phenology, their relative influence across different species and sites has not been evaluated in a single comprehensive analysis. Here, we test the importance of local average spring temperatures, local snowmelt date and regional spring drop in sea-ice extent as controls of variation in long-term time-series of spring leaf out and flowering (average span: 18 years) of 14 species from the

International Tundra Experiment (ITEX) phenology dataset. We show that variation in spring plant phenology is best explained by snowmelt date and, to a lesser extent, by average spring temperature at four tundra sites across the Arctic coasts of Alaska, Canada and Greenland. In contrast to previous studies, sea-ice did not predict spring phenology for any species or site. Our findings highlight that tundra vegetation responses to global change are more complex than a direct response to warming temperatures and emphasize the importance of snowmelt as a local driver of tundra spring phenology.

Introduction

The importance of phenology and global change

Changing phenology is considered one of the most apparent effects of climate change on natural systems world-wide (Cleland, Chuine, Menzel, Mooney, & Schwartz, 2007; IPCC, 2014; Menzel et al., 2006; Parmesan & Yohe, 2003). Phenological processes control ecosystem functions (Ernakovich et al., 2014; Richardson et al., 2013), are linked through feedbacks to the climate system (Richardson et al., 2013) and contribute to structuring food webs through trophic interactions (Kharouba et al., 2018; Visser & Both, 2005). In high latitude ecosystems, the onset of plant growth in spring and senescence in autumn are linked with ecosystem net productivity (Matthias Forkel et al., 2016; Park et al., 2016; Piao et al., 2008; Xu et al., 2013) and food availability for herbivores (Barboza, Van Someren, Gustine, & Bret-Harte, 2018; Doiron, Gauthier, & Lévesque, 2015; Gustine et al., 2017; Kerby & Post, 2013b, 2013a; Post, Pedersen, Wilmers, & Forchhammer, 2008). Particularly for the highly-seasonal Arctic tundra, varying phenological responses to environmental drivers among species or taxa yield a high potential for phenological mismatch (Doiron et al., 2015; Kerby & Post, 2013b; Post et al., 2008). Tundra plants are temperature sensitive, especially at high latitudes (Prevéy et al., 2017), but no net advance in leaf or flowering phenology has been observed across the biome (Bjorkman, Elmendorf, Beamish, Vellend, & Henry, 2015; Steven F. Oberbauer et al., 2013; Post, Kerby, Pedersen, & Steltzer, 2016) despite Arctic surface temperatures rising at twice the global average (IPCC, 2014; Winton, 2006). Instead a more complex picture is emerging, highlighting a considerable amount of unexplained variation in phenology across sites, species and phenological events (Bjorkman et al., 2015; Steven F. Oberbauer et al., 2013; Post & Høye, 2013; Post et al., 2016; Prevéy et al., 2017).

Variation in plant phenology – what controls it?

A detailed understanding of which environmental variables serve as cues for Arctic spring phenology is key for explaining the absence of an overall trend in phenology across sites despite rapid warming, and is critical for predicting future responses of Arctic ecosystems to the effects of climate and environmental change (Richardson et al., 2013). Interannual variation in tundra phenology has been attributed to variation in temperature (Bjorkman et al., 2015; Iler, Inouye, Schmidt, & Høye, 2017; Molau, Urban Nordenhäll, & Bente Eriksen, 2005; Steven F. Oberbauer et al., 2013; Panchen & Gorelick, 2017; Prevéy et al., 2017; H. C. Wheeler, Høye, Schmidt, Svenning, & Forchhammer, 2015), snowmelt (Bjorkman et al., 2015; Iler et al., 2017; Semenchuk et al., 2016) and sea-ice (Kerby & Post, 2013a; Post et al., 2016). To date, no study has combined all three environmental variables to test the degree to which snowmelt, temperature and sea-ice melt influence spring phenological events (leaf-out and flowering time) in the Arctic tundra across multiple coastal sites.

Temperature as a driver

The environmental variable most widely used to explain variation in spring phenological events across latitudes and seasons is temperature (Post, Steinman, & Mann, 2018; Thackeray et al., 2016). This includes the phenology of both Arctic and alpine tundra plants (Bjorkman et al., 2015; Huelber et al., 2006; Iler et al., 2017; Kuoo & Suzuki, 1999; Molau et al., 2005; Steven F. Oberbauer et al., 2013; Panchen & Gorelick, 2017; Prevéy et al., 2017; Thórhallsdóttir, 1998; H. C. Wheeler et al., 2015). Temperature influences phenology because plant metabolism and development increase in response to warmer ambient temperatures (Jones, 2013). Average temperatures over a predefined period (Bjorkman et al., 2015; Iler et al., 2017; Panchen & Gorelick, 2017; Prevéy et al., 2017) as well as cumulative temperatures up to the onset of a phenological event (Barrett, Hollister, Oberbauer, & Tweedie, 2015; G. H. R. Henry & Molau, 1997; Huelber et al., 2006; Kuoo & Suzuki, 1999; Molau et al., 2005; Steven F. Oberbauer et al., 2013; H. C. Wheeler et al., 2015) have been shown to explain variation in Arctic and alpine plant phenology, and a minimum heat energy requirement for phenological progress has been suggested (Huelber et al., 2006; Molau et al., 2005). The strength of phenological responses to temperature within a species is not necessarily conserved across its whole range and may vary at

the site- (Prevéy et al. 2017) and plot-level (Post et al., 2009, Høye et al., 2013) Nonetheless, in highly seasonal tundra ecosystems, temperatures are only one factor determining spring plant phenology.

Snowmelt as a driver

Snow distribution is a major determinant of vegetation composition in Arctic and alpine environments (Billings & Bliss, 1959; Molau et al., 2005; Wipf & Rixen, 2010) and snowmelt date has been shown to explain variation in spring phenology in both Arctic and alpine tundra (Bjorkman et al., 2015; Cooper, Dullinger, & Semenchuk, 2011; Cortés et al., 2014; Iler et al., 2017; Semenchuk et al., 2016; Sherwood, Debinski, Caragea, & Germino, 2017; Molau et al., 2005; Wipf, 2009; Wipf, Stoeckli, & Bebi, 2009; but see Thórhallsdóttir, 1998). During snowmelt, tundra plants experience dramatic changes in their immediate environment: light availability increases and leaf surfaces are exposed to atmospheric temperatures and CO_2 concentrations (Starr & Oberbauer, 2003), which in turn stimulate plant metabolic and developmental activity (Jones, 2013). In addition, snowmelt may act as an indicator for suitable growing conditions (H. C. Wheeler et al., 2015). Prior to melt, the insulation of the snow layer protects the plants from frost damage and desiccation (Mølgaard P. & Christensen K., 2003; Sherwood et al., 2017; H. C. Wheeler et al., 2015; Wipf & Rixen, 2010; Wipf et al., 2009) and reduces early-season herbivory (J. A. Wheeler et al., 2016), while after snowmelt the availability of soil moisture and nutrients is increased (Wipf & Rixen, 2010). Plants may therefore experience strong evolutionary pressure to adapt spring metabolic activity to coincide with the timing of snowmelt (Cortés et al., 2014). In fact, some species can begin development once the snow pack is thin enough to allow sufficient light and diurnal temperature variations (Larsen, Ibrom, Jonasson, Michelsen, & Beier, 2007; Starr & Oberbauer, 2003). Although spring temperatures influence snowmelt date, snowmelt is a complex function of winter precipitation, topography, prevailing wind conditions and radiative exposure across the landscape (Billings & Bliss, 1959; Bjorkman et al., 2015; Molau & Mølgaard, 1996; J. A. Wheeler et al., 2016), and can be partially decoupled from spring temperatures (Bjorkman et al., 2015; H. C. Wheeler et al., 2015).

Sea ice as a driver

Variation in tundra phenology and productivity has also been attributed to sea-ice conditions, including the northern hemisphere annual minimum sea-ice extent and January mean extent (Bhatt et al., 2010; Forchhammer, 2017; Kerby & Post, 2013a; Macias-Fauria, Karlsen, & Forbes, 2017; Macias-Fauria & Post, 2018; Post et al., 2013, 2016). Macias-Fauria et al. (2017) found linkages between regional sea-ice conditions and satellite derived early-season vegetation productivity on eastern Svalbard and suggested that cool sea breeze off sea-ice along the adjacent coast may influence land surface temperatures through cold air advection (Haugen & Brown, 1980). The presence of sea ice in coastal environments could also influence atmospheric humidity (Screen & Simmonds, 2010) and light availability through cloud and fog formation during spring ice melt (Tjernström et al., 2015), thus providing a plausible mechanism that could explain plant phenology at coastal tundra sites separately to the influence of sea-ice on local temperatures via sea-breeze. Alternatively, sea ice conditions could be an aggregate indicator of environmental conditions at regional scales (Kerby & Post, 2013a; Macias-Fauria & Post, 2018; Post et al., 2013) and may not have a direct and localised mechanistic link as a control over tundra plant phenology.

In this study, we test the importance of temperature, snowmelt and onset of regional sea ice melt as controls over variation in spring plant phenology using a dataset of plant phenology observations on 14 species spanning up to 21 years at four coastal tundra sites. Specifically, we address the following three questions: (1) To what extent do trends in plant spring phenological events vary among sites and species? (2) How have the environmental conditions changed at each site over the time-period of monitoring? (3) What is the relative explanatory power of snowmelt date, spring temperatures and the date of spring drop in regional sea-ice extent in a multi-predictor model of spring phenology at the study sites? Our analysis therefore allows us to test the strength of the statistical relationships among the three most commonly suggested cues for tundra spring plant phenology across tundra species and sites: temperature, snowmelt and sea ice, and will contribute to improved predictions of the response of tundra plant communities to changing growing conditions.

Materials and methods

Phenological Observations

The observations of phenology used in this paper are a subset of the most recent version of the International Tundra Experiment (ITEX) (G. H. R. Henry & Molau, 1997; Webber & Walker, 1991) phenology control dataset (Prevéy et al., 2017). The dataset is openly available via the Polar Data Catalogue (CCIN Reference Number 12722, www.polardata.ca/pdcsearch/PDCSearchDOI.jsp?doi_id=12722) and was originally compiled by Oberbauer et al. (2013). All observations were recorded according to methods outlined in the ITEX Manual (Molau & Mølgaard, 1996). See also Oberbauer et al. (2013) and Prevéy et al. (2017), as well as Bjorkman et al. (2015), Cooley et al. (2012), Hollister et al. (2005) and Schmidt et al. (2016) for site-specific descriptions of methods. We obtained a subset of the ITEX dataset for coastal sites by exclusion based on the following criteria: a) coastal proximity (less than 3 km from the sea), b) data record spanning more than 10 years, and c) snowmelt timing data available. Four sites met these criteria: Alexandra Fiord (NU, Canada), Qikiqtaruk – Herschel Island (YT, Canada), Utqiaġvik – formerly Barrow (AK, USA) and Zackenberg (Greenland). We have included additional 2016 data for the Qikiqtaruk site and plot-level data for the Zackenberg site.

Site descriptions

The selected sites include mid Arctic (Qikiqtaruk and Utqiaġvik) and high Arctic (Alexandra Fiord and Zackenberg) sites, and cover a wide geographical range (Figure 2-1) and diversity of tundra types: Alexandra Fiord (75.92 W, 78.88 N) on Ellesmere Island has tundra communities on glacio-fluvial sediment composed of mixtures of granitic and carbonate rocks; Utqiaġvik (156.62 W, 71.317 N) consists of wet meadow and heath tundra; the vegetation at Qikiqtaruk (138.91 W, 69.57 N) is erect dwarf shrub tundra; and the Zackenberg (20.56 W, 74.47 N) site has Arctic tundra on noncarbonated bedrock.

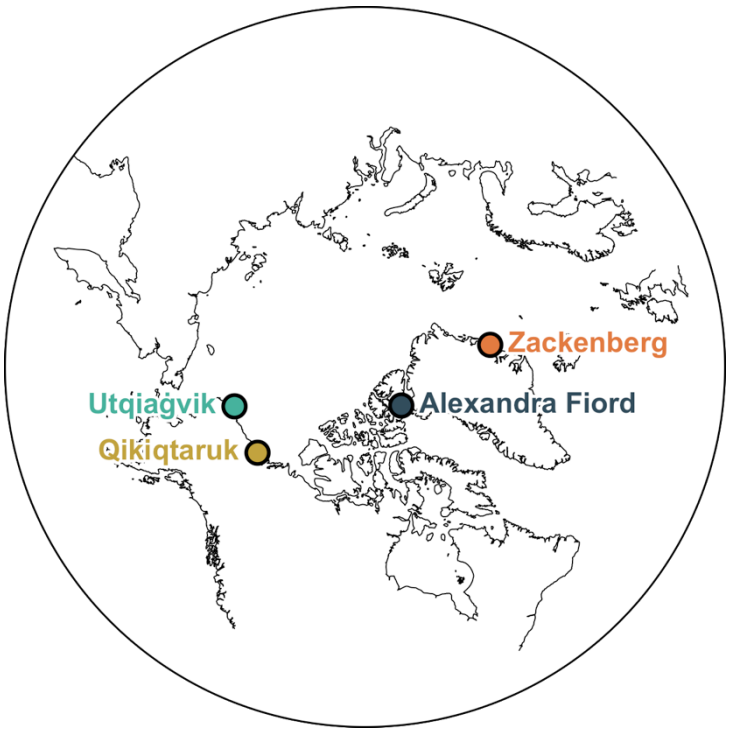

Figure 2-1 | Locations of the four sites included in this study: Alexandra Fiord (NU, Canada), Qikiqtaruk (YT, Canada), Utqiaġvik (AK, USA) and Zackenberg (Greenland).

Selected species and phenological event

Our final subset of the ITEX data contained 14 species (*Cassiope tetragona* D.Don, *Dupontia psilosantha* Ruprecht, *Dryas integrifolia* Vahl, *Dryas octopetala* L., *Eriophorum vaginatum* L., *Luzula arctica* Blytt, *Luzula confusa* Lindeb., *Oxyria digyna* Hill, *Papaver radicatum* Rottb., *Poa arctica* R.Br., *Salix arctica* Pall., *Salix rotundifolia* Trautv., *Saxifraga oppositifolia* L., *Silene acaulis* (L.) Jacq.), which represent the dominant plants in the communities at the selected sites. We selected all species-phenological event combinations that occurred in spring (mean phenological event occurring within 30 days of mean snowmelt at each site). For Utqiaġvik and Qikiqtaruk this selection resulted in 38 and 2 species-phenological event combinations respectively. To obtain a more balanced and biologically representative sample across sites, we narrowed down the Utqiaġvik subset further by selecting only species that make up at least 10% of the ITEX community composition plots at the site and extended the Qikiqtaruk dataset by one additional species whose mean phenological event was the next earliest in the record of the site. The final subset contained a total of 8469 observations for 14 species and two phenological events (spring green up

and flowering), resulting in a total of 24 unique site-species-phenological event combinations (Table 2-1). Phenological events were defined differently for each plant species (Molau & Mølgaard, 1996), but recorded consistently over time (Prevéy et al., 2017). Depending on the species, 'green up' was defined as the date of leaf emergence - the date when the first leaf was visible or open, and 'flowering' was defined as the date when either the first flower was open, the first pollen was visible or the first anthers were exposed (Prevéy et al., 2017).

Table 2-1 | Full species names, phenological event, start, end and length of time-series in years, years with observations in the time-series and colours used for the site-species-phenological event combinations in the dataset.

Site	Species	Phenology Event	Start Year	End Year	Time-Series Length (yrs.)	Years with obs.	Colour
Alexandra Fiord	*Dryas integrifolia*	flowering	1993	2013	21	15	
	Dryas integrifolia	green up	1993	2013	21	14	
	*Luzula spp.**	flowering	1992	2003	12	10	
	Oxyria digyna	flowering	1992	2013	22	18	
	Oxyria digyna	green up	1992	2013	22	18	
	Papaver radicatum	flowering	1992	2013	22	18	
	Papaver radicatum	green up	1992	2013	22	18	
	Salix arctica	flowering	1995	2013	19	14	
Utqiaġvik	*Cassiope tetragona*	green up	1997	2014	18	12	
	Dupontia psilosantha	green up	1995	2014	20	14	
	Luzula arctica	flowering	1994	2014	21	14	
	Luzula arctica	green up	1994	2014	21	14	
	Poa arctica	green up	1994	2014	21	15	
	Salix rotundifolia	flowering	1994	2014	21	15	
	Salix rotundifolia	green up	1994	2014	21	15	
Qikiqtaruk	*Dryas integrifolia*	flowering	2001	2016	16	16	
	Eriophorum vaginatum	flowering	2002	2016	15	15	
	Salix arctica	green up	2001	2016	16	16	
Zackenberg	*Cassiope tetragona*	flowering	1996	2011	16	16	
	Dryas octopetala						
	Papaver radicatum						
	Salix arctica						
	Saxifraga oppositifolia						
	Silene acaulis						

*includes *L. arctica* and *L. confusa*

Snowmelt dates

Snowmelt dates were determined at the plot or site level with site-specific protocols based on the guidelines in the ITEX manual (Molau & Mølgaard, 1996). Alexandra Fiord snowmelt dates were recorded for each plot as the first day of year at which at least 90% of the plot was snow free. Twenty percent of the snowmelt dates at Alexandra Fiord were unobserved. The missing values were gap-filled as detailed in Bjorkman et al. (2015). Utqiaġvik snowmelt dates were based on visual observations of when the plot was 100% snow free or soil surface temperatures when snowmelt occurred in years prior to visual estimates. Snowmelt dates on Qikiqtaruk were determined for each monitored plant individual or plot and recorded as the first date in the year when the individual or plot area was >90% snow free (Cooley et al., 2012). Zackenberg snowmelt dates were determined by multiple visits to the designated plant phenology plots across the landscape. Snowmelt dates were defined as the day at which 50% bare-ground was first visible at a given plot (Schmidt, Hansen, et al., 2016). As not all plant phenology plots at Zackenberg were included in the snowmelt observations, we used the mean snowmelt date of the monitored plots to predict spring phenology at the site. The variation in methods for recording snowmelt are due to the use of different protocols for long-term snowmelt monitoring across these sites.

Spring Temperatures

Daily average air temperatures were obtained from local weather stations (Appendix Table 1) and annual 'spring' averages calculated for each site-species-phenological event time-series. We defined spring average temperature as the mean daily temperature within a calendar year from the earliest snowmelt date on record to the day at which 75% of the phenological event had occurred across the whole length of the time-series. Each time-series therefore had its 'own' specific time-frame across which temperatures were averaged. The period was chosen to capture a static time-window during which the plants are likely to strongly respond to ambient temperatures for each given phenological event. For cross-site comparison of spring temperature change, we calculated spring averages using same approach but applied to the pooled phenology time-series data for each site. These site-specific spring temperatures therefore represent the yearly temperatures from the day of snowmelt to the day when 75% of phenological events occurred within the community across the record of the site.

Day of spring drop in regional sea ice extent

We decided to use the date of spring drop in regional sea-ice extent as it represents the shift from ice covered to ice "free" ocean (the minimum sea ice extent in a given year) in the region surrounding the study site, and hence a change in microclimatic conditions that may act as phenological cues to the tundra plants at our study sites. We hypothesised that, if sea-ice influences plant phenology due to changing light and moisture availability, the time point at which the system shifts its state would carry the highest explanatory power for spring plant phenology at the sites. If air temperatures alone act as the proximate cue, any influence of sea-ice on air temperatures would appear as an effect of temperature in our statistical analysis. We also tested the model using average regional sea-ice extent for the period including the months of May, June and July (Appendix Table 2) and found consistent results to the model with spring drop in sea-ice extent.

The yearly spring drop in sea-ice extent was determined from the NOAA/NSIDC Climate Data Record (CDR) v3 Passive Microwave Sea-Ice Concentrations (Meier et al., 2017; Peng, Meier, Scott, & Savoie, 2013). The data are provided in the NSIDC polar stereographic grid (NSIDC, 2018). We calculated daily regional sea-ice extent for each site within a bounding box of 21 x 21 grid cells (approximately 525 km x 525 km) centred on the cell containing the study site. We used sea ice extent, rather than the raw sea-ice concentrations from the passive microwave data as sea ice extent is more reliable during melt (Worby & Comiso, 2004). To avoid effects of land overspill (Cavalieri, Parkinson, Gloersen, Comiso, & Zwally, 1999), we removed all cells that were directly adjacent to the coastline, retaining only cells that were at least one cell removed from land. Daily regional sea-ice extent was calculated as the total area of cells within the bounding box for which the sea-ice concentration was at least 15%. The day associated with the spring drop in sea ice extent for each year and region was then determined as the day of year (DOY) closest to the annual minimum where the sea-ice extent drops below 85% of the total area (Appendix Figure 1). Our measure therefore picks up the final melt event that leads up to the annual minimum sea-ice extent being reached within a given region and year. Thus, the measure allows for fluctuations in the regional sea-ice extent above and below the 85% mark in the time leading up to the final melt event.

Statistical analysis

We estimated slope parameters for the temporal trends in plant phenological events and environmental predictors using interval-censored and Gaussian-response Bayesian mixed models (respectively) of the MCMCglmm package (Hadfield, 2010) in the R Statistical Environment version 3.4.3 (R Core Team, 2018). We carried out the variance partitioning of the environmental predictors on spring phenology using an interval-censored mixed model using the same package.

Interval-censored phenology observations

For the interval-censored models (Bjorkman et al., 2015; Hadfield, Heap, Bayer, Mittell, & Crouch, 2013), we defined the upper interval bound as the day of year at which the phenological event was first observed. Lower bounds were defined depending on whether prior visits to the monitored individuals / plots were recorded or not. For Alexandra Fiord, Utqiaġvik and Zackenberg no record of prior visits were available and the lower bound was set to the last day at which an observation was recorded at the site prior to the event. The Qikiqtaruk dataset included records of all dates the plots were visited, independent of whether a phenological event was observed or not. We used the last recorded visit prior to the observed phenological event to define the lower bounds of the interval at this site. For phenological observations where no prior date was available (i.e., at the beginning of the year) the lower bound was set as the minimum snowmelt date recorded at the relevant site across the whole study period. Average interval length between observations were 3.2 days for Qikiqtaruk, 3.8 days for Alexandra Fiord and Utqiaġvik, and 6.5 days for Zackenberg.

Phenology trends

Slope estimates for trends in phenological events were determined using a separate model for each site-species-phenological event combination with the following structure:

$$unif[y_{lo}, y_{up}] = \mu + \beta_{year} + \alpha_{plot} + \alpha_{year} + \varepsilon$$

Where y_{lo} and y_{up} are the lower and upper bounds of the interval in which the phenological event occurred, with a uniform likelihood of occurrence across the

interval; μ is the global intercept, β_{year} is the slope parameter for the trend across years; α_{plot} and α_{year} are the random intercepts for plot and year respectively, and ε is the residual error. α_{plot} , α_{year} and ε were normally distributed with a mean of zero and a variance estimated from the data. We included plot and year as categorical random intercepts to account for the replication of phenological observations at each plot over time and at each site in each year.

Environmental predictor trends

Trends in annual mean day of snowmelt, site-specific spring temperature and spring drop in regional sea-ice extent were modelled individually for each site with the following model formula:

$$y = \mu + \beta_{year} + \varepsilon$$

Where y is the value of the environmental predictor for a given year; μ is the global intercept of the model; β_{year} is the slope parameter for the trend across years; and ε the residual error. ε was distributed normally around zero with a variance estimated from the data. We did not include a random intercept for year or plot, as there was no within-year replication of the site-specific environmental variables.

We used weakly informative priors for all parameter estimates (inverse Wishart priors for residual variances and normal priors for the fixed effects) when modelling the trends in phenological events and environmental predictors (Hadfield, 2017). Convergence of these models was assessed through examination of the trace plots.

Prediction analysis

We used a single global model for all site-species-phenological event combinations to estimate the effect of the environmental predictors on spring phenological events. The predictor variables were within subject mean centred for each site-species-phenology event combination (van de Pol & Wright, 2009) and scaled by the standard deviation to allow for direct comparison between the effect sizes (Schielzeth, 2010). The model was structured as follows:

$$unif[y_{lo,i}, y_{up,i}] = \bar{\mu} + \bar{\beta}_{snow} + \bar{\beta}_{temp} + \bar{\beta}_{ice} + \bar{\beta}_{year} + \beta_{snow,i} + \beta_{temp,i} + \beta_{ice,i} + \beta_{year,i} + \alpha_{site} + \alpha_{plot} + \alpha_{year} + \alpha_{site:year} + \varepsilon$$

Where $y_{lo,i}$ and $y_{up,i}$ are the upper and lower bounds of the interval in which a phenological event of the site-species-phenological event combination i occurred, with a uniform likelihood of occurrence across the interval; $\bar{\mu}$ the global intercept; $\bar{\beta}_{snow}$, $\bar{\beta}_{temp}$, $\bar{\beta}_{ice}$ and $\bar{\beta}_{year}$ the mean slope parameters for snowmelt, spring temperature, day of spring drop in sea ice extent and year respectively; $\beta_{snow,i}$, $\beta_{temp,i}$, $\beta_{ice,i}$ and $\beta_{year,i}$ the site-species-phenological event specific slopes for snowmelt, spring temperature, onset of sea-ice melt and year respectively; α_{site}, α_{plot}, α_{year} and $\alpha_{site:year}$ the random intercepts for site, plot, year and site-year interaction; ε the residual error. The random intercepts and the residual error were normally distributed around a mean of zero with variances estimated from the data.

For each fixed effect x, the site-species-phenological event specific effects ($\beta_{x,i}$) were drawn from a normal distribution with estimated variance around the mean slope $\bar{\beta}_x$ of the fixed effect. We included year as a continuous predictor to account for the effects of variables that have changed linearly over years and were not included in the analysis in addition to the modelled fixed effects (Iler et al., 2017; Keogan et al., 2018). Furthermore, we added random intercepts for plot and year to account for the nonindependence of plots measured repeatedly over time as well as the nonindependence of observations conducted in the same year at a given site. Finally, a year-site interaction was included to allow for the year effect to vary among locations (i.e., early year at Alexandra Fiord is not necessarily an early year at Qikiqtaruk). Our model does not allow for: 1) a correlation of responses across species at a site, 2) the correlation of species responses across sites, 3) the correlation of a species' response across phenological events, and 4) plot-level variation in the estimated slope parameters. We did not consider interactions between the environmental predictors, as we had no a priori prediction of a consistent directional interaction effect that would apply across species and locations.

The random slope and intercept parameters of the prediction analysis model were estimated using an unstructured covariance matrix, which allowed for covariance between slopes and the intercept (Hadfield, 2017). We used weakly informative priors for all coefficients (parameter-expanded inverse Wishart priors for the variances and normal priors for the fixed effects). The prediction analysis model was run with four chains and convergence was confirmed through examination of the trace plots and Gelman-Rubin diagnostics (Gelman & Rubin, 1992).

Environmental predictors were tested for multicollinearity with variance inflation factors using the R package usdm (Naimi, Hamm, Groen, Skidmore, & Toxopeus, 2014) prior to execution of the model runs. The variance inflation factors for all three variables were below 1.27, suggesting no problems with multicollinearity. The highest correlation coefficient was observed between spring temperatures and drop in sea ice extent (-0.38). We also ran reduced models of the global model, only containing a single environmental predictor (Appendix Table 5), which allowed us to test for indirect mechanisms linking two of the environmental predictors (e.g., sea-ice and temperature).

Due to the absence of plot-level snowmelt observations at Zackenberg the effect of snowmelt at the Zackenberg site is solely due to among year variation, whereas at Alexandra Fiord, Utqiaġvik and Qikiqtaruk the effect of snowmelt is affected by both among year and among plot variation. Hence, our modelled estimates of the day of snowmelt effect at Zackenberg may be biased up or down due to the loss of within site variation in snowmelt date. We also ran the model with average annual snowmelt values for all sites and observed comparable results to the original model with a slight reduction in the explanatory power for snowmelt date (Appendix Table 2). Our original model may therefore be underestimating the effect of snowmelt date at the Zackenberg site.

We refer to environmental predictors and trends as ‘significant’ when the 95% credible interval (CI) for the corresponding parameter of the fitted models did not overlap zero. Code is available at the following GitHub link: (to be added at the time of publication).

Results

We observed strong variation in both the timing of annual mean spring phenological events and their trends across the study periods for all species-phenological event combinations and sites (Figure 2-2). While the trends indicate that spring is advancing overall at Qikiqtaruk and Zackenberg, not all species or phenological events showed significant trends at the two sites. In addition, we found little to no evidence for changes in the onset of spring at Alexandra Fiord and Utqiaġvik. Estimated rates of change varied from an advance of 10.06 days per decade (CI: -18.77 to -1.35 for *Cassiope tetragona* flowering at Zackenberg) to a delay of 1.67 days per decade (CI: -2.61 to 5.86 for *Oxyria digyna* flowering at Alexandra Fiord), with five site-species-phenological event combinations advancing significantly and 19 combinations showing no significant change (Appendix Table 3).

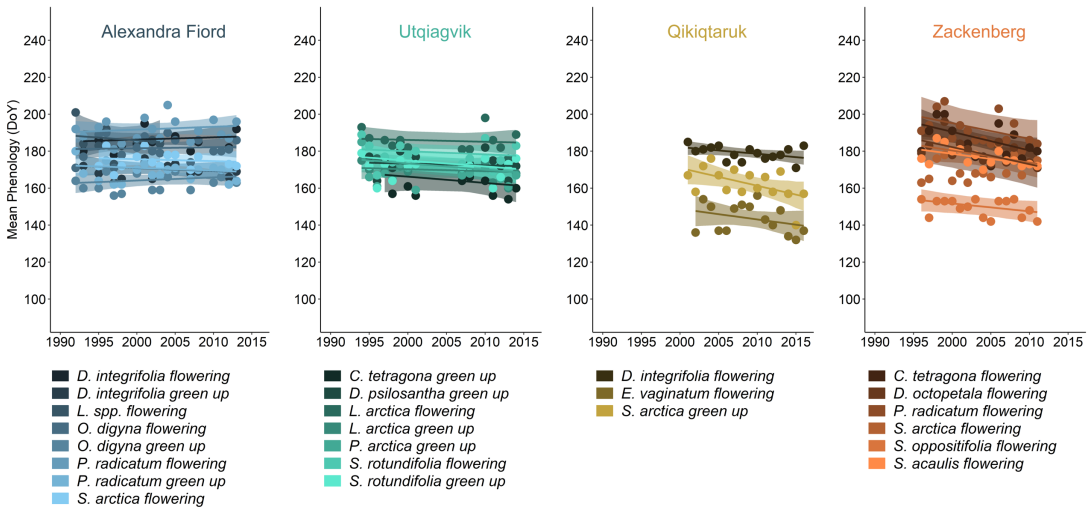

Figure 2-2 | Annual mean spring phenology and trends for the species-phenological event combinations at Alexandra Fiord, Utqiaġvik, Qikiqtaruk and Zackenberg. Trend lines were fitted with Bayesian interval censored models and shaded areas indicate 95% credible intervals. For a detailed list of the phenological event and species combinations monitored see Table 2-1. For graphical clarity, the credible intervals for the *Silene acaulis* flowering time-series at Zackenberg are not shown. A low number of plot-level estimates with high variation in trends resulted in high uncertainties of the model estimates for this time-series. See Appendix Figure 2 for a plot including the credible intervals for the *S. acaulis* time-series.

The observed trends in environmental predictors indicate notable changes in spring climate and environment at all sites across the study periods (Figure 2-3). Snowmelt dates advanced by 8.15 days per decade (CI: -16.19 to 0.31) at Qikiqtaruk and by 10.22 days per decade (CI: -22.51 to 2.06) at Zackenberg, but the trends were marginally non-significant. No significant change was observed at Alexandra Fiord (-0.61 days per decade; CI: -4.19 to 2.98) and Utqiaġvik (-1.41 days per decade; CI: -6.24 to 3.46) (Appendix Table 4). Average spring temperatures across the site-specific "spring" periods increased significantly at all sites during the years monitored respectively, with Qikiqtaruk experiencing the strongest trend of 2.30 °C warming per decade (CI: 0.78, 3.83) and Alexandra Fiord experiencing the weakest trend of 0.63 °C warming per decade (CI: 0.01, 1.24) (Appendix Table 4).The date of spring drop in sea-ice advanced for all sites, roughly mirroring the trends in temperature with onset dates becoming earlier by -10.28 days per decade (CI: -56.07; 34.36 at Zackenberg) to -46.39 days per decade (CI: -73.21, -19.40; at Qikiqtaruk) (Appendix Table 4). However, the variation in onset of sea-ice melt among years was substantial for all sites and particularly high for Zackenberg, and only the declining trend at Qikiqtaruk was statistically significant.

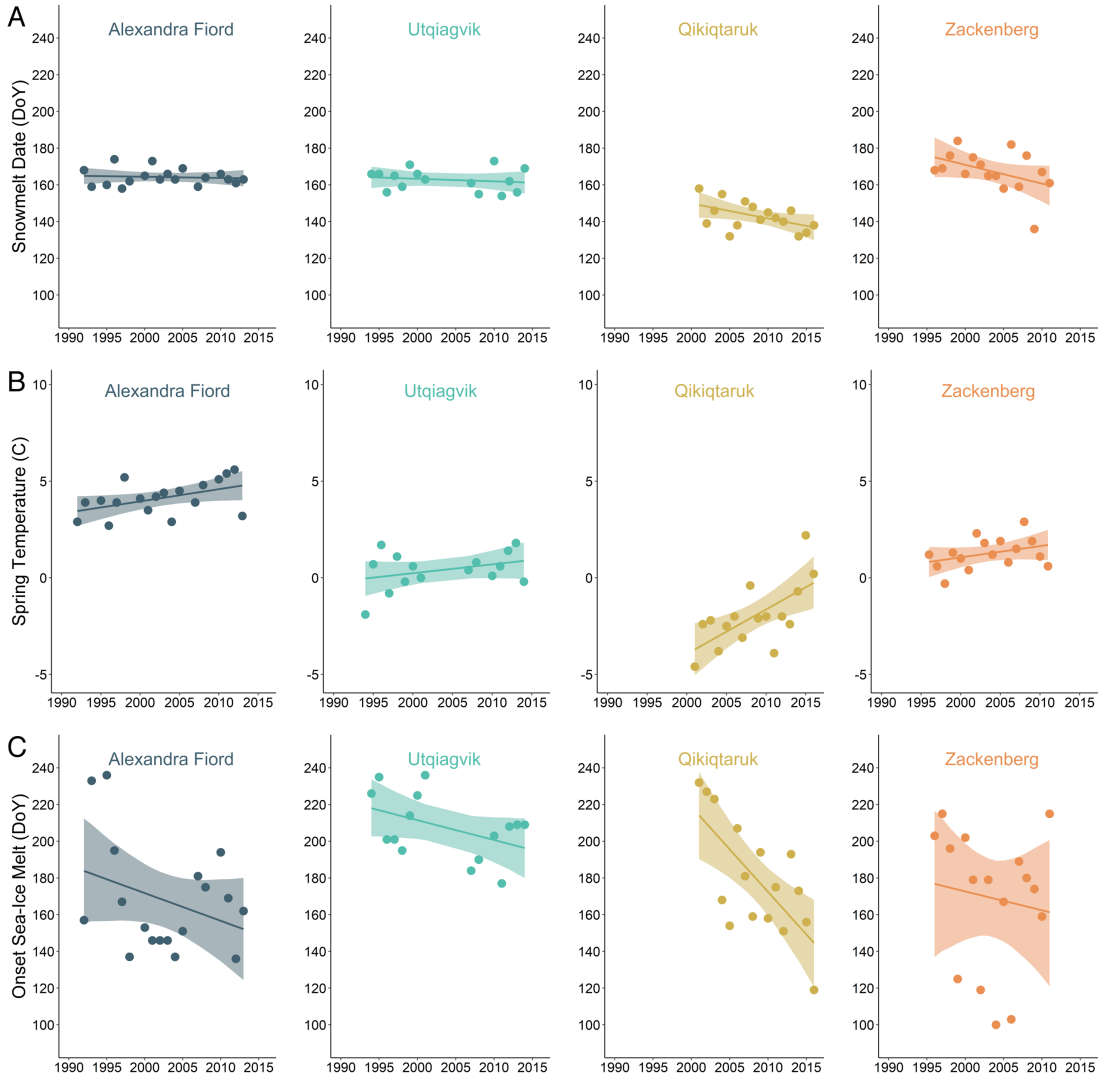

Figure 2-3 | Trends in site averages for snowmelt date (A), 'spring' temperature (B) and onset of regional sea-ice melt (C) for Alexandra Fiord, Utqiaġvik, Qikiqtaruk and Zackenberg for the years in the phenological records. Trend lines were fitted using Bayesian linear models and shaded areas represent 95% credible intervals. 'Spring' temperatures represent yearly averages of daily temperatures within the site-specific time-frames from the earliest day-of-year of snowmelt on record to the day of year where 70% of the spring phenological events occurred in the pooled community record of a given site. Due to these site-specific time-frames Alexandra Fiord represents the 'warmest' spring temperatures despite being the northernmost site.

Snowmelt date consistently predicted phenology (

Figure 2-4 and Appendix Figure 3) with a mean scaled effect size of 3.26 (CI: 2.63 to 3.91) - corresponding to 0.45 days advance in phenology per day advance in snowmelt – and an associated variance in slopes of 1.82 (CI: 0.89 to 3.55), which and 95% of the site-species-phenology event combinations being predicted to respond in the range of 0.09 to 0.82 days advance in phenology per day advance in snowmelt. Temperature explained variation in spring phenology for some, but not all, species-phenological event combinations with a mean scaled effect size of -2.21 (CI -3.04 to -1.39) and associated slope variance of 3.15 (CI: 1.51 to 6.10), which corresponds to 2.39 days advance in phenology per °C increase and 95% of the site-species-phenological event combinations being predicted to respond in the range of 6.16 days advance to 1.38 delay in phenology per °C increase. The spring drop in regional sea-ice extent was a poor predictor in all cases with a mean scaled effect size of -0.01 (CI: -0.94 to 0.91) and associated slope variance of 0.81 (CI: 0.28 to 1.83), which corresponds to less than 0.01 days advance per day delay in regional drop in sea ice extent and 95% of the site-species-phenological event combinations being predicted to respond in the range of 0.07 days advance to 0.07 days delay per day delay in regional drop in sea ice extent. These findings are in broad agreement with the coefficients from the reduced models that tested each environmental predictor separately (Appendix Table 5).

Variation in phenological events of only one species-phenological event combination (*Dryas integrifolia* flowering at Qikiqtaruk) was not significantly explained by snowmelt date, with the 95% confidence intervals overlapping zero for the posterior distributions for all three slope parameters (Figure 4 and Appendix Table 6). Eleven out of the twenty-four species-phenological event combinations were significantly explained by temperature: all Alexandra Fiord species-phenological event combinations, *Salix arctica* green up at Qikiqtaruk, *Cassiope tetragona* and *Salix arctica* flowering at Zackenberg (Appendix Table 6). Finally, the model highlighted a fair amount of unexplained variance among unique site-year combinations (9.40, CI: 5.58 to 14.72), which corresponds to 95% of site-year combinations being in the range of +/- 6.01 days from the predicted values.

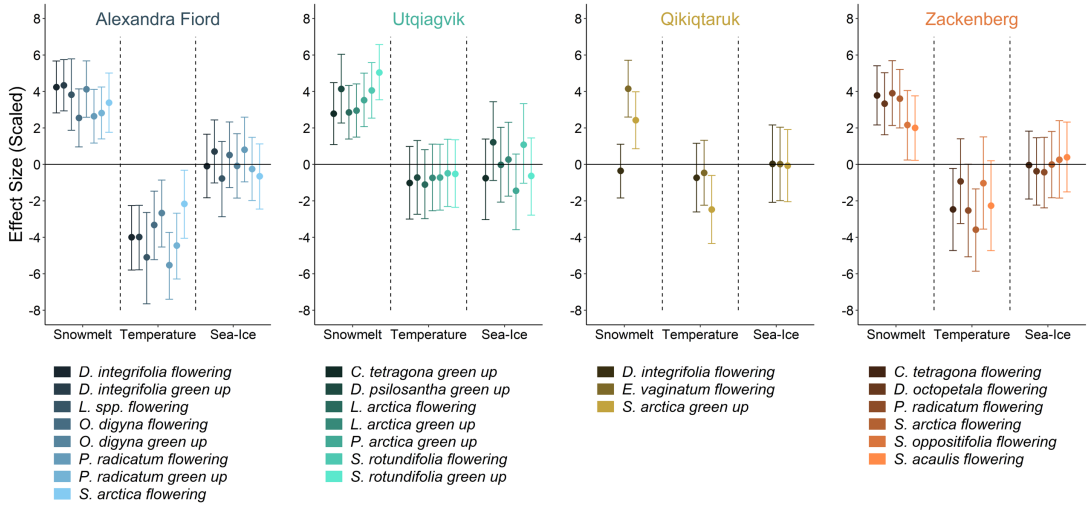

Figure 2-4 | Scaled effect sizes, grouped by the environmental predictors (date of snowmelt, average spring temperature and date of spring drop in regional sea-ice extent), for all species-phenological event combinations at Alexandra Fiord, Utqiaġvik, Qikiqtaruk and Zackenberg. Error bars represent 95% credible intervals. Effect sizes and credible intervals were estimated using a Bayesian mixed model. Environmental predictors were within-subject mean centred and scaled by the standard deviation (date of snowmelt: 7.20, spring temperature: 0.92 and spring drop in regional sea-ice extent: 26.90).

Discussion

Our test of the importance of temperature, snowmelt and drop in spring sea ice extent as controls over coastal Arctic tundra plant phenology highlight three main findings: 1) Trends in spring phenology were highly variable among species across these four sites emphasizing the substantial heterogeneity in plant phenological response across tundra plant communities. 2) While all sites experienced pronounced advances in spring temperatures and onset of regional sea-ice melt, spring phenology did not advance at all sites. Instead spring phenology advanced only at those sites with advancing snowmelt (Qikiqtaruk and Zackenberg) and only for some species-phenological event combinations at these sites. 3) Localised snowmelt was best at predicting variation in spring phenology at the coastal Arctic sites, suggesting that it is a key cue for spring leaf-out and early season flowering in coastal tundra plant communities. Our findings confirm that timing of snowmelt (Bjorkman et al., 2015; Cooper et al., 2011; Cortés et al., 2014; Iler et al., 2017; Kankaanpää et al., 2018; Molau et al., 2005; Semenchuk et al., 2016; Sherwood et al., 2017; Thórhallsdóttir,

1998; Wipf, 2009; Wipf et al., 2009) rather than a localised influence of sea ice (Kerby & Post, 2013a; Macias-Fauria et al., 2017; Post et al., 2016) has important control over spring plant phenology in coastal tundra ecosystems. Furthermore, our results indicate that temperature, despite being the primary driver of spring plant phenology in temperate regions (Cleland et al., 2007; Thackeray et al., 2016; Wolkovich et al., 2012), holds less explanatory power for spring phenology in snow-dominated coastal tundra ecosystems of the Arctic.

Snowmelt needs to be included when studying tundra phenology in a global change context

Our results highlight the importance of considering local snow conditions in addition to temperature when studying and predicting responses of tundra plant phenology to global climate change. To date, snowmelt has yet to be incorporated into pan-Arctic syntheses investigating tundra plant phenology in response to global change (Oberbauer et al., 2013; Prevéy et al., 2017). Snowmelt is also notably absent in multi-biome studies, particularly those that include phenological observations from both tundra and temperate regions (Post et al., 2018; Wolkovich et al., 2012; Xu et al., 2013). Excluding snowmelt from any analysis that includes tundra spring plant phenology may lead to inaccurate estimates of phenological responses to global change in tundra ecosystems. However, obtaining reliable local snowmelt data can be logistically challenging, particularly as most field sites are only visited after the onset of melt and may not have historical snowmelt records. Auto-camera systems (phenocams) could assist in the collection of snowmelt data at a site or plot level in the absence of field teams (Andresen, Tweedie, & Lougheed, 2018; Brown et al., 2016a; Linkosalmi et al., 2016; Westergaard-Nielsen et al., 2017) and satellite data can be used for post-hoc estimations of snowmelt dates at coarser temporal and spatial scales (Dozier, 1989; Hall, Riggs, & Salomonson, 1995). Thus, we advocate the inclusion of snowmelt in future studies of the drivers of phenology change within the tundra biome.

Influence of snowmelt highlights importance of landscape-level heterogeneity in phenology

The high explanatory power of snowmelt date in this study and its inherently high spatial variability highlight the need to consider landscape heterogeneity in tundra

phenology analyses (Kankaanpää et al., 2018). Landscape heterogeneity in phenology integrates a diversity of plant phenological responses and environmental controls (Armstrong, Takimoto, Schindler, Hayes, & Kauffman, 2016). Different plant species, populations and individuals differ in their phenology and as communities change across the landscape, so does community-level phenology (CaraDonna, Iler, & Inouye, 2014; Cleland et al., 2007; Klosterman et al., 2018; Wolkovich, Cook, & Davies, 2014). Furthermore, the environmental controls on phenology also vary substantially across the landscape. For example, snowmelt in the Arctic and alpine tundra is a complex function of winter and spring atmospheric temperatures, precipitation, topography, solar radiation and wind velocity (Billings & Bliss, 1959; Bjorkman et al., 2015; Cortés et al., 2014; Liston, Mcfadden, Sturm, & Pielke, 2008; Molau et al., 2005; Sturm et al., 2001; H. C. Wheeler et al., 2015). Particularly the interplay of micro-topography, radiation and wind can cause highly localised variation in snowmelt at plot and even sub-plot scales (Cortés et al., 2014; Sturm et al., 2001). Individuals and groups of the same species may not only experience differences in the environmental cues they experience across the landscape, but have also been shown to vary in the relative strength of their phenological responses to these cues at the plot level (Post et al., 2009, Høye et al., 2013), likely due to localised interactions and additional environmental influences (Høye et al., 2013). Thus, the locality and distribution of phenological monitoring plots and observations of environmental variables need to encompass this variation in the landscape, if we want to obtain representative estimates of species and community spring phenological events and their drivers at any given site. Emerging technologies such as phenocams (Andresen et al., 2018; Linkosalmi et al., 2016; Richardson et al., 2018), fine-scale aerial imagery from drones (Klosterman et al., 2018) and spatiotemporal modelling of snow properties (Pedersen, Liston, Tamstorf, Westergaard-Nielsen, & Schmidt, 2015) may help facilitate phenological monitoring at the spatial and temporal scales and extents required to understand landscape and community-level phenological change.

Spring drop in sea ice extent did not explain variation in phenology

The spring drop in sea ice extent did not explain spring phenology at the coastal tundra sites in our dataset. As this was the case for the models that included spring drop in sea-ice as the only environmental predictor (Appendix Table 5) as well as for the model containing all three environmental predictors, our findings suggest that

there is neither a direct or indirect mechanism linking spring drop in sea-ice to spring phenology at our study sites. Though we were not able to test directly, we found no particular evidence that the sea-breeze mechanism proposed by Haugen & Brown (1980) and observed by Macias-Fauria et al. (2017) or other indirect sea ice drivers have a significant impact on plant spring phenology across our study sites.

The majority of previous studies that have attributed spring phenology variation and plant productivity to sea-ice used large-scale integrative measures such as annual minimum global sea-ice extent (Bhatt et al., 2010; Forchhammer, 2017; Kerby & Post, 2013a; Post et al., 2013, 2016). Phenology has previously also been linked to other integrative global measures such as ENSO or the North Atlantic Oscillation (NAO) (Chmielewski & Rötzer, 2001; D'Odorico, Yoo, & Jaeger, 2002; Forchhammer, Post, & Stenseth, 1998; Scheifinger, Menzel, Koch, Peter, & Ahas, 2002). Though the integrative measures may correlate well with plant phenology in these cases, our findings highlight the value of statistical analysis that test predictors directly associated with plausible localised ecological mechanisms. We believe that such tests are critical steps to disentangling the complexity of plant phenological responses observed in the tundra biome. We thus advocate for more studies that test localised controls on plant phenology across spatial and temporal scales in tundra ecosystems and beyond.

The challenges of measuring localised sea ice conditions

Determining regional and interannual variation in the onset of sea ice melt can be challenging due to the lack of locally collected data. Globally available satellite products such as the passive microwave data set used in this study (Peng et al., 2013) struggle to detect the ice edge during the melt period (Comiso & Nishio, 2008; Worby & Comiso, 2004) and suffer from land spill-over in cells adjacent to the coast-line (Cavalieri et al., 1999). More accurate manually interpreted datasets based on a mixture of data sources (including optical satellite data) such as those developed by national agencies for navigational purposes could be used, but are often available only for recent years (Canadian Ice Service, 2009) and/or are regionally limited (http://polarview.met.no). We chose the passive microwave satellite data to estimate the timing of drop in spring sea-ice extent as no other data were available for the entire time-period and geographical extent of our study at a daily resolution. Due to

our cautious pre-processing procedure, our measure of onset of sea-ice melt from the NOAA/NSIDC climate data record likely is a conservative estimate and might mask out some of the fine-scale temporal and spatial variation in the sea-ice conditions in the different study regions. Thus, we caution that the interannual variation in regional sea-ice extent may not be entirely comparable to higher-resolution temperature (site level) and snowmelt estimates (site to plot level) used in this study. With advances in technology and growing interest in the northern maritime regions, higher quality sea-ice data are becoming increasingly available (see for example Macias-Fauria et al., 2017), and we encourage future studies to repeat our analyses using such data products.

Photoperiod as a control on spring phenology

Our study was not able to address the separate effect of photoperiod as a control on spring phenology because of the lack of temporal variation required for an analysis such as we have employed here. Arctic and alpine plant phenology can be sensitive to photoperiod as suggested by common garden experiments (Bennington et al., 2012; Bjorkman, Vellend, Frei, & Henry, 2017; Parker, Tang, Clark, Moody, & Fetcher, 2017) and demonstrated in growth chamber experiments (Heide, 1989, 1992; Keller & Körner, 2003). Keller and Körner (2003) found long day requirements for flowering in 54% of the 20 studied alpine plant species and estimated a minimum day length requirement of about 15 h for plants adapted to their study site in the central Alps in Europe. It is therefore likely that minimum daylight requirements were met at all our study sites prior to snowmelt: Alexandra Fiord, Barrow and Zackenberg already experienced 24 hours of daylight two weeks prior to the minimum snowmelt date on record, and Qikiqtaruk experienced 14.5 hours of daylight with no night and only astronomical twilight at this time. However, increases in day length beyond the minimum requirement may accelerate development and phenology of Arctic and alpine plants (Keller & Körner, 2003) and dual requirements based on interactions of temperature and photoperiod have been documented in other studies (Heide, 1989). Thus, understanding the interactive nature of photoperiod and environmental cues on phenology, particularly in the context of range expansions with warming from lower latitudes with stronger diurnal light variation to high latitudes, remains a future challenge for tundra plant ecology.

Phenology, trophic interactions and ecosystem change

Tundra plant phenology impacts ecosystem functions such as net primary productivity (Matthias Forkel et al., 2016; Piao et al., 2008; Xu et al., 2013) thereby creating feedbacks to the global climate system (Richardson et al., 2013). Our study underlines the importance of localised snowmelt dates for spring plant phenology in coastal tundra ecosystems. Snow cover is projected to decrease across the Arctic (AMAP, 2017), but predicted changes in snow conditions differ in direction and magnitude amongst regions and seasons with the highest declines in snow cover expected for warmer coastal areas and during spring (AMAP, 2017). Locally reduced spring snow cover could increase also the susceptibility of plants to freezing events and further affect plant productivity, community composition and evolution through plant health and mortality (Bokhorst, Bjerke, Street, Callaghan, & Phoenix, 2011; Cortés et al., 2014; Jonas, Rixen, Sturm, & Stoeckli, 2008; Phoenix & Bjerke, 2016; J. A. Wheeler et al., 2016; Wipf & Rixen, 2010).

Tundra plant phenology influences resource availability for secondary consumers (Barboza et al., 2018; Doiron et al., 2015; Gustine et al., 2017; Kerby & Post, 2013b) and asynchronous shifts between interacting species due to climate change could result in trophic mismatches (Doiron et al., 2015; Kerby & Post, 2013b, 2013a; Schmidt, Mosbacher, et al., 2016). Reduced spring snow cover could decrease spatial variation in snowmelt timing and thus lessen the extent of landscape-scale heterogeneity in plant phenology, with potentially detrimental impacts on consumers, as these may rely on temporal and spatial variation in their food sources to maximise energy intake across the season (Armstrong et al., 2016; Moorter et al., 2013). This interaction between spatial and temporal patterning and trends in trophic mismatches has only rarely been explored in the tundra and other ecosystems (Bischof et al., 2012; Burgess et al., 2018; Sawyer & Kauffman, 2011). A comprehensive understanding of the mechanistic drivers of plant phenology and how they change is therefore key to our ability to predict and manage the consequences of future environmental change in tundra ecosystems and beyond (Kharouba et al., 2018; Richardson et al., 2013; Thackeray, 2016; Thackeray et al., 2016; Wolkovich et al., 2014)

Conclusions

The Arctic is warming more rapidly than any other region of the planet (IPCC, 2014), with well documented consequences for tundra plant communities, including changes in community composition (Elmendorf, Henry, Hollister, Björk, Bjorkman, et al., 2012; Elmendorf, Henry, Hollister, Björk, Boulanger-Lapointe, et al., 2012; Elmendorf et al., 2015; Ernakovich et al., 2014), trophic mismatch (Doiron et al., 2015; Gustine et al., 2017; Kerby & Post, 2013b, 2013a; Post et al., 2008) and altered plant phenology (Høye, Post, Meltofte, Schmidt, & Forchhammer, 2007; Post et al., 2018). Our findings suggest that snowmelt and temperature, but not spring drop in sea-ice extent are the dominant cues for spring phenology in coastal Arctic plant communities that experience short growing seasons and persistent snow cover. Later snowmelt therefore can delay phenology, even when air temperatures are advancing over time. These results highlight the growing evidence that tundra vegetation responses to rapid environmental change are more complex than a simple response to increasing temperatures and help explain the variation in phenological trends seen across the tundra biome. Thus, to understand and predict future tundra vegetation change and associated feedbacks on the global climate system, we require localised tests of the specific influences of mechanistic drivers of change. Our study illustrates the value of long-term monitoring programmes (sensu Post & Høye, 2013; Schmidt, Christensen, & Roslin, 2017) and cross-site data syntheses for quantifying site- and species-specific responses to environmental change. Only with quantitative tests carried out on comprehensive cross-site datasets, can we attribute variation in plant phenology to localised environmental cues and improve our predictions of tundra ecosystem responses to global change.

Acknowledgements

JJA was supported by a NERC Edinburgh Earth and Environment (E3) doctoral training partnership grant (NE/L002558/1).

Alexandra Fiord

Logistical support was provided by the Polar Continental Shelf Program (Natural Resources Canada) and the Royal Canadian Mounted Police. Financial support was provided through grants to GHRH from the Natural Sciences and Engineering Resource Council (NSERC) of Canada, the Northern Scientific Training Program,

ArcticNet, and the Government of Canada International Polar Year program. Funding to ADB was provided by the University of British Columbia and the Arctic Institute of North America. The research at Alexandra Fiord was conducted under permits from the Nunavut Research Institute and the Nunavut Department of Environment. We thank the Qikiqtani Inuit Association for access to Inuit Owned Land at the site. We especially thank all of the many field assistants, graduate students, postdocs and colleagues who helped to maintain the sites and conduct measurements since 1992.

Utqiaġvik – Barrow

We thank the community of Utqiaġvik for their continued support. We also thank the many researchers responsible for collecting and collating the decades of observations, there are too many to name them all. Funding for this research is provided by the National Science Foundation (NSF) (Award #s 9714103 0632263 0856516 1432277 1504224) with logistics provided by UIC Science.

Qikiqtaruk – Herschel Island

We thank the Herschel Island - Qikiqtaruk Territorial Park and Yukon Government for carrying out this ecological monitoring program. We thank Richard Gordon, Cameron Eckert, Catherine Kennedy, Dorothy Cooley, and Dr. Jill F. Johnstone for establishing and maintaining the phenology monitoring at Qikiqtaruk. We thank the park rangers who collected the observations of phenology including Edward McLeod, Sam McLeod, Ricky Joe, Paden Lennie, Deon Arey, LeeJohn Meyook, Jordan McLeod, Pierre Foisy, Colin Gordon, Jeremy Hansen and Albert Rufus. Funding to JJA and IMS was provided by the UK Natural Environment Research Council ShrubTundra Grant (NE/M016323/1). We thank the Inuvialuit people for the opportunity to conduct research in the Inuvialuit Settlement Region.

Zackenberg

Data from the Zackenberg were provided by Greenland Ecosystem Monitoring Programme. We thank all field assistants and particular Lars Holst Hansen for collecting observations of plant phenology over the years.

We thank Jeffrey T. Kerby for providing valuable feedback on our manuscript, and the Inupiat, Inuvialuit, Inuit and Kalaallit People for the opportunity to conduct research on their traditional lands.

References

AMAP. (2017). *Snow, Water, Ice and Permafrost. Summary for Policy-makers.* (p. 20). Oslo, Norway: Arctic Monitoring and Assessment Programme (AMAP). Retrieved from https://www.amap.no/documents/doc/Snow-Water-Ice-and-Permafrost.-Summary-for-Policy-makers/1532

Andresen, C. G., Tweedie, C. E., & Lougheed, V. L. (2018). Climate and nutrient effects on Arctic wetland plant phenology observed from phenocams. *Remote Sensing of Environment*, *205*, 46–55. https://doi.org/10.1016/j.rse.2017.11.013

Armstrong, J. B., Takimoto, G., Schindler, D. E., Hayes, M. M., & Kauffman, M. J. (2016). Resource waves: phenological diversity enhances foraging opportunities for mobile consumers. *Ecology*, *97*(5), 1099–1112. https://doi.org/10.1890/15-0554.1

Barboza, P. S., Van Someren, L. L., Gustine, D. D., & Bret-Harte, M. S. (2018). The nitrogen window for arctic herbivores: plant phenology and protein gain of migratory caribou (Rangifer tarandus). *Ecosphere*, *9*(1), e02073. https://doi.org/10.1002/ecs2.2073

Barrett, R. T. S., Hollister, R. D., Oberbauer, S. F., & Tweedie, C. E. (2015). Arctic plant responses to changing abiotic factors in northern Alaska. *American Journal of Botany*, *102*(12), 2020–2031. https://doi.org/10.3732/ajb.1400535

Bennington, C. C., Fetcher, N., Vavrek, M. C., Shaver, G. R., Cummings, K. J., & McGraw, J. B. (2012). Home site advantage in two long-lived arctic plant species: results from two 30-year reciprocal transplant studies. *Journal of Ecology*, *100*(4), 841–851. https://doi.org/10.1111/j.1365-2745.2012.01984.x

Bhatt, U. S., Walker, D. A., Raynolds, M. K., Comiso, J. C., Epstein, H. E., Jia, G., … Webber, P. J. (2010). Circumpolar Arctic Tundra Vegetation Change Is Linked to Sea Ice Decline. *Earth Interactions*, *14*(8), 1–20. https://doi.org/10.1175/2010EI315.1

Billings, W. D., & Bliss, L. C. (1959). An Alpine Snowbank Environment and Its Effects on Vegetation, Plant Development, and Productivity. *Ecology*, *40*(3), 388–397. https://doi.org/10.2307/1929755

Bischof, R., Loe, L. E., Meisingset, E. L., Zimmermann, B., Van Moorter, B., & Mysterud, A. (2012). A Migratory Northern Ungulate in the Pursuit of Spring: Jumping or Surfing the Green Wave? *The American Naturalist*, *180*(4), 407–424. https://doi.org/10.1086/667590

Bjorkman, A. D., Elmendorf, S. C., Beamish, A. L., Vellend, M., & Henry, G. H. R. (2015). Contrasting effects of warming and increased snowfall on Arctic tundra plant phenology over the past two decades. *Global Change Biology*, *21*, 4651–4661. https://doi.org/10.1111/gcb.13051

Bjorkman, A. D., Vellend, M., Frei, E. R., & Henry, G. H. R. (2017). Climate adaptation is not enough: warming does not facilitate success of southern tundra plant populations in the high Arctic. *Global Change Biology*, *23*(4), 1540–1551. https://doi.org/10.1111/gcb.13417

Bokhorst, S., Bjerke, J. W., Street, L. E., Callaghan, T. V., & Phoenix, G. K. (2011). Impacts of multiple extreme winter warming events on sub-Arctic heathland: phenology, reproduction, growth, and CO2 flux responses. *Global Change Biology*, *17*(9), 2817–2830. https://doi.org/10.1111/j.1365-2486.2011.02424.x

Brown, T. B., Hultine, K. R., Steltzer, H., Denny, E. G., Denslow, M. W., Granados, J., … Richardson, A. D. (2016). Using phenocams to monitor our changing Earth: toward a global phenocam network. *Frontiers in Ecology and the Environment*, *14*(2), 84–93. https://doi.org/10.1002/fee.1222

Burgess, M. D., Smith, K. W., Evans, K. L., Leech, D., Pearce-Higgins, J. W., Branston, C. J., … Phillimore, A. B. (2018). Tritrophic phenological match–mismatch in space and time. *Nature Ecology & Evolution*, *2*(6), 970–975. https://doi.org/10.1038/s41559-018-0543-1

Canadian Ice Service. (2009). *Canadian Ice Service Arctic Regional Sea Ice Charts in SIGRID-3 Format, Version 1*. Boulder, Colorado USA: NSIDC: National Snow and Ice Data Center. Retrieved from https://doi.org/10.7265/N51V5BW9

CaraDonna, P. J., Iler, A. M., & Inouye, D. W. (2014). Shifts in flowering phenology reshape a subalpine plant community. *Proceedings of the National Academy of Sciences*, *111*(13), 4916–4921. https://doi.org/10.1073/pnas.1323073111

Cavalieri, D. J., Parkinson, C. L., Gloersen, P., Comiso, J. C., & Zwally, H. J. (1999). Deriving long-term time series of sea ice cover from satellite passive-microwave multisensor data sets. *Journal of Geophysical Research: Oceans*, *104*(C7), 15803–15814. https://doi.org/10.1029/1999JC900081

Chmielewski, F.-M., & Rötzer, T. (2001). Response of tree phenology to climate change across Europe. *Agricultural and Forest Meteorology*, *108*(2), 101–112. https://doi.org/10.1016/S0168-1923(01)00233-7

Cleland, E. E., Chuine, I., Menzel, A., Mooney, H. A., & Schwartz, M. D. (2007). Shifting plant phenology in response to global change. *Trends in Ecology & Evolution*, *22*(7), 357–365. https://doi.org/10.1016/j.tree.2007.04.003

Comiso, J. C., & Nishio, F. (2008). Trends in the sea ice cover using enhanced and compatible AMSR-E, SSM/I, and SMMR data. *Journal of Geophysical Research: Oceans*, *113*(C2), C02S07. https://doi.org/10.1029/2007JC004257

Cooley, D., Eckert, C. D., & Gordon, R. R. (2012). *Herschel Island - Qikiqtaruk Inventory, Monitoring and Research Program*. Whitehorse, YT, Canada: Yukon Parks.

Cooper, E. J., Dullinger, S., & Semenchuk, P. R. (2011). Late snowmelt delays plant development and results in lower reproductive success in the High Arctic. *Plant Science*, *180*(1), 157–167. https://doi.org/10.1016/j.plantsci.2010.09.005

Cortés, A. J., Waeber, S., Lexer, C., Sedlacek, J., Wheeler, J. A., van Kleunen, M., … Karrenberg, S. (2014). Small-scale patterns in snowmelt timing affect gene flow and the distribution of genetic diversity in the alpine dwarf shrub Salix herbacea. *Heredity*, *113*(3), 233–239. https://doi.org/10.1038/hdy.2014.19

D'Odorico, P., Yoo, J. C., & Jaeger, S. (2002). Changing Seasons: An Effect of the North Atlantic Oscillation? *Journal of Climate*, *15*(4), 435–445. https://doi.org/10.1175/1520-0442(2002)015<0435:CSAEOT>2.0.CO;2

Doiron, M., Gauthier, G., & Lévesque, E. (2015). Trophic mismatch and its effects on the growth of young in an Arctic herbivore. *Global Change Biology*, *21*(12), 4364–4376. https://doi.org/10.1111/gcb.13057

Dozier, J. (1989). Spectral signature of alpine snow cover from the landsat thematic mapper. *Remote Sensing of Environment*, *28*, 9–22. https://doi.org/10.1016/0034-4257(89)90101-6

Elmendorf, S. C., Henry, G. H. R., Hollister, R. D., Björk, R. G., Bjorkman, A. D., Callaghan, T. V., … Wookey, P. A. (2012). Global assessment of experimental climate warming on tundra vegetation: heterogeneity over space and time. *Ecology Letters*, *15*(2), 164–175. https://doi.org/10.1111/j.1461-0248.2011.01716.x

Elmendorf, S. C., Henry, G. H. R., Hollister, R. D., Björk, R. G., Boulanger-Lapointe, N., Cooper, E. J., … Wipf, S. (2012). Plot-scale evidence of tundra vegetation change and links to recent summer warming. *Nature Climate Change*, *2*(6), 453–457. https://doi.org/10.1038/nclimate1465

Elmendorf, S. C., Henry, G. H. R., Hollister, R. D., Fosaa, A. M., Gould, W. A., Hermanutz, L., … Walker, M. (2015). Experiment, monitoring, and gradient methods used to infer climate change effects on plant communities yield consistent patterns. *Proceedings of the National Academy of Sciences*, *112*(2), 448–452. https://doi.org/10.1073/pnas.1410088112

Ernakovich, J. G., Hopping, K. A., Berdanier, A. B., Simpson, R. T., Kachergis, E. J., Steltzer, H., & Wallenstein, M. D. (2014). Predicted responses of arctic and alpine ecosystems to altered seasonality under climate change. *Global Change Biology*, *20*(10), 3256–3269. https://doi.org/10.1111/gcb.12568

Forchhammer, M. C. (2017). Sea-ice induced growth decline in Arctic shrubs. *Biology Letters*, *13*(8), 20170122. https://doi.org/10.1098/rsbl.2017.0122

Forchhammer, M. C., Post, E., & Stenseth, N. C. (1998). Breeding phenology and climate¨. *Nature*, *391*(6662), 29–30. https://doi.org/10.1038/34070

Forkel, M., Carvalhais, N., Rodenbeck, C., Keeling, R., Heimann, M., Thonicke, K., … Reichstein, M. (2016). Enhanced seasonal CO2 exchange caused by amplified plant productivity in northern ecosystems. *Science*. https://doi.org/10.1126/science.aac4971

Gelman, A., & Rubin, D. B. (1992). Inference from Iterative Simulation Using Multiple Sequences. *Statistical Science*, *7*(4), 457–472.

Gustine, D., Barboza, P., Adams, L., Griffith, B., Cameron, R., & Whitten, K. (2017). Advancing the match-mismatch framework for large herbivores in the Arctic: Evaluating the evidence for a trophic mismatch in caribou. *PLOS ONE*, *12*(2), e0171807. https://doi.org/10.1371/journal.pone.0171807

Hadfield, J. D. (2010). MCMC Methods for Multi-Response Generalized Linear Mixed Models: The **MCMCglmm** *R* Package. *Journal of Statistical Software*, *33*(2). https://doi.org/10.18637/jss.v033.i02

Hadfield, J. D. (2017). MCMCglmm Course Notes. Retrieved 12 March 2018, from https://cran.r-project.org/web/packages/MCMCglmm/vignettes/CourseNotes.pdf

Hadfield, J. D., Heap, E. A., Bayer, F., Mittell, E. A., & Crouch, N. M. A. (2013). Intraclutch Differences in Egg Characteristics Mitigate the Consequences of Age-Related Hierarchies in a Wild Passerine. *Evolution*, *67*(9), 2688–2700. https://doi.org/10.1111/evo.12143

Hall, D. K., Riggs, G. A., & Salomonson, V. V. (1995). Development of methods for mapping global snow cover using moderate resolution imaging spectroradiometer data. *Remote Sensing of Environment*, *54*(2), 127–140. https://doi.org/10.1016/0034-4257(95)00137-P

Haugen, R. K., & Brown, J. (1980). Coastal-Inland Distributions of Summer Air Temperature and Precipitation in Northern Alaska. *Arctic and Alpine Research*, *12*(4), 403–412. https://doi.org/10.2307/1550491

Heide, O. M. (1989). Environmental Control of Flowering and Viviparous Proliferation in Seminiferous and Viviparous Arctic Populations of Two Poa Species. *Arctic and Alpine Research*, *21*(3), 305. https://doi.org/10.2307/1551570

Heide, O. M. (1992). Experimental Control of Flowering in Carex bigelowii. *Oikos*, *65*(3), 371. https://doi.org/10.2307/3545552

Henry, G. H. R., & Molau, U. (1997). Tundra plants and climate change: the International Tundra Experiment (ITEX). *Global Change Biology*, *3*(S1), 1–9. https://doi.org/10.1111/j.1365-2486.1997.gcb132.x

Hollister, R. D., Webber, P. J., & Tweedie, C. E. (2005). The response of Alaskan arctic tundra to experimental warming: differences between short- and long-

term responses. *Global Change Biology*, *11*(4), 525–536. https://doi.org/10.1111/j.1365-2486.2005.00926.x

Høye, T. T., Post, E., Meltofte, H., Schmidt, N. M., & Forchhammer, M. C. (2007). Rapid advancement of spring in the High Arctic. *Current Biology*, *17*(12), R449–R451. https://doi.org/10.1016/j.cub.2007.04.047

Høye, T. T., Post, E., Schmidt, N. M., Trøjelsgaard, K., & Forchhammer, M. C. (2013). Shorter flowering seasons and declining abundance of flower visitors in a warmer Arctic. *Nature Climate Change*, *3*(8), 759–763. https://doi.org/10.1038/nclimate1909

Huelber, K., Gottfried, M., Pauli, H., Reiter, K., Winkler, M., & Grabherr, G. (2006). Phenological Responses of Snowbed Species to Snow Removal Dates in the Central Alps: Implications for Climate Warming. *Arctic, Antarctic, and Alpine Research*, *38*(1), 99–103. https://doi.org/10.1657/1523-0430(2006)038[0099:PROSST]2.0.CO;2

Iler, A. M., Inouye, D. W., Schmidt, N. M., & Høye, T. T. (2017). Detrending phenological time series improves climate–phenology analyses and reveals evidence of plasticity. *Ecology*, *98*(3), 647–655.

IPCC. (2014). *Climate change 2014: Synthesis Report. Contribution of Working Groups I, II and III to the Fifth Assessment Report of the Intergovernmental Panel on Climate Change*. (R. K. Pachauri & L. Mayer, Eds.). Geneva, Switzerland: IPCC.

Jonas, T., Rixen, C., Sturm, M., & Stoeckli, V. (2008). How alpine plant growth is linked to snow cover and climate variability. *Journal of Geophysical Research*, *113*(G3). https://doi.org/10.1029/2007JG000680

Jones, H. G. (2013). *Plants and Microclimate: A Quantitative Approach to Environmental Plant Physiology* (3rd ed.). Cambridge University Press. https://doi.org/10.1017/CBO9780511845727

Kankaanpää, T., Skov, K., Abrego, N., Lund, M., Schmidt, N. M., & Roslin, T. (2018). Spatiotemporal snowmelt patterns within a high Arctic landscape, with implications for flora and fauna. *Arctic, Antarctic, and Alpine Research*, *50*(1), e1415624. https://doi.org/10.1080/15230430.2017.1415624

Keller, F., & Körner, C. (2003). The Role of Photoperiodism in Alpine Plant Development. *Arctic, Antarctic, and Alpine Research*, *35*(3), 361–368. https://doi.org/10.1657/1523-0430(2003)035[0361:TROPIA]2.0.CO;2

Keogan, K., Daunt, F., Wanless, S., Phillips, R. A., Walling, C. A., Agnew, P., … Lewis, S. (2018). Global phenological insensitivity to shifting ocean temperatures among seabirds. *Nature Climate Change*, *8*(4), 313–318. https://doi.org/10.1038/s41558-018-0115-z

Kerby, J. T., & Post, E. (2013a). Advancing plant phenology and reduced herbivore production in a terrestrial system associated with sea ice decline. *Nature Communications*, *4*. https://doi.org/10.1038/ncomms3514

Kerby, J. T., & Post, E. (2013b). Capital and income breeding traits differentiate trophic match–mismatch dynamics in large herbivores. *Philosophical Transactions of the Royal Society of London B: Biological Sciences*, *368*(1624), 20120484. https://doi.org/10.1098/rstb.2012.0484

Kharouba, H. M., Ehrlén, J., Gelman, A., Bolmgren, K., Allen, J. M., Travers, S. E., & Wolkovich, E. M. (2018). Global shifts in the phenological synchrony of species interactions over recent decades. *Proceedings of the National Academy of Sciences*, 201714511. https://doi.org/10.1073/pnas.1714511115

Klosterman, S. T., Melaas, E., Wang, J., Martinez, A., Frederick, S., O'Keefe, J., … Richardson, A. D. (2018). Fine-scale perspectives on landscape phenology from unmanned aerial vehicle (UAV) photography. *Agricultural and Forest Meteorology*, *248*, 397–407. https://doi.org/10.1016/j.agrformet.2017.10.015

Kuoo, G., & Suzuki, S. (1999). Flowering phenology of alpine plant Communities along a gradient of snowmelt timing. *Polar Bioscience*, *12*, 100–113.

Larsen, K. S., Ibrom, A., Jonasson, S., Michelsen, A., & Beier, C. (2007). Significance of cold-season respiration and photosynthesis in a subarctic heath ecosystem in Northern Sweden. *Global Change Biology*, *13*(7), 1498–1508. https://doi.org/10.1111/j.1365-2486.2007.01370.x

Linkosalmi, M., Aurela, M., Tuovinen, J.-P., Peltoniemi, M., Tanis, C. M., Arslan, A. N., … Laurila, T. (2016). Digital photography for assessing the link between vegetation phenology and CO_2 exchange in two contrasting northern ecosystems. *Geoscientific Instrumentation, Methods and Data Systems*, *5*(2), 417–426. https://doi.org/10.5194/gi-5-417-2016

Liston, G. E., Mcfadden, J. P., Sturm, M., & Pielke, R. A. (2008). Modelled changes in arctic tundra snow, energy and moisture fluxes due to increased shrubs. *Global Change Biology*, *8*(1), 17–32. https://doi.org/10.1046/j.1354-1013.2001.00416.x

Macias-Fauria, M., Karlsen, S. R., & Forbes, B. C. (2017). Disentangling the coupling between sea ice and tundra productivity in Svalbard. *Scientific Reports*, *7*(1), 8586. https://doi.org/10.1038/s41598-017-06218-8

Macias-Fauria, M., & Post, E. (2018). Effects of sea ice on Arctic biota: an emerging crisis discipline. *Biology Letters*, *14*(3), 20170702. https://doi.org/10.1098/rsbl.2017.0702

Meier, W. N., Fetterer, F., Savoie, M., Mallory, S., Duerr, R., & Stroeve, J. (2017). *NOAA/NSIDC Climate Data Record of Passive Microwave Sea Ice Concentration, Version 3. NOAA/NSIDC daily sea Ice CDR.* Boulder, Colorado USA: NSIDC: National Snow and Ice Data Center. Retrieved from https://doi.org/10.7265/N59P2ZTG

Menzel, A., Sparks, T. H., Estrella, N., Koch, E., Aasa, A., Ahas, R., … Zust, A. (2006). European phenological response to climate change matches the warming pattern. *Global Change Biology*, *12*(10), 1969–1976. https://doi.org/10.1111/j.1365-2486.2006.01193.x

Molau, U., & Mølgaard, P. (1996). International Tundra Experiment Manual. Retrieved from http://ibis.geog.ubc.ca/itex/PDFs/ITEXmanual.pdf

Molau, U., Urban Nordenhäll, & Bente Eriksen. (2005). Onset of Flowering and Climate Variability in an Alpine Landscape: A 10-Year Study from Swedish Lapland. *American Journal of Botany*, *92*(3), 422–431.

Mølgaard P., & Christensen K. (2003). Response to experimental warming in a population of Papaver radicatum in Greenland. *Global Change Biology*, *3*(S1), 116–124. https://doi.org/10.1111/j.1365-2486.1997.gcb140.x

Moorter, B., Bunnefeld, N., Panzacchi, M., Rolandsen, C. M., Solberg, E. J., Sæther, B., & Fryxell, J. (2013). Understanding scales of movement: animals ride waves and ripples of environmental change. *Journal of Animal Ecology*, *82*(4), 770–780. https://doi.org/10.1111/1365-2656.12045

Naimi, B., Hamm, N. A. S., Groen, T. A., Skidmore, A. K., & Toxopeus, A. G. (2014). Where is positional uncertainty a problem for species distribution modelling. *Ecography*, *37*, 191–203. https://doi.org/10.1111/j.1600-0587.2013.00205.x

NSIDC. (2018). Polar Stereographic Projection and Grid | National Snow and Ice Data Center. Retrieved 7 March 2018, from https://nsidc.org/data/polar-stereo/ps_grids.html

Oberbauer, S. F., Elmendorf, S. C., Troxler, T. G., Hollister, R. D., Rocha, A. V., Bret-Harte, M. S., … Welker, J. M. (2013). Phenological response of tundra plants to background climate variation tested using the International Tundra Experiment. *Philosophical Transactions of the Royal Society of London B: Biological Sciences*, *368*(1624), 20120481. https://doi.org/10.1098/rstb.2012.0481

Panchen, Z. A., & Gorelick, R. (2017). Prediction of Arctic plant phenological sensitivity to climate change from historical records. *Ecology and Evolution*, *7*(5), 1325–1338. https://doi.org/10.1002/ece3.2702

Park, T., Ganguly, S., Tømmervik, H., Euskirchen, E. S., Høgda, K.-A., Karlsen, S. R., … Myneni, R. B. (2016). Changes in growing season duration and productivity of northern vegetation inferred from long-term remote sensing data. *Environmental Research Letters*, *11*(8), 084001. https://doi.org/10.1088/1748-9326/11/8/084001

Parker, T. C., Tang, J., Clark, M. B., Moody, M. M., & Fetcher, N. (2017). Ecotypic differences in the phenology of the tundra species Eriophorum vaginatum reflect sites of origin. *Ecology and Evolution*, *7*(22), 9975–9786. https://doi.org/10.1002/ece3.3445

Parmesan, C., & Yohe, G. (2003). A globally coherent fingerprint of climate change impacts across natural systems. *Nature*, *421*(6918), 37–42. https://doi.org/10.1038/nature01286

Pedersen, S. H., Liston, G. E., Tamstorf, M. P., Westergaard-Nielsen, A., & Schmidt, N. M. (2015). Quantifying Episodic Snowmelt Events in Arctic

Ecosystems. *Ecosystems*, *18*(5), 839–856. https://doi.org/10.1007/s10021-015-9867-8

Peng, G., Meier, W. N., Scott, D. J., & Savoie, M. H. (2013). A long-term and reproducible passive microwave sea ice concentration data record for climate studies and monitoring. *Earth System Science Data*, *5*(2), 311–318. https://doi.org/10.5194/essd-5-311-2013

Phoenix, G. K., & Bjerke, J. W. (2016). Arctic browning: extreme events and trends reversing arctic greening. *Global Change Biology*, *22*(9), 2960–2962. https://doi.org/10.1111/gcb.13261

Piao, S., Ciais, P., Friedlingstein, P., Peylin, P., Reichstein, M., Luyssaert, S., … Vesala, T. (2008). Net carbon dioxide losses of northern ecosystems in response to autumn warming. *Nature*, *451*(7174), 49–52. https://doi.org/10.1038/nature06444

Post, E., Forchhammer, M. C., Bret-Harte, M. S., Callaghan, T. V., Christensen, T. R., Elberling, B., … Aastrup, P. (2009). Ecological Dynamics Across the Arctic Associated with Recent Climate Change. *Science*, *325*(5946), 1355–1358. https://doi.org/10.1126/science.1173113

Post, E., Bhatt, U. S., Bitz, C. M., Brodie, J. F., Fulton, T. L., Hebblewhite, M., … Walker, D. A. (2013). Ecological Consequences of Sea-Ice Decline. *Science*, *341*(6145), 519–524. https://doi.org/10.1126/science.1235225

Post, E., & Høye, T. T. (2013). Advancing the long view of ecological change in tundra systems. *Philosophical Transactions of the Royal Society of London B: Biological Sciences*, *368*(1624), 20120477. https://doi.org/10.1098/rstb.2012.0477

Post, E., Kerby, J. T., Pedersen, C., & Steltzer, H. (2016). Highly individualistic rates of plant phenological advance associated with arctic sea ice dynamics. *Biology Letters*, *12*(12), 20160332. https://doi.org/10.1098/rsbl.2016.0332

Post, E., Pedersen, C., Wilmers, C. C., & Forchhammer, M. C. (2008). Warming, plant phenology and the spatial dimension of trophic mismatch for large herbivores. *Proceedings of the Royal Society of London B: Biological Sciences*, *275*(1646), 2005–2013. https://doi.org/10.1098/rspb.2008.0463

Post, E., Steinman, B. A., & Mann, M. E. (2018). Acceleration of phenological advance and warming with latitude over the past century. *Scientific Reports*, *8*(1), 3927. https://doi.org/10.1038/s41598-018-22258-0

Prevéy, J., Vellend, M., Rüger, N., Hollister, R. D., Bjorkman, A. D., Myers-Smith, I. H., … Rixen, C. (2017). Greater temperature sensitivity of plant phenology at colder sites: implications for convergence across northern latitudes. *Global Change Biology*, *23*(7), 2660–2671. https://doi.org/10.1111/gcb.13619

R Core Team. (2018). *R: A Language and Environment for Statistical Computing*. Vienna, Austria: R Foundation for Statistical Computing. Retrieved from https://www.R-project.org

Richardson, A. D., Hufkens, K., Milliman, T., Aubrecht, D. M., Chen, M., Gray, J. M., … Frolking, S. (2018). Tracking vegetation phenology across diverse North American biomes using PhenoCam imagery. *Scientific Data*, *5*, 180028. https://doi.org/10.1038/sdata.2018.28

Richardson, A. D., Keenan, T. F., Migliavacca, M., Ryu, Y., Sonnentag, O., & Toomey, M. (2013). Climate change, phenology, and phenological control of vegetation feedbacks to the climate system. *Agricultural and Forest Meteorology*, *169*, 156–173. https://doi.org/10.1016/j.agrformet.2012.09.012

Sawyer, H., & Kauffman, M. J. (2011). Stopover ecology of a migratory ungulate. *Journal of Animal Ecology*, *80*(5), 1078–1087. https://doi.org/10.1111/j.1365-2656.2011.01845.x

Scheifinger, H., Menzel, A., Koch, E., Peter, C., & Ahas, R. (2002). Atmospheric mechanisms governing the spatial and temporal variability of phenological phases in central Europe. *International Journal of Climatology*, *22*(14), 1739–1755. https://doi.org/10.1002/joc.817

Schielzeth, H. (2010). Simple means to improve the interpretability of regression coefficients. *Methods in Ecology and Evolution*, *1*(2), 103–113. https://doi.org/10.1111/j.2041-210X.2010.00012.x

Schmidt, N. M., Christensen, T. R., & Roslin, T. (2017). A high arctic experience of uniting research and monitoring. *Earth's Future*, *5*(7), 650–654. https://doi.org/10.1002/2017EF000553

Schmidt, N. M., Hansen, L. H., Hansen, J., Berg, T. B., & Meltofte, H. (2016). BioBasis Manual - 19th Edition. Aarhus University Department of Bioscience. Retrieved from http://zackenberg.dk/fileadmin/Resources/DMU/GEM/Zackenberg/Nye_Zac_files/BioBasis_manual_2016.pdf

Schmidt, N. M., Mosbacher, J. B., Nielsen, P. S., Rasmussen, C., Høye, T. T., & Roslin, T. (2016). An ecological function in crisis? The temporal overlap between plant flowering and pollinator function shrinks as the Arctic warms. *Ecography*, *39*(12), 1250–1252. https://doi.org/10.1111/ecog.02261

Screen, J. A., & Simmonds, I. (2010). The central role of diminishing sea ice in recent Arctic temperature amplification. *Nature*, *464*(7293), 1334–1337. https://doi.org/10.1038/nature09051

Semenchuk, P. R., Gillespie, M. A. K., Rumpf, S. B., Baggesen, N., Elberling, B., & Cooper, E. J. (2016). High Arctic plant phenology is determined by snowmelt patterns but duration of phenological periods is fixed: an example of periodicity. *Environmental Research Letters*, *11*(12), 125006. https://doi.org/10.1088/1748-9326/11/12/125006

Sherwood, J. A., Debinski, D. M., Caragea, P. C., & Germino, M. J. (2017). Effects of experimentally reduced snowpack and passive warming on montane meadow plant phenology and floral resources. *Ecosphere*, *8*(3). https://doi.org/10.1002/ecs2.1745

Starr, G., & Oberbauer, S. F. (2003). Photosynthesis of arctic evergreens under snow: implications for tundra ecosystem carbon balance. *Ecology*, *84*(6), 1415–1420. https://doi.org/10.1890/02-3154

Sturm, M., Holmgren, J., McFadden, J. P., Liston, G. E., Chapin, F. S., & Racine, C. H. (2001). Snow–Shrub Interactions in Arctic Tundra: A Hypothesis with Climatic Implications. *Journal of Climate*, *14*(3), 336–344. https://doi.org/10.1175/1520-0442(2001)014<0336:SSIIAT>2.0.CO;2

Thackeray, S. J. (2016). Casting your network wide: a plea to scale-up phenological research. *Biology Letters*, *12*(6), 20160181. https://doi.org/10.1098/rsbl.2016.0181

Thackeray, S. J., Henrys, P. A., Hemming, D., Bell, J. R., Botham, M. S., Burthe, S., … Wanless, S. (2016). Phenological sensitivity to climate across taxa and trophic levels. *Nature*, *535*(7611), 241–245. https://doi.org/10.1038/nature18608

Thórhallsdóttir, T. E. (1998). Flowering phenology in the central highland of Iceland and implications for climatic warming in the Arctic. *Oecologia*, *114*(1), 43–49. https://doi.org/10.1007/s004420050418

Tjernström, M., Shupe, M. D., Brooks, I. M., Persson, P. O. G., Prytherch, J., Salisbury, D. J., … Wolfe, D. (2015). Warm-air advection, air mass transformation and fog causes rapid ice melt. *Geophysical Research Letters*, *42*(13), 5594–5602. https://doi.org/10.1002/2015GL064373

van de Pol, M., & Wright, J. (2009). A simple method for distinguishing within- versus between-subject effects using mixed models. *Animal Behaviour*, *77*(3), 753–758. https://doi.org/10.1016/j.anbehav.2008.11.006

Visser, M. E., & Both, C. (2005). Shifts in phenology due to global climate change: the need for a yardstick. *Proceedings of the Royal Society of London B: Biological Sciences*, *272*(1581), 2561–2569. https://doi.org/10.1098/rspb.2005.3356

Webber, P. J., & Walker, M. D. (1991). The International Tundra Experiment (ITEX): resolution. *Arctic Antarctic and Alpine Research*, *23*, 124.

Westergaard-Nielsen, A., Lund, M., Pedersen, S. H., Schmidt, N. M., Klosterman, S. T., Abermann, J., & Hansen, B. U. (2017). Transitions in high-Arctic vegetation growth patterns and ecosystem productivity tracked with automated cameras from 2000 to 2013. *Ambio*, *46*(1), 39–52. https://doi.org/10.1007/s13280-016-0864-8

Wheeler, H. C., Høye, T. T., Schmidt, N. M., Svenning, J.-C., & Forchhammer, M. C. (2015). Phenological mismatch with abiotic conditions—implications for flowering in Arctic plants. *Ecology*, *96*(3), 775–787. https://doi.org/10.1890/14-0338.1

Wheeler, J. A., Cortés, A. J., Sedlacek, J., Karrenberg, S., Kleunen, M., Wipf, S., … Cornelissen, H. (2016). The snow and the willows: earlier spring snowmelt

reduces performance in the low-lying alpine shrub Salix herbacea. *Journal of Ecology*, *104*(4), 1041–1050. https://doi.org/10.1111/1365-2745.12579

Winton, M. (2006). Amplified Arctic climate change: What does surface albedo feedback have to do with it? *Geophysical Research Letters*, *33*(3). https://doi.org/10.1029/2005GL025244

Wipf, S. (2009). Phenology, growth, and fecundity of eight subarctic tundra species in response to snowmelt manipulations. *Plant Ecology*, *207*(1), 53–66. https://doi.org/10.1007/s11258-009-9653-9

Wipf, S., & Rixen, C. (2010). A review of snow manipulation experiments in Arctic and alpine tundra ecosystems. *Polar Research*, *29*(1), 95–109. https://doi.org/10.1111/j.1751-8369.2010.00153.x

Wipf, S., Stoeckli, V., & Bebi, P. (2009). Winter climate change in alpine tundra: plant responses to changes in snow depth and snowmelt timing. *Climatic Change*, *94*(1–2), 105–121. https://doi.org/10.1007/s10584-009-9546-x

Wolkovich, E. M., Cook, B. I., Allen, J. M., Crimmins, T. M., Betancourt, J. L., Travers, S. E., … Cleland, E. E. (2012). Warming experiments underpredict plant phenological responses to climate change. *Nature*, *485*(7399), 494–497. https://doi.org/10.1038/nature11014

Wolkovich, E. M., Cook, B. I., & Davies, T. J. (2014). Progress towards an interdisciplinary science of plant phenology: building predictions across space, time and species diversity. *New Phytologist*, *201*(4), 1156–1162. https://doi.org/10.1111/nph.12599

Worby, A., & Comiso, J. C. (2004). Studies of the Antarctic sea ice edge and ice extent from satellite and ship observations. *Remote Sensing of Environment*, *92*(1), 98–111. https://doi.org/10.1016/j.rse.2004.05.007

Xu, L., Myneni, R. B., Iii, F. S. C., Callaghan, T. V., Pinzon, J. E., Tucker, C. J., … Stroeve, J. C. (2013). Temperature and vegetation seasonality diminishment over northern lands. *Nature Climate Change*, *3*(6), 581–586. https://doi.org/10.1038/nclimate1836

Chapter 3 Vegetation monitoring using multispectral sensors – best practices and lessons learned from high latitudes

The author retrieving a drone after a successful flight on Qikiqtaruk.
Photo by Sandra Angers-Blondin.

Chapter 3 Vegetation monitoring using multispectral sensors – best practices and lessons learned from high latitudes

The following chapter has been accepted by the Journal for Unmanned Vehicle Systems as a primary research article. At the time of submission of this thesis, the article was in press.

Authors: Jakob J Assmann[1,2], Jeffrey T Kerby[3], Andrew M Cunliffe[1,4] and Isla H Myers-Smith[1]

Affiliations:
[1] School of GeoSciences, The University of Edinburgh, Edinburgh, UK
[2] School of Biology, The University of Edinburgh, Edinburgh, UK
[3] Neukom Institute for Computational Science, Institute of Arctic Studies, Dartmouth College, USA
[4] School of Geography, University of Exeter, Exeter, UK

Author Contributions: JJA and IHMS conceived the study. JJA performed the analysis and wrote the manuscript with input from all authors

Abstract

Rapid technological advances have dramatically increased affordability and accessibility of Unmanned Aerial Vehicles (UAVs) and associated sensors. Compact multispectral drone sensors capture high-resolution imagery in visible and near-infrared parts of the electromagnetic spectrum, allowing for the calculation of vegetation indices such as the Normalised Difference Vegetation Index (NDVI) for productivity estimates and vegetation classification. Despite the technological advances, challenges remain in capturing high-quality data, highlighting the need for standardized workflows. Here, we discuss challenges, technical aspects and practical considerations of vegetation monitoring using multispectral drone sensors and propose a workflow based on remote sensing principles and our field experience in high-latitude environments, using the Parrot Sequoia (Pairs, France) sensor as an example. We focus on the key error sources associated with solar angle, weather conditions, geolocation and radiometric calibration and estimate their relative contributions that can lead to uncertainty of greater than ±10% in peak season NDVI estimates of our tundra field site. Our findings show that these errors can be accounted for by improved flight planning, meta-data collection, ground control point deployment, use of reflectance targets and quality control. With standardized best practice, multispectral sensors can provide meaningful spatial data that is reproducible and comparable across space and time.

Introduction

Aerial imagery collected with drones is increasingly recognised by the ecological research community as an important tool for monitoring vegetation and ecosystems (Anderson and Gaston 2013, Salamí et al. 2014, Cunliffe et al. 2016, Pádua et al. 2017, Torresan et al. 2017, Manfreda et al. 2018). Rapid advances in technology have resulted in increasing affordability and use of light-weight multispectral sensors for drones for a variety of scientific applications. Despite the increased presence of drone-sensor derived products in the published literature, standardized protocols and best practices for fine-grain multispectral drone-based mapping have yet to be developed by the ecological research community (Manfreda et al. 2018). In this methods paper, we lay out the challenges of collecting and analysing multispectral data acquired with drone platforms and propose common protocols that could be implemented in the field, drawing from examples of applying drone technology to research in high-latitude ecosystems. The concepts developed herein are aimed at researchers with limited prior experience in remote sensing and spectroscopy, providing the tools and guidance needed to plan high quality drone-based multispectral data collection.

Multispectral imagery is widely used in satellite- and airplane-based remote sensing and has many benefits for vegetation monitoring when compared to conventional broad band visible-spectrum imagery. Including near-infrared parts of the spectrum, certain vegetation indices (VIs) can be calculated that allow for more detailed spectral discrimination among plant types and development stages. Such VIs can be highly useful for estimating biological parameters such as vegetation productivity and the leaf-area index (LAI; e.g. see Aasen et al. 2015, Wehrhan et al. 2016), and for the purpose of vegetation classification (Juszak et al. 2017, Ahmed et al. 2017, Müllerová et al. 2017, Samiappan et al. 2017, Dash et al. 2017). Particularly in remote high-latitude ecosystems, where satellite records suggest a ‘greening’ of tundra ecosystems from NDVI time series (Fraser et al. 2011, Guay et al. 2014, Ju and Masek 2016), multispectral drone monitoring could play an important role in validating satellite remotely-sensed productivity trends (Laliberte et al. 2011, Matese et al. 2015).

A variety of multispectral camera and sensor options are available and have been deployed with drones. These range from modified off-the-shelf digital cameras (Lebourgeois et al. 2008, for examples see Berra et al. 2017, Müllerová et al. 2017), to compact purpose-built multi-band drone sensors such as the Parrot Sequoia (Ahmed et al. 2017, Fernández-Guisuraga et al. 2018) and the MicaSense Red-Edge (Samiappan et al. 2017, Dash et al. 2017). The Parrot Sequoia and MicaSense Red-Edge sensors are compact bundles (rigs) of 4-5 cameras with Complementary Metal-Oxide-Semiconductor (CMOS) (Weste 2011) sensors, a type of imaging sensor commonly found in phones and digital single lens reflex (DSLRs) consumer cameras. Each camera in the rig is equipped with an individual narrow-band filter that removes all but a discrete section of the visible and/or near-infrared parts of the spectrum (Table 3-1). New multispectral camera and sensor options continue to be released as technologies develop rapidly, yet many common considerations exist with the use of these type of sensors for the collection of vegetation monitoring data that we describe below.

The purpose-made design of the recent generation of multiband drone sensors provide many improvements that increase the ease of use, quality and accuracy of the collected multispectral aerial imagery. These include: precise co-registration of bands, characterised sensor responses, well defined narrow bands, sensor attitude correction, ambient light sensors, geo-tagged imagery, and seamless integration into photogrammetry software such as Pix4Dmapper (Pix4D SA, Lausanne, Switzerland) and PhotoScan Pro (Aigsoft, St. Petersburg, Russia). Despite these advances, acquiring multispectral drone imagery that is comparable across sensors, space, and time requires careful planning and best practices to minimise the effect of measurement errors caused by three main sources 1) differences among sensors and sensor units, 2) changes in ambient light (weather and position of sun), and 3) spatially-constraining the imagery (Kelcey and Lucieer 2012, Turner et al. 2014, Salamí et al. 2014, Aasen et al. 2015, Pádua et al. 2017).

Table 3-1 | Band wavelengths (nm) of the Parrot Sequoia and MicaSense Red-Edge Sensors with comparable Sentinel, Landsat, MODIS and AVHRR bands (Barnes et al. 1998, NOAA 2014, Barsi et al. 2014, European Space Agency 2015, MicaSense 2016a, 2016b). Vegetation indices such as the NDVI, derived from the read and near-infrared bands, can be notably affected by differences in spectral bandwidth. For the NDVI the position of the red band has been found to be of particular importance (Teillet 1997).

Sensor	Blue	Green	Red	Red-Edge	Near-Infrared
Parrot Sequoia	-	530 - 570	640 - 680	730 - 740	770 - 810
Mica Sense RedEdge	465 - 485	550 - 570	663 - 673	712 - 722	820 - 860
Sentinel 2 (10 m)	457.5 - 522.5	542.5 - 577.5	650 - 680		784.5 - 899.5
Sentinel 2 (20 m)				697.5 - 712.5 (Band 5)	
				732.5 - 747.5 (Band 6)	838.75 -891.25 (Band 8b)
				773 - 793 (Band 7)	

With the goal of collecting comparable and reproducible drone imagery in mind, we discuss the fundamental technical background of multispectral drone sensors (Section 1), outline the proposed workflow for data collection and processing (Section 2) and conclude by reviewing the most important steps of the protocol in more detail (Section 3-6). These perspectives emerged from protocols originally developed for the High Latitude Drone Ecology Network (HiLDEN – arcticdrones.org) and build on examples drawn from data collected with a Parrot Sequoia at our focal study site Qikiqtaruk – Herschel Island (QHI), Yukon Territory, in north-western Canada and processed in Pix4Dmapper. Nonetheless, much of the discussed content should transfer directly to other multispectral drone sensors, including the MicaSense RedEge and Tetracam products, as well as to a lesser degree modified conventional cameras.

Technical Background on Multispectral Drone Sensors (Section 1)

A fundamental aim of vegetation surveys with multispectral drone sensors is to measure surface reflectance across space for two or more specific bands of wavelengths (e.g. the red and near-infrared bands), which then serve as a base for calculating VIs (such as the NDVI) or to inform surface cover classifications. Reflectance is the fraction of incident light reflected at the interface of a surface. VIs enhance the characteristic electromagnetic reflectance signatures of different surfaces (such as bare ground, sparse or dense vegetation), whereas classifications

often partition images based on these differences. Leaf structure and chlorophyll content influence the spectral signatures of plants, and VIs transform spectra-specific variability into single variables that can be related to other measures of vegetation productivity and leaf area index (LAI) (Tucker 1979, Guay et al. 2014, e.g. see Aasen et al. 2015). In practice, drone-based reflectance maps are usually created by collecting many overlapping images of an area of interest, which are then combined into a single orthomosaic (map) with a photogrammetry software package (such as Pix4Dmapper or Agisoft PhotoScan).

Reflectance is not directly measured by multispectral imaging sensors, instead they measure at-sensor radiance, the radiant flux received by the sensor (Figure 3-1). Surface reflectance is a property of the surface independent on the incident radiation (ambient light), whereas at-sensor radiance is a function of surface radiance (flux of radiation from the surface) and atmospheric disturbance between surface and sensor (see Wang and Myint 2015 for a detailed discussion). Surface radiance itself is highly dependent on the incident radiation, and disturbance between surface and sensors is often assumed to be negligible for drone-based surveys (Duffy et al. 2017). At-sensor radiance measurements are stored as arbitrary digital numbers (DN) in the image files for each band at a determined bit depth. Without modification, the DNs may serve as a proxy for relative differences of surface reflectance during the ambient light conditions of a particular survey, but if absolute surface reflectance measurements are desired - e.g. for cross site, sensor or time comparison - a conversion (“calibration”) of the digital numbers into absolute surface reflectance values is essential (Figure 3-1).

There are several ways to convert image DNs into absolute surface reflectance, but the most common is the so-called empirical line approach: Images of surfaces with known reflectance are used to establish an assumed linear relationship (empirical line) between image DNs and surface reflectance under the specific light conditions of the survey (Laliberte et al. 2011, Turner et al. 2014, Wang and Myint 2015, Aasen et al. 2015, Wehrhan et al. 2016, Ahmed et al. 2017, Crusiol et al. 2017, Dash et al. 2017). Additionally, information from incident light sensors, such as the Parrot Sequoia sunshine sensor may be incorporated to account for changes in irradiation during the flight. We would like to highlight here that this is not a calibration of the

sensor itself, but a calibration of the output data. Practical aspects of radiometric calibration are discussed later in Section 6.

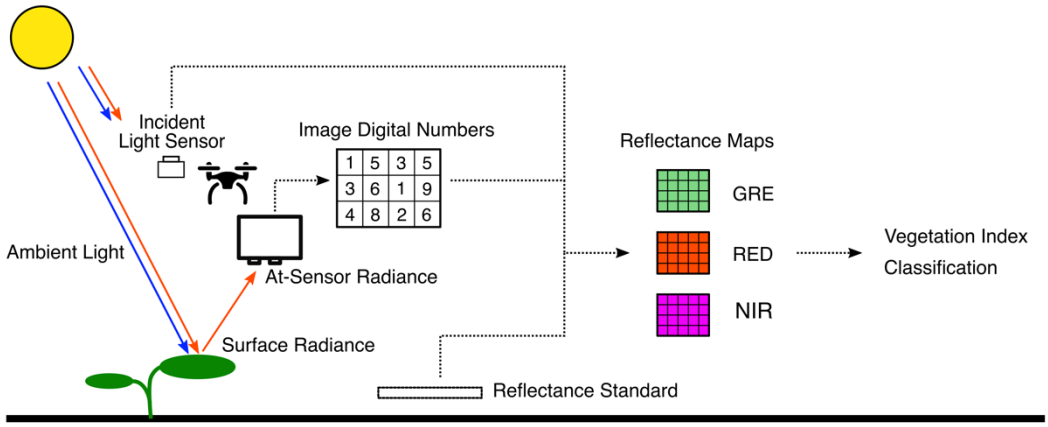

Figure 3-1 | Simplified flow of information from surface radiance to reflectance maps using multispectral drone sensors. Surface radiance is measured as at-sensor radiance for each band by the drone sensor and saved as digital numbers (DNs) in an image file. Image DNs are then converted ("calibrated") into reflectance values using an image of a reflectance standard acquired at the time point of the survey. The resulting reflectance maps for each of the sensor's bands can then be used to calculate vegetation indices or as direct inputs for classification. Drone symbol by Mike Rowe from the Noun Project (CC-BY, http://thenounproject.com).

The relationship between DN and the surface reflectance value of a pixel is also influenced by the optical apparatus and the spectral response of the sensor, which require additional corrections (see Kelcey and Lucieer 2012 and, Wang and Myint 2015 for in-depth discussions). For the latest generation of sensors (e.g. MicaSense RedEdge and Parrot Sequoia) the processing software packages (such as Pix4Dmapper) automatically apply these corrections and little input is required from the user in this respect. Instructions on how to carry out the calibrations manually has been made available by some manufacturers (Parrot 2017a, Agisoft 2018, MicaSense 2018c) and may be used by advanced users to develop their own processing workflow. However, understanding the principles of these corrections and why they are required can be helpful to all users when planning multispectral drone surveys and handling the data outputs.

Firstly, the optical apparatus (i.e. filters and lenses) distort the light on its way to the sensor and therefore influence the relative amount of radiation reaching each pixel.

Effects such as vignetting - pixels on the outsides of the images receive less light than those in the centre of the image (Kelcey and Lucieer 2012) – can produce desirable aesthetic effects in conventional photography, but bias data in different parts of the images when mapping surface reflectance. Converting the DNs of all pixels the same way would incorrectly estimate reflectance values towards the extremes of each image. This can be corrected for if the effects of the optical apparatus of the sensor have been characterised sufficiently (Kelcey and Lucieer 2012, Salamí et al. 2014).

Secondly, the relationship between DN and radiant flux is dependent on the sensitivity of the CMOS sensor unit in the specific band of the spectrum, the shutter speed, as well as the aperture and ISO value (signal current amplification at the sensor pixel level) settings during image capture. In the case of the Parrot Sequoia, this relationship is a linear function for which the parameters are characterised for each individual sensor unit at production. This is one of the major advantages of using purpose-built sensors such as the Parrot Sequoia and alike over modified consumer cameras. The relevant parameters of this relationship can be extracted from the image EXIF tags and applied to each image to obtain arbitrary reflectance values common to all Sequoias. These arbitrary reflectance values can then be converted into absolute reflectance using a standard of known reflectance (see Parrot 2017c).

When using Pix4Dmapper for processing Parrot Sequoia or MicaSense RedEdge data these corrections are automatically carried out by the software (Pix4d Personal Communication June 2017). Apart from defining the radiometric calibration image to establish the empirical line relationship, no additional input is required. The exact algorithms of Pix4Dmapper are proprietary and will likely remain a black box to the scientific community and may change between software versions. To the best of our knowledge, at this time, there is no open source software currently available with the same scope and ease of handling of Pix4Dmapper for processing multispectral drone data. During the completion of this manuscript, radiometric calibration features have been added to recent releases of Agisoft PhotoScan Pro (St. Petersburg, Russia), a similar proprietary photogrammetric software (Agisoft 2018).

Multispectral Drone Sensor

- A light-weight camera rig with at least two digital imaging sensors that capture monochromatic imagery in well-characterised and narrow bands of the electromagnetic spectrum. Often include bands outside the visible spectrum. Used to determine surface reflectance across space.

Surface Reflectance

- Proportion of electromagnetic radiation reflected by a surface. Here specifically, the proportion of electromagnetic radiation reflected by a surface within narrow bands of the electromagnetic spectrum.

Vegetation Index (VI)

- Mathematical transformation of surface reflectance values across multiple bands to allow for the estimation of vegetation productivity and surface cover type classifications.

Digital Number (DN)

- Sensor-specific value used to denote strength of radiant flux to a sensor pixel. Arbitrary in nature, it requires knowledge of sensor response, optical apparatus and ambient light conditions to allow for conversion into surface reflectance values.

Ground Sampling Distance (GSD)

- Distance between pixel centres or pixel-width measured on the ground of a digital aerial image.

Ground Control Points (GCPs)

- Artificial or natural features with (often very accurately) known locations used to geo-rectify aerial imagery.

Structure from Motion (SfM)

- Computational technique (computer vision) that uses relative positions of pixels from overlapping imagery of the same scene obtained at different angles to construct 3D models and composite orthomosaic images.

Orthomosaic

- Mosaic of geometrically corrected (orthorectified) images so that scale is uniform across the mosaic from a nadir perspective (viewer 90° above viewing plane).

Reflectance Map

- Orthomosaic of monochromatic imagery in a specific spectral band obtained with a multiband drone sensor. Pixel values contain (often radiometrically calibrated) surface reflectance values (ranging from 0 to 1). Can be used to calculate maps of vegetation indices.

Data collection and processing – Workflow overview (Section 2)

Specific research questions and scientific objectives should be used to determine the exact methods used and the data outputs required from a multispectral drone survey (Figure 3-2). However, using a standardized workflow will help users avoid common pitfalls that affect data quality, and thus ensure repeatable and comparable data collection through time and across sites. We suggest starting by identifying the spatial and temporal scales required to address the research questions and scientific objectives (Step 1). Explicit consideration of scale is critical to the quantification and interpretation of any environmental pattern (Turner et al. 1989, Levin 1992), thus particular attention is required when planning drone surveys due to the scale-dependent nature of these inherently spatial data and its associated errors.

The selected spatial and temporal scales, together with the capabilities of the drone platform form the basis for flight planning (Step 2). Flight paths and image overlap (Section 3), as well as weather conditions and solar position (Section 4) are especially important to consider when planning multispectral drone surveys because of their impact on mosaicking and radiometric calibration. Once the flight plan is established, ground control points (GCPs) and radiometric in-flight targets need to be deployed on site, their locations determined with a high-accuracy global navigation satellite systems (GNSS) device (e.g. a survey-grade GPS receiver), and radiometric calibration imagery taken (Steps 3 and 4). We will discuss practical aspects of GCPs deployment and radiometric calibration in the final two sections (Section 5 and 6, respectively).

Once pre-flight preparations are completed, the drone is launched and the image data collected (Step 5). Though this may sound straight forward, in practice this can be challenging. Technical issues such as aircraft material failure, weather impacts on realized vs. planned flight path, and/or compass issues are not uncommon. Operator skill and logistical experience in the field should not be discounted, particularly when operating in extreme environments such as those found in the high latitudes (Duffy et al. 2017). Manufacturer guidance, online discussion boards and email lists (such as the HiLDEN network: arcticdrones.org) can provide help and information on these technical problems. Upon completion of the flight, image data can be retrieved from the sensors and transferred to a computer for processing. We recommend backing

up the drone / sensor memory after every flight to reduce the risk of data loss due to hardware failure and crashes.

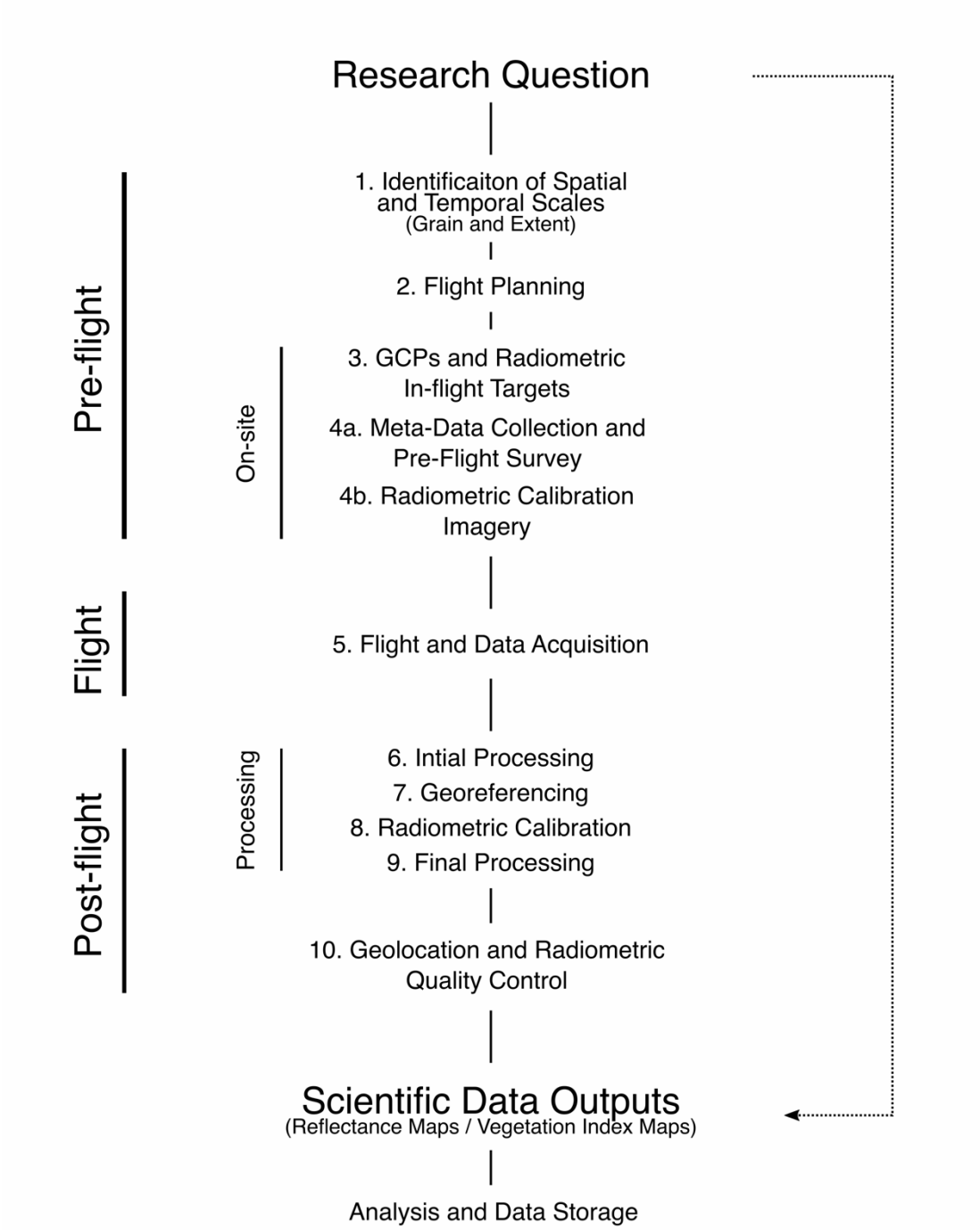

Figure 3-2 | Overview of the proposed workflow for scientific data collection using multispectral drone sensors and guide to the sections of this publication. Flight planning is discussed in Sections 3 (Image Overlap and Ground Sampling Distance) and Section 4 (Weather and Sun) of this manuscript. Geo-location and use of ground control points (GCPs) in Section 5 and Radiometric Calibration in Section 6.

Processing will vary with the type of sensor / software that is used. Figure 3-2 outlines the core steps when processing Parrot Sequoia data with Pix4Dmapper Desktop. The initial processing step (Step 6) creates a rough model of the area surveyed using Structure from Motion – Multiview Stereo algorithms (SfM-MVS) (Westoby et al. 2012). The user then manually places GCP markers for improving estimates of the camera positions and lens model parameters (Step 7) and carries out the radiometric calibration (Step 8). These inputs are then incorporated by the software in a final processing step (Step 9), producing reflectance map and VI map outputs.

We suggest a final quality control step (Step 10) to assess the accuracy of the geo-location and radiometric calibration of the outputs, before using them in the analysis to answer the research questions. We also highlight that drone surveys can produce large amounts of data that can create challenges for data handling and archiving. It is helpful to produce a storage and archiving plan before data collection begins, test flights can provide valuable insights on data volume expectations for the project.

Flight planning and overlap (Section 3)

A well-designed flight plan ensures that the full extent of the area of interest is covered at the appropriate grain size to fulfil the scientific objectives of the survey. The capabilities of drone and sensor, the terrain and meteorological conditions, as well as local regulations will constrain what is practically achievable. Flight planning software and manufacture guidance can assist, and a wealth of information on flight planning and practise is available on the internet, including guidance on the legal aspects of operating drones in different jurisdictions. Furthermore, pre-flight site visits (“recces”) can be highly valuable for identifying obstacles and can inform about topographic constraints that may affect flight planning and geolocation. Here, we will focus on two aspects of mission planning particularly important for multispectral surveys: 1) image overlap - the proportion of overlap between neighbouring individual images in the pool of images covering the area of interest; and 2) spatial grain size or ground sampling distance (GSD) - the width of the ground area represented by each pixel in the imagery. Both are closely linked to, and limited by, flight height and speed, as well as sensor size, resolution, focal length and trigger rate.

Image overlap influences the percentage of pixels captured near to nadir view angles (sensor at 90° above surface of interest). Vegetative surfaces do not have lambertian reflectance properties; *i.e.*, they do not reflect light evenly in all directions, instead their reflectance is a function of both angle of incident light and angle of view. These relationships can be complex and are commonly described with so called bidirectional reflectance distribution functions (BRDFs) (Kimes 1983, for example Bicheron and Leroy 2000). For multispectral drone surveys, non-uniform reflectance functions pose a challenge as they hamper the comparison of pixels captured at different angles of view (Aasen and Bolten 2018).

When obtaining surface reflectance imagery with wide-angled lenses, as those employed in many drone sensors, pixels near to the edges of the image have viewing angles notably different from 90° (up to 32° different for the Parrot Sequoia and up to 23.6° for the MicaSense RedEdge-M). If a nadir angle of view (observer 90° above observed point) is assumed for these pixels the reflectance values in the extremes of the image maybe under or overestimated. High amounts of image overlap (75% - 90% front lap and side lap) ensure that the whole area of interest is captured by pixels taken at near-nadir view. During processing these pixels can then be preferentially selected as best estimates for surface reflectance at nadir view. Pix4Dmapper carries out such a selection when creating reflectance maps (Pix4D Personal Communication, June 2017).

We recommend a minimum of 75% of for multispectral flights for both side- and front-lap (also recommended by MicaSense 2018a). Greater overlap might not always be better as there are penalties for very high amounts of overlap, affecting data storage and processing requirements. However, imagery can be thinned to reduce excessive overlap at the processing stage. We found that 80% overlap worked well for our data collection in low canopy tundra environments, in this case all parts of the area surveyed are within 10% of the image centre (near nadir-view for a stabilised sensor) in at least one image and support reliable reconstructions and good quality reflectance map outputs using Pix4Dmapper.

If high amounts of side- and front-lap are not achievable due to limitations of the aircraft or shutter speed of the sensor (*e.g.,* due to high flight speeds and wide turns

required by fixed-wing aircraft), adding cross-flight lines to the flight plan (Figure 3-3 A) or repeating the flight plan twice with a slightly shifted grid of the same orientation may be two of the many possible solutions. This will allow the coverage of larger proportions of the surveyed area at near-nadir angles and may reduce BRDF effects. In the case of the Parrot Sequoia, the RGB camera can also be disabled to increase trigger rates for the monochromatic multiband imagery. If problems occur with reconstruction of uniform vegetated surfaces or because of complicated terrains, two diagonal cross-flight lines may be added to the flight plan (Figure 3-3 B), this provides additional coverage of the area and may result in improved reconstructions.

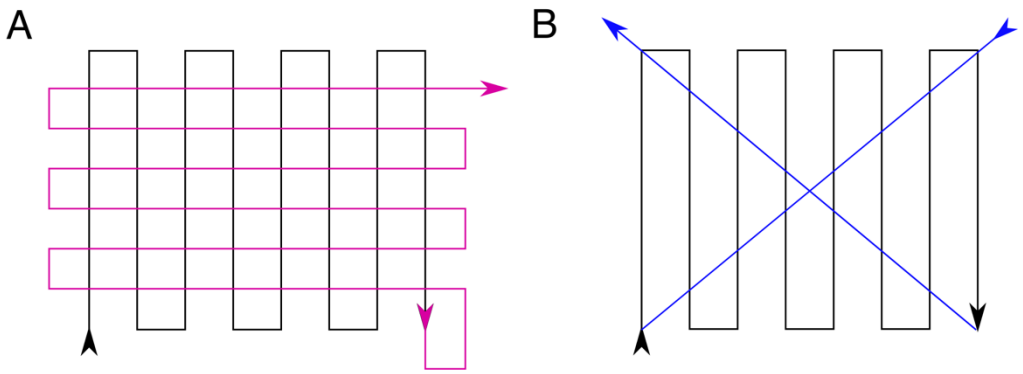

Figure 3-3 | A) Lawn-mower flight pattern (black) with perpendicular flight lines (pink) to achieve higher overlap and reduce BRDF effects when overlap is limited by aircraft or sensor triggering speed, and B) Lawn-mover pattern flight path (black) with additional diagonal flight lines (blue) that may aid reconstruction.

The ground sampling distance has a strong influence on the signal to noise ratio. GSD is a function of flight altitude, sensor resolution and optics. Imagery of vegetated surfaces at very small GSDs may contain a lot of noise due to non-uniform reflectance functions and movement of plant parts, such as leaves, between image acquisitions. High amounts of noise hamper key-point matching during SfM-MVS model reconstructions and can reduce the quality of reflectance map outputs, resulting in artefacts, blurry patches and distorted geometry. Pix4D recommends a GSD of 10 cm or coarser for densely vegetated areas (Pix4D 2018a). Nonetheless, we obtained consistently good results with slightly finer (5 cm) and coarser (15 cm) GSDs for the tussock sedge and shrub tundra vegetation types at our field site QHI in Arctic Canada during the data collection campaigns in 2016 and 2017.

When selecting a GSD it is particularly important to consider the scientific objectives of the survey and factor in the scale at which reflectance varies across the area of interest: If the objective is to monitor the distribution of large shrubs, then a larger GSD might be sufficient with the added benefits of reduced noise, the potential to cover larger areas due to higher flight altitudes, less required data storage and faster processing times. In contrast, if the objective is to monitor distribution of small grass tussocks, a smaller GSD might be required with potential penalties due to increased noise in the imagery and reduction in area that can be covered.

Weather and Sun (Section 4)

Weather and sun are additional factors that influence drone-captured multispectral imagery quality. Most drones will be unable to operate in high winds and rain; but cloud cover and solar position also influence the spectral composition of the ambient light and shadows, thus affecting image acquisition with multispectral drone sensors (Salamí et al. 2014, Pádua et al. 2017) . Variation in solar angle may introduce variation in VI estimates even within a single day or flight period (Figure 3-4). Radiometric calibration of the imagery (Section 6) is a key tool to account for the majority of this variation, but additional steps during flight planning and in-field data collection can be taken to control for some of these factors.

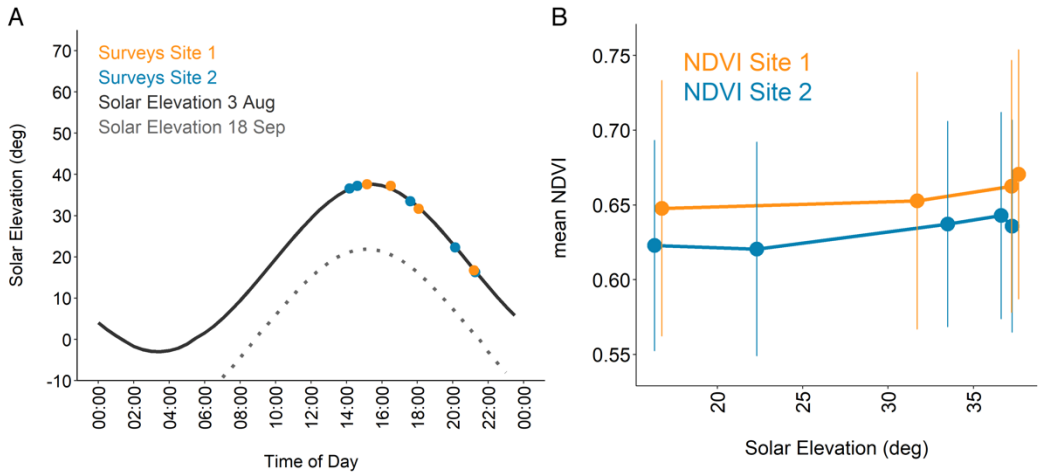

Figure 3-4 | Effect of diurnal solar variation on measured landscape scale mean NDVI. A) Time of day vs. solar elevation for Qikiqtaruk – Herschel Island on 3rd of August 2016 with time-points of repeat surveys shown in B. Light-grey dashed line shows the solar elevation curve for the 18th September 2016, illustrating similar magnitudes of seasonal and diurnal variation across the season at high latitude studies sites such as Qikiqtaruk. B) Effect of solar elevation on mean NDVI for repeat flights of sites on the 3rd of August 2016 on Qikiqtaruk – Herschel Island, highlighting the impact of solar angle and clouds on the mean NDVI values despite radiometric calibration in Pix4D mapper. Bars represent the standard deviation from the mean NDVI (5 cm GSD), illustrating within-site variation at the two 1-ha sites. Absolute differences between highest and lowest solar elevation are just above 0.02 NDVI. Thin stratus cloud cover for all flights except for the flight closest to peak solar elevation (37.22°) at site 2, with low dense cloud, potentially explaining its outlier character.

To minimise variations in solar angle, flights should be conducted as close to solar noon as possible. As a rule of thumb, we recommend a maximum of 2-3 hours before and after solar noon. Seasonal and diurnal variation in solar angle and position can be calculated using solar calculators (such as https://www.esrl.noaa.gov/gmd/grad/solcalc/index.html). At high latitude sites, solar angle will vary across the year in more dramatic ways than at lower latitudes, whereas lower latitudes experience stronger variation in diurnal angle. On clear days, solar position also determines the size and direction of shadows cast on the landscape by micro- and macro-variation in topography (i.e. furrows and ridges, vegetation and hills) (Figure 3-5).

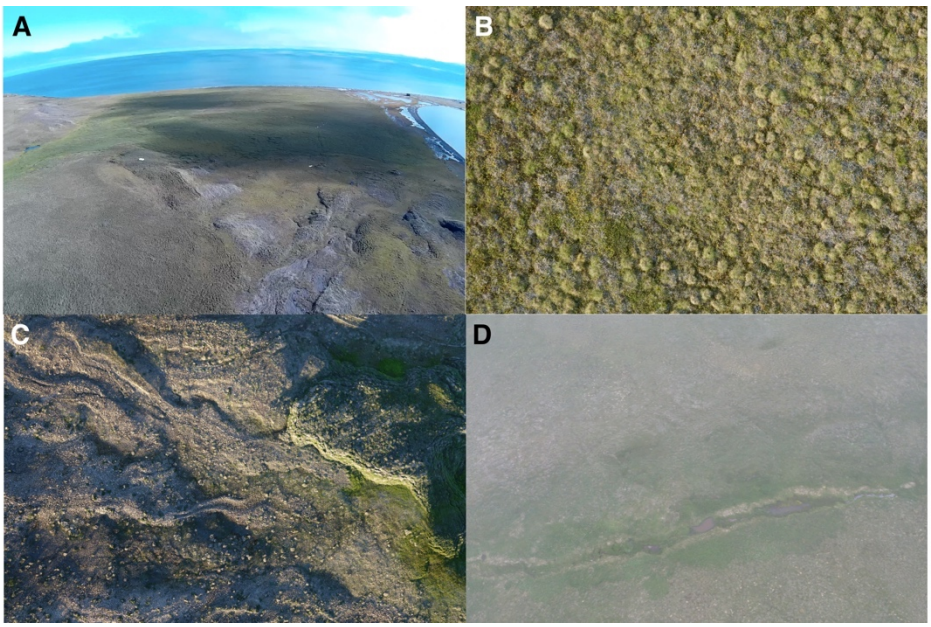

Figure 3-5 | RGB photographs of different cloud and sun angle conditions and their effect on scene illumination. A) “Popcorn” clouds casting well delimitated shadows across the landscape. B) Thin continuous stratus scattering light, resulting in even illumination of the scene and reduced shadows. C) Low solar angle interacting with microtopography, casting shadows across the landscape. D) Fog blurring the imagery and causing uneven illumination.

Under clear sky conditions, sun glint and hotspots can be present in the imagery, creating radiometric inaccuracies and potential issues for photogrammetric processing. Some efforts have been made towards detecting and mitigating these effects through post-processing of the imagery, and the relative position of sun and aircraft can be incorporated during flight planning to reduce their impact (Ortega-Terol et al. 2017). However, due to the low solar angles, sun glint and hotspots are less of a problem at high latitudes.

We recommend recording sky conditions during the flight (Table 3-2) to account for cloud-induced changes in the spectral composition of light and avoiding days where scattered cumulus clouds (“popcorn-clouds”) are partially shading survey area(s) (Figure 3-5). The collection of additional meteorological observations such as wind speed (may impact movement of vegetation), temperature and presence of dew/snow may be helpful to account for additional sources of variation in surface reflectance estimates.

Table 3-2 | Sky-Codes for qualitative classification of cloud related ambient light conditions. Table courtesy of NERC Field Spectroscopy Facility, Edinburgh UK (2018) based on work by Milton et al. (2009). See also WMO Cloud Identification Guide (World Meteorological Association 2017).

Sky-Code	Condition
0	Clear sky
1	Haze
2	Thin cirrus – sun not obscured
3	Thin cirrus – sun obscured
4	Scattered cumulus – sun not obscured
5	Cumulus over most of sky – sun not obscured
6	Cumulus – sun obscured
7	Complete cumulus cover
8	Stratus – sun obscured
9	Drizzle

Geolocation and Ground Control Points (Section 5)

Accurate geolocation is essential when the image data is: part of a time-series, combined with other sources of geo-referenced data such as satellite or ground-based observations, or used to build structural models. Photogrammetry software packages commonly use two sources of geolocation information: the coordinates of the of the camera during each image capture as recorded by the sensor or drone, and/or coordinates of ground control points (GCPs) identified in the imagery. Two problems complicate the accurate geolocation of multispectral imagery products: 1) The accuracy of image geo-tags may be insufficient (at best ca. ± 2-3 m horizontally) for some applications, and 2) conventional GCP designs can be difficult to identify in the low-resolution monochromatic images.

The accuracy of geo-tags is limited by the low precision of common drone / sensor GNSS modules. On-board differential positioning systems can be deployed for high accuracy direct georeferencing of the images, but integration can be time consuming and the modules may increase the cost of the aircraft system considerably (Ribeiro-Gomes et al. 2016). A common and practical alternative for the generation of sub-meter geo-located reflectance maps is to incorporate GCPs in the photogrammetry process, whose location is determined in-field with a high accuracy survey grade GNSS.

When mapping with the Parrot Sequoia and processing with Pix4D, we recommend the use of around five GCPs well distributed across the area of interest (Harwin et al. 2015; Pix4D 2018b). More may be required for large sites (>1 ha) or sites with varying topography, but higher numbers might not substantially improve geolocation (Pix4D 2018b). We tested the influence of number of GCPs and marking effort (images marked per GCP) on 2D geolocation accuracy for small (1 ha) and flat tundra plots and found rapidly diminishing improvements in geolocation accuracy beyond 4 GCPs marked on 3 images each (Figure 3-6 A). Additional GCPs not included in constraining the photogrammetric reconstructions should be used to assess the accuracy of each reconstruction (Step 10), we recommend at least one additional independent GCP for this purpose.

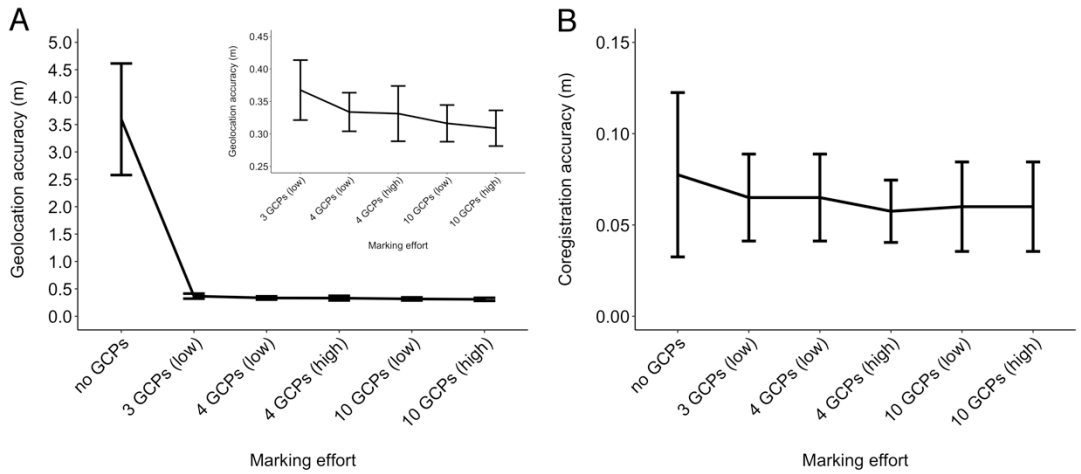

Figure 3-6 | A) Ground Control Point (GCP) marker placement effort and mean geolocation accuracy for eight reflectance maps (red and near-infrared bands) collected at four sites on Qikiqtaruk – Herschel Island. Insert shows data on finer scale excluding the “no GCPs” data point. Images were captured with a Parrot Sequoia at 5 cm per pixel GSD and processed in Pix4D. Error bars indicate standard deviation of the sites from the grand mean. Marking effort was staggered by incorporating 0, 3, 4 or 10 GCPs and increasing the number of images marked per GCP from low (3 images per GCP) to high (8 images per GCP). The relationship suggests diminishing returns for efforts of more than 3 GCPs, with a potential optimum effort-return ratio for 4 GCPs marked at low effort (accuracy approx. 7 x GSD). Sites are 1 ha in size and composed of graminoid dominated tundra on predominantly flat terrain with medium amounts of variation in altitude (max 30 m). GCP locations were determined with a survey grade GNSS with a horizontal accuracy of 0.02 m. GCP marker dimensions were 0.265 m x 0.265 m (ca. 5 x 5 GSD) and made from soft plastic or plastic fibres with a black and white triangular sand-dial pattern. Marker contrast was uneven across the monochromatic imagery, resulting in sometimes difficult to distinguish markers. We estimate marker centres were manually identified to ca. two pixels (0.05-0.10 m). Geolocation accuracy of the reflectance maps was assessed by visually locating centre points of 13 GCPs on the final reflectance map outputs in QGIS (QGIS

Development Team 2017), this included all GCPs incorporated in the processing. For each reflectance map, the mean absolute distance between visually estimated and computed position was calculated. B) GCP marker placement effort and mean accuracy of co-registration of red and near-infrared reflectance maps from the four sites as in A). The same methods were employed, except the co-registration accuracy was measured as the mean absolute distance between the visually determined locations of the 13 GCPs. The resulting relationship suggests a benefit of including GCPs, but we found no evidence for an improvement with effort of marker placement beyond three GCPs at this flat tundra site.

The compact size and power requirements limit the spatial resolution of CMOS imaging sensors used in multi-camera rigs such as the Parrot Sequoia. This, combined with the reduced spectral bandwidth, can cause difficulties when identifying GCPs in the monochromatic single-band imagery. To achieve maximum visibility of the GCPs, we suggest using square targets composed of four alternating black and white fields arranged in a checkerboard pattern (Figure 3-7 A) with an overall side length of 7-10x the GSD. The choice of material is important, as white areas of the targets need to reflect strongly across the whole spectrum of the sensor independently of the angle of view (near-lambertian), while black areas should have a low reflectivity to provide a strong contrast. What appears distinctly black and white to the human eye may have similar reflectance properties in the NIR. In our experience, painted canvas and sailcloth are suitable materials that are affordable, readily available and reasonably light. We also achieved good results success with vinyl flooring tiles; however, these can be heavy and therefore impractical in remote field conditions. We strongly recommend testing the visibility of the targets using the multispectral sensors prior field deployment.

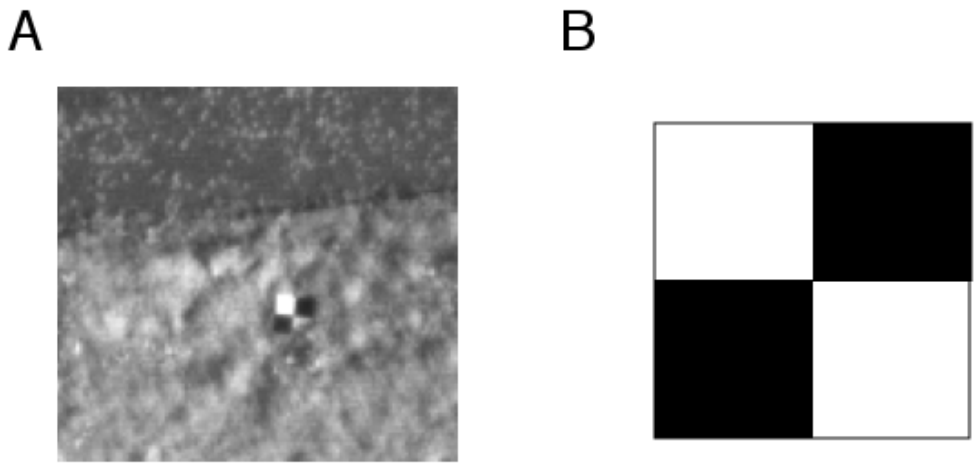

Figure 3-7 | A) Parrot Sequoia near-infrared image of 0.6 m x 0.6 m GCP on grass. This GCP is made from self-adhesive vinyl tiles obtained in a local hardware store. Ground sampling distance: approx. 0.07 m per pixel. Image curtsey of Tom Wade and Charlie Moriarty, The University of Edinburgh. B) Chequerboard pattern suggested for improved visibility of GCP in coarse resolution Parrot Sequoia imagery. Aligning the chequerboard pattern with the sensor orientation can further aid visibility.

Accurate co-registration of pixels among bands is essential when calculating VIs (Turner et al. 2014). Incorporating GCPs in the processing can aid in constraining the relative shifts between the bands. However, we found that increasing the effort in GCP placement (number of GCPs and images marked per GCP) in Pix4D for Parrot Sequoia imagery had little impact on constraining the co-registration between bands. High degrees of co-registration (1-2 pixels) were achieved even with the lowest effort of marker placement (Figure 3-6 B). Turner et al. (2014) reported similar levels of co-registration accuracy between reflectance maps of bands collected with a multiband Tetracam mini-MCA (GSD 0.03 m / pixel) at moss sites in Antarctica.

Radiometric calibration (Section 6)

The aim of the radiometric calibration is to convert at-sensor radiance (in form of DNs) into absolute surface reflectance values, accounting for variation caused by differences in ambient light due to weather and sun, and between sensors types and units (Kelcey and Lucieer 2012). The relationship (empirical line) between image DN values and surface reflectance is established from a sample of pixels covering areas of known reflectance, theoretically this could be a naturally occurring homogeneous

area in the area of interest measured with a field spectrometer, but artificial standards ("reflectance targets") of known reflectance are more commonly used to carry out the calibration.

When processing Parrot Sequoia outputs in Pix4Dmapper a single image is used to calibrate each band (Step 8). A single image is sufficient to establish the empirical line if the sensor response is known and linear (Wang and Myint 2015), as is the case for the Parrot Sequoia (Parrot 2017c). The calibration is carried out by manually selecting the area of the reflectance target on the calibration image (Figure 3-8) and assigning the known reflectance value of the target. In our experience, a larger sample of pixels produces better calibration results, *i.e.* the more pixels that are taken up by the reflectance target the better. Sample size is likely to be of importance here as it mitigates for variations caused by the inherent noise across the image stemming from the sensor, illumination of the target, and bleeding effects from adjacent non-target surfaces. These findings are consistent with advice from Pix4D (2018b) and MicaSense, who recommend at least 1/3 of the total image footprint to be covered by the calibration area of the reflectance target (MicaSense 2018b).

Calibration images can be collected either before, after or during the flight. For pre- and post-flight calibration, drone and sensor are held manually above the target and images for all bands are acquired (Step 4). In-flight calibration targets are placed within the area of interest and calibration images acquired during the survey. In-flight targets need to be sufficiently large to ensure a good sample of pixels. Especially when operating in remote areas, weight and size of targets may be limited and quality in-fight calibration imagery can be difficult to obtain. Nonetheless, smaller in-flight reflectance targets (about 100+ pixels = 10+ x 10+ GSD) can be of great use for quality control of the final reflectance map output (see for example Aasen et al., 2015) and may serve as an emergency back-up should pre-/post-flight calibration imagery fail. It is important that both in-flight and pre-/post- flight reflectance targets are placed as level as possible to ensure even illumination of the target surface.

Figure 3-8 | Parrot Sequoia pre-flight radiometric calibration image of a MicaSense Ltd. (Seattle, WA, USA) reflectance target in the near-infrared band. Red box: surface with known reflectance value used for calibration.

We recommend always obtaining both pre-/post-flight calibration imagery of a reflectance target and, if possible, the use of at least two in-flight reflectance targets for quality control and redundancy. Avoiding overexposure (saturated sensor) and shading of all reflectance targets is critical as this will render the images unusable for radiometric calibration. The Parrot Sequoia has a calibration image acquisition feature for pre-/post-flight calibration accessible via the Wi-Fi interface, which obtains a bracketed exposure reducing the risk of over-exposure.

When taking pre-/post-flight calibration imagery, ensure that as little radiation as possible is reflected onto the target by surrounding objects, including the person taking the calibration picture. Avoiding bright clothing and taking the image with the sun to the photographer's rear while stepping aside to avoid casting a shadow over the target may reduce the risk of contamination by light scattered from the body (see MicaSense 2018b and, Pix4D 2018b for additional guidance). Aasen and Bolten

(2018) observed notable errors introduced to their calibration imagery by the presence and position of the person / drone in the hemisphere above the target, suggesting that the development of reliable calibration methods requires further attention.

It is key that all reflectance targets employed have homogenous and near-lambertian reflectance properties. For pre-/post-flight imagery, we recommend medium sized (approx. 15 x 15 cm) Polytetrafluoroethylene (PTFE) based targets, such as Spectralon (Labsphere 2018), Zenith (Sphereoptics 2018) or similar, due to their durability, off-the shelf calibration and ease of maintenance. Durability and ease of maintenance are particularly important when working in environments with harsh climates. We experienced substantial degradation in commercially manufactured reflectance targets over a single field season (3 months), likely due to exposure to dust, insects, moisture and temperature fluctuations experienced in the Arctic tundra (Figure 3-9). For larger targets used in-flight, we recommend tarpaulins made of canvas, sailcloth, felt or similar materials (see Ahmed et al. 2017, Crusiol et al. 2017, Mosaic Mill Ltd. 2018). A variety of other materials have also been successfully employed as reflectance targets (Laliberte et al. 2011, Turner et al. 2014, Wang and Myint 2015, Aasen et al. 2015, Wehrhan et al. 2016, Dash et al. 2017).

Target maintenance and quality control is essential (also discussed by Wang and Myint 2015). Changes in target reflectance can have notable effects on the calibration outputs (Figure 3-10). It is key to handle targets as carefully as possible to avoid surface degradation. We recommend regular cleaning according to manufacturers' guidance and frequent re-measurement of reflectance values. Field spectroscopy facilities can provide assistance and expertise in obtaining and maintaining targets. Re-measurement of the reflectance values can be carried out in-field prior each flight (e.g. Laliberte et al. 2011). However, this might not always be feasible when operating in remote areas, in which case careful handling, maintenance and measurements of reflectance values before and after a field season may have to suffice.

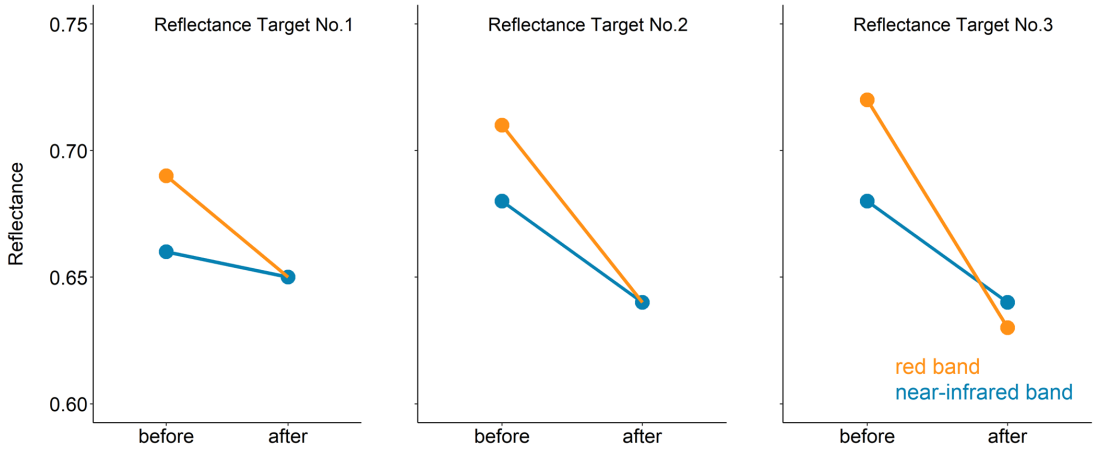

Figure 3-9 | Decrease in reflectance values of three reflectance targets before and after a three-month field season in the Arctic tundra on Qikiqtaruk – Herschel Island. Loss in reflectance is likely due to degradation in the harsh environmental conditions (dust, insect debris, moisture and temperature fluctuations). Across the field seasons in 2016 and 2017 we saw 4-10% reduction in reflectance across targets from different suppliers, composed of different materials.

Optical filters directly affect the radiation reaching the sensor and influence the relationship between surface radiance and image DN, see Kelcey and Lucieer (2012) for further discussion. It is therefore essential that all radiometric calibration imagery and survey photographs are consistently taken either with or without the removable filter. The Parrot Sequoia is shipped with a protective lens cover (a clear filter), which can be useful when operating in difficult terrains such as the tundra where rough landings are possible, which could scratch the sensor lenses. Parrot does not characterise the transmissivity of the protective lens covers shipped with the Sequoia. As the presence / absence of filters is difficult to detect *post hoc* during automated processing (such as online cloud services), Parrot recommends refraining from using them during multispectral data acquisition flights (Parrot 2017b).

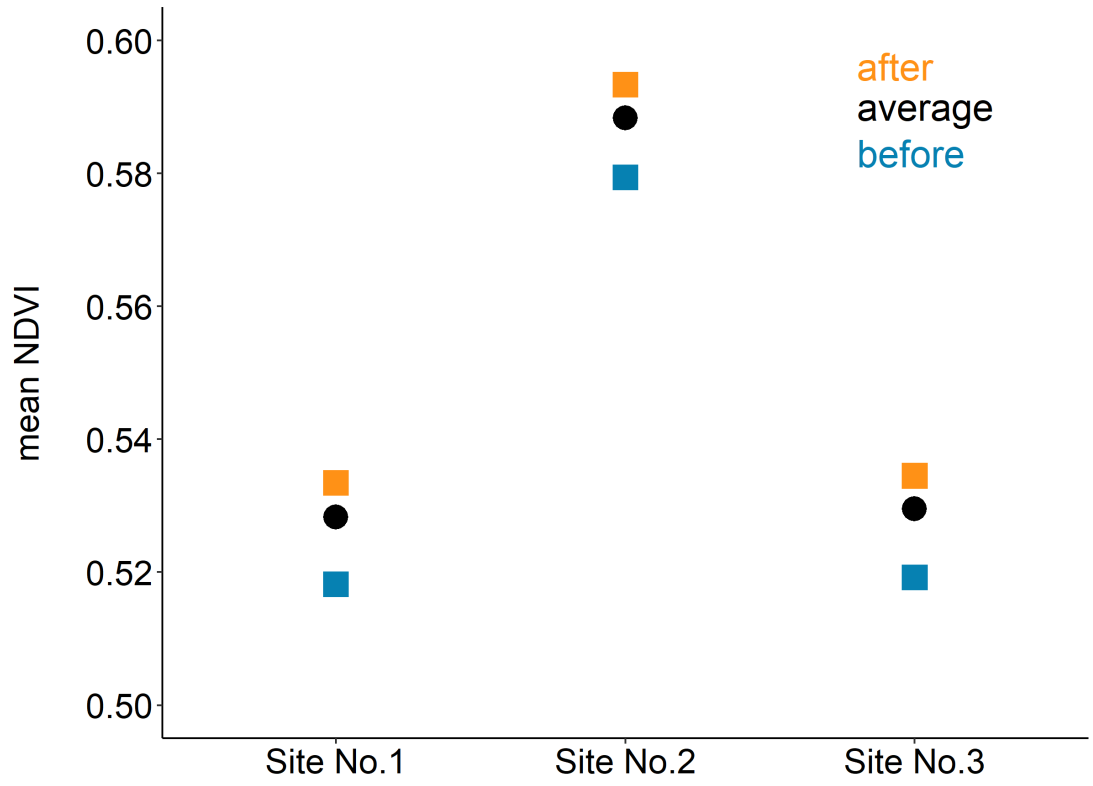

Figure 3-10 | Mean NDVI value for three graminoid tundra sites (1 ha each) on Qikiqtaruk – Herschel Island based on red and near-infrared reflectance maps calibrated with three different reflectance values for the reflectance target No. 1 (Figure 3-9): before and after degradation, and the average between the two values. Surveys where flown at the beginning of the season when little to no degradation of the target is expected to have occurred. Before and after values differ by about 0.015 in absolute NDVI, suggesting an overestimation of NDVI when after values are used for the early season surveys.

We measured the transmissivity of the filters shipped with two Sequoias obtained in 2016 (Figure 3-11). We observed a small reduction in transmitted radiation across all four bands (see also Figure 3-12), and a small effect of angle of view across the horizontal field of view on the radiation transmitted in the near-infrared band. These findings suggest that the protective lens cover may be used with little to no effect on the final reflectance map outputs, if the filter is applied consistently for all flights under comparison.

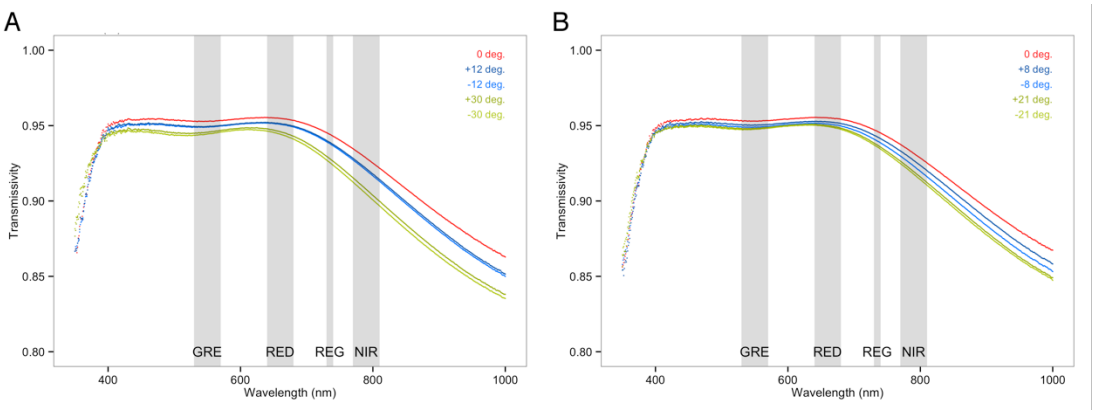

Figure 3-11 | Transmissivity of Parrot Sequoia Lens-Protector filter across the a) horizontal and b) vertical field-of-view of the Sequoia Sensor. The overall small reductions in transmitted light and the small effect of angle across field-of-view suggest that little to no impact on reflectance map outputs acquired with the filter can be expected.

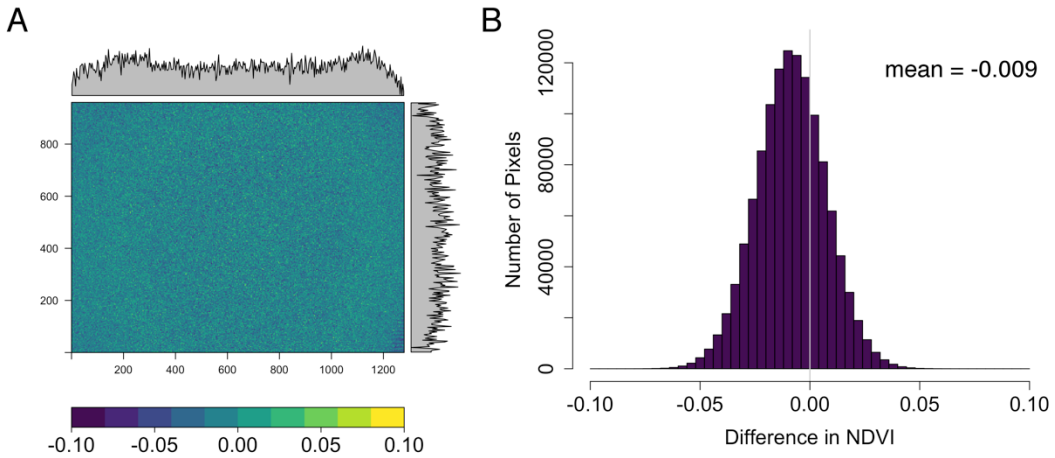

Figure 3-12 | Raster plot (A) and histogram (B) of pixel by pixel differences in NDVI values of a homogenously illuminated integrating sphere with and without the Parrot Sequoia protective lens cover. Margins in the raster plot show mean differences for the pixel columns and rows respectively.

Estimated combined error

We estimate that the combined effect of the main sources of error discussed in this manuscript – if not properly accounted for - could be as much as 0.094 in magnitude for landscape level estimates (1 ha mean) in NDVI for the drone surveys conducted with a Parrot Sequoia at 5 cm GSD at our Arctic research site Qikiqtaruk during the 2016 field campaign (Figure 3-13). This combined error equates to approximately 10-13% of the peak growing season NDIV (0.60 - 0.68) of the tussock-sedge and dryas-

vetch tundra types at the site. These estimates highlight the importance of controlling for these sources of error, by carrying out radiometric calibration, surveying at constant solar angles, monitoring reflectance target degradation and using the protective lens cover consistently. Nonetheless, a notable error will remain even if everything except cloud conditions is controlled for, we estimate that our ability to then confidently detect change in landscape scale (1 ha) mean NDVI is limited to differences above 0.02 - 0.03 in absolute magnitude across space and time.

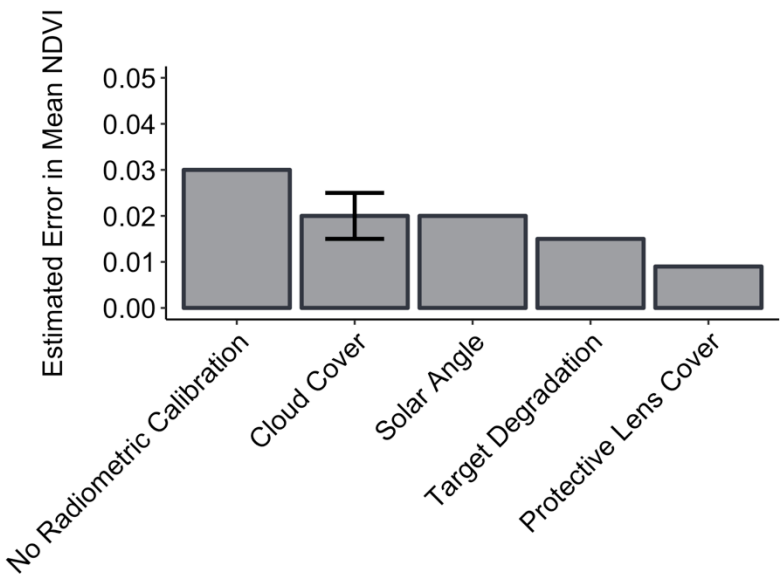

Figure 3-13 | Estimated effects of the five main sources of errors discussed in this manuscript on the mean NDVI of 1 ha tundra plots on Qikiqtaruk surveyed in 2016 with a Parrot Sequoia at 50m flight altitude (5 cm GSD). The five sources of error sum up to a combined error of 0.094 NDVI (assuming the mean error for cloud cover variation) and were calculated as: 1) The estimated average deviation from the calibrated mean NDVI compared to a survey without radiometric calibration carried out. 2) The deviation in estimated mean NDVI when comparing clear sky to continuous cloud cover conditions (lower error bar: thick stratus, upper error bar: thick cumulus) even if radiometric calibration is carried out. 3) The estimated deviation of mean NDVI caused by changes in solar elevation from solar noon to evening during peak growing season at our field site in the Arctic (about 20° drop – roughly equivalent to the difference between start/end and mid growing season) even if radiometric calibration is carried out. 4) The estimated effect of target degradation on mean NDVI across a three-month field season. 5) The error introduced by the protective lens cover if used and removed inconsistently between flights in comparison. These estimates are based on both data presented in this manuscript and manuscripts in preparation. We would like to urge caution when transferring these estimates to other sensors / set ups and ecological systems. The estimates are presented here with the

purpose of giving the reader a feel for the relative importance of the sources of error discussed in this manuscript.

Conclusions

Vegetation monitoring using drones could provide key datasets to quantify vegetation responses to global change (Anderson and Gaston 2013, Salamí et al. 2014, Torresan et al. 2017). However, accurately quantifying and accounting for the common sources of error and variation in multispectral data collection is a key part of the workflow for scientific applications (Aasen et al. 2015, Manfreda et al. 2018). As technologies advance and our understanding of multispectral drone products increases we may be able to better quantify the sources of error and improve our measures to account for them; however, it is critical that the drone data collection of today is done as cautiously and rigorously as possible as it will provide the baseline for future ecological monitoring studies.

The rapid and ongoing development of drone and sensor technology (Anderson and Gaston 2013, Pádua et al. 2017) has made the collection of multispectral imagery with drones accessible to many ecological research projects, even those operating with small budgets. Despite the plug-and-play nature of the latest generation of multispectral sensors, such as the Parrot Sequoia and the MicaSense RedEdge, a handful of factors require careful consideration if the aim is to collect high-quality multispectral data that is comparable across sensors, space and time. For example, variation in ambient light and sensors require radiometric calibration of the imagery, and ground control points may be necessary to achieve accurate geolocation of reflectance and vegetation index maps (Kelcey and Lucieer 2012, Turner et al. 2014, Salamí et al. 2014, Aasen et al. 2015, Pádua et al. 2017).

Standardized workflows for multispectral drone surveys that incorporate flight planning, the influence of weather and sun, as well as aspects of geolocation and radiometric calibration will produce data that is comparable across different study regions, plots, sensors and time. We encourage drone survey practitioners in the field of ecology and beyond to incorporate these methods and perspectives in their planning and data collection to promote higher data quality and allow for cross site comparisons. Standardised procedures and practises across research groups (*e.g.*,

those developed by the HiLDEN network) have the potential to provide highly-valuable baseline data that can be used to address urgent and emerging topics, such as identifying the landscape patterns and processes of vegetation responses to global change at high latitudes and across the world's biomes.

Acknowledgements

Much of this manuscript would have not been possible without the valuable input from Chris MacLellan and Andrew Gray at the NERC Field Spectroscopy Facility at the Grant Institute in Edinburgh. We would also like to thank Andrew Gray for providing feedback on an earlier version of this manuscript and Tom Wade from the University of Edinburgh Airborne GeoSciences Facility University of Edinburgh Airborne GeoScience facility for his ongoing support of our drone-based endeavours in the Arctic. Finally, we would like to thank two anonymous reviewers for feedback and suggestions that have improved this manuscript.

Funding for this research was provided by NERC through the ShrubTundra standard grant (NE/M016323/1), a NERC E3 Doctoral Training Partnership PhD studentship for Jakob Assmann (NE/L002558/1), a research grant from the National Geographic Society (CP-061R-17) and a Parrot Climate Innovation Grant for Jeffrey Kerby, a NERC support case for use of the NERC Field Spectroscopy Facility (738.1115), equipment loans from the University of Edinburgh Airborne GeoSciences Facility and the NERC Geophysical Equipment Facility (GEF 1063 and 1069).

References

Aasen, H., and Bolten, A. 2018. Multi-temporal high-resolution imaging spectroscopy with hyperspectral 2D imagers – From theory to application. Remote Sens. Environ. 205: 374–389. doi:10.1016/j.rse.2017.10.043.

Aasen, H., Burkart, A., Bolten, A., and Bareth, G. 2015. Generating 3D hyperspectral information with lightweight UAV snapshot cameras for vegetation monitoring: From camera calibration to quality assurance. ISPRS J. Photogramm. Remote Sens. 108: 245–259. doi:10.1016/j.isprsjprs.2015.08.002.

Agisoft. 2018. Radiometric calibration using reflectance panels in PhotoScan Professional 1.4. Available from http://www.agisoft.com/pdf/PS_1.4_(IL)_Refelctance_Calibration.pdf [accessed 5 September 2018].

Ahmed, O.S., Shemrock, A., Chabot, D., Dillon, C., Williams, G., Wasson, R., and Franklin, S.E. 2017. Hierarchical land cover and vegetation classification using multispectral data acquired from an unmanned aerial vehicle. Int. J. Remote Sens. 38(8–10): 2037–2052. doi:10.1080/01431161.2017.1294781.

Anderson, K., and Gaston, K.J. 2013. Lightweight unmanned aerial vehicles will revolutionize spatial ecology. Front. Ecol. Environ. 11(3): 138–146. doi:10.1890/120150.

Barnes, W.L., Pagano, T.S., and Salomonson, V.V. 1998. Prelaunch characteristics of the Moderate Resolution Imaging Spectroradiometer (MODIS) on EOS-AM1. IEEE Trans. Geosci. Remote Sens. 36(4): 1088–1100. doi:10.1109/36.700993.

Barsi, J.A., Lee, K., Kvaran, G., Markham, B.L., and Pedelty, J.A. 2014. The Spectral Response of the Landsat-8 Operational Land Imager. Remote Sens. 6(10): 10232–10251. doi:10.3390/rs61010232.

Berra, E.F., Gaulton, R., and Barr, S. 2017. Commercial Off-the-Shelf Digital Cameras on Unmanned Aerial Vehicles for Multitemporal Monitoring of Vegetation Reflectance and NDVI. IEEE Trans. Geosci. Remote Sens. PP(99): 1–9. doi:10.1109/TGRS.2017.2655365.

Bicheron, P., and Leroy, M. 2000. Bidirectional reflectance distribution function signatures of major biomes observed from space. J. Geophys. Res. Atmospheres 105(D21): 26669–26681. doi:10.1029/2000JD900380.

Crusiol, L.G.T., Nanni, M.R., Silva, G.F.C., Furlanetto, R.H., Gualberto, A.A. da S., Gasparotto, A. de C., and Paula, M.N.D. 2017. Semi professional digital camera calibration techniques for Vis/NIR spectral data acquisition from an unmanned aerial vehicle. Int. J. Remote Sens. 38(8–10): 2717–2736. doi:10.1080/01431161.2016.1264032.

Cunliffe, A.M., Brazier, R.E., and Anderson, K. 2016. Ultra-fine grain landscape-scale quantification of dryland vegetation structure with drone-acquired structure-from-motion photogrammetry. Remote Sens. Environ. 183: 129–143. doi:10.1016/j.rse.2016.05.019.

Dash, J.P., Watt, M.S., Pearse, G.D., Heaphy, M., and Dungey, H.S. 2017. Assessing very high resolution UAV imagery for monitoring forest health during a simulated disease outbreak. ISPRS J. Photogramm. Remote Sens. 131: 1–14. doi:10.1016/j.isprsjprs.2017.07.007.

Duffy, J.P., Cunliffe, A.M., DeBell, L., Sandbrook, C., Wich, S.A., Shutler, J.D., Myers-Smith, I.H., Varela, M.R., and Anderson, K. 2017. Location, location, location: considerations when using lightweight drones in challenging environments. Remote Sens. Ecol. Conserv.: n/a-n/a. doi:10.1002/rse2.58.

European Space Agency. 2015. Sentinel 2 - User Handbook Revison 2. Available from https://sentinel.esa.int/documents/247904/685211/Sentinel-2_User_Handbook [accessed 30 May 2018].

Fernández-Guisuraga, J., Sanz-Ablanedo, E., Suárez-Seoane, S., and Calvo, L. 2018. Using Unmanned Aerial Vehicles in Postfire Vegetation Survey Campaigns through Large and Heterogeneous Areas: Opportunities and Challenges. Sensors 18(2): 586. doi:10.3390/s18020586.

Fraser, R.H., Olthof, I., Carrière, M., Deschamps, A., and Pouliot, D. 2011. Detecting long-term changes to vegetation in northern Canada using the Landsat satellite image archive. Environ. Res. Lett. 6(4): 045502. doi:10.1088/1748-9326/6/4/045502.

Guay, K.C., Beck, P.S.A., Berner, L.T., Goetz, S.J., Baccini, A., and Buermann, W. 2014. Vegetation productivity patterns at high northern latitudes: a multi-sensor satellite data assessment. Glob. Change Biol. 20(10): 3147–3158. doi:10.1111/gcb.12647.

Harwin, S., Lucieer, A., and Osborn, J. 2015. The Impact of the Calibration Method on the Accuracy of Point Clouds Derived Using Unmanned Aerial Vehicle Multi-View Stereopsis. Remote Sens. 7(9): 11933–11953. doi:10.3390/rs70911933.

Ju, J., and Masek, J.G. 2016. The vegetation greenness trend in Canada and US Alaska from 1984–2012 Landsat data. Remote Sens. Environ. 176: 1–16. doi:10.1016/j.rse.2016.01.001.

Juszak, I., Iturrate-Garcia, M., Gastellu-Etchegorry, J.-P., Schaepman, M.E., Maximov, T.C., and Schaepman-Strub, G. 2017. Drivers of shortwave radiation fluxes in Arctic tundra across scales. Remote Sens. Environ. 193: 86–102. doi:10.1016/j.rse.2017.02.017.

Kelcey, J., and Lucieer, A. 2012. Sensor Correction of a 6-Band Multispectral Imaging Sensor for UAV Remote Sensing. Remote Sens. 4(5): 1462–1493. doi:10.3390/rs4051462.

Kimes, D.S. 1983. Dynamics of directional reflectance factor distributions for vegetation canopies. Appl. Opt. 22(9): 1364–1372. doi:10.1364/AO.22.001364.

Labsphere. 2018. Labsphere. Available from https://www.labsphere.com [accessed 23 January 2018].

Laliberte, A.S., Goforth, M.A., Steele, C.M., and Rango, A. 2011. Multispectral Remote Sensing from Unmanned Aircraft: Image Processing Workflows and Applications for Rangeland Environments. Remote Sens. 3(12): 2529–2551. doi:10.3390/rs3112529.

Lebourgeois, V., Bégué, A., Labbé, S., Mallavan, B., Prévot, L., and Roux, B. 2008. Can Commercial Digital Cameras Be Used as Multispectral Sensors? A Crop Monitoring Test. Sensors 8(11): 7300–7322. doi:10.3390/s8117300.

Levin, S.A. 1992. The Problem of Pattern and Scale in Ecology: The Robert H. MacArthur Award Lecture. Ecology 73(6): 1943–1967. doi:10.2307/1941447.

Manfreda, S., McCabe, M., Miller, P., Lucas, R., Madrigal, V.P., Mallinis, G., Dor, E.B., Helman, D., Estes, L., Ciraolo, G., Müllerová, J., Tauro, F., Lima, M.I.D., Lima, J.L.M.P.D., Frances, F., Caylor, K., Kohv, M., Maltese, A., Perks, M., Ruiz-Pérez, G., Su, Z., Vico, G., and Toth, B. 2018. On the Use of Unmanned Aerial Systems for Environmental Monitoring. doi:10.20944/preprints201803.0097.v1.

Matese, A., Toscano, P., Di Gennaro, S.F., Genesio, L., Vaccari, F.P., Primicerio, J., Belli, C., Zaldei, A., Bianconi, R., and Gioli, B. 2015. Intercomparison of UAV, Aircraft and Satellite Remote Sensing Platforms for Precision Viticulture. Remote Sens. 7(3): 2971–2990. doi:10.3390/rs70302971.

MicaSense. 2016a. What is the center wavelength and bandwidth of each filter on the RedEdge camera? Available from http://support.micasense.com/hc/en-us/articles/214878778-What-is-the-center-wavelength-and-bandwidth-of-each-filter-on-the-RedEdge-camera- [accessed 19 October 2017].

MicaSense. 2016b. What spectral bands does the Sequoia camera capture? Available from http://support.micasense.com/hc/en-us/articles/217112037-What-spectral-bands-does-the-Sequoia-camera-capture- [accessed 19 October 2017].

MicaSense. 2018a. How much overlap is needed? Available from http://support.micasense.com/hc/en-us/articles/215206828-How-much-overlap-is-needed- [accessed 18 January 2018].

MicaSense. 2018b. Best practices: Collecting Data with MicaSense RedEdge and Parrot Sequoia. Available from http://support.micasense.com/hc/en-us/articles/224893167-Best-practices-Collecting-Data-with-MicaSense-RedEdge-and-Parrot-Sequoia [accessed 18 January 2018].

MicaSense. 2018c. MicaSense RedEdge image processing tutorials. Jupyter Notebook, MicaSense, Inc. Available from https://github.com/micasense/imageprocessing [accessed 29 May 2018].

Milton, E.J., Schaepman, M.E., Anderson, K., Kneubühler, M., and Fox, N. 2009. Progress in field spectroscopy. Remote Sens. Environ. 113: S92–S109. doi:10.1016/j.rse.2007.08.001.

Mosaic Mill Ltd. 2018. EnsoMOSAIC Agri Reflectance Targets. Available from http://www.mosaicmill.com/download/EnsoMOSAIC_Agri_overview.pdf [accessed 23 January 2018].

Müllerová, J., Bartaloš, T., Brůna, J., Dvořák, P., and Vítková, M. 2017. Unmanned aircraft in nature conservation: an example from plant invasions. Int. J. Remote Sens. 38(8–10): 2177–2198. doi:10.1080/01431161.2016.1275059.

NOAA. 2014. KLM Users Guide. U.S. Dept. of Commerce, National Oceanic and Atmospheric Administration, National Environmental Satellite, Data, and Information Service, National Climatic Data Center, Climate Services Division, Satellite Services Branch, Asheville, NC, USA. Available from https://www1.ncdc.noaa.gov/pub/data/satellite/publications/podguides/N-

15%20thru%20N-19/pdf/0.0%20NOAA%20KLM%20Users%20Guide.pdf [accessed 8 February 2018].

Ortega-Terol, D., Hernandez-Lopez, D., Ballesteros, R., and Gonzalez-Aguilera, D. 2017. Automatic Hotspot and Sun Glint Detection in UAV Multispectral Images. Sensors 17(10): 2352. doi:10.3390/s17102352.

Pádua, L., Vanko, J., Hruška, J., Adão, T., Sousa, J.J., Peres, E., and Morais, R. 2017. UAS, sensors, and data processing in agroforestry: a review towards practical applications. Int. J. Remote Sens. 38(8–10): 2349–2391. doi:10.1080/01431161.2017.1297548.

Parrot. 2017a. Release of application notes. Available from http://forum.developer.parrot.com/t/parrot-announcement-release-of-application-notes/5455 [accessed 29 May 2018].

Parrot. 2017b. Parrot Developers Forum. Available from http://forum.developer.parrot.com/t/transmissivity-of-protective-lens-cover/5907 [accessed 14 May 2018].

Parrot. 2017c, April 25. SEQ AN 01 - Applicaiton Note - Pixel to Irradiance. Available from http://forum.developer.parrot.com/uploads/default/original/2X/3/383261d35e33f1f375ee49e9c7a9b10071d2bf9d.pdf [accessed 1 December 2018].

Pix4D. 2018a. Support Website - Ground Sampling Distance. Available from http://support.pix4d.com/hc/en-us/articles/202557459-Step-1-Before-Starting-a-Project-1-Designing-the-Image-Acquisition-Plan-a-Selecting-the-Image-Acquisition-Plan-Type [accessed 18 January 2018].

Pix4D. 2018b. Step 1. Before Starting a Project > 4. Getting GCPs on the field or through other sources (optional but recommended). Available from http://support.pix4d.com/hc/en-us/articles/202557489-Step-1-Before-Starting-a-Project-4-Getting-GCPs-on-the-field-or-through-other-sources-optional-but-recommended- [accessed 30 August 2018].

Pix4D. 2018c. Support - Radiometric Calibration Target. Available from http://support.pix4d.com/hc/en-us/articles/206494883-Radiometric-Calibration-Target [accessed 23 January 2018].

QGIS Development Team. 2017. QGIS Geographic Information System. Open Source Geospatial Foundation Project. Available from http://qgis.osgeo.org.

Ribeiro-Gomes, K., Hernandez-Lopez, D., Ballesteros, R., and Moreno, M.A. 2016. Approximate georeferencing and automatic blurred image detection to reduce the costs of UAV use in environmental and agricultural applications. Biosyst. Eng. 151: 308–327. doi:10.1016/j.biosystemseng.2016.09.014.

Salamí, E., Barrado, C., and Pastor, E. 2014. UAV Flight Experiments Applied to the Remote Sensing of Vegetated Areas. Remote Sens. 6(11): 11051–11081. doi:10.3390/rs61111051.

Samiappan, S., Turnage, G., Hathcock, L.A., and Moorhead, R. 2017. Mapping of invasive phragmites (common reed) in Gulf of Mexico coastal wetlands using multispectral imagery and small unmanned aerial systems. Int. J. Remote Sens. 38(8–10): 2861–2882. doi:10.1080/01431161.2016.1271480.

Sphereoptics. 2018. Sphereoptics. Available from http://sphereoptics.de/ [accessed 23 January 2018].

Teillet, P. 1997. Effects of spectral, spatial, and radiometric characteristics on remote sensing vegetation indices of forested regions. Remote Sens. Environ. 61(1): 139–149. doi:10.1016/S0034-4257(96)00248-9.

Torresan, C., Berton, A., Carotenuto, F., Gennaro, S.F.D., Gioli, B., Matese, A., Miglietta, F., Vagnoli, C., Zaldei, A., and Wallace, L. 2017. Forestry applications of UAVs in Europe: a review. Int. J. Remote Sens. 38(8–10): 2427–2447. doi:10.1080/01431161.2016.1252477.

Tucker, C.J. 1979. Red and photographic infrared linear combinations for monitoring vegetation. Remote Sens. Environ. 8(2): 127–150. doi:10.1016/0034-4257(79)90013-0.

Turner, M.G., O'Neill, R.V., Gardner, R.H., and Milne, B.T. 1989. Effects of changing spatial scale on the analysis of landscape pattern. Landsc. Ecol. 3(3): 153–162. doi:10.1007/BF00131534.

Turner, D., Lucieer, A., Malenovský, Z., King, D.H., and Robinson, S.A. 2014. Spatial Co-Registration of Ultra-High Resolution Visible, Multispectral and Thermal Images Acquired with a Micro-UAV over Antarctic Moss Beds. Remote Sens. 6(5): 4003–4024. doi:10.3390/rs6054003.

Wang, C., and Myint, S.W. 2015. A Simplified Empirical Line Method of Radiometric Calibration for Small Unmanned Aircraft Systems-Based Remote Sensing. IEEE J. Sel. Top. Appl. Earth Obs. Remote Sens. 8(5): 1876–1885. doi:10.1109/JSTARS.2015.2422716.

Wehrhan, M., Rauneker, P., and Sommer, M. 2016. UAV-Based Estimation of Carbon Exports from Heterogeneous Soil Landscapes—A Case Study from the CarboZALF Experimental Area. Sensors 16(2): 255. doi:10.3390/s16020255.

Weste, N.H.E. 2011. CMOS VLSI design : a circuits and systems perspective. *In* Fourth edition / Neil H.E. Weste, David Harris..

Westoby, M.J., Brasington, J., Glasser, N.F., Hambrey, M.J., and Reynolds, J.M. 2012. 'Structure-from-Motion' photogrammetry: A low-cost, effective tool for geoscience applications. Geomorphology 179: 300–314. doi:10.1016/j.geomorph.2012.08.021.

World Meteorological Association. 2017. Cloud Identification Guide. Available from https://ane4bf-datap1.s3-eu-west-1.amazonaws.com/wmocms/s3fs-public/ckeditor/files/WMD2017_poster_JN162028_EN.pdf?nYgh.wIczIOQE7LTllgPL2S0Zbwwn0A3 [accessed 19 January 2017].

Chapter 4 Drone data reveals fine-scale variation of tundra greenness and phenology that is missed by satellite and *in situ* monitoring

Drone images of the Herschel (left) and Komakuk (right) vegetation types. Supervisor Isla H. Myers-Smith (top left) at the ground control station.

Chapter 4 Drone data reveals fine-scale variation of tundra greenness and phenology that is missed by satellite and in situ monitoring

The following chapter has been prepared as a manuscript for submission, but at the time point of submission of this thesis, this manuscript had not yet been submitted to any journal.

Authors: Jakob J Assmann[1,2], Isla H Myers-Smith[1], Andrew M Cunliffe[1,4] and Jeffrey T Kerby[3]

Affiliations:
[1] School of GeoSciences, The University of Edinburgh, Edinburgh, UK
[2] School of Biology, The University of Edinburgh, Edinburgh, UK
[3] Neukom Institute for Computational Science, Institute of Arctic Studies, Dartmouth College, USA
[4] School of Geography, University of Exeter, Exeter, UK

Author Contributions: JJA and IHMS conceived the study with input from JTK. JJA carried out the data processing and analysis. AMC lead the field campaign for the drone data collection in 2017. JJA wrote the manuscript with input from all authors.

Abstract

The Arctic is undergoing rapid environmental change with dramatic consequences for tundra vegetation. Satellite observations suggest that tundra vegetation productivity is increasing (greening) and that the growing season is becoming longer. Vegetation productivity and phenology are key components of the tundra ecosystems, influencing ecosystem function and providing potential feedbacks to the global climate system. Despite the overall greening trend, a large amount of unexplained spatial variation persists in the amount of greening and phenological changes. Our ability to explain this variation and the underlying ecological processes causing it has been limited by the coarse grain sizes of satellite observations. Here, we combine a novel dataset of within-growing season time-series of fine-grain multispectral drone imagery from two years (2016 and 2017) with MODIS and Sentinel 2 satellite data to quantify the correspondence amongst platforms and study the fine-scale distribution of vegetation greenness at our study site in the Canadian Arctic across space and time. Our results show cross-platform correspondence of drone and satellite measures of tundra greenness at the landscape-scale for our eight 1 ha plots at the field site in both years, but highlight a notable loss of variation when aggregating from fine-grain drone (approx. 0.05 m) to medium-grain satellite pixel sizes (10 m), potentially obscuring

key ecological variation in productivity and phenology. For example, the observed fine-scale variation (sub-metre) in tundra greenness at our field site likely reflects ecological variation in productivity caused by large tussock sedges, microtopography and disturbances. Finally, our time-series analysis shows a decline of landscape-level variation in greeness over the course of the growing season, suggesting that not only the timing, but also the heterogeneity of tundra landscape productivity can vary within and amongst years. If with warming, tundra phenological heterogeneity is reduced at an earlier point in the growing season, interactions between the tundra plants and their consumers may be affected. Overall, our findings illustrate the potential for multispectral drone imagery to provide fine-grain measures at landscape-level extent that can bridge the gap between satellite and *in situ* measures of tundra vegetation greenness and phenology.

Introduction

The Arctic is undergoing rapid environmental change, surface temperatures are rising at twice the rate then the rest of the globe (IPCC, 2014) with dramatic consequences for tundra vegetation. Satellite observations show increases in tundra vegetation productivity or "greening" (Guay et al., 2014; Keenan & Riley, 2018; Myneni, Keeling, Tucker, Asrar, & Nemani, 1997) and changes in growing season phenology (Zeng, Jia, & Epstein, 2011; Zeng, Jia, & Forbes, 2013; Zhao et al., 2015) over the recent decades. Tundra vegetation productivity and phenology influence ecosystem function through carbon and nutrient cycles with potential feedbacks on the global climate system (Chapin et al., 2005; Ernakovich et al., 2014; Loranty & Goetz, 2012; Pearson et al., 2013; Richardson et al., 2013) and have direct impacts on plant-consumer and -pollinator interactions (Barboza, Van Someren, Gustine, & Bret-Harte, 2018; Doiron, Gauthier, & Lévesque, 2015; Gustine et al., 2017; Kerby & Post, 2013a, 2013b; Post, Pedersen, Wilmers, & Forchhammer, 2008). Yet the satellite greening trends and phenology measures calculated across different platforms do not always correspond (e.g. Guay et al., 2014) and repeated calls for ground validation have been made (Fraser, Olthof, Carrière, Deschamps, & Pouliot, 2011; Guay et al., 2014; Ju & Masek, 2016; Stow et al., 2004).

Satellites show heterogenous greening of the tundra

Long-term time series of satellite observations suggest the Arctic has been undergoing greening over recent decades. Observations are mainly based on changes in surface reflectance derived Normalised Difference Vegetation Index (NDVI) (Tucker, 1979) and were first recognised at the turn of the millennium (Myneni et al., 1997; Myneni, Tucker, Asrar, & Keeling, 1998; Tucker et al., 2001). More recent studies have confirmed the Arctic wide trends (Bhatt et al., 2010; Guay et al., 2014; Keenan & Riley, 2018; Zhu et al., 2016), but also highlight a notable amount of variation at global (Bhatt et al., 2010; Guay et al., 2014; Tucker et al., 2001), continental (Fraser et al., 2011; Jia, Epstein, & Walker, 2003, 2009; Ju & Masek, 2016) and regional scales (Lara, Nitze, Grosse, Martin, & McGuire, 2018; Macias-Fauria, Forbes, Zetterberg, & Kumpula, 2012; Miles & Esau, 2016; Raynolds, Walker, Verbyla, & Munger, 2013; Thompson & Koenig, 2018; Vickers et al., 2016; Walker et al., 2009) including many areas that show either no trends in NDVI or even significant "browning" (e.g. Guay et al., 2014; Lara et al., 2018; Walker et al., 2009) and a recent slowdown of the arctic wide greening trend has been suggested (Bhatt et al., 2013).

What explains satellite trends

Satellite greening trends of the tundra have been linked directly to trends in temperatures (Bhatt et al., 2013; Keenan & Riley, 2018; Raynolds, Comiso, Walker, & Verbyla, 2008; Vickers et al., 2016) and indirectly to changes in sea-ice conditions (Fauchald, Park, Tømmervik, Myneni, & Hausner, 2017; Macias-Fauria et al., 2012; Walker et al., 2009). Furthermore, tundra vegetation changes reported by *in situ* (ground-based) studies support the overall greening trend: Tundra vegetation community composition is changing (Elmendorf et al., 2012, 2015) including the expansion of more productive shrubs (Myers-Smith, Forbes, et al., 2011; Tape, Hallinger, Welker, & Ruess, 2012; Tape, Strum, & Racine, 2006), and vegetation height is increasing in many communities across the biome (Bjorkman et al., 2018). Yet few studies have been able to directly link on-the-ground ecological changes to satellite trends in NDVI (Macias-Fauria et al., 2012; Pattison, Jorgenson, Raynolds, & Welker, 2015; Walker et al., 2009).

Growing season phenology - how is it changing?

Satellite observations of tundra growing season phenology have suggested advances in the start and delays in the end of the growing season, and associated increases in growing season length have been reported (Zhou et al., 2001; Zeng et al., 2011, 2013; but see White et al., 2009). However, no coherent directional trend of phenological change has been reported from long-term *in situ* phenological observations across the biome (Chapter 2): while spring and summer advances have been reported for some locations (Høye, Post, Meltofte, Schmidt, & Forchhammer, 2007; Kerby & Post, 2013a; Post, Kerby, Pedersen, & Steltzer, 2016) others show no evidence or delays (Bjorkman, Elmendorf, Beamish, Vellend, & Henry, 2015; Oberbauer et al., 2013; Prevéy et al., 2017). Little is known about *in situ* trends of autumn phenology in the tundra (Gallinat, Primack, & Wagner, 2015; Prevéy et al., 2017; Myers-Smith et al., 2018). Snowmelt, temperature and sea-ice have been identified as drivers of *in situ* phenology in the tundra (Bjorkman et al., 2015; Post et al., 2016; Prevéy et al., 2017; Semenchuk et al., 2016), but few studies have attributed variation in regional and landscape level phenology to environmental factors (Kerby, 2015, 2015; Macias-Fauria et al., 2012; Miles & Esau, 2016) or ground validated satellite-derived phenology (Beck et al., 2007; Gamon, Huemmrich, Stone, & Tweedie, 2013; White et al., 2009). Furthermore, the importance of heterogeneity in tundra phenology for plant-consumer and -pollinator interactions is poorly understood (Armstrong, Takimoto, Schindler, Hayes, & Kauffman, 2016; Kerby, 2015). Frequent cloud cover within the short growing seasons of the Arctic complicates time-series analysis based on optical satellite imagery and increases uncertainties in the derived predictions of start, peak and end of season (Gamon et al., 2013; Jia et al., 2003, 2009; Stow et al., 2004).

The scale discrepancy problem and the ecology of NDVI

A major problem in linking satellite observed trends of tundra greenness and phenology to *in situ* observations and ecological processes is the discrepancy in scales between the two types of observations (Myers-Smith, Forbes, et al., 2011; Raynolds et al., 2013; Stow et al., 2004; Woodcock & Strahler, 1987): While satellite datasets with long-term records are limited by their moderate- to coarse-grain sizes, ranging from 30 m (Landsat) to 250 m (MODIS) and 8 km (AVHRR-GIMMS3g), *in situ* ecological monitoring in tundra ecosystems is logistically challenging and therefore

restricted to few sites in the biome and small plot-scales (plot sizes of one square metre or below are common, see for example Molau & Mølgaard, 1996). The interpretation of satellite-scale NDVI is furthermore complicated by methodological artefacts and uncertainties about the ecological meaning of the trends in the vegetation index. Though overall related to the amount of photosynthetically active biomass (Blok et al., 2011; Raynolds, Walker, Epstein, Pinzon, & Tucker, 2012), long-term coarse-scale observations of NDVI may be subject to errors relating to sensor calibration (Martínez-Beltrán, Jochum, Calera, & Meliá, 2009; Teillet, Staenz, & William, 1997) and non-linearity of the vegetation index (Huete et al., 2002; Martínez-Beltrán et al., 2009), while spectral mixing at the sub-pixel level integrates a complexity of ecological processes (Huemmrich et al., 2010; Loranty et al., 2018; Walker et al., 2009) and may cause contradicting trends in tundra NDVI from satellite observations at different spatial grain sizes (Pattison et al., 2015). Recently emerging drone technologies and associated sensors allow for the collection of fine-grain multispectral imagery at landscape scales that has the potential to bridge the scale-gap between satellite and ground-based observations (Anderson & Gaston, 2013; Klosterman et al., 2018; Klosterman & Richardson, 2017).

Novel drone data to study variation in greenness

In this study, we combine a novel data set of twelve within-growing season time-series of fine-grain drone-derived tundra greenness of two years (2016 and 2017) with medium- to coarse- grain satellite observations to test the correspondence between drone and satellite datasets and asses how fine-scale variation in tundra greenness is distributed across space and time at our study site in the mid-Arctic of Canada. Specifically, we address the following four questions: (1) How well do satellite and drone measures of tundra greenness correspond? (2) How is fine-grain variation in tundra greenness distributed across space? (3) Does local spatial variation in tundra greenness increase or decline across the growing season? And, (4) are the trend estimates in variation over time influenced by the scale of observation? Our analysis therefore allows us to validate satellite derived landscape estimates of vegetation greenness with fine-grain drone data and describe spatial and temporal variation in tundra productivity at grain sizes and extents that were not previously accessible.

Methods

Site description

The research for this study was conducted on Qikiqtaruk – Herschel Island (138.91 W, 69.57 N). The island is located in the Beaufort Sea along the coastline of the Yukon North Slope in the Yukon Territory, Canada. It was formed as a push moraine by the Laurentide Ice Sheet and the soils are composed of glacial and marine deposits (Burn & Zhang, 2009). Continuous ice-rich permafrost underlies the active layer top-soils and is subject to frequent disturbance, such as soil creep and thaw slumping (Obu et al., 2015). Climate and vegetation are currently undergoing pronounced changes: Ground-based observations show autumn warming, increases in shrub and graminoid abundance, decline of bare ground cover, advancement of spring and a lengthening of the growing season (Myers-Smith et al., 2018); and satellites demonstrate a greening of the landscape (Fraser et al., 2011).

The vegetation of Qikiqtaruk has been described as shrub tundra (Myers-Smith, Hik, et al., 2011) and is characteristic for the lowlands of the North-Slope of the Yukon Territory and adjacent Alaska. The two most common plant communities on the island are found in the “Herschel“ and “Komakuk” vegetation types (Obu et al., 2015; Smith, Kennedy, Hargrave, & McKenna, 1989). Herschel vegetation is dominated by the tussock forming sedge *Eriophorum vaginatum* L. with varying cover of *Salix pulchra* Cham.. Komakuk vegetation is found on previously disturbed ground and is characterised by the ubiquitous presence of *Dryas integrifolia* Vahl., the willow *Salix arctica* Phall., various grass species including *Arctagrostis latifolia*. (R.Br.) Griseb. and forb species including *Lupinus arcticus* S. Wats. (Myers-Smith, Hik, et al., 2011). The Komakuk vegetation type has greater cover of bare ground relative to the Herschel vegetation type.

Study design

In 2016, we established four research sites on the south-east corner of Qikiqtaruk (Figure 4-1). At each site two 100 m x 100 m (1 ha) plots were set up, one in the Herschel and one in the Komakuk vegetation type. The plots were approximately north-south oriented and generously staked out to account for measurement error in the field. The maximum distance between two sites is 2.74 km and the plots at each site are on average 300 m apart. The sites varied somewhat in altitude and

topographic location: Collinson Head (73 m), Bowhead Ridge (82 m) and Hawk Ridge (79 m) are located on ridge tops, whereas Hawk Valley (63 m) is located on a shallow north facing slope (Komakuk plot) and a valley bottom (Herschel plot). All plots are relatively level and show little variation in terrain across each plot. The mean altitudinal range within a plot is 5.0 m with a maximum range of 8.7 m for the Hawk Valley Komakuk plot.

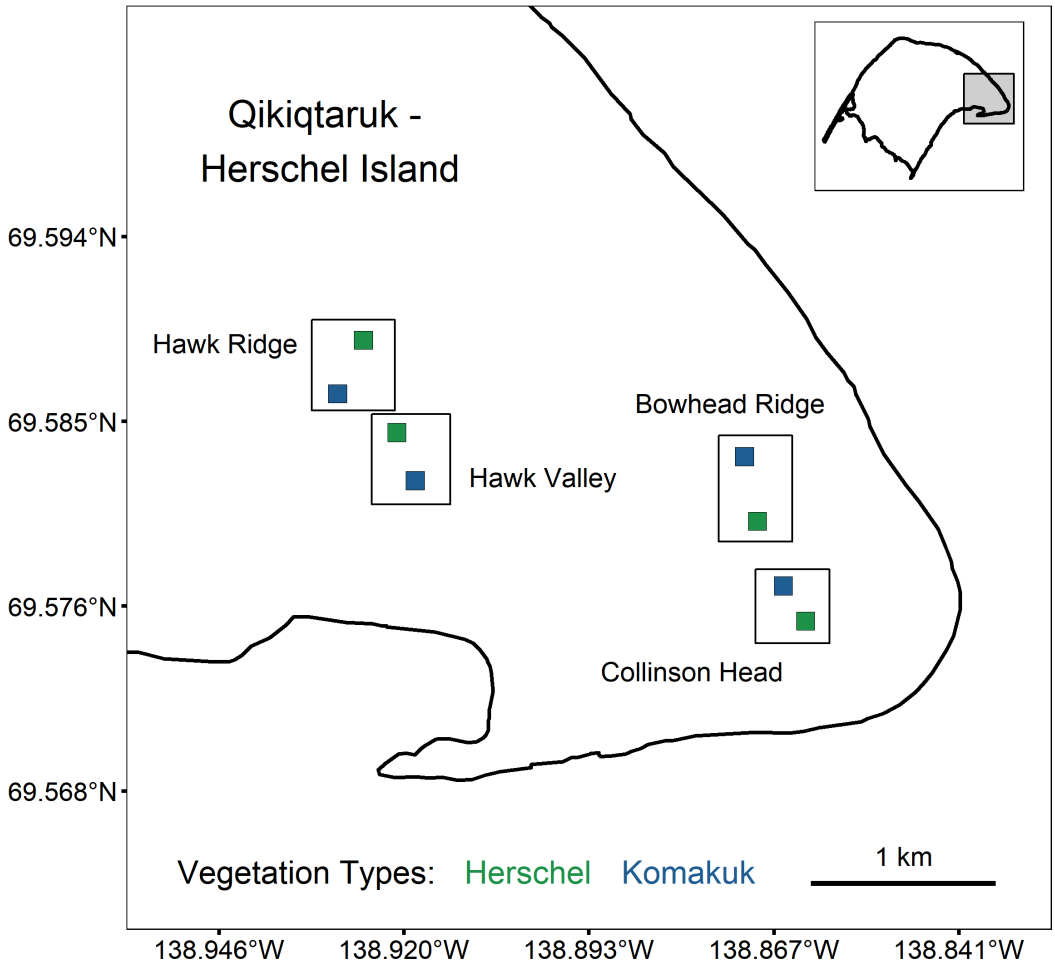

Figure 4-1 | Map of the study sites and paired Herschel and Komakuk vegetation plots on Qikiqtaruk – Herschel Island in the Canadian Yukon. The map is projected in UTM Zone 7N, WGS84. Latitude and longitude coordinate pairs are shown for ease of interpretation. Shoreline data provided by the GSHHG: http://www.soest.hawaii.edu/wessel/gshhg/ (Wessel & Smith, 1996).

Satellite data acquisition

Moderate Resolution Imaging Spectrometer Vegetation (MODIS) images were obtained through the Google Earth Engine (Gorelick et al., 2017). We used the MOD13Q1 Terra v6 vegetation index product (Didan, 2015) with pixel sizes of 250 m pixel. The MOD13Q1 product provides 16-day composite vegetation index values with quality scores on a per pixel basis. We extracted the NDVI values for the pixels containing each plot for the two study periods (May to September 2016 and May to September 2017) and discarded all values with a quality score (Summary QA) of -1 (no data) or 3 (cloudy). The MODIS NDVI is calculated from the MODIS bands 1 (near-infrared) and 2 (red), which cover the wavelengths of 841 nm – 876 nm and 620 nm – 670 nm respectively.

Sentinel 2 L1C products were obtained by querying the Copernicus Open Access Hub (https://scihub.copernicus.eu/) for all accessible imagery during the two study periods (same as MODIS) and downloading the resulting tile bundles (2016) or tiles (2017). For each image / acquisition day, the tile containing Qikiqtaruk and the surrounding area (T07WET) was then processed to the L2A product using Sen2Cor 2.4.0 (Mueller-Wilm, 2017). We retained all L2A rasters with 10 m resolution (Band 1, 2, 3 and 8), applied the L2A cloud mask and created true colour composites for each image. We further inspected all true colour images manually for cloud contamination not detected by the cloud mask and discarded all images where the study area was cloudy or partially cloudy, 78% of the satellite imagery for the 2016 period and 74% for the 2017 period had to be discarded due to cloud contamination. The resulting dataset contained 9 cloud-free L2A - 10 m resolution - 4-band images for 2016 and 15 for 2017.

The sentinel imagery was further processed by clipping to the 10 x 10 cells of the sentinel grid that had the highest overlap with the plot area established on the ground. The coordinates for the extents of the plots can be found in Appendix Table 7. Pixel by pixel NDVI values were then calculated for each Sentinel image and each plot using the rasters of band 8 (near-infrared, 784.5 nm - 899.5 nm) and band 4 (red, 650 nm - 680 nm).

Drone imagery

Multispectral drone imagery of the plots were obtained using Parrot Sequoia (Paris, France) compact multispectral sensors mounted on multi-rotor drone platforms during spring to early autumn (June – August) in 2016 and 2017. All 2016 flights were conducted with a Tarot 680 Pro based hexa-copter and the same Parrot Sequoia sensor unit (#1), which was mounted on the drone with a gimbal to stabilise the sensor for image acquisition at nadir. The 2017 surveys were carried out with two different quad-copter platforms and two Sequoia units. Three-quarters of the surveys in 2017 were flown with a 3DR Iris+ and the remaining quarter with a DJI Phantom 4 Pro. On both platforms the Sequoia units were not stabilised, and the image acquisition angle was therefore affected by the drone's attitude. All but four flights in 2017 were conducted with the Sequoia unit (#1) used for the 2016 surveys. A second, different Sequoia sensor unit (#2), was used for surveying the Site 1 Herschel and Komakuk plots on the 24 June 2017 and 9 July 2017.

Surveys were conducted with a lawn-mower flight pattern at an altitude of 50 m, which, for the Parrot Sequoia sensor, resulted in ground sampling distances between 0.05 m and 0.06 m. Images were acquired with a minimum of 75% forward and side overlap and in 2016 the plot areas marked on the ground were overshot generously. The 2017 surveys were carried out with a lower overshoot and the resulting rasters might therefore be subject to larger edge-effects. Flight times ranged between 5-17 minutes depending on the platform, flight plan and weather conditions. All survey flights were conducted as close to solar noon as possible. In 2016, the average difference to solar noon between the time of the survey and solar noon was 2 hours 47 min (maximum 6 hours 42 min) and in 2017 the mean 2 hours 15 min (maximum 6 hours 15 min).

The Parrot Sequoia imagery from each survey flight was processed in the photogrammetry software Pix4D Desktop 4.0.21 (Pix4D SA, Lausanne, Switzerland) to generate co-registered reflectance maps for each sensor band (red, green, blue and near-infrared). We used the Pix4D Desktop agMultispectral template with the "merge reflectance map tiles" option set to true. Radiometric calibration and geolocation with ground control points (GCPs) were carried out using the respective routines in Pix4D Desktop. Pre- and post-flight imagery of a pre-calibrated reflectance panel was acquired for each survey. A MicaSense (Seattle, USA) reflectance panel

was used in 2016 and SpereOptics (Herrsching, Germany) Zenith Lite panels were used in 2017. Panel reflectance for the Sequoia bands was measured pre- and post-season and the average reflectance between those two time points were used to carry out the radiometric calibration.

Thirteen GCP targets were deployed in each plot and their horizontal and vertical position measured to a horizontal accuracy of ±0.02 m using a survey-grade RTK-GNSS system in the middle of each field season. We used 4-6 of the GCPs to geolocate the imagery in Pix4D Desktop, placing markers on a minimum of three images per band per GCP. Higher marking efforts resulted in diminishing returns in geo-location accuracy, partially due to the at times poor visibility of the GCP targets in the monochromatic imagery (Chapter 3). We estimate that the co-registration between the reflectance maps of the four bands lies between 1-2 pixels for any given survey (Chapter 3) and an average horizontal geo-location accuracy of a set of co-registered reflectance maps to be between 0.1 and 0.3 m (2-6 x GSD).

The drone reflectance maps were cropped to the extent of the plots covered by the 10 x 10 subset of the sentinel grid (Appendix Table 7) Depending on the next step in the statistical analysis (see below), reflectance maps were then either a) not further processed, b) resampled to the 10 m cell size of the sentinel grid or c) resampled to 1 m, 5 m, 10 m, 20 m and 30 m cell sizes. Finally, pixel-by-pixel NDVI values were calculated from the native or resampled reflectance maps using the red (640 nm - 680 nm) and near-infrared (770 nm - 810 nm) bands of the Parrot Sequoia.

We carried out a total of 122 drone surveys across the two field-seasons. However, we did not use all drone surveys in our analyses due to overexposed radiometric calibration imagery, including all the 2016 imagery obtained for Hawk Valley (Site 3) and Hawk Ridge (Site 4). We retained two flights without calibration imagery for the Collinson Head Herschel and Komakuk plots obtained at peak growing season in 2016 for which we only used the mean NDVI and standard deviation in the analysis. We estimate an associated error of about 5% in the NDVI plot mean for those surveys due to the lack of calibration (Chapter 3). Our final dataset included 68 surveys: 19 in 2016 and 49 in 2017 (Table 4-1).

Table 4-1 | Number of drone surveys / time-points included in the time-series for each plot-site combination in the 2016 and 2017 growing seasons.

Site Name	Vegetation Type	No. flights 2016	No. flights 2017
Collinson Head (Site 1)	Herschel	6	7
	Komakuk	5	7
Bowhead Ridge (Site 2)	Herschel	4	6
	Komakuk	4	6
Hawk Valley (Site 3)	Herschel	-	5
	Komakuk	-	6
Hawk Ridge (Site 4)	Herschel	-	6
	Komakuk	-	6

Correspondence between drone and satellites

To test the correspondence between the landscape-level estimates of tundra vegetation greenness between the drone and satellite products, we calculated the mean NDVI values from the drone and Sentinel imagery for each 1 ha plot and time-point and visually compared their correspondence across the growing season with the MODIS pixel values containing each plot. We then plotted the Sentinel and drone rasters, native and resampled to the sentinel grid, for direct visual comparison. We further obtained histograms and summary statistics of the NDVI distributions to assess the change in grain size from the native to resampled drone raster and for direct comparison of the two with the Sentinel NDVI maps.

Finally, we tested the correlation between Sentinel and re-sampled 10 m drone pixel values. For this, we first created a subset of the 2017 imagery for all drone and sentinel images that were acquired within 48 hours from each other and then modelled the relationship between the NDVI rasters using a Bayesian linear mixed model. We used a mixed model to allow - and test for - an effect of plot vegetation type (Herschel or Komakuk), Sentinel satellite id (2A or 2B) and day difference between image drone and sentinel image acquisition (-2 days to +2 days) on the statistical relationship. Specifically, we modelled the relationship using the following formula:

$$NDVI_{drone} = \mu + \beta_{NDVI_{sentinel}} + \alpha_{veg.type} + \alpha_{sent.id} + \alpha_{diff.}$$
$$\beta_{NDVI_{sentinel}}: veg.type +$$
$$\beta_{NDVI_{sentinel}}: sent.id +$$
$$\beta_{NDVI_{sentinel}}: diff. + \varepsilon$$

Where $NDVI_{drone}$ is the pixel value of the resampled 10 m drone pixel, μ the global intercept; $\beta_{NDVI_{sentinel}}$ the slope value for the linear relationship between the drone pixel and the corresponding sentinel pixel; $\alpha_{veg.type}$,$\alpha_{sent.id}$ and $\alpha_{diff.}$ the fixed intercepts for vegetation type, sentinel satellite id and difference in acquisition data between drone and sentinel imagery; $\beta_{NDVI_{sentinel}}: veg.type$, $\beta_{NDVI_{sentinel}}: sen.id$ and $\beta_{NDVI_{sentinel}}: diff.$ the interactions between vegetation type, Sentinel id and difference in acquisition date and the continuous predictor – the Sentinel pixel NDVI value; and ε the residual error. ε was distributed normally with a variance estimated from the data. We used weakly informative priors for all parameter estimates: inverse Wishart priors for the residual variance and normal priors for the fixed effects (Hadfield, 2017). We were unable to model random intercepts or slopes as there was insufficient replication in the auxiliary predictors (including difference in acquisition date and plot id) for the model to converge.

Fine-scale variation across space

To study the fine-scale distribution of variation in vegetation greenness across space, we first selected six drone NDVI maps at native grain-size from the Bowhead Ridge (Site 2) 2017 time-series: three maps from each vegetation type obtained at the beginning peak and end of the growing season (26 June, 27 July and 9 August 2017 respectively). We then obtained variograms and model fits for the NDVI rasters using the gstat package of the statistical computing environment R and calculated the mean range estimate of all variogram model fits. We were unable to fully sample the large native grain-size drone rasters (up to 4 million cells) for the variograms due to computational limitations. Instead we obtained variogram estimate based on a random sample of 5% of the cells in each rasters. Semi-variance of NDVI was estimated for bin-widths of 0.15 m for all point-pair distances up to 15 m and bin-widths of 3 m for all point-pair distances up to 45 m. A minimum sample of 1.6 million

point-pairs (mean: 39 million) per bin was obtained to estimate the semi-variance of the 0.15 m bins, and a minimum sample of 430 million point-pairs (mean: 666 million) per bin was used to estimate the semi-variance of the 3 m bins. The variogram-model fit function of the gstat package automatically chooses the best model of fit. In all cases a spherical model provided the best fit. The model parameters (range, nugget, sill) were extracted and the mean range for the three rasters calculated.

Variation across the growing season

To assess the variation in tundra greenness across the growing season we analysed the trends over time in the standard deviation of plot-level NDVI for the time-series in 2016 (4 time-series) and 2017 (8 time-series). For each plot and time-point of observation the standard deviation of NDVI in the 1 ha plot was calculated. We then fitted a Bayesian linear mixed model to test for a trend over time. We hypothesised potential effects of vegetation type and year on the intercept of the model, and fitted the model with the following formula:

$$SD_{NDVI} = \mu + \beta_{day\ of\ year} + \alpha_{veg.type} + \alpha_{year} + \varepsilon$$

Where SD_{NDVI} is the standard deviation in NDVI across a plot; μ is the global intercept; $\beta_{day\ of\ year}$ the slope between the day of year and the standard deviation in NDVI; $\alpha_{veg.type}$ and α_{year} the fixed intercepts for vegetation type and year; and ε the residual error. ε was distributed normally with a variance estimated from the data. We used weakly informative priors for all parameter estimates: inverse Wishart priors for the residual variance and normal priors for the fixed effects.

We repeated the above analysis with the coefficient of variance instead of the standard variation and obtained comparable results, and tested for an effect of vegetation type on $\beta_{day\ of\ year}$ (veg. type:day of year interaction), but found no significant effect.

Influence of grain size on trends in variation

In our final analytical step, we tested whether the trend in standard deviation across the growing season was affected by grain size. We repeated the analysis for the previous section using the drone NDVI map resampled to the five cell sizes: 1 m, 5

m, 10 m, 20 m and 30 m. In addition to vegetation type and year we modelled a fixed intercept for grain size and a day of year:grain size interaction to test for an effect of grain size on the slope of the relationship:

$$SD_{NDVI} = \mu + \beta_{day\ of\ year} + \alpha_{veg.type} + \alpha_{year} + \alpha_{grain\ size} + \beta_{day\ of\ year}: grain\ size + \varepsilon.$$

Where SD_{NDVI} is the standard deviation in NDVI across a plot; μ is the global intercept; $\beta_{day\ of\ year}$ the slope between the day of year and the standard deviation in NDVI; $\alpha_{veg.type}$, α_{year} and $\alpha_{grain\ size}$ the fixed intercepts for vegetation type, year and grain size; $\beta_{day\ of\ year}: grain\ size$ the interaction between grain size and the slope; and ε the residual error. ε was distributed normally with a variance estimated from the data. We used weakly informative priors for all parameter estimates: inverse Wishart priors for the residual variance and normal priors for the fixed effects.

Data handling and packages

All data handled and analysis was carried out in the R statistical environment (version 3.4.2). Clipping , resampling, summary statistics and general spatial data handling was performed with the raster version 2.5-8 (Hijmans, 2016), sp version 1.2-5 (R. S. Bivand, Pebesma, & Gomez-Rubio, 2013; Pebesma & Bivand, 2005) and rgdal version 1.2-15 (R. Bivand, Keitt, & Rowlingson, 2017) packages. Raster visualisations were created with rasterVis version 0.41 (Perpiñán & Hijmans, 2018) and the gstat version 1.1-6 (Gräler, Pebesma, & Heuvelink, 2016; Pebesma, 2004) package was used obtain variograms and model fits. General data visualisations were created using ggplot2 version 2.3.0.0 (Wickham, 2016). Finally, the MCMCglmm package (version 2.25) was used for Bayesian linear mixed modelling. Model convergence was confirmed through examinations of the trace plots. We refer to effects as “significant” if the 95% credible intervals do not overlap zero.

Results

Correspondence across platforms at landscape level

Landscape-scale estimates of tundra greenness of our study plots corresponded well between the satellite and drone platforms in the 2016 and 2017 growing seasons, even though the time-series suggest a small offset between the drone and satellite

mean NDVI estimates of the 1 ha tundra plots (Table 4-2 and Figure 4-2 A). The July mean NDVI for the Herschel and Komakuk vegetation types showed stark differences in landscape-level greenness between the two vegetation types in the 2017 growing season, but no clear difference was observed in the 2016 growing season (Figure 4-2 B). July landscape-level greenness in 2017 was notably higher for the Komakuk plots than the Herschel plots (Figure 4-2 B). When resampling the native grain-size drone rasters to the 10-m Sentinel grid a substantial amount of variation in NDVI was lost (Figure 4-3). Nonetheless, we observed a strong linear relationship between Sentinel pixel NDVI values and the NDVI values of the re-sampled 10 m drone rasters (Figure 4-4). The intercept (and slope of this relationship were significantly dependent on the vegetation type, the specific Sentinel satellite from which the imagery were obtained and the acquisition time difference in days between the drone and Sentinel image (Appendix Table 8).

Table 4-2 | Difference in July plot-level NDVI between the three sensing platforms (drone, Sentinel and MODIS) for the 1 ha study plots on Qikiqtaruk. Drone and Sentinel observations represent July mean NDVI values of the plots, whereas the MODIS observations represent the July mean NDVI value of the MODIS pixels containing the plots.

Platform Comparison	Difference in July Plot NDVI	Standard Deviation in July Plot NDVI
Drone to MODIS	0.060	0.026
Drone to Sentinel	0.066	0.017
Sentinel to MODIS	-0.006	0.026

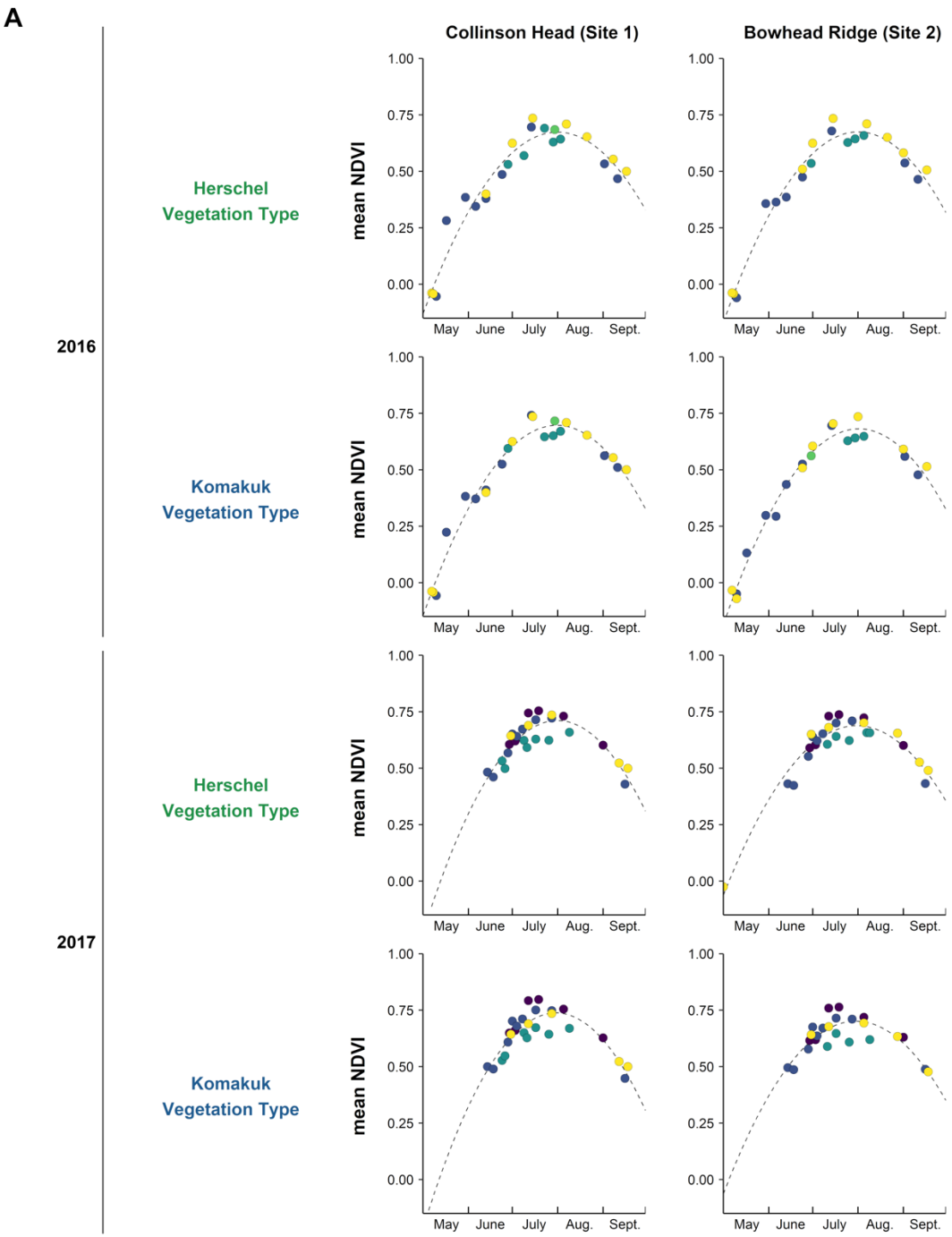

Figure 4-2 | A) Time-series of drone, Sentinel 2 and MODIS estimates of landscape greenness of the four one-hectare plots in the two vegetation types (Herschel and Komakuk) on Qikiqtaruk across the growing seasons of 2016 and 2017. Drone and Sentinel observations represent site-averages in NDVI, whereas the MODIS observations represent the NDVI value of the MDIS pixel containing each respective plot. B) Drone-derived mid-season NDVI estimates for the Herschel and Komakuk vegetation types in 2016 and 2017. Values and error bars represent the mean and

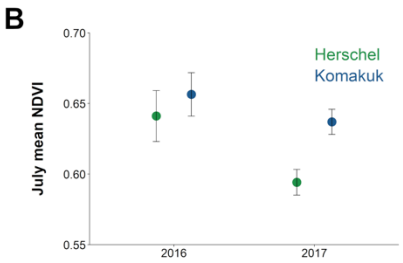

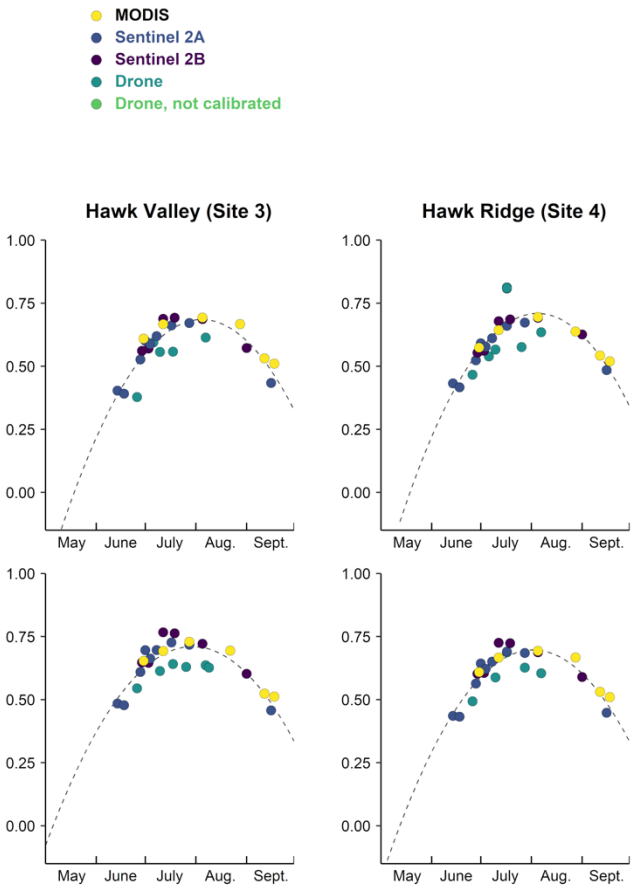

associated standard error for all drone surveys conducted over the 1 ha vegetation plots during the month of July in the respective year. Growing-season NDVI curves are shown for illustrative purposes and represent a simple quadratic model fit of the plot-level NDVI from all sensors and the day of year (doy): NDVI = $\alpha doy^2 + \beta doy + \gamma$.

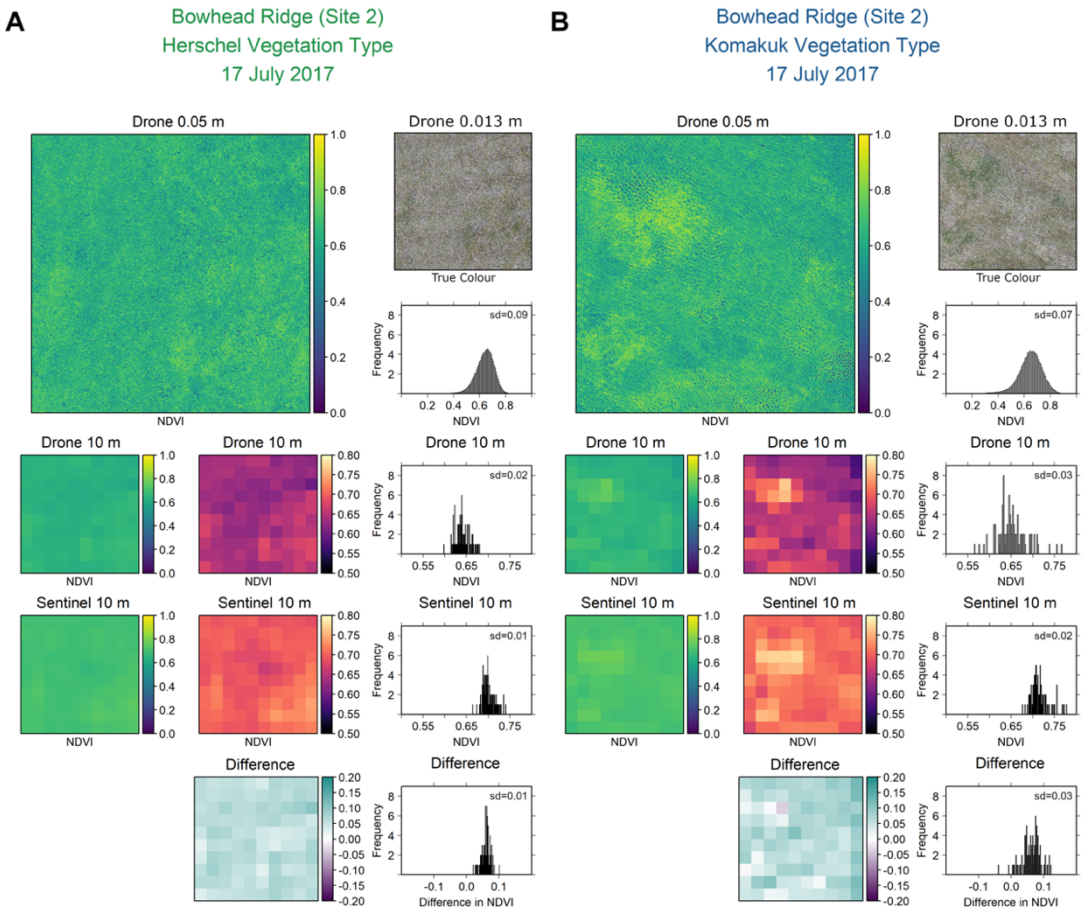

Figure 4-3 | Spatial variation and pixel-by-pixel differences in NDVI for the Bowhead Ridge (Site 2) Herschel (A) and Komakuk (B) plots as observed by drone and Sentinel 2A on the 17 July 2017. Drone reflectance maps were re-sampled to the 10 m Sentinel 2 grid prior calculation of the NDVI for the pixel-by-pixel comparisons. Ten-metre resolution NDVI maps are shown with two colour-scales to visualise the reduced pixel-by-pixel variation in the coarser grain rasters. Histograms and standard deviation visualise variation for each NDVI map. True colour orthomosaics are shown for illustrative purposes. RGB imagery was obtained on the same date with the native DJI Phantom 4 Pro camera and subsequently processed with Pix4D Desktop.

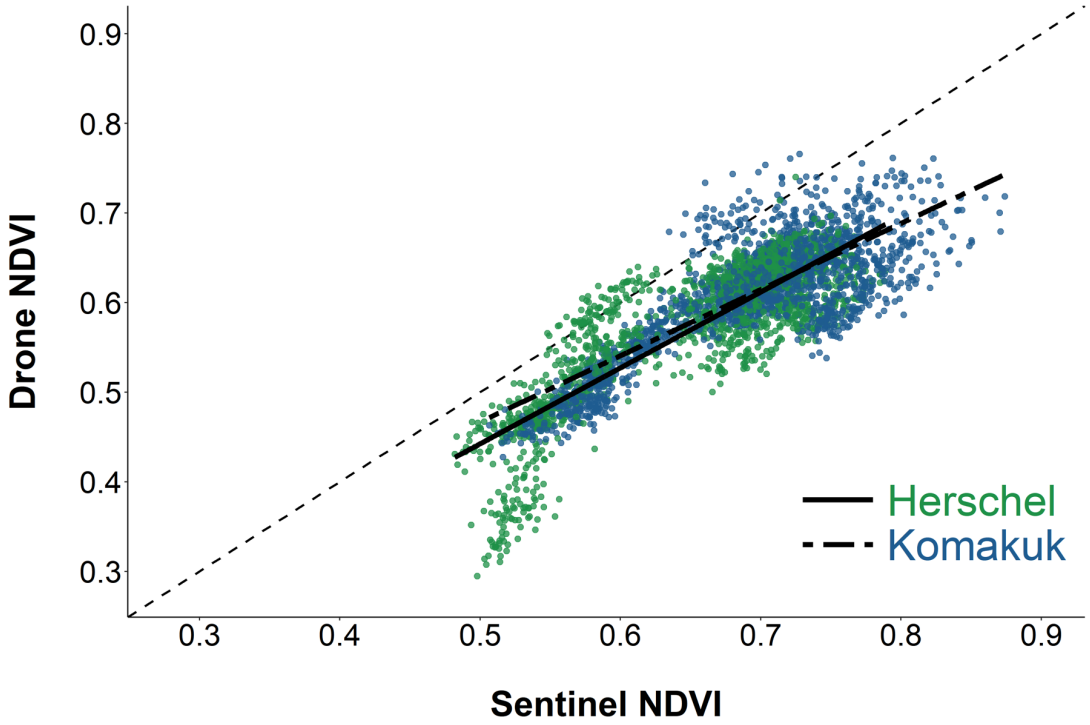

Figure 4-4 | Pixel by pixel comparison between Sentinel 2 L2A pixel values and resampled drone data for our study sites on Qikiqtaruk in 2017. Drone red and near-infrared drone reflectance maps were re-sampled from their native (approximately 0.05 m) ground sampling distance to match the Sentinel grid with a 10 m grain size. All Sentinel-drone pixel pairs were matched from images acquired less than 48 hours apart. We estimated slope and intercept of the linear relationship using Bayesian mixed models, testing for the effect of day difference in acquisition time (days), vegetation type (Herschel and Komakuk) and Sentinel satellite platform (Sentinel 2A and 2B). All of these factors had a significant effect on intercept and slope (Appendix Table 8). Here, we show a simpler version of the linear model for graphical clarity, which includes only the effect of vegetation type on intercept and slope of the relationship (Appendix Table 9). The dataset contained a total of 68 drone surveys with nine distinct Sentinel image and drone survey date-pairs obtained from up to four plots per vegetation type.

Fine-scale variation in landscape greenness

Semi-variance of vegetation greenness for the Herschel and Komakuk vegetation plots at Bowhead Ridge (Site 2) derived from the native-scale drone rasters steadily increased from zero to about a half of a metre distance and levelled off thereafter (Figure 4-5). The spherical variogram models confirmed the visual trend and returned a mean range of 0.52 m (Figure 4-5 B). We found no notable difference in the behaviour of NDVI semi-variance with distance for both vegetation types but generally observed lower semi-variance values for the Herschel vegetation type (Figure 4-5).

Likewise, the NDVI semi-variance pattern was consistent among different time-points of the growing season, though overall semi-variance decreased with progression of the season in 2017 (Figure 4-5).

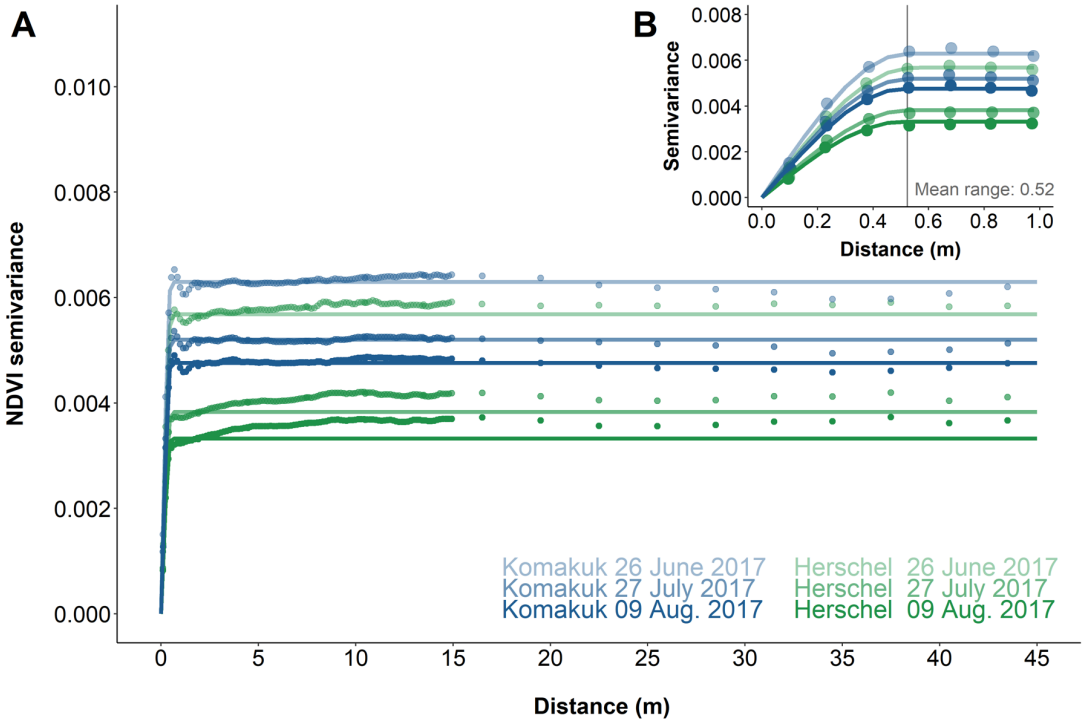

Figure 4-5 I A) Variograms and model fits of drone derived NDVI maps with ground sampling distances of approximately 0.05 m for the Herschel and Komakuk vegetation plots at Bowhead Ridge (Site 2) on three time-points during the growing season of 2017. B) Close up of the semi-variograms and model fits for bin distances below 1 m.

Variation across the growing season

We observed a decline in standard deviation of NDVI derived from the native-scale drone imagery for all plots across the growing season of both years (Figure 4-6). The slopes of linear mixed models were statistically significant with significant effects for the intercept for vegetation type and year (Appendix Table 10). No significant interaction between vegetation type and the slope of the relationship was observed (Appendix Table 11). We also tested the relationship using the coefficient of variation instead of the standard deviation and obtained comparable results (Appendix Table 12). Four of the 12 time-series showed a notable dip in standard deviation in the middle of the growing season (Figure 4-6 B).

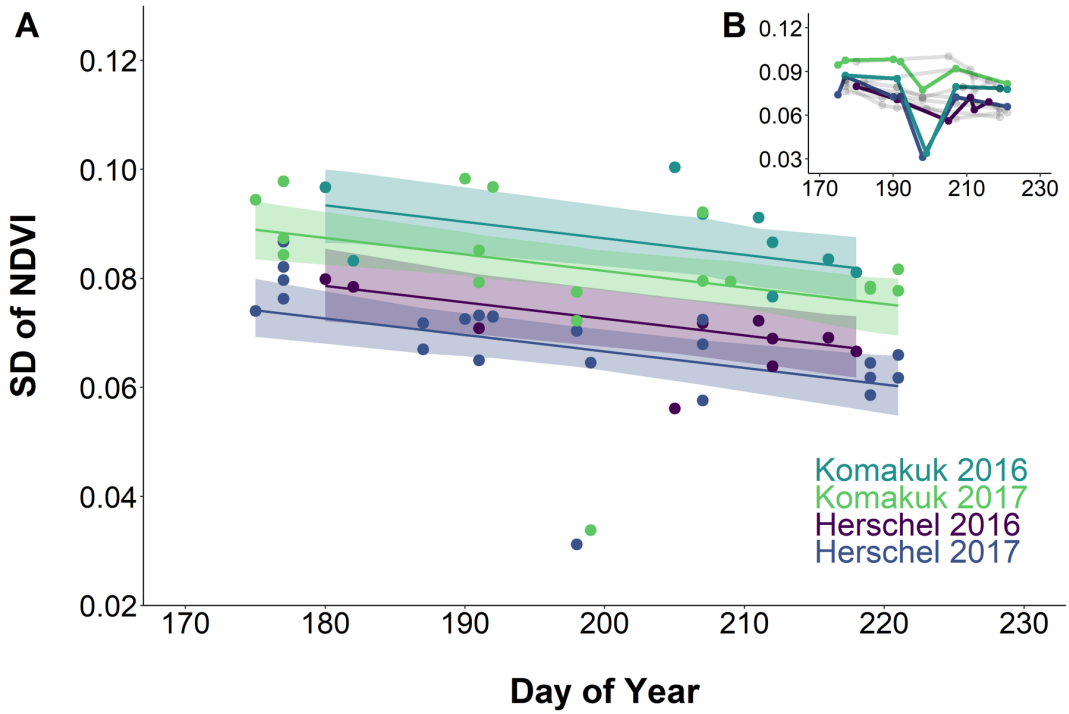

Figure 4-6 l (A) Change in the standard deviation of NDVI for 1 ha plots surveyed with drones at a ground sampling distance of approximately 0.05 m for the Herschel and Komakuk vegetation types in the years 2016 (4 time-series) and 2017 (8 time-series). See Appendix Table 10 for slope and intercept estimates. (B) Two time-series in each year showed a pronounced dip in the standard deviation at peak-growing season: The time-series of the Collinson Head (Site 1) Herschel plot in 2016 (purple) and 2017 (dark blue), as well as the time-series of the Collinson Head (Site 1) Komakuk plot in 2016 (light blue) and the Hawk Valley (Site 3) Herschel plot in 2017 (green). The remaining time-series are shown in light grey.

Influence of grain size on trends in variation

The slope of the linear trend in the standard deviation of plot-level NDVI across the growing season was not affected by grain size (Figure 4-7). We found no significant effect of the grain size on the slope of the linear mixed model (Appendix Table 13). For all grain sizes the slope declined as the growing seasons progressed. Nonetheless, the standard deviation decreased with grain size (Figure 4-7), which was also confirmed by a mixed model analysis, for which grain size and vegetation type significantly affected the intercept of the relationship if a grain size:slope interaction was not included (Appendix Table 14). Year did not significantly impact the intercept with or without interaction.

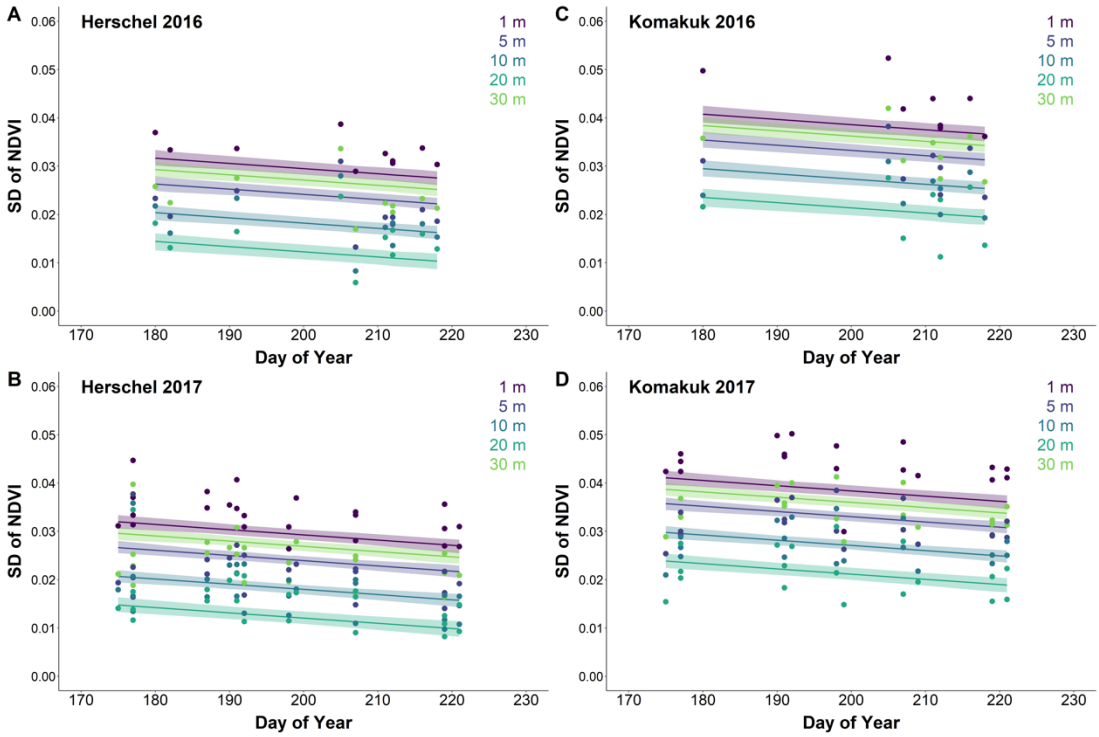

Figure 4-7 | Influence of grain size on the trends in standard deviation of NDVI across the growing seasons for the 1 ha plots in the drone dataset. The drone reflectance map rasters were resampled to 5 different cell sizes (1 m, 5 m, 10 m, 20 m and 30 m), the NDVI calculated and the standard deviation determined. Trend lines represent Bayesian linear mixed model fits with fixed intercept estimates for vegetation type (Herschel and Komakuk) and the years 2016 (A and C) and 2017 (B and D) for the five cell sizes indicated by colour. See Appendix Table 14 for the posterior parameter estimates of the model. The slightly lowered trendline for the 1 m cell size is likely caused by the tendency of generalised mixed models to pull the effect sizes of extreme groupings towards the overall mean effect.

Discussion

Our analysis of correspondence between drone and satellite measures of tundra productivity, and study of fine-grain variation of tundra productivity highlight the following main findings: (1) Drone and satellite derived measures of tundra productivity correspond well at the landscape level (grain sizes of 10 m - 100 m). However, a substantial amount of variation is lost when the fine-scale drone data is aggregated to the grain sizes of even the most high-resolution satellite products that are publicly available, such as those from the Sentinel 2 satellites. (2) Tundra vegetation productivity in the 1 ha study plots at our field site is auto-correlated for distances below 0.5 m, but variation plateaus just above this distance and increases very little or not at all for distances of up to 45 m thereafter. (3) We observed a

significant decline in the variation of tundra greenness across the growing season of both studied years. (4) This trend in standard deviation was not affected by variation in grain sizes for grain sizes up to 30 m. Our findings therefore validate landscape-level measures of vegetation productivity derived from coarse-grain satellite data but highlight a substantial amount of spatial and temporal variation in tundra vegetation greenness at fine-scales, currently not captured by publicly available satellite products. Understanding plant phenology trends at finer resolutions, and also the changing heterogeneity of phenology, will be key for understanding of how tundra ecosystems will respond as the climate continues to warm.

Correspondence across platforms at landscape level

Drone and satellite measures of landscape-level tundra greenness corresponded well and so did pixel by pixel comparisons of Sentinel L2A products and resampled drone NDVI. Whereas these findings validate the landscape-level measures of tundra vegetation greenness for our study plots across the platforms, the observed offset (approximately 0.06 for July-mean plot-level NDVI) between drone and satellite NDVI and the random variation over time indicated in imagery from all platforms underline the broader challenges of cross-platform comparison of NDVI values. Despite being a normalised ratio, absolute NDVI values are not necessarily directly comparable across platforms and time-points of acquisition due to a variety of error sources associated with the underlying reflectance measurements, which apply to both drone (Chapter 3; Aasen & Bolten, 2018; Aasen, Burkart, Bolten, & Bareth, 2015) and satellite derived NDVI measurements (Fan & Liu, 2016; Martínez-Beltrán et al., 2009; Teillet et al., 1997).

The main error sources complicating comparisons of NDVI values across sensors, space and time are (in no particular order): atmospheric disturbance and solar illumination, differences in optical apparatus between sensors, calibration accuracies, differences in spectral bands and ground sampling distance, spatial integration of reflectance measurements across different grain sizes, as well as image geometry, geolocation and co-registration between bands (Fan & Liu, 2016; Martínez-Beltrán et al., 2009; Teillet et al., 1997). We accounted for these error sources through standardising our drone data acquisition method (Chapter 3) and using post processed satellite products that include atmospheric corrections and cross sensor

calibration such as the MOD13Q1 and Sentinel L2A products, but caution that some error will remain in our analysis. With the rapid development of drone technologies and sensors, we advocate for continued cross-platform and sensor comparisons using improved and standardized methods between drone- and satellite-derived measures of tundra vegetation greenness.

Loss of variation with increasing grain size

A notable amount of variation was lost when resampling the drone data to coarser grain sizes and comparing the native resolution drone NDVI maps to the Sentinel products. The loss of variation and diversity with increasing grain size is a classic phenomenon well discussed in the ecological and geographic literature (Jelinski & Wu, 1996; Marceau, 1999; Turner, O'Neill, Gardner, & Milne, 1989; Woodcock & Strahler, 1987) and often referred to as the "scale problem" component of the modifiable area unit problem (MAUP) (Openshaw & Taylor, 1981). Our study provides yet another example and demonstrates that this problem also applies when shifting from fine-grain drone imagery to medium grain satellite-based measurements of tundra vegetation greenness. However, whether this loss of variation and hence information matters is highly dependent on the ecological phenomena under consideration (Levin, 1992; Marceau, 1999; Turner et al., 1989). As a first step to finding an answer to this question, we investigated how fine-scale variation in vegetation greenness on Qikiqtaruk is spatially structured in the two studied vegetation types.

Spatial structure of vegetation greenness on Qikiqtaruk

Our findings suggest that the maximum in spatial variation of tundra greenness for the Herschel and Komakuk vegetation types on Qikiqtaruk is reached at distances of just over half a metre. In our study plots, little to no additional spatial variation was observed for distances greater than half a metre and notable auto-correlation in vegetation greenness was found for distances shorter than a half of a metre. These findings correspond well with the ecological structure of the two tundra vegetation types: Tussock sedges and ice-wedge polygons dominate the structure of the Herschel vegetation type at small scales, while soil disturbances create characteristic patterning of the Komakuk vegetation over short distances, but beyond this both vegetation types are homogenous (Obu et al., 2015; Smith et al., 1989). Tussock

sedge diameter commonly ranges between 0.1 m and 0.3 m (see for example Mark, Fetcher, Shaver, & Iii, 1985) and ice-wedge polygons harbour characteristic plant communities on their rims and troughs with widths of 0.0 m – 1.0 m (Fritz et al., 2016). Komakuk vegetation is commonly found on gently sloping uplands or gentle slopes and the soil is subject to slow downslope movements and gelifluction (Obu et al., 2015). Active layer disturbances lead to a distinctive pattern of alternating vegetation and elongated bare-ground patches perpendicular to the slope with approximate dimensions of 0.3 m – 0.5 m width and 0.4 – 1.0 m length. Thus, for both of the dominant vegetation types at this site, vegetation and disturbance patterning create variation in tundra greenness at scales of less than a metre.

The marked differences between the Komakuk and Herschel vegetation types in their July mean NDVI values in the 2017 growing season demonstrate that there is variation in vegetation greenness amongst the vegetation types at the landscape level and corresponds well satellite derived vegetation type classifications of the island previously conducted (Obu et al., 2015). The absence of a clear difference in greenness between the two vegetation types in 2016 could be an artefact of the smaller sample size in that year or may suggests that differences between the vegetation types could be subject to inter-growing season variation. A multi-year satellite-based analysis or repeated drone surveys with a larger extent could be used to test how generalizable the vegetation type differences are at this site and to understand the spread of variation in greenness values among sites and community types across the tundra biome.

The observed decline in variation in NDVI within the 1 ha study plots over the progress of the growing season highlights that landscape phenology does not only relate to variation in distinct events amongst years, but that there are also temporal-patterns in the degree of spatial variation within the landscape (Armstrong et al., 2016; Kerby, 2015; Klosterman et al., 2018). The start of season for both of our study years was very similar (ground-based observations of *Salix arctica* spring leaf out on Qikiqtaruk show 5 days difference between 2016 and 2017) and indeed we did not detect any significant influence of year on the slope of the decline in standard deviation with the progression of the growing season. However, it is plausible that there are stark differences in the timing of when the minimum in variation is reached among

extremely early and late years and further exploration using an extended time-series would be warranted .

The onset of the growing season on Qikiqtaruk has been advancing (Myers-Smith et al., 2018; Chapter 2) and should this trend continue, the minimum in variation of vegetation greenness might be reached notably earlier in the year. Variation in the timing of the heterogeneity in plant phenology could alter plant consumer and pollinator interactions that rely on spatial variation in resources or “resource waves” across the landscape (Armstrong et al., 2016; Kerby, 2015). Indeed, lemming species in the Canadian Arctic (Rodgers & Lewis, 1986) and mammalian herbivores in Greenland (Klein & Bay, 1994) have been shown to change their home ranges according to the seasonal availability of their preferred food sources. Furthermore, multi-level trophic interactions in the tundra can be strongly related to snow conditions (Berg et al., 2008) which themselves can be highly localised (Pedersen et al., 2018). The ability of drone technologies to unpick fine-scale spatial and temporal variation in tundra vegetation greenness demonstrated by our study therefore provides novel opportunities to investigate plant-herbivore interactions in the tundra landscape.

We did not observe an influence of vegetation type on the slope of the decline in variation of NDVI across the growing season, suggesting that this trend holds true at the landscape level at our field site independent on vegetation type. However, the absolute magnitude of variation in NDVI (intercept) between the two vegetation types differed significantly. Vegetation indices such as the NDVI reflect plant community composition and surface cover diversity (for example, Campbell and Wynne, 2011; Gould, 2000) and the higher variation in NDVI of the Komakuk vegetation type could be explained by the higher diversity in plant species and increased bare soil cover compared to the Herschel vegetation type dominated by almost continuous growth of tussocks sedges. In addition, the species specificity of tundra plant phenological responses (Chapter 2) would suggest that higher species diversity would correlate with a higher variation in trends of vegetation greenness over small spatial scales. Further investigations using quadratic or polynomial models fitted to time-series of fine-grain drone data could improve our understanding of how species diversity influences trends and variation in vegetation greenness across the growing season in the tundra landscape.

Overall, our study underlines that drone technologies can transform the way we study landscape phenology (Anderson & Gaston, 2013; Klosterman et al., 2018; Klosterman & Richardson, 2017). Particularly in the tundra, where the plants are small in size and important environmental factors such as snow cover, carbon, nutrient and water availability vary over short distances (Hubbard et al., 2013; Muster, Langer, Heim, Westermann, & Boike, 2012; Wainwright et al., 2015), uncovering patterns in the fine-scale variation of phenology and greenness is key to improving our understanding of the mechanistic basis for landscape-scale productivity to improve predictions of future tundra vegetation change. Our ability to study the tundra landscape at sub-metre grain sizes had previously been limited by the available observational methods. Drone studies of tundra vegetation patterns and processes will likely play a critical role in improving our understanding of the hierarchical structure of the ecosystems of the north (sensu Allen & Starr, 1982).

Conclusions

The Arctic is undergoing rapid environmental change (IPCC, 2014) with dramatic consequences for the ecosystems. *In situ* observations demonstrate changes in tundra community composition (Elmendorf et al., 2015; Ernakovich et al., 2014; Myers-Smith, Forbes, et al., 2011), plant height (Bjorkman et al., 2018) and altered phenology (Høye et al., 2007; Post, Steinman, & Mann, 2018) while satellite observations suggest a highly heterogenous increase in vegetation productivity with variation in trends across the tundra and between satellite platforms (Guay et al., 2014; Keenan & Riley, 2018), as well as longer growing season caused by earlier onsets of spring and delayed onset of autumn (Zeng et al., 2011, 2013; Zhao et al., 2015). However, uncertainty remains in which ecological processes are responsible for the heterogeneity in these satellite trends and what causes disagreement across platforms (Guay et al., 2014; Zeng et al., 2013). Scale-discrepancies and methodological differences have complicated our ability to link *in situ* variation to the medium - coarse grain satellite data (Guay et al., 2014; Myers-Smith, Forbes, et al., 2011; Stow et al., 2004; Woodcock & Strahler, 1987).

Our findings demonstrate high cross-platform correspondence of drone and satellite measures of tundra greenness at the landscape-scale for our field site Qikiqtaruk, but also show a notable offset (approximately 0.06 for mean July plot-level NDVI)

between drone and satellite data. We observed a loss of variation in tundra greenness when aggregating from fine-grain drone (approx. 0.05 m) to medium-grain satellite pixel sizes (10 m). While the studied vegetation types were homogenous in vegetation greenness at the landscape scale (metres to tens of metres) we observed notable fine-scale variation below the grain sizes (sub-metre) of the most recent generation of publicly available satellite products, caused in part by variable bare-ground, vegetation cover and ice-wedge polygonal terrain. Our time-series analysis suggested a cross-growing season decline of landscape-level variation within the vegetation types, which if altered by climate change could impact plant-consumer interactions.

Our study illustrates the potential for drone derived observations to bridge the gap between satellite-derived landscape-level and small-scale *in situ* observations of vegetation productivity and phenology. Particularly in the tundra, where growth and variation occur at small scales, fine-resolution drone data can assist in advancing our understanding of the ecosystem and biome-wide processes that govern changes in vegetation productivity and phenology, and therefore will likely play a critical role in improving our forecasts of future tundra ecosystems and their feedbacks to global climate change.

Acknowledgements

We would like to thank the Team Shrub field crews of the 2016 and 2017 field seasons for their hard work and effort invested in collecting the data presented in this research, this includes Will Palmer, Santeri Lehtonen, Callum Tyler, Gergana Daskalova, Sandra Angers-Blondin and Haydn Thomas. Furthermore, we would like to thank Tom Wade and Simon Gibson-Poole from the University of Edinburgh Airborne GeoSciences Facility, as well as Chris McLellan and Andrew Gray from the NERC Field Spectroscopy Facility for their ongoing support in our drone endeavours.

We thank the Herschel Island - Qikiqtaruk Territorial Park Team and Yukon Government for providing logistical support for our field research on Qikiqtaruk including: Richard Gordon, Cameron Eckert and the park rangers Edward McLeod, Sam McLeod, Ricky Joe and Paden Lennie. All airborne activities were lincesed under

the Transport Canada special flight operations certificates ATS 16-17-00008441 RDIMS 11956834 (2016) and ATS 16-17-00072213 RDIMS 12929481 (2017).

Funding for this research was provided by NERC through the ShrubTundra standard grant (NE/M016323/1), a NERC E3 Doctoral Training Partnership PhD studentship for Jakob Assmann (NE/L002558/1), a research grant from the National Geographic Society (CP-061R-17) and a Parrot Climate Innovation Grant for Jeffrey Kerby, a NERC support case for use of the NERC Field Spectroscopy Facility (738.1115), equipment loans from the University of Edinburgh Airborne GeoSciences Facility and the NERC Geophysical Equipment Facility (GEF 1063 and 1069).

Finally, we would like to thank the Inuvialuit people for the opportunity to conduct research in the Inuvialuit Settlement Region.

References

Aasen, H., & Bolten, A. (2018). Multi-temporal high-resolution imaging spectroscopy with hyperspectral 2D imagers – From theory to application. *Remote Sensing of Environment*, *205*, 374–389. https://doi.org/10.1016/j.rse.2017.10.043

Aasen, H., Burkart, A., Bolten, A., & Bareth, G. (2015). Generating 3D hyperspectral information with lightweight UAV snapshot cameras for vegetation monitoring: From camera calibration to quality assurance. *ISPRS Journal of Photogrammetry and Remote Sensing*, *108*, 245–259. https://doi.org/10.1016/j.isprsjprs.2015.08.002

Allen, T. F. H., & Starr, T. B. (1982). *Hierarchy*. Chicago: Univeristy of Chicago Press. Retrieved from https://www.press.uchicago.edu/ucp/books/book/chicago/H/bo26850242.html

Anderson, K., & Gaston, K. J. (2013). Lightweight unmanned aerial vehicles will revolutionize spatial ecology. *Frontiers in Ecology and the Environment*, *11*(3), 138–146. https://doi.org/10.1890/120150

Armstrong, J. B., Takimoto, G., Schindler, D. E., Hayes, M. M., & Kauffman, M. J. (2016). Resource waves: phenological diversity enhances foraging opportunities for mobile consumers. *Ecology*, *97*(5), 1099–1112. https://doi.org/10.1890/15-0554.1

Barboza, P. S., Van Someren, L. L., Gustine, D. D., & Bret-Harte, M. S. (2018). The nitrogen window for arctic herbivores: plant phenology and protein gain of migratory caribou (Rangifer tarandus). *Ecosphere*, *9*(1), e02073. https://doi.org/10.1002/ecs2.2073

Beck, P. S. A., Jönsson, P., Høgda, K.-A., Karlsen, S. R., Eklundh, L., & Skidmore, A. K. (2007). A ground-validated NDVI dataset for monitoring vegetation dynamics and mapping phenology in Fennoscandia and the Kola peninsula. *International Journal of Remote Sensing*, *28*(19), 4311–4330. https://doi.org/10.1080/01431160701241936

Berg, T. B., Schmidt, N. M., Høye, T. T., Aastrup, P. J., Hendrichsen, D. K., Forchhammer, M. C., & Klein, D. R. (2008). High-Arctic Plant—Herbivore Interactions under Climate Influence. In *Advances in Ecological Research* (Vol. 40, pp. 275–298). Academic Press. https://doi.org/10.1016/S0065-2504(07)00012-8

Bhatt, U. S., Walker, D. A., Raynolds, M. K., Comiso, J. C., Epstein, H. E., Jia, G., … Webber, P. J. (2010). Circumpolar Arctic Tundra Vegetation Change Is Linked to Sea Ice Decline. *Earth Interactions*, *14*(8), 1–20. https://doi.org/10.1175/2010EI315.1

Bhatt, U. S., Walker, D., Raynolds, M., Bieniek, P., Epstein, H., Comiso, J., … Polyakov, I. V. (2013). Recent Declines in Warming and Vegetation Greening Trends over Pan-Arctic Tundra. *Remote Sensing*, *5*(9), 4229–4254. https://doi.org/10.3390/rs5094229

Bivand, R., Keitt, T., & Rowlingson, B. (2017). *rgdal: Bindings for the 'Geospatial' Data Abstraction Library*. Retrieved from https://CRAN.R-project.org/package=rgdal

Bivand, R. S., Pebesma, E., & Gomez-Rubio, V. (2013). *Applied spatial data analysis with R, Second edition*. Springer, NY. Retrieved from http://www.asdar-book.org/

Bjorkman, A. D., Elmendorf, S. C., Beamish, A. L., Vellend, M., & Henry, G. H. R. (2015). Contrasting effects of warming and increased snowfall on Arctic tundra plant phenology over the past two decades. *Global Change Biology*, *21*, 4651–4661. https://doi.org/10.1111/gcb.13051

Bjorkman, A. D., Myers-Smith, I. H., Elmendorf, S. C., Normand, S., Rüger, N., Beck, P. S. A., … Weiher, E. (2018). Plant functional trait change across a warming tundra biome. *Nature*, *562*(7725), 57–62. https://doi.org/10.1038/s41586-018-0563-7

Blok, D., Schaepman-Strub, G., Bartholomeus, H., Heijmans, M. M. P. D., Maximov, T. C., & Frank Berendse. (2011). The response of Arctic vegetation to the summer climate: relation between shrub cover, NDVI, surface albedo and temperature. *Environmental Research Letters*, *6*(3), 035502. https://doi.org/10.1088/1748-9326/6/3/035502

Burn, C. R., & Zhang, Y. (2009). Permafrost and climate change at Herschel Island (Qikiqtaruq), Yukon Territory, Canada. *Journal of Geophysical Research: Earth Surface*, *114*(F2). https://doi.org/10.1029/2008JF001087

Campbell, J. B., & Wynne, R. H. (2011). *Introduction to Remote Sensing, Fifth Edition*. New York, UNITED STATES: Guilford Publications.

Chapin, F. S., Sturm, M., Serreze, M. C., McFadden, J. P., Key, J. R., Lloyd, A. H., … Welker, J. M. (2005). Role of Land-Surface Changes in Arctic Summer Warming. *Science*, *310*(5748), 657–660. https://doi.org/10.1126/science.1117368

Didan, K. (2015). MOD13Q1 MODIS/Terra Vegetation Indices 16-Day L3 Global 250m SIN Grid V006. NASA EOSDIS Land Processes DAAC. Retrieved from doi: 10.5067/MODIS/MOD13Q1.006

Doiron, M., Gauthier, G., & Lévesque, E. (2015). Trophic mismatch and its effects on the growth of young in an Arctic herbivore. *Global Change Biology*, *21*(12), 4364–4376. https://doi.org/10.1111/gcb.13057

Elmendorf, S. C., Henry, G. H. R., Hollister, R. D., Björk, R. G., Boulanger-Lapointe, N., Cooper, E. J., … Wipf, S. (2012). Plot-scale evidence of tundra vegetation change and links to recent summer warming. *Nature Climate Change*, *2*(6), 453–457. https://doi.org/10.1038/nclimate1465

Elmendorf, S. C., Henry, G. H. R., Hollister, R. D., Fosaa, A. M., Gould, W. A., Hermanutz, L., … Walker, M. (2015). Experiment, monitoring, and gradient methods used to infer climate change effects on plant communities yield consistent patterns. *Proceedings of the National Academy of Sciences*, *112*(2), 448–452. https://doi.org/10.1073/pnas.1410088112

Ernakovich, J. G., Hopping, K. A., Berdanier, A. B., Simpson, R. T., Kachergis, E. J., Steltzer, H., & Wallenstein, M. D. (2014). Predicted responses of arctic and alpine ecosystems to altered seasonality under climate change. *Global Change Biology*, *20*(10), 3256–3269. https://doi.org/10.1111/gcb.12568

Fan, X., & Liu, Y. (2016). A global study of NDVI difference among moderate-resolution satellite sensors. *ISPRS Journal of Photogrammetry and Remote Sensing*, *121*, 177–191. https://doi.org/10.1016/j.isprsjprs.2016.09.008

Fauchald, P., Park, T., Tømmervik, H., Myneni, R., & Hausner, V. H. (2017). Arctic greening from warming promotes declines in caribou populations. *Science Advances*, *3*(4), e1601365. https://doi.org/10.1126/sciadv.1601365

Fraser, R. H., Olthof, I., Carrière, M., Deschamps, A., & Pouliot, D. (2011). Detecting long-term changes to vegetation in northern Canada using the Landsat satellite image archive. *Environmental Research Letters*, *6*(4), 045502. https://doi.org/10.1088/1748-9326/6/4/045502

Fritz, M., Wolter, J., Rudaya, N., Palagushkina, O., Nazarova, L., Obu, J., … Wetterich, S. (2016). Holocene ice-wedge polygon development in northern Yukon permafrost peatlands (Canada). *Quaternary Science Reviews*. https://doi.org/10.1016/j.quascirev.2016.02.008

Gallinat, A. S., Primack, R. B., & Wagner, D. L. (2015). Autumn, the neglected season in climate change research. *Trends in Ecology & Evolution*, *30*(3), 169–176. https://doi.org/10.1016/j.tree.2015.01.004

Gamon, J. A., Huemmrich, K. F., Stone, R. S., & Tweedie, C. E. (2013). Spatial and temporal variation in primary productivity (NDVI) of coastal Alaskan tundra: Decreased vegetation growth following earlier snowmelt. *Remote Sensing of Environment*, *129*, 144–153. https://doi.org/10.1016/j.rse.2012.10.030

Gorelick, N., Hancher, M., Dixon, M., Ilyushchenko, S., Thau, D., & Moore, R. (2017). Google Earth Engine: Planetary-scale geospatial analysis for everyone. *Remote Sensing of Environment*, *202*, 18–27. https://doi.org/10.1016/j.rse.2017.06.031

Gould, W. (2000). Remote sensing of vegetation, plant species richness, and regional biodiversity hotspots. *Ecological Applications*, *10*(6), 1861–1870. https://doi.org/10.1890/1051-0761(2000)010[1861:RSOVPS]2.0.CO;2

Gräler, B., Pebesma, E., & Heuvelink, G. (2016). Spatio-Temporal Interpolation using gstat. *The R Journal*, *8*(1), 204–218.

Guay, K. C., Beck, P. S. A., Berner, L. T., Goetz, S. J., Baccini, A., & Buermann, W. (2014). Vegetation productivity patterns at high northern latitudes: a multi-sensor satellite data assessment. *Global Change Biology*, *20*(10), 3147–3158. https://doi.org/10.1111/gcb.12647

Gustine, D., Barboza, P., Adams, L., Griffith, B., Cameron, R., & Whitten, K. (2017). Advancing the match-mismatch framework for large herbivores in the Arctic: Evaluating the evidence for a trophic mismatch in caribou. *PLOS ONE*, *12*(2), e0171807. https://doi.org/10.1371/journal.pone.0171807

Hadfield, J. D. (2017). MCMCglmm Course Notes. Retrieved 12 March 2018, from https://cran.r-project.org/web/packages/MCMCglmm/vignettes/CourseNotes.pdf

Hijmans, R. J. (2016). *raster: Geographic Data Analysis and Modeling*. Retrieved from https://CRAN.R-project.org/package=raster

Høye, T. T., Post, E., Meltofte, H., Schmidt, N. M., & Forchhammer, M. C. (2007). Rapid advancement of spring in the High Arctic. *Current Biology*, *17*(12), R449–R451. https://doi.org/10.1016/j.cub.2007.04.047

Hubbard, S. S., Gangodagamage, C., Dafflon, B., Wainwright, H., Peterson, J., Gusmeroli, A., … Wullschleger, S. D. (2013). Quantifying and relating land-surface and subsurface variability in permafrost environments using LiDAR and surface geophysical datasets. *Hydrogeology Journal*, *21*(1), 149–169. https://doi.org/10.1007/s10040-012-0939-y

Huemmrich, K. F., Gamon, J. A., Tweedie, C. E., Oberbauer, S. F., Kinoshita, G., Houston, S., … Oechel, W. C. (2010). Remote sensing of tundra gross ecosystem productivity and light use efficiency under varying temperature and moisture conditions. *Remote Sensing of Environment*, *114*(3), 481–489. https://doi.org/10.1016/j.rse.2009.10.003

Huete, A., Didan, K., Miura, T., Rodriguez, E. P., Gao, X., & Ferreira, L. G. (2002). Overview of the radiometric and biophysical performance of the MODIS

vegetation indices. *Remote Sensing of Environment*, *83*(1), 195–213. https://doi.org/10.1016/S0034-4257(02)00096-2

IPCC. (2014). *Climate change 2014: Synthesis Report. Contribution of Working Groups I, II and III to the Fifth Assessment Report of the Intergovernmental Panel on Climate Change*. (R. K. Pachauri & L. Mayer, Eds.). Geneva, Switzerland: IPCC.

Jelinski, D. E., & Wu, J. (1996). The modifiable areal unit problem and implications for landscape ecology. *Landscape Ecology*, *11*(3), 129–140. https://doi.org/10.1007/BF02447512

Jia, G. J., Epstein, H. E., & Walker, D. A. (2003). Greening of arctic Alaska, 1981–2001. *Geophysical Research Letters*, *30*(20), 2067. https://doi.org/10.1029/2003GL018268

Jia, G. J., Epstein, H. E., & Walker, D. A. (2009). Vegetation greening in the canadian arctic related to decadal warming. *Journal of Environmental Monitoring*, *11*(12), 2231. https://doi.org/10.1039/b911677j

Ju, J., & Masek, J. G. (2016). The vegetation greenness trend in Canada and US Alaska from 1984–2012 Landsat data. *Remote Sensing of Environment*, *176*, 1–16. https://doi.org/10.1016/j.rse.2016.01.001

Keenan, T. F., & Riley, W. J. (2018). Greening of the land surface in the world's cold regions consistent with recent warming. *Nature Climate Change*, 1. https://doi.org/10.1038/s41558-018-0258-y

Kerby, J. T. (2015). Phenology in a chancing Arctic: Linking trophic interactions across scales. Retrieved from https://etda.libraries.psu.edu/catalog/26992

Kerby, J. T., & Post, E. (2013a). Advancing plant phenology and reduced herbivore production in a terrestrial system associated with sea ice decline. *Nature Communications*, *4*. https://doi.org/10.1038/ncomms3514

Kerby, J. T., & Post, E. (2013b). Capital and income breeding traits differentiate trophic match–mismatch dynamics in large herbivores. *Philosophical Transactions of the Royal Society of London B: Biological Sciences*, *368*(1624), 20120484. https://doi.org/10.1098/rstb.2012.0484

Klein, D. R., & Bay, C. (1994). Resource partitioning by mammalian herbivores in the high Arctic. *Oecologia*, *97*(4), 439–450. https://doi.org/10.1007/BF00325880

Klosterman, S. T., Melaas, E., Wang, J., Martinez, A., Frederick, S., O'Keefe, J., … Richardson, A. D. (2018). Fine-scale perspectives on landscape phenology from unmanned aerial vehicle (UAV) photography. *Agricultural and Forest Meteorology*, *248*, 397–407. https://doi.org/10.1016/j.agrformet.2017.10.015

Klosterman, S. T., & Richardson, A. D. (2017). Observing Spring and Fall Phenology in a Deciduous Forest with Aerial Drone Imagery. *Sensors*, *17*(12), 2852. https://doi.org/10.3390/s17122852

Lara, M. J., Nitze, I., Grosse, G., Martin, P., & McGuire, A. D. (2018). Reduced arctic tundra productivity linked with landform and climate change interactions. *Scientific Reports*, *8*(1), 2345. https://doi.org/10.1038/s41598-018-20692-8

Levin, S. A. (1992). The Problem of Pattern and Scale in Ecology: The Robert H. MacArthur Award Lecture. *Ecology*, *73*(6), 1943–1967. https://doi.org/10.2307/1941447

Loranty, M. M., Davydov, S., Kropp, H., Alexander, H., Mack, M., Natali, S., … Zimov, N. S. (2018). Vegetation Indices Do Not Capture Forest Cover Variation in Upland Siberian Larch Forests. *Remote Sensing*, *10*(11), 1686. https://doi.org/10.3390/rs10111686

Loranty, M. M., & Goetz, S. J. (2012). Shrub expansion and climate feedbacks in Arctic tundra. *Environmental Research Letters*, *7*(1), 011005. https://doi.org/10.1088/1748-9326/7/1/011005

Macias-Fauria, M., Forbes, B. C., Zetterberg, P., & Kumpula, T. (2012). Eurasian Arctic greening reveals teleconnections and the potential for structurally novel ecosystems. *Nature Climate Change*, *2*(8), 613–618. https://doi.org/10.1038/nclimate1558

Marceau, D. J. (1999). The Scale Issue in the Social and Natural Sciences. *Canadian Journal of Remote Sensing*, *25*(4), 347–356. https://doi.org/10.1080/07038992.1999.10874734

Mark, A. F., Fetcher, N., Shaver, G. R., & Iii, F. S. C. (1985). Estimated Ages of Mature Tussocks of Eriophorum vaginatum along a Latitudinal Gradient in Central Alaska, U.S.A. *Arctic and Alpine Research*, *17*(1), 1. https://doi.org/10.2307/1550957

Martínez-Beltrán, C., Jochum, M. A. O., Calera, A., & Meliá, J. (2009). Multisensor comparison of NDVI for a semi-arid environment in Spain. *International Journal of Remote Sensing*, *30*(5), 1355–1384. https://doi.org/10.1080/01431160802509025

Miles, V. V., & Esau, I. (2016). Spatial heterogeneity of greening and browning between and within bioclimatic zones in northern West Siberia. *Environmental Research Letters*, *11*(11), 115002. https://doi.org/10.1088/1748-9326/11/11/115002

Molau, U., & Mølgaard, P. (1996). International Tundra Experiment Manual. Retrieved from http://ibis.geog.ubc.ca/itex/PDFs/ITEXmanual.pdf

Mueller-Wilm, U. (2017, January 7). Sen2Cor Software Release Note: Ref.: S2-PDGS-MPC-L2A-SRN-V2.4.0. Retrieved from http://step.esa.int/thirdparties/sen2cor/2.4.0/Sen2Cor_240_Documenation_PDF/S2-PDGS-MPC-L2A-SRN-V2.4.0.pdf

Muster, S., Langer, M., Heim, B., Westermann, S., & Boike, J. (2012). Subpixel heterogeneity of ice-wedge polygonal tundra: a multi-scale analysis of land

cover and evapotranspiration in the Lena River Delta, Siberia. *Tellus B: Chemical and Physical Meteorology*, *64*(1), 17301. https://doi.org/10.3402/tellusb.v64i0.17301

Myers-Smith, I. H., Forbes, B. C., Wilmking, M., Hallinger, M., Lantz, T., Blok, D., … Hik, D. S. (2011). Shrub expansion in tundra ecosystems: dynamics, impacts and research priorities. *Environmental Research Letters*, *6*(4), 045509. https://doi.org/10.1088/1748-9326/6/4/045509

Myers-Smith, I. H., Grabowski, M. M., Thomas, H. J. D., Angers-Blondin, S., Daskalova, G. N., Bjorkman, A. D., … Eckert, C. D. (2018). Eighteen years of ecological monitoring reveals multiple lines of evidence for tundra vegetation change. *Ecological Monographs*. Retrieved from accepted

Myers-Smith, I. H., Hik, D. S., Kennedy, C., Cooley, D., Johnstone, J. F., Kenney, A. J., & Krebs, C. J. (2011). Expansion of Canopy-Forming Willows Over the Twentieth Century on Herschel Island, Yukon Territory, Canada. *AMBIO*, *40*(6), 610–623. https://doi.org/10.1007/s13280-011-0168-y

Myneni, R. B., Keeling, C. D., Tucker, C. J., Asrar, G., & Nemani, R. R. (1997). Increased plant growth in the northern high latitudes from 1981 to 1991. *Nature*, *386*(6626), 698–702. https://doi.org/10.1038/386698a0

Myneni, R. B., Tucker, C. J., Asrar, G., & Keeling, C. D. (1998). Interannual variations in satellite-sensed vegetation index data from 1981 to 1991. *Journal of Geophysical Research: Atmospheres*, *103*(D6), 6145–6160. https://doi.org/10.1029/97JD03603

Oberbauer, S. F., Elmendorf, S. C., Troxler, T. G., Hollister, R. D., Rocha, A. V., Bret-Harte, M. S., … Welker, J. M. (2013). Phenological response of tundra plants to background climate variation tested using the International Tundra Experiment. *Philosophical Transactions of the Royal Society of London B: Biological Sciences*, *368*(1624), 20120481. https://doi.org/10.1098/rstb.2012.0481

Obu, J., Lantuit, H., Myers-Smith, I., Heim, B., Wolter, J., & Fritz, M. (2015). Effect of Terrain Characteristics on Soil Organic Carbon and Total Nitrogen Stocks in Soils of Herschel Island, Western Canadian Arctic. *Permafrost and Periglacial Processes*, n/a-n/a. https://doi.org/10.1002/ppp.1881

Openshaw, S., & Taylor, P. (1981). The modifiable areal unit problem. In N. Wrigley & R. Bennet (Eds.), *Quantitative Geography: A British View* (pp. 60–69). London: Kegan Paul.

Pattison, R. R., Jorgenson, J. C., Raynolds, M. K., & Welker, J. M. (2015). Trends in NDVI and Tundra Community Composition in the Arctic of NE Alaska Between 1984 and 2009. *Ecosystems*, *18*(4), 707–719. https://doi.org/10.1007/s10021-015-9858-9

Pearson, R. G., Phillips, S. J., Loranty, M. M., Beck, P. S. A., Damoulas, T., Knight, S. J., & Goetz, S. J. (2013). Shifts in Arctic vegetation and associated

feedbacks under climate change. *Nature Climate Change*, *3*(7), 673–677. https://doi.org/10.1038/nclimate1858

Pebesma, E. J. (2004). Multivariable geostatistics in S: the gstat package. *Computers & Geosciences*, *30*, 683–691.

Pebesma, E. J., & Bivand, R. S. (2005). Classes and methods for spatial data in R. *R News*, *5*(2), 9–13.

Pedersen, S. H., Liston, G. E., Tamstorf, M. P., Abermann, J., Lund, M., & Schmidt, N. M. (2018). Quantifying snow controls on vegetation greenness. *Ecosphere*, *9*(6), e02309. https://doi.org/10.1002/ecs2.2309

Perpiñán, O., & Hijmans, R. (2018). *rasterVis*. Retrieved from http://oscarperpinan.github.io/rastervis/

Post, E., Kerby, J. T., Pedersen, C., & Steltzer, H. (2016). Highly individualistic rates of plant phenological advance associated with arctic sea ice dynamics. *Biology Letters*, *12*(12), 20160332. https://doi.org/10.1098/rsbl.2016.0332

Post, E., Pedersen, C., Wilmers, C. C., & Forchhammer, M. C. (2008). Warming, plant phenology and the spatial dimension of trophic mismatch for large herbivores. *Proceedings of the Royal Society of London B: Biological Sciences*, *275*(1646), 2005–2013. https://doi.org/10.1098/rspb.2008.0463

Post, E., Steinman, B. A., & Mann, M. E. (2018). Acceleration of phenological advance and warming with latitude over the past century. *Scientific Reports*, *8*(1), 3927. https://doi.org/10.1038/s41598-018-22258-0

Prevéy, J., Vellend, M., Rüger, N., Hollister, R. D., Bjorkman, A. D., Myers-Smith, I. H., … Rixen, C. (2017). Greater temperature sensitivity of plant phenology at colder sites: implications for convergence across northern latitudes. *Global Change Biology*, *23*(7), 2660–2671. https://doi.org/10.1111/gcb.13619

Raynolds, M. K., Comiso, J. C., Walker, D. A., & Verbyla, D. (2008). Relationship between satellite-derived land surface temperatures, arctic vegetation types, and NDVI. *Remote Sensing of Environment*, *112*(4), 1884–1894. https://doi.org/10.1016/j.rse.2007.09.008

Raynolds, M. K., Walker, D. A., Epstein, H. E., Pinzon, J. E., & Tucker, C. J. (2012). A new estimate of tundra-biome phytomass from trans-Arctic field data and AVHRR NDVI. *Remote Sensing Letters*, *3*(5), 403–411. https://doi.org/10.1080/01431161.2011.609188

Raynolds, M. K., Walker, D. A., Verbyla, D., & Munger, C. A. (2013). Patterns of Change within a Tundra Landscape: 22-year Landsat NDVI Trends in an Area of the Northern Foothills of the Brooks Range, Alaska. *Arctic, Antarctic, and Alpine Research*, *45*(2), 249–260. https://doi.org/10.1657/1938-4246-45.2.249

Richardson, A. D., Keenan, T. F., Migliavacca, M., Ryu, Y., Sonnentag, O., & Toomey, M. (2013). Climate change, phenology, and phenological control of

vegetation feedbacks to the climate system. *Agricultural and Forest Meteorology*, *169*, 156–173. https://doi.org/10.1016/j.agrformet.2012.09.012

Rodgers, A. R., & Lewis, M. C. (1986). Diet selection in Arctic lemmings (Lemmus sibiricus and Dicrostonyx groenlandicus): demography, home range, and habitat use. *Canadian Journal of Zoology*, *64*(12), 2717–2727. https://doi.org/10.1139/z86-396

Semenchuk, P. R., Gillespie, M. A. K., Rumpf, S. B., Baggesen, N., Elberling, B., & Cooper, E. J. (2016). High Arctic plant phenology is determined by snowmelt patterns but duration of phenological periods is fixed: an example of periodicity. *Environmental Research Letters*, *11*(12), 125006. https://doi.org/10.1088/1748-9326/11/12/125006

Smith, C., Kennedy, C., Hargrave, A., & McKenna, K. (1989). *Soil and Vegetation of Herschel Island* (Yukon Soil Survey No. No 1). Whitehorse, Yukon Terriotry, Canada: Agriculture Canada.

Stow, D. A., Hope, A., McGuire, D., Verbyla, D., Gamon, J., Huemmrich, F., … Myneni, R. (2004). Remote sensing of vegetation and land-cover change in Arctic Tundra Ecosystems. *Remote Sensing of Environment*, *89*(3), 281–308. https://doi.org/10.1016/j.rse.2003.10.018

Tape, K. D., Hallinger, M., Welker, J. M., & Ruess, R. W. (2012). Landscape Heterogeneity of Shrub Expansion in Arctic Alaska. *Ecosystems*, *15*(5), 711–724. https://doi.org/10.1007/s10021-012-9540-4

Tape, K. D., Strum, & Racine, C. H. (2006). The evidence for shrub expansion in Northern Alaska and the Pan-Arctic. Glob. Change Biol. 12, 686–702 (2006). *Global Change Biology*, *12*, 686–702.

Teillet, P. M., Staenz, K., & William, D. J. (1997). Effects of spectral, spatial, and radiometric characteristics on remote sensing vegetation indices of forested regions. *Remote Sensing of Environment*, *61*(1), 139–149. https://doi.org/10.1016/S0034-4257(96)00248-9

Thompson, J. A., & Koenig, L. S. (2018). Vegetation phenology in Greenland and links to cryospheric change. *Annals of Glaciology*, 1–10. https://doi.org/10.1017/aog.2018.24

Tucker, C. J. (1979). Red and photographic infrared linear combinations for monitoring vegetation. *Remote Sensing of Environment*, *8*(2), 127–150. https://doi.org/10.1016/0034-4257(79)90013-0

Tucker, C. J., Slayback, D. A., Pinzon, J. E., Los, S. O., Myneni, R. B., & Taylor, M. G. (2001). Higher northern latitude normalized difference vegetation index and growing season trends from 1982 to 1999. *International Journal of Biometeorology*, *45*(4), 184–190. https://doi.org/10.1007/s00484-001-0109-8

Turner, M. G., O'Neill, R. V., Gardner, R. H., & Milne, B. T. (1989). Effects of changing spatial scale on the analysis of landscape pattern. *Landscape Ecology*, *3*(3), 153–162. https://doi.org/10.1007/BF00131534

Vickers, H., Høgda, K. A., Solbø, S., Karlsen, S. R., Tømmervik, H., Aanes, R., & Hansen, B. B. (2016). Changes in greening in the high Arctic: insights from a 30 year AVHRR max NDVI dataset for Svalbard. *Environmental Research Letters*, *11*(10), 105004. https://doi.org/10.1088/1748-9326/11/10/105004

Wainwright, H. M., Dafflon, B., Smith, L. J., Hahn, M. S., Curtis, J. B., Wu, Y., … Hubbard, S. S. (2015). Identifying multiscale zonation and assessing the relative importance of polygon geomorphology on carbon fluxes in an Arctic tundra ecosystem. *Journal of Geophysical Research: Biogeosciences*, *120*(4), 788–808. https://doi.org/10.1002/2014JG002799

Walker, D. A., Leibman, M. O., Epstein, H. E., Forbes, B. C., Bhatt, U. S., Raynolds, M. K., … Yu, Q. (2009). Spatial and temporal patterns of greenness on the Yamal Peninsula, Russia: interactions of ecological and social factors affecting the Arctic normalized difference vegetation index. *Environmental Research Letters*, *4*(4), 045004. https://doi.org/10.1088/1748-9326/4/4/045004

Wessel, P., & Smith, W. H. F. (1996). A global, self-consistent, hierarchical, high-resolution shoreline database. *Journal of Geophysical Research: Solid Earth*, *101*(B4), 8741–8743. https://doi.org/10.1029/96JB00104

White, M. A., de BEURS, K. M., Didan, K., Inouye, D. W., Richardson, A. D., Jensen, O. P., … Lauenroth, W. K. (2009). Intercomparison, interpretation, and assessment of spring phenology in North America estimated from remote sensing for 1982-2006. *Global Change Biology*, *15*(10), 2335–2359. https://doi.org/10.1111/j.1365-2486.2009.01910.x

Wickham, H. (2016). *ggplot2: Elegant Graphics for Data Analysis*. Springer-Verlag New York. Retrieved from http://ggplot2.org

Woodcock, C. E., & Strahler, A. H. (1987). The factor of scale in remote sensing. *Remote Sensing of Environment*, *21*(3), 311–332. https://doi.org/10.1016/0034-4257(87)90015-0

Zeng, H., Jia, G., & Epstein, H. (2011). Recent changes in phenology over the northern high latitudes detected from multi-satellite data. *Environmental Research Letters*, *6*(4), 045508. https://doi.org/10.1088/1748-9326/6/4/045508

Zeng, H., Jia, G., & Forbes, B. C. (2013). Shifts in Arctic phenology in response to climate and anthropogenic factors as detected from multiple satellite time series. *Environmental Research Letters*, *8*(3), 035036. https://doi.org/10.1088/1748-9326/8/3/035036

Zhao, J., Zhang, H., Zhang, Z., Guo, X., Li, X., & Chen, C. (2015). Spatial and Temporal Changes in Vegetation Phenology at Middle and High Latitudes of the Northern Hemisphere over the Past Three Decades. *Remote Sensing*, *7*(8), 10973–10995. https://doi.org/10.3390/rs70810973

Zhou, L., Tucker, C. J., Kaufmann, R. K., Slayback, D., Shabanov, N. V., & Myneni, R. B. (2001). Variations in northern vegetation activity inferred from satellite

data of vegetation index during 1981 to 1999. *Journal of Geophysical Research: Atmospheres*, *106*(D17), 20069–20083. https://doi.org/10.1029/2000JD000115

Zhu, Z., Piao, S., Myneni, R. B., Huang, M., Zeng, Z., Canadell, J. G., … Zeng, N. (2016). Greening of the Earth and its drivers. *Nature Climate Change*, *6*(8), 791–795. https://doi.org/10.1038/nclimate3004

Chapter 5 Discussion

The Arctic willow *Salix arctica* Pall. in autumn colours on Qikiqtaruk.

Chapter 5 Discussion

The Arctic is warming at twice the rate than the rest of the globe and the rapid increase in temperatures is causing pronounced changes in the ecosystems of the north (IPCC, 2014). Particularly, the vegetation in the tundra is responding, often in rapid and dramatic ways (Elmendorf et al., 2015; Guay et al., 2014; Høye, Post, Meltofte, Schmidt, & Forchhammer, 2007; Myers-Smith et al., 2011). Tundra vegetation change could result in feedbacks to the global climate system (F. Stuart Chapin, Shaver, Giblin, Nadelhoffer, & Laundre, 1995; Ernakovich et al., 2014; Loranty & Goetz, 2012) and could alter key plant-herbivore and pollinator interactions (Doiron, Gauthier, & Lévesque, 2015; Kerby & Post, 2013b; Post, Pedersen, Wilmers, & Forchhammer, 2008). Predicting the future of the tundra biome and its role in the global system requires improved knowledge of the links between tundra vegetation change and the resulting changes to ecosystem functions. Recently emerging drone technology and associated sensors now allow us to map vegetation productivity of tundra landscapes at higher levels of detail (Anderson & Gaston, 2013; Fraser, Olthof, Lantz, & Schmitt, 2016; Klosterman & Richardson, 2017). Drone technology therefore enables us to bridge the gap between conventional medium- to coarse-grain satellite observations and *in situ* monitoring, and enhances our ability to observe ecosystem changes at multiple scales. In this thesis I combined data from all three sources to contribute to our understanding of how tundra plant phenology and productivity are changing across space, time and observational scales, and to further our ability to predict the future tundra and its role in the planetary system. My main findings were (see also Figure 5-1):

Chapter 2:

1. Trends in spring phenology at the studied coastal tundra sites in Alaska, Canada and Greenland show varied directional changes, mirroring the absence of a globally coherent directional trend across the tundra biome.

2. Localised snowmelt and regional temperature – but not sea-ice – are best at explaining spring plant phenology in the studied coastal tundra communities.

Chapter 3:

1. The key error sources associated with multispectral drone surveys of tundra greenness include solar angle, weather conditions, geolocation and radiometric calibration. Cumulatively they can lead to uncertainties of greater than ± 10% in peak season NDVI of one-hectare tundra plots on Qikiqtaruk.

2. The key error sources can be accounted for by improved flight planning, meta-data collection, ground control point deployment, use of reflectance targets and quality control.

Chapter 4:

1) Observations of tundra greenness on Qikiqtaruk correspond well between drone and satellites at landscape-scales (10 m – 100 m), but considerable variation is lost when aggregating from fine-grain drone (approx. 0.05 m) to medium-grain satellite pixel sizes (10 m).

2) The maximum in spatial variation of tundra greenness within the one-hectare study plots on Qikiqtaruk is reached at distances of just over half a metre, little to no additional spatial variation was observed for greater distances. The fine-scale variation in tundra greenness likely reflects ecological variation in productivity caused by large tussock sedges, microtopography and disturbances.

3) Landscape-level variation in greenness in the one-hectare tundra plots declined over the course of the growing seasons in 2016 and 2017. Thus, spatial heterogeneity of tundra greenness varies across the growing season, and if affected by warming trends in heterogeneity could shift over time.

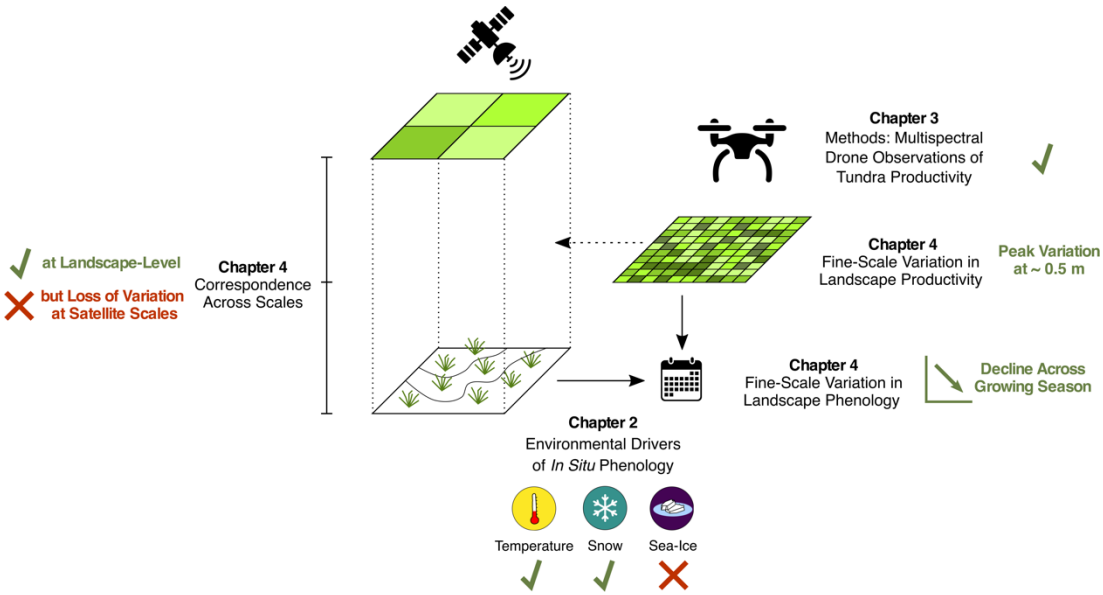

Figure 5-1 I Updated flow diagram of the thesis. Illustrating the main findings of the research in Chapters 2,3 and 4. Satellite symbol by ProSymbols and drone symbol by Mike Rowe, both reproduced under a creative-commons license from the Noun Project [www.thenounproject.com].

In the remainder of this chapter, I discuss the implications of the main findings and highlight associated future research needs. First, I focus on the influence of localised and regional drivers on tundra plant phenology. Second, I elaborate on how drones can bridge the scale gap between satellite and *in situ* observations. Third, I discuss the fine-scale variation in tundra productivity and phenology and how this influences our understanding of key ecological processes. Finally, I conclude by considering the findings in the context of scale and its importance for ecological research in the tundra and beyond.

Localised and regional drivers of tundra phenology

Spring phenology influenced by localised snowmelt and regional temperature

Using long-term records of *in situ* phenological observations, my findings indicate the importance of both highly localised (snowmelt) and regional (temperature) environmental factors as controls on spring phenology in coastal Arctic tundra systems (Chapter 2). Local snow conditions have been recognised early as an important influence on key parameters of tundra ecosystems (Billings & Bliss, 1959; Molau, 1993), and more recently the impact of snow conditions on productivity (Thompson & Koenig, 2018), biodiversity (Niittynen, Heikkinen, & Luoto, 2018) and phenology (Bjorkman, Elmendorf, Beamish, Vellend, & Henry, 2015; Semenchuk et

al., 2016) has been demonstrated. However, the influence of snowmelt has also been shown to become less important as the summer progresses, when air temperatures are considered to exert more control (Bjorkman et al., 2015; Molau, 1993). By demonstrating the importance of localised snowmelt and regional temperature for the timing of spring at multiple sites across the biome (Chapter 2), my findings re-emphasize that both act as key drivers for tundra spring phenology.

The scale at which environmental data are collected can influence the estimated strength of the ecological relationships under statistical investigation. When testing the influence of temperature on tundra plant phenology, temperature is generally measured at regional to landscape levels (Bjorkman et al., 2015; Oberbauer et al., 2013; Panchen & Gorelick, 2017; Post, Steinman, & Mann, 2018) under the assumption that regional temperature is highly corelated with the microclimate that the tundra plants experience. This assumption is generally not made when considering snow conditions or snow melt (Bjorkman et al., 2015; Semenchuk et al., 2016), as a high variation across the landscape is expected. However, tundra plants are small in stature, microclimate therefore likely plays an important role in controlling individual plant responses to changing conditions. High-resolution observations of microclimate combined with observations of phenological variation of tundra vegetation based on fine-grain landscape phenology data such as produced in Chapter 4, will allow us to explicitly test the strength of regional versus microclimate variation as predictors of tundra phenology. Despite the improvements in our understanding of spring and summer phenology and the roles of snowmelt and temperatures as driver thereof, three important additional research areas in the field of tundra phenology remain (Figure 5-2): autumn phenology (Gallinat, Primack, & Wagner, 2015), the influence of photo-period (Richardson et al., 2013) and the interactions of above and below ground phenological processes (Blume-Werry, Wilson, Kreyling, & Milbau, 2016; Eisenhauer et al., 2018).

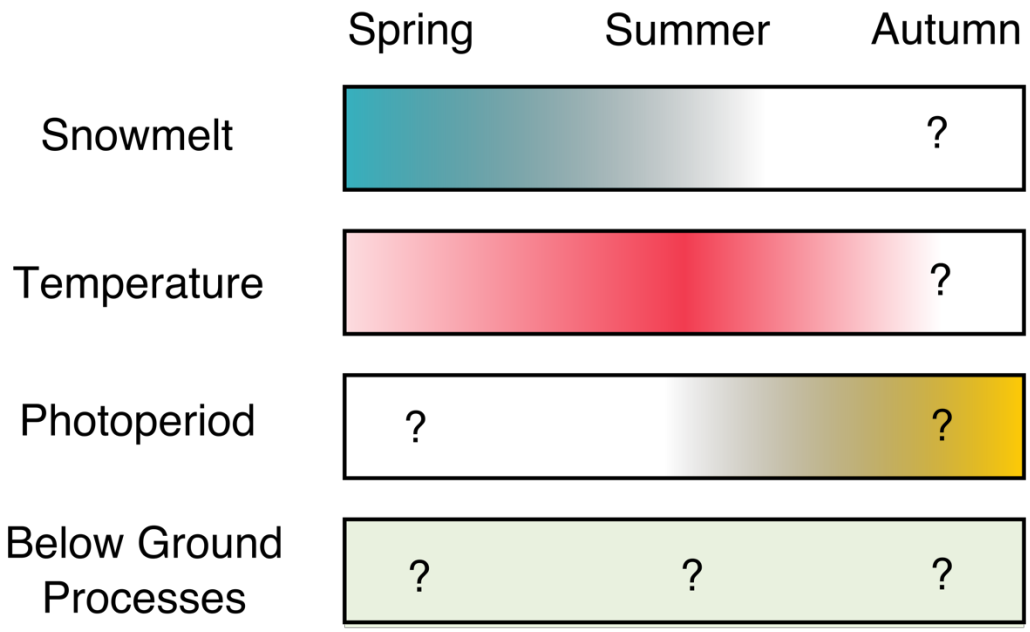

Figure 5-2 | Conceptual heat-map of the relative importance of the key environmental drivers of tundra plant phenology in spring, summer and autumn. Question marks highlight limitations to our understanding and illustrate future research needs. Below ground processes that could influence above ground phenology include for example, temporal variation in soil temperature, moisture availability and active layer depth.

Tundra autumn phenology

Little is known about the drivers of autumn phenology in the tundra and around the globe (Gallinat et al., 2015). Few studies have used *in situ* observations to test for trends of late-season phenology in the tundra (Bjorkman et al., 2015; Myers-Smith et al., 2018) and the majority of trends have been reported from satellite derived end-of-season phenology metrics (Garonna, de Jong, & Schaepman, 2016; Zeng, Jia, & Epstein, 2011; Zeng, Jia, & Forbes, 2013) associated with high uncertainties (Beck et al., 2007; White et al., 2009). Likewise, the drivers of late-season tundra phenology are little understood, though an important influence of photoperiod has been suggested (Gallinat et al., 2015). The emerging drone technologies provide an excellent opportunity to test the influence of photoperiod on autumn senescence in the tundra: If photoperiod is the key driver of senescence, a homogenous response across the landscape could be hypothesised. My findings indicate that variation in tundra greenness at Qikiqtaruk is indeed low at the beginning of autumn (Chapter 4), which would support this hypothesis. Combined with *in situ* measurements of

senescence and coarse grain satellite data, extended drone observations in the autumn season could be used to further test the uniformity of phenological responses across the landscape, at regional scales and for the tundra biome as a whole (Klosterman et al., 2018; Klosterman & Richardson, 2017).

Photoperiod as a driver of phenology

Photoperiod in addition to temperature is thought to be a key controlling factor of tundra plant phenology (Bjorkman et al., 2015; Huelber et al., 2006; Kremers, Hollister, & Oberbauer, 2015; Oberbauer et al., 2013; Panchen & Gorelick, 2017; Wipf, 2009). For example, the interaction between photoperiod has been suggested to explain non-linear responses in the phenology of tundra plants to temperature (Iler, Høye, Inouye, & Schmidt, 2013). Day length can be 24 hours during midsummer in the Arctic (Chapter 2), but changes in the spectral composition of light could be sensed by the plants and rapid changes in day and night patterns occur in the shoulder seasons. And indeed a few common garden (Bennington et al., 2012; Bjorkman, Vellend, Frei, & Henry, 2017; Parker, Tang, Clark, Moody, & Fetcher, 2017) and laboratory experiments (Heide, 1989, 1992; Keller & Körner, 2003) have highlighted the sensitivity of tundra plant phenology to photoperiod or light quality. However, more experimental work is needed to determine the magnitude of influence and the specific mechanistic cues of light variation, particularly on late season phenology (Gallinat et al., 2015)

Below and above ground phenology

Recent studies have highlighted important knowledge gaps in our understanding of below ground phenology and its relationship with above ground processes in tundra ecosystems and beyond (Blume-Werry et al., 2016; Eisenhauer et al., 2018). Blume-Werry et al. (2016) demonstrated a later peak in below-ground biomass and a notably extended below-ground growing season in their tundra study system. Particularly in the Arctic where over 80% of the plant biomass has been shown to be below ground (Iversen et al., 2015; Mokany, Raison, & Prokushkin, 2006), additional attention on the phenology of plant below-ground processes is required to fully understand the implications of environmental change in the tundra (Blume-Werry, 2016). In the context of this thesis, research is needed to understand the interactions of below-ground processes on above ground phenology (Eisenhauer et al., 2018), particularly

in the tundra where soil temperatures and active layer depth are highly important at influencing water and nutrient ability (Dafflon et al., 2017; Hubbard et al., 2013; Wainwright et al., 2015). Fine-grain drone data (Chapter 4) could assist in studying the interaction of above-ground phenology and the - often highly varied - below-ground conditions.

Regional and localised influences on tundra phenology

The importance of localised snowmelt and regional temperature on tundra plant phenology (Chapter 2) highlight the need to improve our abilities to forecast local snow conditions and regional temperatures in the tundra with future climate change. Climate models are good at predicting future temperature change under different emission scenarios; however, uncertainties persist in modelling localised snowfall (AMAP, 2017; Bintanja & Andry, 2017; Bokhorst et al., 2016). More studies are needed that use predictions of future snow scenarios (Niittynen et al., 2018) and study the influence of landscape heterogeneity of snowfall and its influence on tundra vegetation change (Thompson & Koenig, 2018). My results indicated the absence of an effect of regional sea-ice conditions on spring phenology (Chapter 2) despite other studies suggesting a link between circum-Arctic sea-ice and localised tundra plant phenology (Kerby & Post, 2013a; Post, Kerby, Pedersen, & Steltzer, 2016). The contrasting effect of regional and circum-Arctic sea-ice measures further underlines the importance of identifying the key scales at which environmental influences on tundra phenology act and suggests that more sophisticated approaches are needed to unravel the teleconnections that may link regional sea-ice conditions to local climate and hence the arctic biota on adjacent coastal lands (Macias-Fauria, Forbes, Zetterberg, & Kumpula, 2012; Macias-Fauria, Karlsen, & Forbes, 2017; Macias-Fauria & Post, 2018).

Drones can bridge the scale gap between satellite and *in situ* observations

High-quality data collection with drones is challenging

I synthesised the challenges associated with collecting high-quality drone observations that are comparable across platforms, space and time in extreme environments such as those of the high-latitude tundra (Chapter 3). I identified the key error sources associated with solar angle, weather conditions, geolocation and radiometric calibration and estimated that they can lead to uncertainties of up to ±10%

in the mean NDVI of the 1 ha tundra study plots on Qikiqtaruk – Herschel Island in the Canadian Arctic. However, I also demonstrated that we can control for error using best practice (Box 1 – Key recommendations for high-latitude drone ecologists collecting time-series data with multispectral drone sensors). High sensitivity of multi-temporal multi- and hyperspectral drone observations to error sources have also been documented by other research groups (Aasen & Bolten, 2018; Aasen, Burkart, Bolten, & Bareth, 2015) and our call for the coordination and uptake of best practises and standardised methods for monitoring tundra vegetation using compact multispectral drone sensors have been echoed for the wider field of drone spectroscopy by Aasen and Bolten (2018). Ongoing development of methods and coordination between ecologists using drones for vegetation surveys in ecology is required in the light of the continuous advancement in drone technology and sensors.

Development of best-practises for collecting accompanying ground data

A critical next step forward for the ecological community utilising drones for vegetation monitoring will be the development of best-practises for the collection of high-quality ground-based observations that accompany the optical drone data. Without accompanying plot-based observations our ability to make well founded ecological inferences based on drone data products will be highly limited. Techniques to acquire these data may make use conventional vegetation monitoring approaches, including point-framing (e.g. Myers-Smith et al., 2018), destructive biomass sampling techniques (Raynolds et al., 2012), as well as phenology (Chapter 2) and trait measurements (Bjorkman et al., 2018), but could also use field spectroscopy (Díaz-Delgado et al., 2019) and novel approaches utilising ground-based photography combined with emerging machine learning techniques or virtual point framing methods (Liu and Treitz, 2016). During the field work for this thesis, ground-validation data was collected for all drone surveys conducted for Chapter 4 in the form of phenology stage observations as well as leaf- and stem-growth increments, but time-constraints prevented the incorporation of this data into the chapter prior the deadline of this doctoral project. Whether or not these collected data and methods were useful will therefore require further investigation.

Box 1 | Key recommendations for high-latitude drone ecologists collecting time-series data with multispectral drone sensors. (Overleaf)

Survey and plot design

- **Identify the right plot size.**
  The plot size will need to be large enough to contain the variation in the tundra landscape under study and small enough to allow for the limitations of the drone platforms available.
- **Factor in the time it will take to survey it.**
  Survey length will limit the amount of repeat surveys that can be achieved within a day. Longer surveys may be subject to increased variation in light conditions, which can be difficult to control for.
- **Design the flight plans so that there is a comfortable overshoot of the target area.**
  Collecting data beyond the target area will reduce edge-effects.

Repeat measurements

- **Keep the time of day as consistent and as close to solar noon as possible.**
  This may affect the number of plots that can be surveyed in any one day.
- **Estimate the number of flights that can be done in a week. Factor in the weather.**
  Weather conditions including wind, rain, fog, cloud cover, etc. can vary substantially day to day, particularly in harsher climates and thus can limit the number of repeat measurements possible**.**
- **Develop a triage system.**
  If multiple plots are involved, decided on which one(s) will be prioritised if the weather is suitable, establish the minimum required to answer the research question and focus on obtaining this, everything else is a bonus.

Redundancy in technology

- **Use as simple a drone system as possible.**
  When working in remote areas, maintenance can be difficult. Employing drone systems that are easy to use and maintain is key to efficient and productive data collection.
- **Ensure you have redundancy on all fronts including drones and sensors.**
  Even the best pilots experience mechanical failures and/or crashes due to material failure and unexpected behaviour particularly at high latitude sites. Compass systems get confused closer to the magnetic north pole and weather conditions can be harsh. Deploying multiple drone systems will allow data collection to continue in the event of loss of functionality in a platform or sensor.

Radiometric calibration and quality control

- **Combine pre-/post- and inflight targets.**
  Incorporate multiple sets of information within multispectral data collection to assess spectral accuracy and changes to light conditions throughout the flight. This is key to ensuring high-quality data collection.
- **Use inflight targets with multiple reflectance values (e.g. canvas).**
  These are invaluable for testing the accuracy of your radiometric calibration. Measure with a field spectrometer in the field if available, but be aware of the extra work involved.
- **Handle your targets carefully and carry out regular maintenance.**
  Spectral targets get dirty over time. The more carefully they are handled and maintained, the higher the quality of the calibration data.

Geo-location

- **Geo-location with differential GNSS is essential.**
  Use Ground Control Points (GCP) whose locations is measured with a survey grade RTK dGNSS system. **Use six GCPs to start with**, but test how many are actually needed if the landscape is heterogeneous. Alternatively, on-board dGNSS may reduce the need for GCPs; but if it fails, *in situ* GCPs will maintain the quality of the data.

Collect Meta-data

Time and date, weather, sensor, aircraft and pilot are the minimum of meta data to collect. Without detailed records of the flight conditions, data cannot be compared across time and across sites.

Data Storage

Expect to produce a lot of data (in the order of TBs for a single campaign), develop a system to store and handle data efficiently**.**

Do not underestimate the amount of work involved!

Hardware maintenance, surveys, calibrations, data processing and analysis take a lot of time. If you're new to drone data collection, do not underestimate the number of hours required to get up and running.

Drones and satellites correspond at a landscape level

I demonstrated correspondence between landscape level measures of satellite and drones (Chapter 4). The cross-validation of the medium-grain satellite observations gives us added confidence in their measures of tundra greenness at the landscape level. In addition, is shows that drones can provide fine-grain observations at landscape extents that are directly comparable to satellite data, therefore demonstrating that they could be used to link plot-scale observations to satellite observations (Anderson & Gaston, 2013) in the tundra. However, we observed an offset between drone and satellite greenness: drone-derived July mean plot NDVI (one-hectare) was on average about 0.06 lower than Sentinel and MODIS satellite NDVI estimates (Chapter 4). The exact mechanistic reason for this offset between drone and satellite data remains unknown but may relate in part to landscape-level heterogeneity (Kerby et al. unpublished – cross-site drone synthesis). Furthermore, the ability of satellite data to capture localised tundra greenness may not extrapolate to coarse grained satellite observations such as the GIMSS (8 km) products derived from the AVHRR sensors (see for example Pattison, Jorgenson, Raynolds, & Welker, 2015). Thus, future work should continue to test the correspondence of observations between the various drone and satellite products available. Such tests should include a variety tundra locations (see https://arcticdrones.org/), only by studying homogenous and heterogeneous tundra sites, with markedly different vegetation communities, can we begin to understand the importance of landscape-level covariates on Arctic greening patterns at the tundra biome scale.

Establishing the link: in situ *– drones – satellites*

Linking *in situ* via fine-grain drone observations to the landscape scale and then connecting them to regional and global-scale satellite measurements will be a critical step in identifying the key drivers in the complexity ecological processes integrated in the observed trends of satellite vegetation indices over time (Walker et al., 2009). Furthermore, linking ground-based, satellite and drone observations will allow us to identify and characterise characterising scale-dependent phenomena (Levin, 1992; Marceau, 1999; Turner, O'Neill, Gardner, & Milne, 1989) and hence improve our abilities capture tundra vegetation change and the associated feedbacks at landscape to biome scales (Ernakovich et al., 2014). Further to the multispectral methods presented in this thesis (Chapters 3 and 4), RGB imagery from drones can monitor

the timing of flowering within the landscape (Hill et al., 2017) and structure-from-motion data can be used to quantify changes in vegetation canopy structure (Fraser et al., 2016). Phenocam imagery (Andresen, Tweedie, & Lougheed, 2018; Linkosalmi et al., 2016; Richardson et al., 2018) could complement conventional *in situ* observations and integrate well with the image based observations for satellites and drones (Kerby, 2015). By combining data collection across scales, key ecological processes can be captured in ways that were previously not possible and will allow us to better understand and predict responses of tundra ecosystems to global change.

Drones reveal fine-scale variation in tundra productivity and phenology

Fine-scale variation in vegetation productivity is missed by satellite data

I reveal that key fine-scale variation in tundra productivity on Qikiqtaruk is not captured by satellite observations (Chapter 4). Fine-scale variation in tundra NDVI has also been observed with a tram-mounted spectrometer at a site with similar tussock-sedge vegetation on the North-Slope of Alaska (Gamon et al., 2013). The small-scale variation in the tundra types of the North Slope in the Yukon and Alaska likely reflects microtopography (Gamon, Huemmrich, Stone, & Tweedie, 2013; Wainwright et al., 2015) and localised disturbance processes (Obu et al., 2015) which are not captured in medium-grain satellite time series. Three key questions emerge from these findings: 1) Do patterns of fine-scale heterogeneity of vegetation greenness in relation to microtopography hold true for other tundra ecosystems and across the biome as a whole? 2) Does this variation capture the key ecological processes that govern landscape-level variation in plant phenology? 3) If so, are the small-scale variation observations required to appropriately estimate the landscape-level processes or are approximations using coarse-scale data sufficient? Finally, it remains to be shown whether we can use the uncovered fine-scale variation to quantify the mechanistic processes leading to tundra vegetation change and greening that we have previously been unable to detect. For example, does the loss of small bare ground patches (Myers-Smith et al., 2018) with warming, caused by reductions in localised cryoturbation (Obu et al., 2015), contribute significantly to the greening observed on Qikiqtaruk? Drone data provides a new way to sense the land-surface at fine-scales and thus opens a new window on the global change responses of tundra ecosystems.

Decline in variation across the growing season

My results indicate a decline in the variation of vegetation productivity across the growing season (Chapter 4). This finding suggests that plant resources such as mature leaves, flower pollen or fruits become more homogeneously available across the growing season when approaching the period of peak biomass. The change in landscape variation of productivity over time might influence plant herbivore and pollinator interactions that are dependent on resource heterogeneity across the landscape (Armstrong, Takimoto, Schindler, Hayes, & Kauffman, 2016; Kerby, 2015; Richardson et al., 2018). Little is known about how herbivores and pollinators utilise landscape heterogeneity in tundra ecosystems and beyond (Armstrong et al., 2016) and more research is needed on which animals and insects "surf" resource waves across tundra landscapes. Time-series of drone surveys open up novel opportunities to study heterogeneity in the availability of tundra resources and how this might influences trophic interactions in a warming tundra biome.

Fine-scale variation in tundra phenology

Finally, the fine-scale variation and dynamics in tundra productivity over time (Chapter 4) and the importance of the highly-localised snowmelt as a driver of spring phenology (Chapter 2) raise the question of how fine-scale variation in phenology is distributed across the tundra landscape. Time-series of fine-grain drone data such as those presented in this thesis now allow us to describe tundra variation in phenology at meter and sub-meter scales and identify its association with the ecological drivers and causes (Klosterman et al., 2018; Klosterman & Richardson, 2017). Quadratic or double logistic growing season curves such as those common in satellite phenological studies (Beck, Atzberger, Høgda, Johansen, & Skidmore, 2006; White et al., 2009; Zeng et al., 2011) could be fitted to the NDVI time-series on a pixel-by-pixel basis or to aggregations of the data (e.g. with a one metre cell size to account for uncertainties associated with the geo-location of the individual images). Combined with ground-based phenological observations of green up and senescence, such an analysis would allow us to quantify how representative long-term *in situ* observations of plot and individuals are of the variation in phenology across the landscape. Finally, an aggregation analysis (Jelinski & Wu, 1996; Kerby, 2015; Turner et al., 1989) of this data would allow us to test for scale dependency of the observations to identify scale thresholds and indicate which data products are required (drone and/or satellite) for the quantification of key variation in tundra landscape phenology (Figure 5-3). Thus,

fine-scale observations of tundra phenology obtained with drones can provide us with new perspectives on scale-dependent process in tundra ecosystems and beyond.

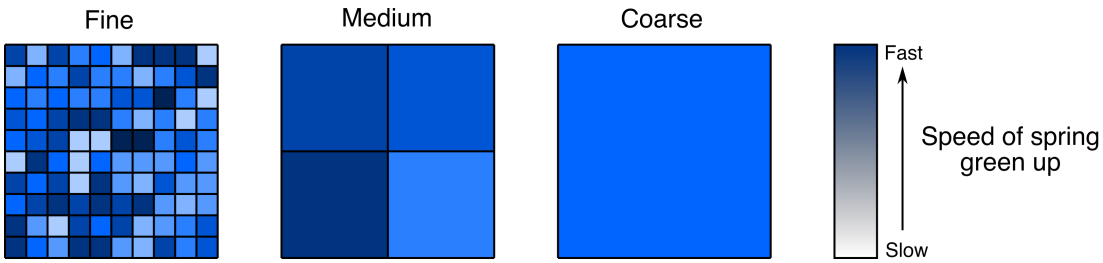

Figure 5-3 | Conceptual illustration of the loss of variation in tundra landscape phenology across scales.

Conclusions

Localised processes influencing large-scale patterns

Overall, the research presented in this PhD highlights how localised processes can influence large-scale patterns and trends of plant phenology and productivity in tundra ecosystems. This is particularly exemplified by the influence of highly localised snowmelt on tundra phenology across Arctic coastal tundra sites (Chapter 2). The fine-scale variation in tundra productivity observed with drone data (Chapter 4) further suggests that we have yet to uncover all of the localised processes that mediate tundra greenness. Understanding at which scales the key ecological processes and phenomena work and how they interact across scales is critical for obtaining a comprehensive understanding of the hierarchical organisation of the planet's ecosystems (Allen & Starr, 1982; Levin, 1992; Marceau, 1999). Revealing the hierarchical structure of tundra ecosystem responses to global change is particularly required if we want to better predict their feedbacks to the global climate system (F. S. Chapin et al., 2005; Ernakovich et al., 2014).

Drones help to identify the relevant scales of ecological processes

Identifying the right scale at which to observe ecological phenomena is a challenge with no simple solution (Levin, 1992), yet it can be tackled by studying systems across a variety of scales (Levin, 1992; Marceau, 1999; Marceau & Hay, 1999). Previously, we were limited in our ability to link *in situ* observations to global satellite measures due to the coarse-grained nature of the satellite observations. Emerging technologies such as true colour and multispectral drone imagery can fill this scale gap (Anderson

& Gaston, 2013; Klosterman et al., 2018). My PhD research demonstrates that drones can be used to obtain fine-grained observations of tundra productivity and phenology at landscape-level extents that are directly comparable to global-scale satellite data. This fine-scale landscape-level data can be used to test the mechanisms of vegetation change and quantify their influences on ecosystem functions and climate feedbacks. By combining *in situ*, satellite and drone data, we can therefore overcome scale issues in the observation of ecological phenomena and processes such as those involved in tundra vegetation change and better predict their role in global climate change.

References

Aasen, H., & Bolten, A. (2018). Multi-temporal high-resolution imaging spectroscopy with hyperspectral 2D imagers – From theory to application. *Remote Sensing of Environment*, *205*, 374–389. https://doi.org/10.1016/j.rse.2017.10.043

Aasen, H., Burkart, A., Bolten, A., & Bareth, G. (2015). Generating 3D hyperspectral information with lightweight UAV snapshot cameras for vegetation monitoring: From camera calibration to quality assurance. *ISPRS Journal of Photogrammetry and Remote Sensing*, *108*, 245–259. https://doi.org/10.1016/j.isprsjprs.2015.08.002

Allen, T. F. H., & Starr, T. B. (1982). *Hierarchy*. Chicago: Univeristy of Chicago Press.

AMAP. (2017). *Snow, Water, Ice and Permafrost. Summary for Policy-makers.* (p. 20). Oslo, Norway: Arctic Monitoring and Assessment Programme (AMAP). Retrieved from https://www.amap.no/documents/doc/Snow-Water-Ice-and-Permafrost.-Summary-for-Policy-makers/1532

Anderson, K., & Gaston, K. J. (2013). Lightweight unmanned aerial vehicles will revolutionize spatial ecology. *Frontiers in Ecology and the Environment*, *11*(3), 138–146. https://doi.org/10.1890/120150

Andresen, C. G., Tweedie, C. E., & Lougheed, V. L. (2018). Climate and nutrient effects on Arctic wetland plant phenology observed from phenocams. *Remote Sensing of Environment*, *205*, 46–55. https://doi.org/10.1016/j.rse.2017.11.013

Armstrong, J. B., Takimoto, G., Schindler, D. E., Hayes, M. M., & Kauffman, M. J. (2016). Resource waves: phenological diversity enhances foraging opportunities for mobile consumers. *Ecology*, *97*(5), 1099–1112. https://doi.org/10.1890/15-0554.1

Beck, P. S. A., Atzberger, C., Høgda, K. A., Johansen, B., & Skidmore, A. K. (2006). Improved monitoring of vegetation dynamics at very high latitudes: A new

method using MODIS NDVI. *Remote Sensing of Environment*, *100*(3), 321–334. https://doi.org/10.1016/j.rse.2005.10.021

Beck, P. S. A., Jönsson, P., Høgda, K.-A., Karlsen, S. R., Eklundh, L., & Skidmore, A. K. (2007). A ground-validated NDVI dataset for monitoring vegetation dynamics and mapping phenology in Fennoscandia and the Kola peninsula. *International Journal of Remote Sensing*, *28*(19), 4311–4330. https://doi.org/10.1080/01431160701241936

Bennington, C. C., Fetcher, N., Vavrek, M. C., Shaver, G. R., Cummings, K. J., & McGraw, J. B. (2012). Home site advantage in two long-lived arctic plant species: results from two 30-year reciprocal transplant studies. *Journal of Ecology*, *100*(4), 841–851. https://doi.org/10.1111/j.1365-2745.2012.01984.x

Billings, W. D., & Bliss, L. C. (1959). An Alpine Snowbank Environment and Its Effects on Vegetation, Plant Development, and Productivity. *Ecology*, *40*(3), 388–397. https://doi.org/10.2307/1929755

Bintanja, R., & Andry, O. (2017). Towards a rain-dominated Arctic. *Nature Climate Change*, *7*(4), 263–267. https://doi.org/10.1038/nclimate3240

Bjorkman, A. D., Elmendorf, S. C., Beamish, A. L., Vellend, M., & Henry, G. H. R. (2015). Contrasting effects of warming and increased snowfall on Arctic tundra plant phenology over the past two decades. *Global Change Biology*, *21*, 4651–4661. https://doi.org/10.1111/gcb.13051

Bjorkman, A. D., Vellend, M., Frei, E. R., & Henry, G. H. R. (2017). Climate adaptation is not enough: warming does not facilitate success of southern tundra plant populations in the high Arctic. *Global Change Biology*, *23*(4), 1540–1551. https://doi.org/10.1111/gcb.13417

Bjorkman, A. D., Myers-Smith, I. H., Elmendorf, S. C., Normand, S., Rüger, N., Beck, P. S. A., … Weiher, E. (2018). Plant functional trait change across a warming tundra biome. *Nature*, *562*(7725), 57–62. https://doi.org/10.1038/s41586-018-0563-7

Blume-Werry, G. (2016). *The hidden life of plants - Fine root dynamics in northern ecosystems*. Umeå Universitet, Umeå, Sweden.

Blume-Werry, G., Wilson, S. D., Kreyling, J., & Milbau, A. (2016). The hidden season: growing season is 50% longer below than above ground along an arctic elevation gradient. *New Phytologist*, *209*(3), 978–986. https://doi.org/10.1111/nph.13655

Bokhorst, S., Pedersen, S. H., Brucker, L., Anisimov, O., Bjerke, J. W., Brown, R. D., … Callaghan, T. V. (2016). Changing Arctic snow cover: A review of recent developments and assessment of future needs for observations, modelling, and impacts. *Ambio*, *45*(5), 516–537. https://doi.org/10.1007/s13280-016-0770-0

Chapin, F. S., Sturm, M., Serreze, M. C., McFadden, J. P., Key, J. R., Lloyd, A. H., … Welker, J. M. (2005). Role of Land-Surface Changes in Arctic Summer

Warming. *Science*, *310*(5748), 657–660. https://doi.org/10.1126/science.1117368

Chapin, F. Stuart, Shaver, G. R., Giblin, A. E., Nadelhoffer, K. J., & Laundre, J. A. (1995). Responses of Arctic Tundra to Experimental and Observed Changes in Climate. *Ecology*, *76*(3), 694–711. https://doi.org/10.2307/1939337

Dafflon, B., Oktem, R., Peterson, J., Ulrich, C., Tran, A. P., Romanovsky, V., & Hubbard, S. S. (2017). Coincident above- and below-ground autonomous monitoring to quantify co-variability in permafrost, soil and vegetation properties in Arctic Tundra: Above- and below-ground co-dynamics. *Journal of Geophysical Research: Biogeosciences*. https://doi.org/10.1002/2016JG003724

Díaz-Delgado, R., Ónodi, G., Kröel-Dulay, G., & Kertész, M. (2019). Enhancement of Ecological Field Experimental Research by Means of UAV Multispectral Sensing. *Drones*, *3*(1), 7. https://doi.org/10.3390/drones3010007

Doiron, M., Gauthier, G., & Lévesque, E. (2015). Trophic mismatch and its effects on the growth of young in an Arctic herbivore. *Global Change Biology*, *21*(12), 4364–4376. https://doi.org/10.1111/gcb.13057

Eisenhauer, N., Herrmann, S., Hines, J., Buscot, F., Siebert, J., & Thakur, M. P. (2018). The Dark Side of Animal Phenology. *Trends in Ecology & Evolution*. https://doi.org/10.1016/j.tree.2018.09.010

Elmendorf, S. C., Henry, G. H. R., Hollister, R. D., Fosaa, A. M., Gould, W. A., Hermanutz, L., … Walker, M. (2015). Experiment, monitoring, and gradient methods used to infer climate change effects on plant communities yield consistent patterns. *Proceedings of the National Academy of Sciences*, *112*(2), 448–452. https://doi.org/10.1073/pnas.1410088112

Ernakovich, J. G., Hopping, K. A., Berdanier, A. B., Simpson, R. T., Kachergis, E. J., Steltzer, H., & Wallenstein, M. D. (2014). Predicted responses of arctic and alpine ecosystems to altered seasonality under climate change. *Global Change Biology*, *20*(10), 3256–3269. https://doi.org/10.1111/gcb.12568

Fraser, R., Olthof, I., Lantz, T. C., & Schmitt, C. (2016). UAV Photogrammetry for Mapping Vegetation in the Low-Arctic. *Arctic Science*. https://doi.org/10.1139/AS-2016-0008

Gallinat, A. S., Primack, R. B., & Wagner, D. L. (2015). Autumn, the neglected season in climate change research. *Trends in Ecology & Evolution*, *30*(3), 169–176. https://doi.org/10.1016/j.tree.2015.01.004

Gamon, J. A., Huemmrich, K. F., Stone, R. S., & Tweedie, C. E. (2013). Spatial and temporal variation in primary productivity (NDVI) of coastal Alaskan tundra: Decreased vegetation growth following earlier snowmelt. *Remote Sensing of Environment*, *129*, 144–153. https://doi.org/10.1016/j.rse.2012.10.030

Garonna, I., de Jong, R., & Schaepman, M. E. (2016). Variability and evolution of global land surface phenology over the past three decades (1982-2012).

Global Change Biology, *22*(4), 1456–1468. https://doi.org/10.1111/gcb.13168

Guay, K. C., Beck, P. S. A., Berner, L. T., Goetz, S. J., Baccini, A., & Buermann, W. (2014). Vegetation productivity patterns at high northern latitudes: a multi-sensor satellite data assessment. *Global Change Biology*, *20*(10), 3147–3158. https://doi.org/10.1111/gcb.12647

Heide, O. M. (1989). Environmental Control of Flowering and Viviparous Proliferation in Seminiferous and Viviparous Arctic Populations of Two Poa Species. *Arctic and Alpine Research*, *21*(3), 305. https://doi.org/10.2307/1551570

Heide, O. M. (1992). Experimental Control of Flowering in Carex bigelowii. *Oikos*, *65*(3), 371. https://doi.org/10.2307/3545552

Hill, D. J., Tarasoff, C., Whitworth, G. E., Baron, J., Bradshaw, J. L., & Church, J. S. (2017). Utility of unmanned aerial vehicles for mapping invasive plant species: a case study on yellow flag iris (Iris pseudacorus L.). *International Journal of Remote Sensing*, *38*(8–10), 2083–2105. https://doi.org/10.1080/01431161.2016.1264030

Høye, T. T., Post, E., Meltofte, H., Schmidt, N. M., & Forchhammer, M. C. (2007). Rapid advancement of spring in the High Arctic. *Current Biology*, *17*(12), R449–R451. https://doi.org/10.1016/j.cub.2007.04.047

Hubbard, S. S., Gangodagamage, C., Dafflon, B., Wainwright, H., Peterson, J., Gusmeroli, A., … Wullschleger, S. D. (2013). Quantifying and relating land-surface and subsurface variability in permafrost environments using LiDAR and surface geophysical datasets. *Hydrogeology Journal*, *21*(1), 149–169. https://doi.org/10.1007/s10040-012-0939-y

Huelber, K., Gottfried, M., Pauli, H., Reiter, K., Winkler, M., & Grabherr, G. (2006). Phenological Responses of Snowbed Species to Snow Removal Dates in the Central Alps: Implications for Climate Warming. *Arctic, Antarctic, and Alpine Research*, *38*(1), 99–103. https://doi.org/10.1657/1523-0430(2006)038[0099:PROSST]2.0.CO;2

Iler, A. M., Høye, T. T., Inouye, D. W., & Schmidt, N. M. (2013). Nonlinear flowering responses to climate: are species approaching their limits of phenological change? *Philosophical Transactions of the Royal Society of London B: Biological Sciences*, *368*(1624), 20120489. https://doi.org/10.1098/rstb.2012.0489

IPCC. (2014). *Climate change 2014: Synthesis Report. Contribution of Working Groups I, II and III to the Fifth Assessment Report of the Intergovernmental Panel on Climate Change*. (R. K. Pachauri & L. Mayer, Eds.). Geneva, Switzerland: IPCC.

Iversen, C. M., Sloan, V. L., Sullivan, P. F., Euskirchen, E. S., McGuire, A. D., Norby, R. J., … Wullschleger, S. D. (2015). The unseen iceberg: plant roots

in arctic tundra. *New Phytologist*, *205*(1), 34–58. https://doi.org/10.1111/nph.13003

Jelinski, D. E., & Wu, J. (1996). The modifiable areal unit problem and implications for landscape ecology. *Landscape Ecology*, *11*(3), 129–140. https://doi.org/10.1007/BF02447512

Keller, F., & Körner, C. (2003). The Role of Photoperiodism in Alpine Plant Development. *Arctic, Antarctic, and Alpine Research*, *35*(3), 361–368. https://doi.org/10.1657/1523-0430(2003)035[0361:TROPIA]2.0.CO;2

Kerby, J. T. (2015). Phenology in a chancing Arctic: Linking trophic interactions across scales. Retrieved from https://etda.libraries.psu.edu/catalog/26992

Kerby, J. T., & Post, E. (2013a). Advancing plant phenology and reduced herbivore production in a terrestrial system associated with sea ice decline. *Nature Communications*, *4*. https://doi.org/10.1038/ncomms3514

Kerby, J. T., & Post, E. (2013b). Capital and income breeding traits differentiate trophic match–mismatch dynamics in large herbivores. *Philosophical Transactions of the Royal Society of London B: Biological Sciences*, *368*(1624), 20120484. https://doi.org/10.1098/rstb.2012.0484

Klosterman, S. T., Melaas, E., Wang, J., Martinez, A., Frederick, S., O'Keefe, J., … Richardson, A. D. (2018). Fine-scale perspectives on landscape phenology from unmanned aerial vehicle (UAV) photography. *Agricultural and Forest Meteorology*, *248*, 397–407. https://doi.org/10.1016/j.agrformet.2017.10.015

Klosterman, S. T., & Richardson, A. D. (2017). Observing Spring and Fall Phenology in a Deciduous Forest with Aerial Drone Imagery. *Sensors*, *17*(12), 2852. https://doi.org/10.3390/s17122852

Kremers, K. S., Hollister, R. D., & Oberbauer, S. F. (2015). Diminished Response of Arctic Plants to Warming over Time. *PLoS ONE*, *10*(3). https://doi.org/10.1371/journal.pone.0116586

Levin, S. A. (1992). The Problem of Pattern and Scale in Ecology: The Robert H. MacArthur Award Lecture. *Ecology*, *73*(6), 1943–1967. https://doi.org/10.2307/1941447

Linkosalmi, M., Aurela, M., Tuovinen, J.-P., Peltoniemi, M., Tanis, C. M., Arslan, A. N., … Laurila, T. (2016). Digital photography for assessing the link between vegetation phenology and CO_2 exchange in two contrasting northern ecosystems. *Geoscientific Instrumentation, Methods and Data Systems*, *5*(2), 417–426. https://doi.org/10.5194/gi-5-417-2016

Liu, N., & Treitz, P. (2016). Modelling high arctic percent vegetation cover using field digital images and high resolution satellite data. *International Journal of Applied Earth Observation and Geoinformation*, *52*, 445–456. https://doi.org/10.1016/j.jag.2016.06.023

Loranty, M. M., & Goetz, S. J. (2012). Shrub expansion and climate feedbacks in Arctic tundra. *Environmental Research Letters*, *7*(1), 011005. https://doi.org/10.1088/1748-9326/7/1/011005

Macias-Fauria, M., Forbes, B. C., Zetterberg, P., & Kumpula, T. (2012). Eurasian Arctic greening reveals teleconnections and the potential for structurally novel ecosystems. *Nature Climate Change*, *2*(8), 613–618. https://doi.org/10.1038/nclimate1558

Macias-Fauria, M., Karlsen, S. R., & Forbes, B. C. (2017). Disentangling the coupling between sea ice and tundra productivity in Svalbard. *Scientific Reports*, *7*(1), 8586. https://doi.org/10.1038/s41598-017-06218-8

Macias-Fauria, M., & Post, E. (2018). Effects of sea ice on Arctic biota: an emerging crisis discipline. *Biology Letters*, *14*(3), 20170702. https://doi.org/10.1098/rsbl.2017.0702

Marceau, D. J. (1999). The Scale Issue in the Social and Natural Sciences. *Canadian Journal of Remote Sensing*, *25*(4), 347–356. https://doi.org/10.1080/07038992.1999.10874734

Marceau, D. J., & Hay, G. J. (1999). Remote Sensing Contributions to the Scale Issue. *Canadian Journal of Remote Sensing*, *25*(4), 357–366. https://doi.org/10.1080/07038992.1999.10874735

Mokany, K., Raison, R. J., & Prokushkin, A. S. (2006). Critical analysis of root : shoot ratios in terrestrial biomes. *Global Change Biology*, *12*(1), 84–96. https://doi.org/10.1111/j.1365-2486.2005.001043.x

Molau, U. (1993). Relationships between Flowering Phenology and Life History Strategies in Tundra Plants. *Arctic and Alpine Research*, *25*(4), 391–402. https://doi.org/10.2307/1551922

Myers-Smith, I. H., Forbes, B. C., Wilmking, M., Hallinger, M., Lantz, T., Blok, D., … Hik, D. S. (2011). Shrub expansion in tundra ecosystems: dynamics, impacts and research priorities. *Environmental Research Letters*, *6*(4), 045509. https://doi.org/10.1088/1748-9326/6/4/045509

Myers-Smith, I. H., Grabowski, M. M., Thomas, H. J. D., Angers-Blondin, S., Daskalova, G. N., Bjorkman, A. D., … Eckert, C. D. (2018). Eighteen years of ecological monitoring reveals multiple lines of evidence for tundra vegetation change. *Ecological Monographs (Manuscript in Press)*.

Niittynen, P., Heikkinen, R. K., & Luoto, M. (2018). Snow cover is a neglected driver of Arctic biodiversity loss. *Nature Climate Change*, 1. https://doi.org/10.1038/s41558-018-0311-x

Oberbauer, S. F., Elmendorf, S. C., Troxler, T. G., Hollister, R. D., Rocha, A. V., Bret-Harte, M. S., … Welker, J. M. (2013). Phenological response of tundra plants to background climate variation tested using the International Tundra Experiment. *Philosophical Transactions of the Royal Society of London B:*

Biological Sciences, *368*(1624), 20120481. https://doi.org/10.1098/rstb.2012.0481

Obu, J., Lantuit, H., Myers-Smith, I., Heim, B., Wolter, J., & Fritz, M. (2015). Effect of Terrain Characteristics on Soil Organic Carbon and Total Nitrogen Stocks in Soils of Herschel Island, Western Canadian Arctic. *Permafrost and Periglacial Processes*, n/a-n/a. https://doi.org/10.1002/ppp.1881

Panchen, Z. A., & Gorelick, R. (2017). Prediction of Arctic plant phenological sensitivity to climate change from historical records. *Ecology and Evolution*, *7*(5), 1325–1338. https://doi.org/10.1002/ece3.2702

Parker, T. C., Tang, J., Clark, M. B., Moody, M. M., & Fetcher, N. (2017). Ecotypic differences in the phenology of the tundra species Eriophorum vaginatum reflect sites of origin. *Ecology and Evolution*, *7*(22), 9975–9786. https://doi.org/10.1002/ece3.3445

Pattison, R. R., Jorgenson, J. C., Raynolds, M. K., & Welker, J. M. (2015). Trends in NDVI and Tundra Community Composition in the Arctic of NE Alaska Between 1984 and 2009. *Ecosystems*, *18*(4), 707–719. https://doi.org/10.1007/s10021-015-9858-9

Post, E., Kerby, J. T., Pedersen, C., & Steltzer, H. (2016). Highly individualistic rates of plant phenological advance associated with arctic sea ice dynamics. *Biology Letters*, *12*(12), 20160332. https://doi.org/10.1098/rsbl.2016.0332

Post, E., Pedersen, C., Wilmers, C. C., & Forchhammer, M. C. (2008). Warming, plant phenology and the spatial dimension of trophic mismatch for large herbivores. *Proceedings of the Royal Society of London B: Biological Sciences*, *275*(1646), 2005–2013. https://doi.org/10.1098/rspb.2008.0463

Post, E., Steinman, B. A., & Mann, M. E. (2018). Acceleration of phenological advance and warming with latitude over the past century. *Scientific Reports*, *8*(1), 3927. https://doi.org/10.1038/s41598-018-22258-0

Raynolds, M. K., Walker, D. A., Epstein, H. E., Pinzon, J. E., & Tucker, C. J. (2012). A new estimate of tundra-biome phytomass from trans-Arctic field data and AVHRR NDVI. *Remote Sensing Letters*, *3*(5), 403–411. https://doi.org/10.1080/01431161.2011.609188

Richardson, A. D., Hufkens, K., Milliman, T., Aubrecht, D. M., Chen, M., Gray, J. M., … Frolking, S. (2018). Tracking vegetation phenology across diverse North American biomes using PhenoCam imagery. *Scientific Data*, *5*, 180028. https://doi.org/10.1038/sdata.2018.28

Richardson, A. D., Keenan, T. F., Migliavacca, M., Ryu, Y., Sonnentag, O., & Toomey, M. (2013). Climate change, phenology, and phenological control of vegetation feedbacks to the climate system. *Agricultural and Forest Meteorology*, *169*, 156–173. https://doi.org/10.1016/j.agrformet.2012.09.012

Semenchuk, P. R., Gillespie, M. A. K., Rumpf, S. B., Baggesen, N., Elberling, B., & Cooper, E. J. (2016). High Arctic plant phenology is determined by snowmelt

patterns but duration of phenological periods is fixed: an example of periodicity. *Environmental Research Letters*, *11*(12), 125006. https://doi.org/10.1088/1748-9326/11/12/125006

Thompson, J. A., & Koenig, L. S. (2018). Vegetation phenology in Greenland and links to cryospheric change. *Annals of Glaciology*, 1–10. https://doi.org/10.1017/aog.2018.24

Turner, M. G., O'Neill, R. V., Gardner, R. H., & Milne, B. T. (1989). Effects of changing spatial scale on the analysis of landscape pattern. *Landscape Ecology*, *3*(3), 153–162. https://doi.org/10.1007/BF00131534

Wainwright, H. M., Dafflon, B., Smith, L. J., Hahn, M. S., Curtis, J. B., Wu, Y., … Hubbard, S. S. (2015). Identifying multiscale zonation and assessing the relative importance of polygon geomorphology on carbon fluxes in an Arctic tundra ecosystem. *Journal of Geophysical Research: Biogeosciences*, *120*(4), 788–808. https://doi.org/10.1002/2014JG002799

Walker, D. A., Leibman, M. O., Epstein, H. E., Forbes, B. C., Bhatt, U. S., Raynolds, M. K., … Yu, Q. (2009). Spatial and temporal patterns of greenness on the Yamal Peninsula, Russia: interactions of ecological and social factors affecting the Arctic normalized difference vegetation index. *Environmental Research Letters*, *4*(4), 045004. https://doi.org/10.1088/1748-9326/4/4/045004

White, M. A., De BEURS, K. M., Didan, K., Inouye, D. W., Richardson, A. D., Jensen, O. P., … Lauenroth, W. K. (2009). Intercomparison, interpretation, and assessment of spring phenology in North America estimated from remote sensing for 1982–2006. *Global Change Biology*, *15*(10), 2335–2359. https://doi.org/10.1111/j.1365-2486.2009.01910.x

Wipf, S. (2009). Phenology, growth, and fecundity of eight subarctic tundra species in response to snowmelt manipulations. *Plant Ecology*, *207*(1), 53–66. https://doi.org/10.1007/s11258-009-9653-9

Zeng, H., Jia, G., & Epstein, H. (2011). Recent changes in phenology over the northern high latitudes detected from multi-satellite data. *Environmental Research Letters*, *6*(4), 045508. https://doi.org/10.1088/1748-9326/6/4/045508

Zeng, H., Jia, G., & Forbes, B. C. (2013). Shifts in Arctic phenology in response to climate and anthropogenic factors as detected from multiple satellite time series. *Environmental Research Letters*, *8*(3), 035036. https://doi.org/10.1088/1748-9326/8/3/035036

Appendix

Contents

Chapter 3

Appendix Table 1 | Daily air temperature weather station data sources.....176
Appendix Table 2 | Effect size estimates of full models including the original model and those using spring average regional sea-ice extent and spring average temperatures 177
Appendix Figure 1 | Daily regional sea-ice extent and annual spring drop in regional sea-ice extent. 178
Appendix Table 3 | Slope estimates for trends in phenological events over time.....179
Appendix Figure 2 | Annual mean spring phenology and trends for all species-phenological events including credible intervals for *S. acaulis* flowering at Zackenberg. 180
Appendix Table 4 | Slope estimates for trends in the environmental predictors. 181
Appendix Figure 3 | Estimated mean effect sizes and associated distribution for the effect of environmental predictors on spring phenological events across all site-species-phenological event combinations. 182
Appendix Table 5 | Effect size estimates with reduced models (single environmental predictor). 183
Appendix Table 6 | Slope estimates for effects of environmental predictors on phenology events for each site-species-phenological event combinations 184

Chapter 4

Appendix Table 7 | Coordinates of the study plots 188
Appendix Table 8 | Sentinel vs. resampled drone model posterior parameter estimates....188
Appendix Table 9 | Sentinel vs resampled drone model posterior parameter estimates – model with effects for vegetation type only - utilised for visualisation purposes 188
Appendix Table 10 | Trends in NDVI standard deviation over time - model posterior parameter estimates 189
Appendix Table 11 | Trends in NDVI standard deviation over time model - posterior parameter estimates including year fixed effect and slope : vegetation type interaction.....189
Appendix Table 12 | Trends in NDVI coefficient of variance over time - model posterior parameter estimates 189
Appendix Table 13 | Effect of grain size on NDVI standard deviation trends - model posterior parameter estimates with interaction 190
Appendix Table 14 | Effect of grain size on NDVI standard deviation trends - model posterior parameter estimates without interaction 190

Appendix for Chapter 3

Appendix Table 1 | Daily air temperature weather station data sources

Site	Source
Alexandra Fiord	Alexandra Fiord climate station ambient air temperature (1.5 m). (Bjorkman et al., 2015)
Utqiaġvik	Utqiaġvik - Barrow ambient air temperature (2 m), hourly observations averaged to daily means NOAA Earth System Research Laboratory Global Monitoring Division https://www.esrl.noaa.gov/gmd/obop/brw/ (NOAA ESRL Global Monitoring Division, 2018)
Qikiqtaruk	Environment Canada Qikiqtaruk - Herschel Island weather station (ID 1560) Daily mean air temperatures gap filled with Environment Canada Komakuk weather satiation daily means (ID 10822), located at approx. distance to Qikiqtaruk: 50 km http://climate.weather.gc.ca/historical_data/search_historic_data_e.html
Zackenberg	Greenland Ecological Monitoring Programme, Climate Basis Zackenberg, air temperature (2 m) hourly data averaged to daily means. http://data.g-e-m.dk.

Appendix Table 2 | Slope parameter and random intercept estimates with associated 95% credible intervals for the original prediction model, the model using site-averages of snowmelt instead of plot-level snowmelt observations for Alexandra Fiord, Utqigavik and Qiqkitaruk, as well as the model using average regional spring sea-ice extent (May – July) instead of date of drop in regional spring sea-ice extent.

	Slope Parameters											
	Snowmelt Parameter			Temperature Parameter			Sea-Ice Parameter			Year (cont.)		
Model	**Mean**	**l-95% CI**	**u-95% CI**	**Mean**	**l-95% CI**	**u-95% CI**	**Mean**	**l-95% CI**	**u-95% CI**	**Mean**	**l-95% CI**	**u-95% CI**
Original Model	3.26	2.62	3.91	-2.21	-3.03	-1.39	-0.01	-0.94	0.91	-0.09	-1.29	1.08
Snowmelt Site Averages	2.99	2.04	3.99	-2.44	-3.17	-1.69	-0.14	-1.06	0.77	0.08	-1.14	1.25
Regional Sea-Ice Extent (May-July avg.)	3.17	2.54	3.82	-2.07	-2.84	-1.31	-0.21	-1.23	0.78	-0.20	-1.37	0.91
	Random Intercepts											
	Site			Plot			Year			Site: Year Interaction		
Model	**Mean**	**l-95% CI**	**u-95% CI**	**Mean**	**l-95% CI**	**u-95% CI**	**Mean**	**l-95% CI**	**u-95% CI**	**Mean**	**l-95% CI**	**u-95% CI**
Original Model	153.30	0.08	968.94	21.45	17.15	26.67	2.12	0.00	8.03	9.40	5.58	14.72
Snowmelt Site Averages	280.26	0.00	1081.50	30.09	23.90	36.47	2.56	0.00	7.32	9.21	4.91	14.02
Regional Sea-Ice Extent (May-July avg.)	140.00	0.00	530.64	21.69	17.07	26.55	2.00	0.00	6.31	9.36	5.21	13.98

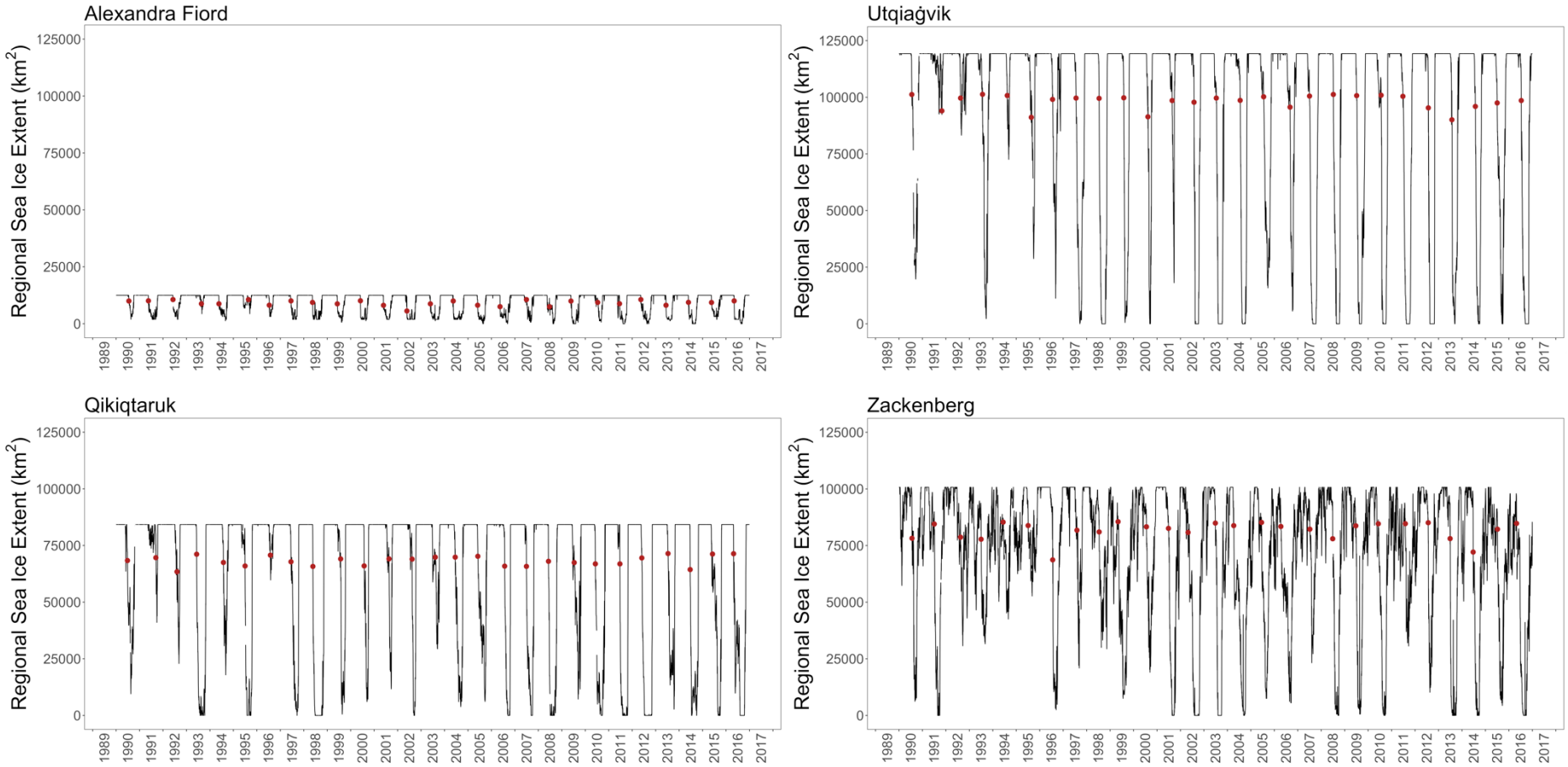

Appendix Figure 1 | Daily regional sea-ice extent in km² (black lines) and the day of spring drop in regional sea ice extent (red dots – drop below 85% leading up to annual minimum) for Alexandra Fiord, Utqiaġvik, Qikiqtaruk and Zackenberg determined from NOAA/NSIDC CDR v3 sea-ice concentrations. The sea-ice extent represents the total area of cells with sea-ice concentrations larger than 15% in the 525 km x 525 km bounding box of the polar stereographic grid centred on the respective site. Due to Alexandra Fiord's position along the Nares Strait between Ellesmere Island and Greenland, the total area of open sea in the bounding box is approximately 1/10 of the area at other sites.

Appendix Table 3 | Slope estimates for trends in the site-species-phenological event combinations, credible intervals, effective sample sizes, pMCMC and estimated change per decade.

Site Name	Species	Phenology Event	Slope	Lower 95% CI	Upper 95% CI	eff. sample size	pMCMC	Change days/decade
Alexandra Fiord	*Dryas integrifolia*	flowering	0.12	-0.42	0.65	99806	0.63	1.23
	Dryas integrifolia	green up	-0.16	-0.64	0.32	99700	0.48	-1.61
	*Luzula spp.**	flowering	-0.30	-2.16	1.49	99700	0.71	-3.03
	Oxyria digyna	flowering	0.05	-0.41	0.51	99700	0.81	0.54
	Oxyria digyna	green up	0.17	-0.26	0.59	50512	0.42	1.67
	Papaver radicatum	flowering	0.16	-0.31	0.62	99700	0.49	1.56
	Papaver radicatum	green up	-0.15	-0.58	0.30	99700	0.47	-1.52
	Salix arctica	flowering	-0.10	-0.59	0.40	100843	0.65	-1.05
Utqiaġvik	*Cassiope tetragona*	green up	-0.34	-1.22	0.55	99700	0.42	-3.39
	Dupontia psilosantha	green up	-0.09	-0.58	0.39	101160	0.69	-0.92
	Luzula arctica	flowering	-0.10	-0.63	0.43	99700	0.69	-0.99
	Luzula arctica	green up	-0.11	-0.56	0.38	96585	0.63	-1.06
	Poa arctica	green up	-0.34	-0.84	0.18	100062	0.18	-3.35
	Salix rotundifolia	flowering	-0.17	-0.68	0.34	99700	0.48	-1.71
	Salix rotundifolia	green up	-0.32	-0.87	0.24	99700	0.24	-3.16
Qikiqtaruk	*Dryas integrifolia*	flowering	-0.36	-0.76	0.04	99700	0.08	-3.60
	Eriophorum vaginatum	flowering	-0.57	-1.57	0.42	99700	0.24	-5.69
	Salix arctica	green up	-0.96	-1.83	-0.09	99700	0.03	-9.61
Zackenberg	*Cassiope tetragona*	flowering	-1.01	-1.88	-0.14	99700	0.03	-10.06
	Dryas octopetala		-0.92	-1.61	-0.24	98227	0.01	-9.23
	Papaver radicatum		-0.85	-1.67	-0.03	99700	0.04	-8.48
	Salix arctica		-0.65	-1.37	0.07	99700	0.07	-6.50
	Saxifraga oppositifolia		-0.43	-0.90	0.04	99700	0.07	-4.28
	Silene acaulis		-0.55	-0.95	-0.16	99700	0.01	-5.47

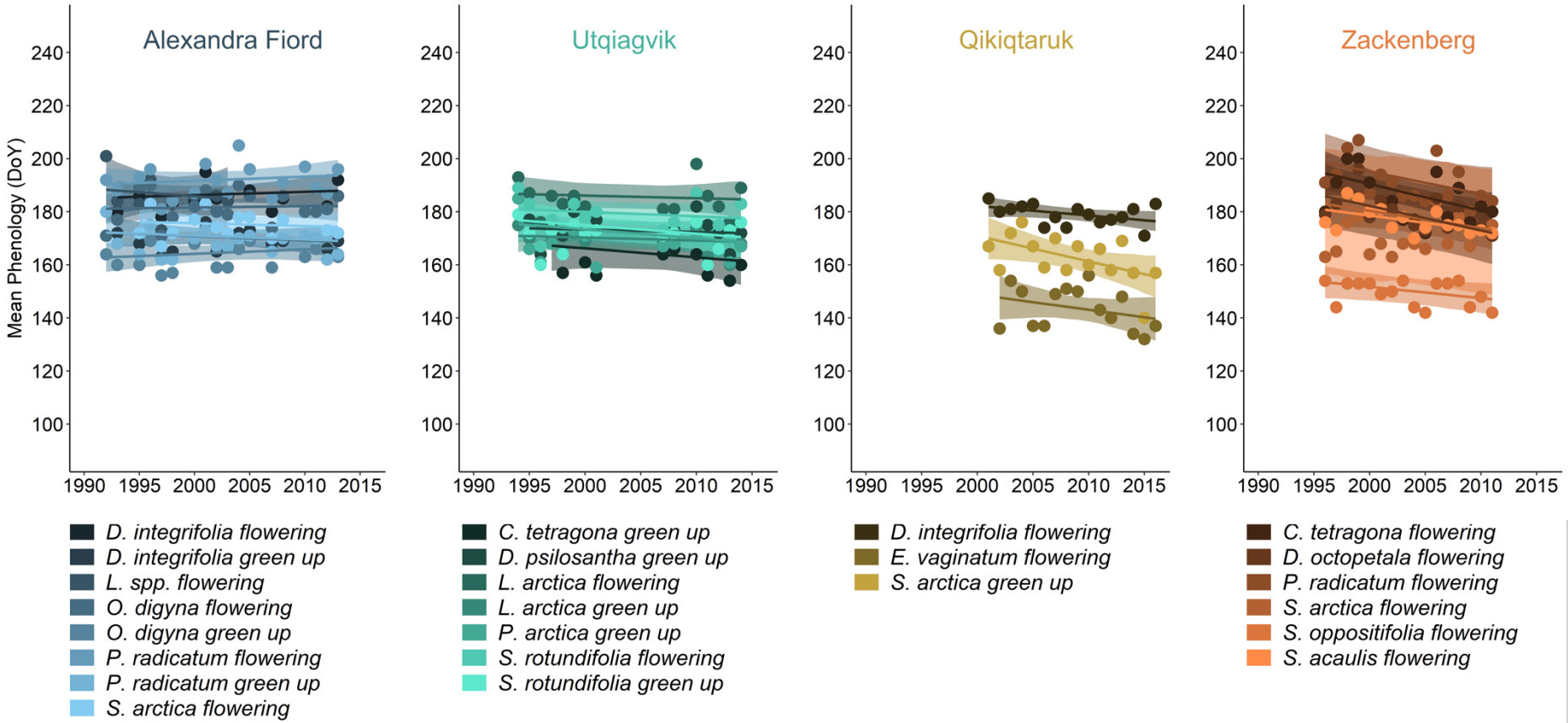

Appendix Figure 2 | Annual mean spring phenology and trends for the species-phenological event combinations at Alexandra Fiord, Utqiaġvik, Qikiqtaruk and Zackenberg with added credible intervals for *Silene acaulis* flowering. Trend lines were fitted with Bayesian interval censored models and shaded areas indicate 95% credible intervals. This figure is identical to

Figure 2-2 in the main manuscript except for the added credible intervals for *S. acaulis* flowering.

Appendix Table 4 | Slope estimates for trends in the environmental predictors, credible intervals, effective sample sizes, pMCMC and estimated change per decade (days/decade for snowmelt and spring drop in regional sea-ice extend, °C per decade for temperature) of all sites.

Site Name	Predictor	Slope	Lower 95% CI	Upper 95% CI	eff. sample size	pMCMC	Change unit/decade
Alexandra Fiord	Sea-Ice	-1.51	-3.80	0.76	499700	0.18	-15.09
	Snowmelt	-0.06	-0.42	0.30	502333	0.72	-0.61
	Temperature	0.06	0.00	0.12	504651	0.05	0.63
Utqiaġvik	Sea-Ice	-1.08	-2.38	0.22	495574	0.09	-10.83
	Snowmelt	-0.14	-0.62	0.35	499700	0.54	-1.41
	Temperature	0.05	-0.03	0.12	501721	0.22	0.46
Qikiqtaruk	Sea-Ice	-4.64	-7.32	-1.94	499700	0.00	-46.39
	Snowmelt	-0.82	-1.62	-0.03	499700	0.04	-8.15
	Temperature	0.23	0.08	0.38	499700	0.01	2.30
Zackenberg	Sea-Ice	-1.03	-5.61	3.44	503032	0.63	-10.28
	Snowmelt	-1.02	-2.25	0.21	499700	0.10	-10.22
	Temperature	0.06	-0.03	0.15	499700	0.18	0.59

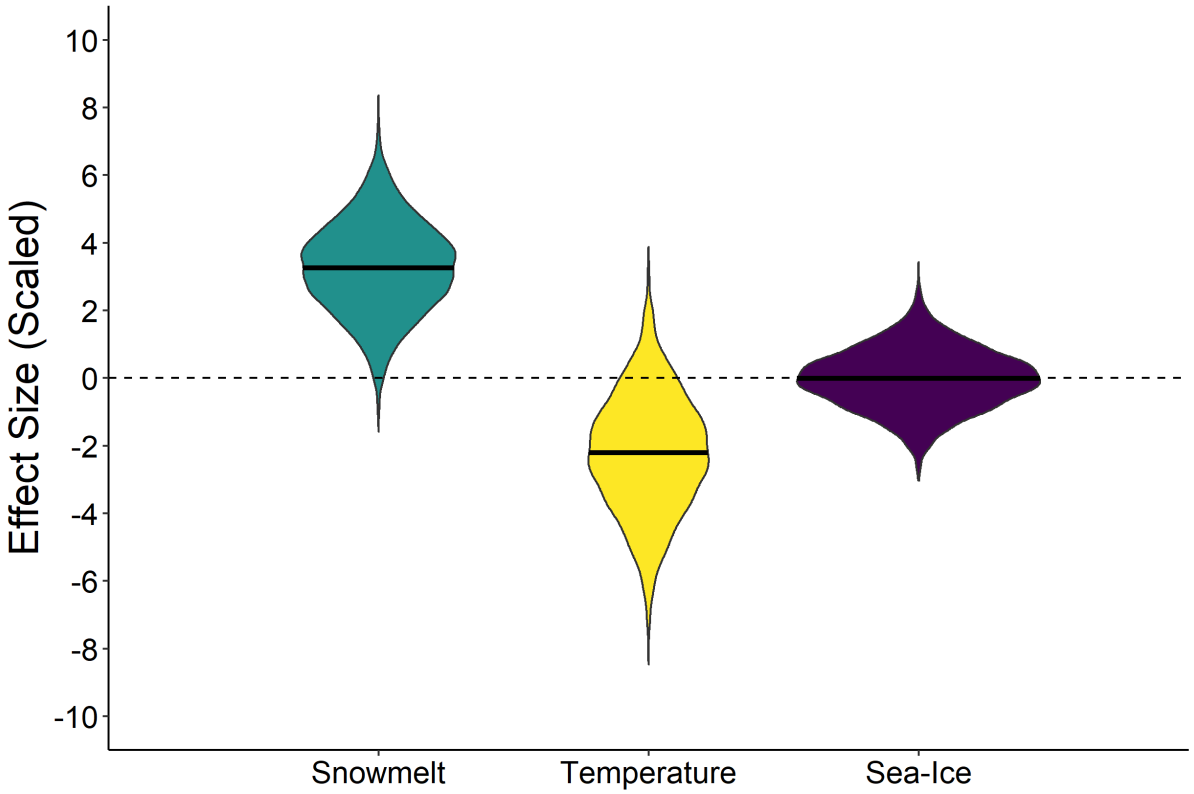

Appendix Figure 3 I Means (black lines) and estimated posterior distributions for the scaled effect sizes of the three environmental predictors (snowmelt, spring temperature and spring drop in regional sea-ice extent) across all site-species-phenological event combinations in the dataset. These posterior distributions demonstrate that overall snowmelt was best at explaining variation in spring phenology, whereas temperature explained variation for some site-species-phenological event combinations and sea-ice was a poor explanatory factor. See also the site-species-phenological event estimates in

Figure 2-4. The back transformed (unscaled) posterior estimates for the mean slope parameters and associated variances are: snowmelt date mean slope: 0.45 (CI: 0.37 to 0.54) and variance: 0.25 (CI: 0.12 to 0.49); spring temperature mean slope: 2.39 (CI: -3.30 to -1.51) and variance: 3.42 (CI: 1.64 to 6.63); drop in regional sea-ice extent mean slope: >-0.01 (CI: -0.14 to 0.13) and variance: 0.12 (CI: 0.04 to 0.27).

Appendix Table 5 | Slope parameter and random intercept estimates for the single environmental predictor models. The models were run with a lower number of iterations than the original model (20,000 instead of 1,200,000), which still ensured sufficient effective sample sizes for the slope parameters of interest but resulted in reduced confidence in the intercept estimates due to lower effective sample sizes for these effects.

Slope Parameters

Environmental Predictor	Environmental Predictor			Year (continuous)		
	Mean	l-95 CI%	u-95% CI	Mean	l-95% CI	u-95% CI
Snowmelt	3.36	2.78	3.97	-0.93	-1.90	0.15
Spring Temperature	-2.46	-3.17	-1.69	-0.53	-1.82	0.79
Spring Drop in Sea-Ice	-0.33	-1.59	1.18	-1.81	-3.44	-0.33
Regional Sea-Ice Extent (May-July avg.)	-0.39	-1.89	1.17	-1.84	-3.39	-0.32

Random Intercepts

Environmental Predictor	Site			Plot ID			Year (factor)			Year (site)		
	Mean	l-95% CI	u-95% CI	Mean	l-95% CI	u-95% CI	Mean	l-95% CI	u-95% CI	Mean	l-95% CI	u-95% CI
Snowmelt	5.27	0.00	4.13	21.16	16.59	25.88	0.11	0.00	0.29	13.35	8.75	19.03
Spring Temperature	9.64	0.00	33.63	29.78	23.84	36.21	0.00	0.00	0.00	22.98	15.37	32.08
Spring Drop in Sea-Ice	3.14	0.00	1.87	29.46	23.35	35.63	0.10	0.00	0.39	31.36	20.16	43.65
Regional Sea-Ice Extent (May-July avg.)	6.33	0.00	19.23	29.59	23.82	36.40	0.00	0.00	0.00	31.91	20.39	43.60

Appendix Table 6 | Estimated mean scaled and back-transformed (unscaled) effect sizes with associated 95% credible intervals for snowmelt, temperature and spring drop in sea-ice extent for all site-species-phenological event combinations. Unscaled effect sizes for snowmelt, temperature and drop in regional sea ice extent represent day advance/delay in phenology per (i) day change in snowmelt date, (ii) °C spring temperature change and (iii) day change in drop in regional sea-ice extent.

Predictor	Site Name	Species	Phenology Event	Effect Size (Scaled)	Lower 95% CI	Upper 95% CI	Effect Size (back transf.)	Lower 95% CI (back transf.)	Upper 95% CI (back transf.)
Snowmelt Date	Alexandra Fiord	*Dryas integrifolia*	flowering	4.24	2.82	5.67	0.59	0.39	0.79
		Dryas integrifolia	green up	4.34	2.94	5.75	0.60	0.41	0.80
		*Luzula spp.**	flowering	3.83	1.87	5.79	0.53	0.26	0.80
		Oxyria digyna	flowering	2.55	0.96	4.14	0.35	0.13	0.58
		Oxyria digyna	green up	4.12	2.58	5.68	0.57	0.36	0.79
		Papaver radicatum	flowering	2.64	1.17	4.12	0.37	0.16	0.57
		Papaver radicatum	green up	2.82	1.4	4.24	0.39	0.19	0.59
		Salix arctica	flowering	3.38	1.76	5.01	0.47	0.24	0.70
	Utqiaġvik	*Cassiope tetragona*	green up	2.78	1.09	4.48	0.39	0.15	0.62
		Dupontia psilosantha	green up	4.14	2.27	6.04	0.58	0.32	0.84
		Luzula arctica	flowering	2.86	1.39	4.33	0.40	0.19	0.60
		Luzula arctica	green up	2.95	1.5	4.42	0.41	0.21	0.61
		Poa arctica	green up	3.53	2.07	5	0.49	0.29	0.69
		Salix rotundifolia	flowering	4.06	2.54	5.58	0.56	0.35	0.78
		Salix rotundifolia	green up	5.04	3.54	6.57	0.70	0.49	0.91
	Qikiqtaruk	*Dryas integrifolia*	flowering	-0.35	-1.84	1.11	-0.05	-0.26	0.15
		Eriophorum vaginatum	flowering	4.15	2.6	5.71	0.58	0.36	0.79
		Salix arctica	green up	2.43	0.86	3.98	0.34	0.12	0.55
	Zackenberg	*Cassiope tetragona*	flowering	3.79	2.16	5.41	0.53	0.30	0.75
		Dryas octopetala		3.33	1.63	5.03	0.46	0.23	0.70
		Papaver radicatum		3.91	2.13	5.69	0.54	0.30	0.79
		Salix arctica		3.61	2	5.21	0.50	0.28	0.72
		Saxifraga oppositifolia		2.16	0.24	4.05	0.30	0.03	0.56
		Silene acaulis		2.01	0.22	3.76	0.28	0.03	0.52

Predictor	Site Name	Species	Phenology Event	Effect Size (Scaled)	Lower 95% CI	Upper 95% CI	Effect Size (back transf.)	Lower 95% CI (back transf.)	Upper 95% CI (back transf.)
Spring Temperature	Alexandra Fiord	*Dryas integrifolia*	flowering	-3.99	-5.79	-2.26	-4.34	-6.29	-2.46
		Dryas integrifolia	green up	-3.98	-5.78	-2.25	-4.33	-6.28	-2.45
		*Luzula spp.**	flowering	-5.09	-7.65	-2.64	-5.53	-8.32	-2.87
		Oxyria digyna	flowering	-3.32	-5.23	-1.47	-3.61	-5.68	-1.60
		Oxyria digyna	green up	-2.67	-4.53	-0.86	-2.90	-4.92	-0.93
		Papaver radicatum	flowering	-5.53	-7.4	-3.73	-6.01	-8.04	-4.05
		Papaver radicatum	green up	-4.45	-6.28	-2.68	-4.84	-6.83	-2.91
		Salix arctica	flowering	-2.16	-4.05	-0.32	-2.35	-4.40	-0.35
	Utqiaġvik	*Cassiope tetragona*	green up	-1.02	-3	0.98	-1.11	-3.26	1.07
		Dupontia psilosantha	green up	-0.72	-2.74	1.31	-0.78	-2.98	1.42
		Luzula arctica	flowering	-1.1	-2.98	0.81	-1.20	-3.24	0.88
		Luzula arctica	green up	-0.74	-2.54	1.11	-0.80	-2.76	1.21
		Poa arctica	green up	-0.72	-2.51	1.1	-0.78	-2.73	1.20
		Salix rotundifolia	flowering	-0.48	-2.31	1.38	-0.52	-2.51	1.50
		Salix rotundifolia	green up	-0.52	-2.36	1.35	-0.57	-2.57	1.47
	Qikiqtaruk	*Dryas integrifolia*	flowering	-0.73	-2.6	1.16	-0.79	-2.83	1.26
		Eriophorum vaginatum	flowering	-0.46	-2.24	1.32	-0.50	-2.43	1.43
		Salix arctica	green up	-2.48	-4.34	-0.61	-2.70	-4.72	-0.66
	Zackenberg	*Cassiope tetragona*	flowering	-2.47	-4.72	-0.22	-2.68	-5.13	-0.24
		Dryas octopetala		-0.93	-3.25	1.4	-1.01	-3.53	1.52
		Papaver radicatum		-2.52	-5.07	0.01	-2.74	-5.51	0.01
		Salix arctica		-3.58	-5.86	-1.34	-3.89	-6.37	-1.46
		Saxifraga oppositifolia		-1.03	-3.55	1.51	-1.12	-3.86	1.64
		Silene acaulis		-2.26	-4.73	0.2	-2.46	-5.14	0.22

Predictor	Site Name	Species	Phenology Event	Effect Size (Scaled)	Lower 95% CI	Upper 95% CI	Effect Size (back transf.)	Lower 95% CI (back transf.)	Upper 95% CI (back transf.)
Spring drop in sea-ice Extent	Alexandra Fiord	*Dryas integrifolia*	flowering	-0.09	-1.83	1.65	0.00	-0.07	0.06
		Dryas integrifolia	green up	0.71	-1.01	2.44	0.03	-0.04	0.09
		*Luzula spp.**	flowering	-0.77	-2.87	1.26	-0.03	-0.11	0.05
		Oxyria digyna	flowering	0.52	-1.27	2.33	0.02	-0.05	0.09
		Oxyria digyna	green up	-0.08	-1.85	1.69	0.00	-0.07	0.06
		Papaver radicatum	flowering	0.81	-0.96	2.59	0.03	-0.04	0.10
		Papaver radicatum	green up	-0.25	-1.98	1.48	-0.01	-0.07	0.06
		Salix arctica	flowering	-0.65	-2.45	1.13	-0.02	-0.09	0.04
	Utqiaġvik	*Cassiope tetragona*	green up	-0.76	-3.03	1.39	-0.03	-0.11	0.05
		Dupontia psilosantha	green up	1.22	-0.88	3.44	0.05	-0.03	0.13
		Luzula arctica	flowering	-0.02	-2.07	2.03	0.00	-0.08	0.08
		Luzula arctica	green up	0.27	-1.74	2.31	0.01	-0.06	0.09
		Poa arctica	green up	-1.45	-3.58	0.57	-0.05	-0.13	0.02
		Salix rotundifolia	flowering	1.08	-1.03	3.33	0.04	-0.04	0.12
		Salix rotundifolia	green up	-0.63	-2.78	1.45	-0.02	-0.10	0.05
	Qikiqtaruk	*Dryas integrifolia*	flowering	0.03	-2.08	2.16	0.00	-0.08	0.08
		Eriophorum vaginatum	flowering	0.02	-1.99	2.04	0.00	-0.07	0.08
		Salix arctica	green up	-0.07	-2.05	1.91	0.00	-0.08	0.07
	Zackenberg	*Cassiope tetragona*	flowering	-0.04	-1.9	1.83	0.00	-0.07	0.07
		Dryas octopetala		-0.37	-2.23	1.46	-0.01	-0.08	0.05
		Papaver radicatum		-0.43	-2.39	1.49	-0.02	-0.09	0.06
		Salix arctica		-0.01	-1.83	1.81	0.00	-0.07	0.07
		Saxifraga oppositifolia		0.26	-1.85	2.4	0.01	-0.07	0.09
		Silene acaulis		0.39	-1.51	2.32	0.01	-0.06	0.09

Appendix for Chapter 4

Appendix Table 7 | Coordinates for the extent of the Herschel and Komakuk vegetation plots based on the Sentinel grid. Coordinates are given in WGS84 UTM Zone 7N (EPSG:32607).

Site Name	Vegetation Type	Min x	Max x	Min y	Max y
Collinson Head (Site 1)	Herschel	583120	583220	7719870	7719970
	Komakuk	583000	583100	7720060	7720160
Bowhead Ridge (Site 2)	Herschel	582860	582960	7720410	7720510
	Komakuk	582790	582890	7720760	7720860
Hawk Valley (Site 3)	Herschel	580910	581010	7720890	7720990
	Komakuk	581010	581110	7720630	7720730
Hawk Ridge (Site 4)	Herschel	580730	580830	7721390	7721490
	Komakuk	580590	580690	7721100	7721200

Appendix Table 8 | Posterior parameter estimates for the Sentinel vs. resampled 10 m drone pixel model including estimates for the effect on intercept and interaction effects on the slope for vegetation type, Sentinel id and the difference in days between drone and sentinel images.

Model parameter	Posterior mean	Lower 95% CI	Upper 95% CI	Eff. sample size	pMCMC
Intercept (μ)	-0.020	-0.029	-0.011	4700	$< 2 \times 10^{-4}$
Slope ($\beta_{Sentinel}$)	0.944	0.930	0.958	4700	$< 2 \times 10^{-4}$
Veg. type Intercept ($\alpha_{veg.type}$)	-0.026	-0.030	-0.022	4700	$< 2 \times 10^{-4}$
Sentinel ID Intercept ($\alpha_{sent.id}$)	0.094	0.082	0.107	4700	$< 2 \times 10^{-4}$
Diff. Days Intercept (α_{diff})	0.065	0.042	0.089	4700	$< 2 \times 10^{-4}$
$\beta_{NDVI_{sentinel}}: veg.type$	0.012	0.005	0.018	4700	$< 2 \times 10^{-4}$
$\beta_{NDVI_{sentinel}}: sent.id$	-0.128	-0.146	-0.110	4700	$< 2 \times 10^{-4}$
$\beta_{NDVI_{sentinel}}: diff$	-0.167	-0.199	-0.134	4700	$< 2 \times 10^{-4}$
Residual Variance (ε)	0.00069	0.00067	0.00071	4700	NA

Appendix Table 9 | Posterior parameter estimates for the reduced sentinel vs. resampled 10 m drone pixel model including only estimates for the effect on intercept and interaction effects on the slope for vegetation type, utilised for visualisation purposes only in Figure 4-4.

Model parameter	Posterior mean	Lower 95% CI	Upper 95% CI	Eff. sample size	pMCMC
Intercept (μ)	0.019	0.008	0.030	4921	0. 000851
Slope ($\beta_{Sentinel}$)	0.847	0.831	0.865	4934	$< 2 \times 10^{-4}$
Veg. type Intercept ($\alpha_{veg.type}$)	0.079	0.061	0.096	4700	$< 2 \times 10^{-4}$
$\beta_{NDVI_{sentinel}}: veg.type$	-0.109	-0.133	-0.083	5240	$< 2 \times 10^{-4}$
Residual Variance (ε)	0.00160	0.00155	0.00165	0.00160	NA

Appendix Table 10l Posterior parameter estimates for the linear mixed models of trends in the standard deviation in NDVI of native grain-size drone raster across the growing seasons, including fixed intercept estimates for vegetation type and year. Trend lines are visualised in Figure 4-6.

Model parameter	Posterior mean	Lower 95% CI	Upper 95% CI	Eff. sample size	pMCMC
Intercept (μ)	0.1331	0.0995	0.1681	1700	< 6 x 10^{-4}
Slope ($\beta_{day\ of\ year}$)	-0.0003	-0.0005	-0.0001	1700	< 6 x 10^{-4}
Veg. type Intercept ($\alpha_{veg.type}$)	0.0148	0.0097	0.0192	1404	< 6 x 10^{-4}
Year Intercept (α_{year})	-0.0060	-0.0115	-0.0005	1700	0.0329
Residual Variance (ε)	0.00010	0.00006	0.00014	1700	NA

Appendix Table 11 l Posterior parameter estimates for the linear mixed models of trends in the standard deviation in NDVI of native grain-size drone raster across the growing seasons, including fixed intercept estimates for vegetation type and year, and an interaction between slope and vegetation type.

Model parameter	Posterior mean	Lower 95% CI	Upper 95% CI	Eff. sample size	pMCMC
Intercept (μ)	0.1480	0.1024	0.1939	1527	< 6 x 10^{-4}
Slope ($\beta_{day\ of\ year}$)	-0.0004	-0.0006	-0.0002	1525	< 6 x 10^{-4}
Veg. type Intercept ($\alpha_{veg.type}$)	-0.0139	-0.0839	0.0480	1700	0.6906
Year Intercept (α_{year})	-0.0059	-0.0113	0.0001	1700	0.0447
$\beta_{day\ of\ year}: veg.type$	0.0001	-0.0002	0.0005	1700	0.3776
Residual Variance (ε)	0.00010	0.00007	0.00014	1700	NA

Appendix Table 12 l Posterior parameter estimates for the linear mixed models of trends in the coefficient of variance for the NDVI of native grain-size drone raster across the growing seasons, including fixed intercept estimates for vegetation type and year, and an interaction between slope and vegetation type.

Model parameter	Posterior mean	Lower 95% CI	Upper 95% CI	Eff. sample size	pMCMC
Intercept (μ)	0.4234	0.3273	0.5260	1700	< 6 x 10^{-4}
Slope ($\beta_{day\ of\ year}$)	-0.0015	-0.0020	-0.0010	1700	< 6 x 10^{-4}
Veg. type Intercept ($\alpha_{veg.type}$)	-0.0864	-0.2323	0.0446	1700	0.219
Year Intercept (α_{year})	-0.0058	-0.0180	0.0051	1700	0.322
$\beta_{day\ of\ year}: veg.type$	0.0005	-0.0002	0.0012	1700	0.131
Residual Variance (ε)	0.00045	0.00030	0.00062	1823	NA

Appendix Table 13 | Posterior parameter estimates for the linear mixed models of effect of grain size on the trends standard deviation of NDVI across the growing seasons, including fixed intercept estimates for vegetation type and year, and an interaction between grain size and slope.

Model parameter	Posterior mean	Lower 95% CI	Upper 95% CI	Eff. sample size	pMCMC
Intercept (μ)	0.050030	0.037550	0.062110	1974	$< 6 \times 10^{-4}$
Slope ($\beta_{day\ of\ year}$)	-0.000100	-0.000156	-0.000035	1939	0.00118
Grain size Intercept ($\alpha_{grain\ size}$)	-0.000472	-0.001212	0.000271	1700	0.23059
Veg. type Intercept ($\alpha_{veg.type}$)	0.009118	0.007915	0.010160	1700	$< 6 \times 10^{-4}$
Year Intercept (α_{year})	-0.000180	-0.001509	0.001069	1506	0.78
$\beta_{day\ of\ year}: grain\ size$	-0.000001	-0.000004	0.000003	1700	0.75412
Residual Variance (ε)	0.000027	0.000023	0.000032	1700	NA

Appendix Table 14 | Posterior parameter estimates for the linear mixed models of effect of grain size on the trends standard deviation of NDVI across the growing seasons, including fixed intercept estimates for vegetation type and year with no interaction between grain size and slope.

Model parameter	Posterior mean	Lower 95% CI	Upper 95% CI	Eff. sample size	pMCMC
Intercept (μ)	0.05171	0.04292	0.05938	1877	$< 6 \times 10^{-4}$
Slope ($\beta_{day\ of\ year}$)	-0.00011	-0.00015	-0.00007	1896	$< 6 \times 10^{-4}$
Grain size Intercept ($\alpha_{grain\ size}$)	-0.00059	-0.00065	-0.00055	1700	$< 6 \times 10^{-4}$
Veg. type Intercept ($\alpha_{veg.type}$)	0.00910	0.00783	0.01014	1700	$< 6 \times 10^{-4}$
Year Intercept (α_{year})	-0.00024	-0.00164	0.00094	1387	0.74
Residual Variance (ε)	0.000027	0.000023	0.000031	1700	NA